Rev.	Publish date	Description	Made by	Checked by	Project appro.	Client appro.
0	28.11.19	Final issue	LYAN	SIGU	FKAM	
A	30.08.19	First issue	LYAN	SIGU	FKAM	

Client

Statens vegvesen

Contractor

DNV·GL

Contract no.:

15/255967

Document name:

Independent Analyses of AMC Floating Bridge BJF 2019

Document no.:	Rev.:	Pages:
SBJ-32-C5-DNV-62-RE-023	0	188

FERJEFRI E39 - RAMMEAVTALE FJORDKRYSNINGSPROSJEKTET

Independent Analyses of AMC Floating Bridge BJF 2019

Statens vegvesen region vest

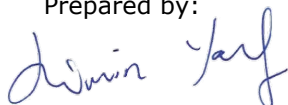**Report No.:** 2019-0297, Rev. 0
Document No.: 110UE04C-59
Date: 2019-11-28

Project name:	Ferjefri E39 - Rammeavtale fjordkrysningsprosjektet	DNV GL AS Oil & Gas Offshore Structures
Report title:	Independent Analyses of AMC Floating Bridge BJF 2019	Veritasveien 1 1363 Høvik
Customer:	Statens vegvesen region vest, Askedalen 4 6863 LEIKANGER Norway	Norway Tel: NO 945 748 931 MVA
Customer contact:	Tore Askeland	
Date of issue:	2019-11-28	
Project No.:	10042624	
Organisation unit:	Offshore Structures	
Report No.:	2019-0297, Rev. 0	
Document No.:	110UE04C-59	

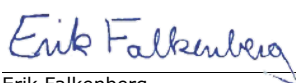Applicable contract(s) governing the provision of this Report:

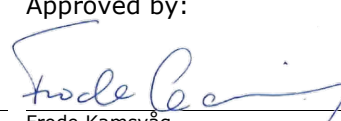Objective: Perform independent global analyses of AMC K12 concept.

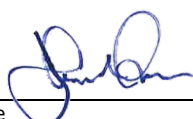| Prepared by:	Verified by:	Approved by:
Limin Yang Senior Engineer	Erik Falkenberg Senior Principal Engineer	Frode Kamsvåg Business Development Leader Marine Structures
Marius Skinlo Clausen Senior Engineer	Gudfinnur Sigurdson SVP	
Harald Rove Principal Engineer	Vigleik Hansen PM	

DNV GL Distribution:

☐ OPEN. Unrestricted distribution, internal and external.

☐ INTERNAL use only. Internal DNV GL document.

☒ CONFIDENTIAL. Distribution within DNV GL according to applicable contract*

☐ SECRET. Authorized access only.

*Specify distribution:

Keywords:

Floating bridge, E39, West Coast, Dynamics, Ferjefri

Rev. No.	Date	Reason for Issue	Prepared by	Verified by	Approved by
A	2019-08-30	First issue	L. Yang	G. Sigurdsson	F. Kamsvåg
0	2019-11-28	Final Issue	L. Yang	G. Sigurdsson	F. Kamsvåg

Table of contents

1 EXECUTIVE SUMMARY

1.1 General

This report documents the independent analyses for AMC concept K12 alternative for Bjørnafjorden crossing. The independent analyses are focused on the capacity of the bridge girder and the mooring lines.

Per agreement with SVV, revision 0 of this report has been issued without any adjustments compared to revision A.

Independent analyses are based on a coupled time domain analysis model in SIMO/RIFLEX. Each simulation has an effective duration of 3 hours, and each ULS/ALS simulation has been repeated with 30 different realizations of wind and waves.

The geometry of the bridge has been received from the designer.

Cross-section properties of the steel girder have been based on latest drawings while designer's cross section data has been used for tower, columns, cables and concrete sections.

Hydrodynamic loads on the pontoons are based on WADAM.

Analysis cases are based on DNV GL interpretation of the Metocean report.

The independent analyses show that the designer's strong axis bending moment at axis 2 may have been underpredicted, and that reinforcements are needed in this area. Their screening analysis was based on an uncoupled approach where the different load effects were superimposed, thus ignoring coupling effects. Our results have identified a different critical environmental direction for this response.

Our results show that the dynamic response in the bridge increases with decreasing current speed. Designers documentation show that a current speed of 1.7 m/s was used for all analyses. This is non-conservative.

1.2 Conclusions

1.2.1 ULS

The calculated stresses exceed the ULS capacity of the box girder at Axis 2 (tower) and need to be reinforced. At the North end the capacity is at the limit and reinforcements may be needed. This agrees with the checks done by the designer. The rest of the bridge girder satisfy the specified requirements.

1.2.2 FLS

The independent analyses carried out by DNV GL determines the contribution to damage from environmental loads in the bridge girder. The results from the screening analysis show a minimum fatigue life of 482 years. This number should be reduced due to the local stress increase as shown in Section 7.3.5. A reduction similar to the example in Section 7.3.6 could be expected that will bring the fatigue damage from environmental loads close to the required life of 250 years.

The contributions from traffic and tidal variation are not part of the independent analyses by DNV GL. The contributions will add to the damage only at certain details in the bridge. Tidal variation will only lead to damage close to the ends and traffic will predominantly give damage in the bridge deck. However, the fatigue loading as determined by DNV GL show that it should be expected that in certain areas

details as assumed in the fatigue screening with SCF of 1.5 and SN-curve D may not be allowed even from environmental actions alone.

1.2.3 Mooring

The loads in the mooring system give a safety factor well above the requirement of 2.2

The calculated fatigue life for the top chain is just above the requirement of 50 years design life and DDF of 10, while the bottom chain goes below 100 years design life and DDF of 10. These results are with a SCF of 1.15, which may be conservative.

2 INTRODUCTION

2.1 General

During fall of 2018 SVV set out two conceptual studies to develop a floating bridge concept for crossing Bjørnafjorden (BJF). DNV GL has been chosen as independent verifier by SVV for this conceptual work. This is reflected in Frame agreement no 15/255967. DNV GL scope of work related to 'BJF 2019' is described in Ctrs 610, 615, 620, 625 and 630. For this report reference is made to Ctr 620 with focus on independent analyses of AMC chosen bridge concept. This DNV GL report is charged to Ctr 630, reporting to SVV.

This report deals with the concepts evaluated by design group AMC. A total of four (4) concepts have been investigated by each of the design groups and one of these considered concepts will be recommended for the next phase (part B, Dec. 2019 – Dec. 2020). The activity plan (part A) set up by SVV were as follows:

Time	SVV activity plan	Responsible
19/11-18	SVV hand over design basis documentation to the two chosen design groups for Part A and project kick-off	SVV
18/01-19	Routing of roads for the 4 bridge alternatives accepted by SVV	AMC
28/01-19	Status report no 1 with concept ranking issued by AMC	AMC
29/03-19	Status report no 2 with estimates of masses, costs and updated drawings/descriptions for all 4 alternatives issued by AMC	AMC
07/05-19	Verification of technical quality completed based on review of existing documentation for the 4 bridge alternatives. This verification also including interviews of AMC. Interviews to be performed by DNV GL.	SVV
24/05-19	Report from AMC on their chosen bridge concept including evaluations for the three other bridge concepts.	AMC
30/06-19	Documentation basis (drawings and descriptions) for investment estimates of chosen bridge concept	AMC
15/08-19	Final documentation delivery of recommended bridge concept	AMC
31/08-19	Final documentation of the three (3) other bridge concepts	AMC
31/08-19	Resource-diagram prognosis for the period Dec. 2019 – Dec- 2020 (part B)	AMC
31/08-19	Part A completed	AMC

For Bjørnafjorden several different bridge alternatives have been considered over the last 2 – 3 years for crossing. Currently the BJF crossing is into phase 5 and the following 4 floating bridge concepts have been up for evaluations:

K11 – Curved, end-anchored floating bridge in accordance with phase 4 of the project.

K12 – Curved, end-anchored floating bridge with supplementary side moorings

K13 – Straight, side anchored floating bridge

K14 – 'Straight' S-shaped, side anchored bridge

2.2 Objective

The objective of the analyses is to check that the conceptual design is sound and that the concept can be realized according to the designers plans. This is achieved through identification of the most onerous environmental conditions and ULS code checks for these, and fatigue damage estimation due to environmental loads for selected regions and details in the bridge girder.

2.3 Scope of work

The work includes developing a global analysis model for the bridge.

The global model is established as follows:

1. WADAM frequency domain hydrodynamic model for calculation of first and second order (drift) wave loads on the pontoons. It is assumed that the hydrodynamic coupling between the different pontoons is negligible.

2. SIMO model for time domain simulations of the pontoon response. In addition to 1st and 2nd order wave loads on the pontoons (based on results from 1.), the model incorporates current and wind loads on the pontoons as relevant.

3. RIFLEX model of the global bridge structure: bridge girder, columns, tower, cables and mooring lines. The model incorporates load coupling to the SIMO pontoon models (from 2.) and aerodynamic loads on the bridge structure where relevant.

4. The 3-dimensional and 3-component wind field will be simulated using TURBSIM and imported to the integrated SIMO-RIFLEX model.

The critical conditions for ULS are analysed to evaluate structural capacity. In addition, a series of sensitivity analysis are carried out to gain insight in bridge performance.

Fatigue damage on the bridge girder and the mooring lines due to environmental loading is calculated based on the long-term conditions for Bjørnafjorden.

2.4 Changes from previous revision

The report has been updated as indicated in Table 2-1.

Table 2-1   Changes from previous revision

Section	What is updated
All	This is the first revision

3 BASIS FOR WORK

3.1 Nomenclature and coordinate system

3.1.1 Overview of the bridge structure

The bridge will cross Bjørnafjorden, south of Bergen.

The position of axis 1 is specified in UTM32 coordinates as 6666163.33 N, 297947.86 E. The profile line level is 62 m above baseline/still water line.

The North abutment is located at Gulholmane and its calculated coordinates are 6671331.58 N, 299015.79 E in UTM32 system.

The overall bridge heading is therefore 11.67 degrees from True North.
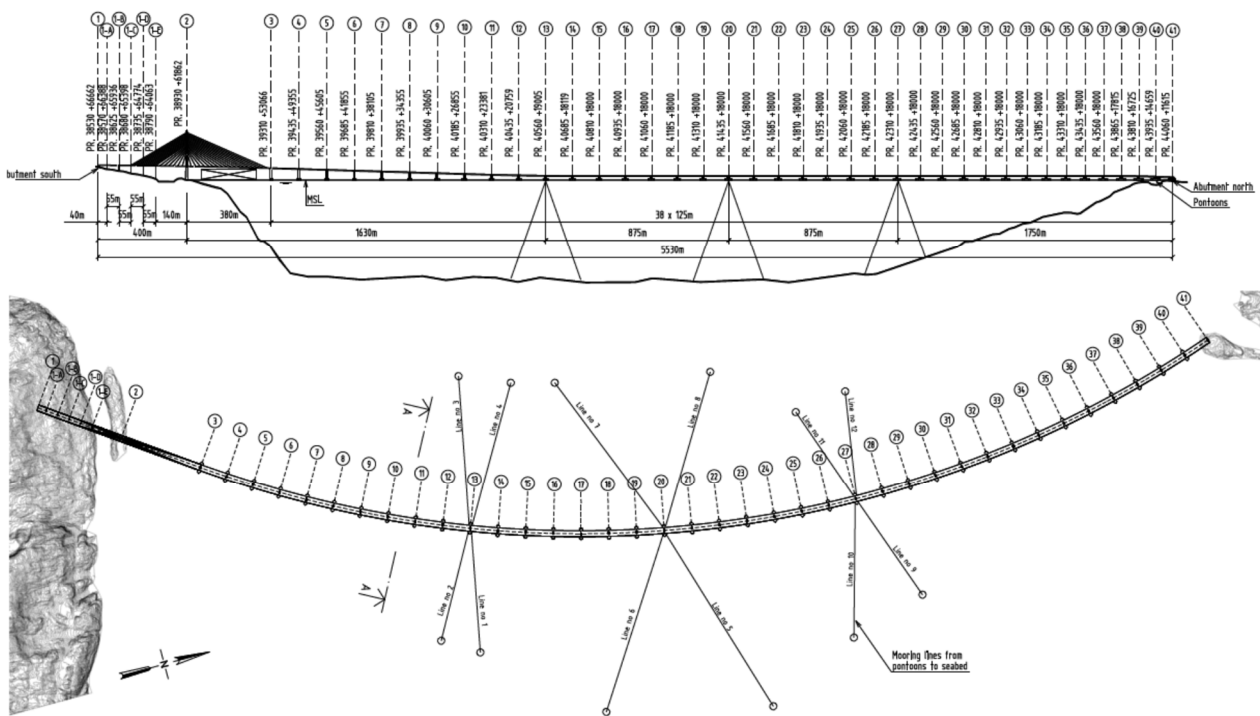
Figure 3-1   Curved bridge overview /1/.

3.1.2 Global metocean coordinate system

A right-handed earth-fixed coordinate system is used for all reference to meteorological and ocean data and environmental conditions, unless otherwise noted. It is defined as follows:

- X-axis points towards North.

- Y-axis points towards East.

- Z-axis points downwards.

- Rotations in the XY-plane are positive clockwise from North.

- Wind, wave and current are defined as "coming from" (note that in met ocean reports current is often specified with "going to" direction). This definition is used for environmental directions presented in this report.

3.1.3 Global model coordinate system

The right-handed and earth-fixed global model coordinate system is defined as

- X-axis points towards North.

- Y-axis points towards West.

- Z-axis points upwards.

- Rotations in the XY-plane are positive counter-clockwise from North.

- Wind, wave and current directions are defined as propagation directions (i.e. "going to"). This definition is used in the input files for the analyses.

- The baseline (Z=0m) is the mean surface level (MSL).

- The origin of the coordinate system is set at 6668744.33 N, 299215.63 E (UTM32) at MSL. Consequently, the positions of Axes 1 and 41 in the global coordinate system are:

  - Axis 1: x = -2581.00 m, y = 1267.77 m

  - Axis 41: x = 2587.25 m, y = 199.84 m
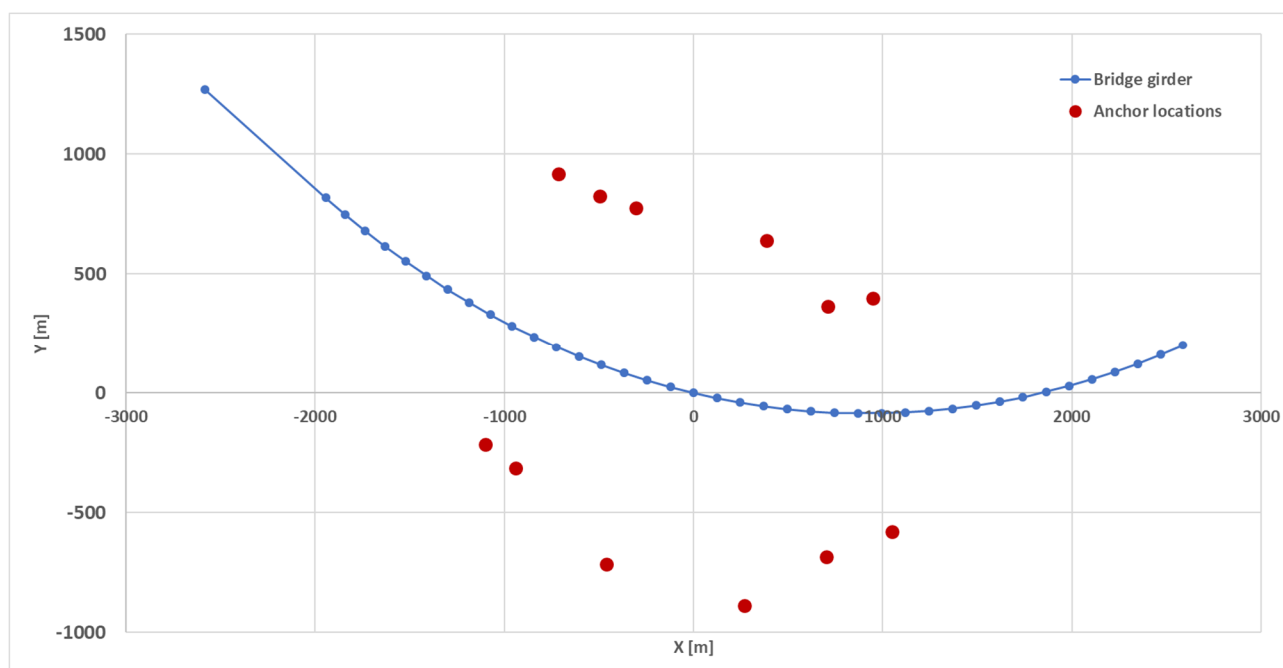
Figure 3-2   Coordinates in the analysis model

3.1.4 Pontoon coordinate system

The right-handed pontoon coordinate system is defined as

- X-axis points towards pontoon's longitudinal direction, towards bridge's West.

- Y-axis points towards pontoon's transversal direction, towards bridge's South.

- Z-axis points upwards.

The origin is located at the still water line (coincide with global baseline), and the longitudinal and transverse mid-point.

All pontoons (axes 3- 40) are oriented perpendicular to bridge's girder.
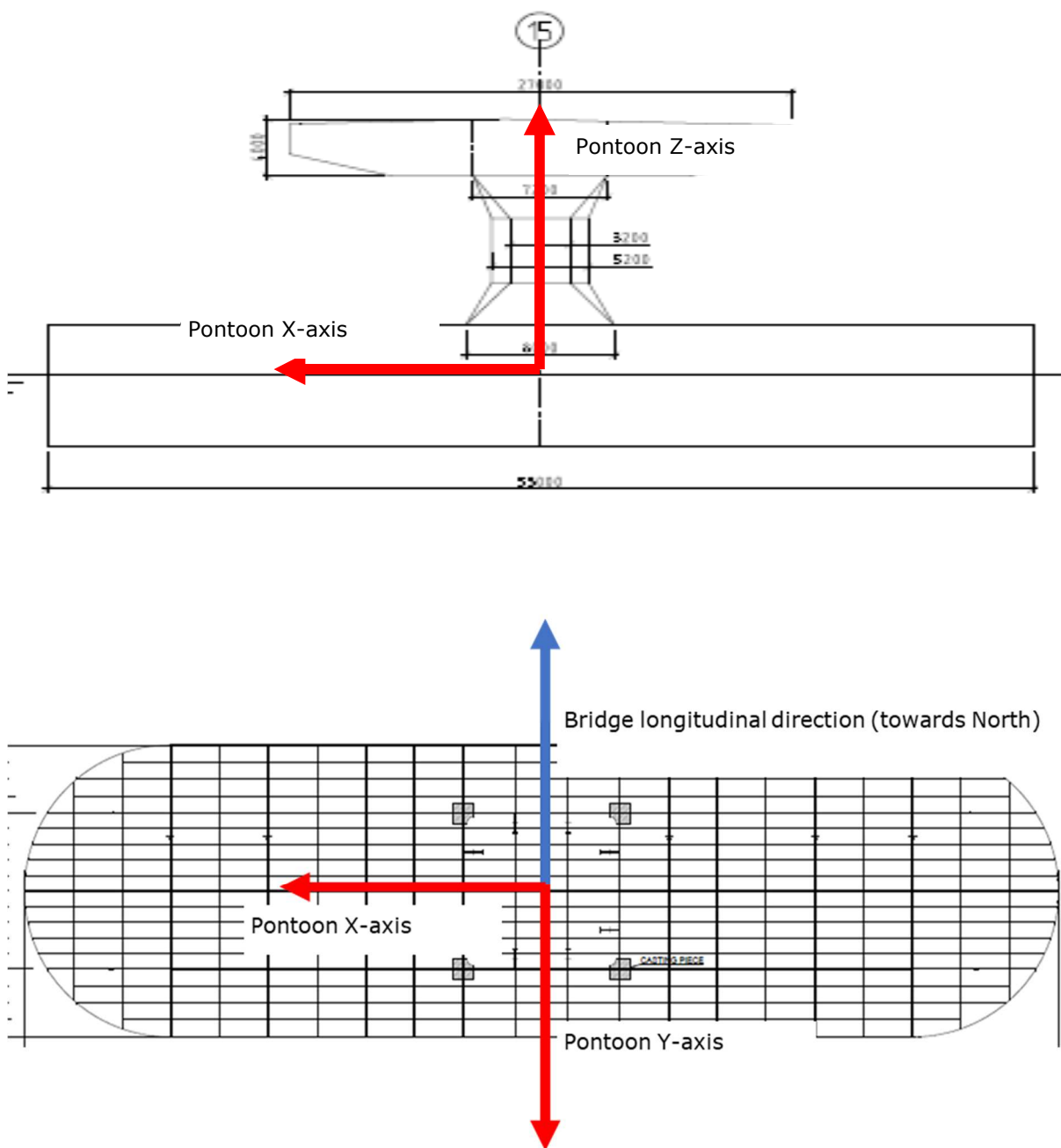
Figure 3-3 Pontoon local coordinate system

3.1.5 RIFLEX local element coordinate system

The right-handed local element coordinate system is defined as:

- X-axis is oriented along the secant between the two end nodes 1 and 2 of the element and goes through the centroid of the cross-section.

- Y-axis is defined towards bridge west direction. In the tower cross-beam, it points towards bridge south.

- Z-axis is in general perpendicular to the global X-Y plane, except for the vertical elements where it can be defined as the cross-product between the local X- and Y-axes.

3.1.6 Definition of load effects

3.1.6.1 Bridge girder, tower and stay cables

Motions (displacement, accelerations etc.) refer to the global coordinate system.

The following load effects refer to the local element coordinate system:

- Axial force (X-axis)

- Shear forces (Y- and Z-axis, only beam elements)

- Bending moments about weak and strong axis (Y- and Z-axis, only beam elements)

- Torque (about X-axis, only beam elements)

3.1.6.2 Pontoons

The pontoon instantaneous position (X, Y and Z coordinate) refers to the global coordinate system. The pontoon motions e.g. roll and pitch, forces and moments refer to the pontoon coordinate system.

3.1.7 Units

Applied units in this report are unless otherwise noted:

- Length is given in meters (m)

- Time is given in seconds (s)

- Mass is given in 10^3 kg (ton)

- Force is given in 10^6 N (MN)

- Stress is given in 10^6 Pa (MPa)

3.2 Model description

3.2.1 General arrangement

The general arrangement of the bridge is modelled per drawings listed in Appendix A.

The bridge consists of

a) cable-stayed part called the "high bridge" arching the navigation channel in the South end

b) "floating bridge" supported by pontoons

The limits for the global model are axis 1 (South abutment) and axis 41 (abutment North).

The 400 m back-span of the "high bridge" starts at axis 1 and ends at the tower at axis 2. The 380m "main-span" starts at axis 2, arches the navigation channel and ends at axis 3. There are 18 pairs of tendons in each span of the "high bridge".

The "floating bridge" between axis 3 and axis 41 is supported by 38 floating pontoons separated by 125 metres. The "floating bridge" is moored at three pontoons located in axes 13, 20 and 27. The mooring system consists of two lines at each side of the pontoons.

3.2.2 Boundary conditions

Table 3-1 summarizes the boundary conditions applied to the global analysis model. All boundary conditions are applied in the RIFLEX local element coordinate system, defined in Section 3.1.5.

Table 3-1   Model boundary conditions

Location	X motion	Y motion	Z motion	X rotation	Y rotation	Z rotation
Axis 1	Fixed	Fixed	Fixed	Fixed	Fixed	Fixed
Axis 41	Fixed	Fixed	Fixed	Fixed	Fixed	Fixed
Bottom of East tower leg	Fixed	Fixed	Fixed	Fixed	Fixed	Fixed
Bottom of West tower leg	Fixed	Fixed	Fixed	Fixed	Fixed	Fixed
All anchors	Fixed	Fixed	Fixed	Fixed*	Fixed*	Fixed*
Bridge girder at axis 2	Free	Fixed	Fixed	Fixed	Free	Free
Bottom of column at axis 1B	Fixed	Fixed	Fixed	Fixed	Fixed	Fixed
Bottom of column at axis 1C	Fixed	Fixed	Fixed	Fixed	Fixed	Fixed
Bottom of column at axis 1D	Fixed	Fixed	Fixed	Fixed	Fixed	Fixed
Bottom of column at axis 1E	Fixed	Fixed	Fixed	Fixed	Fixed	Fixed

* Since the anchor lines are modelled as bar elements, these boundary conditions have no effect.

Figure 3-4 to Figure 3-7 show different views of the independent global response analysis model.

The bridge geometry is described in more detail with coordinates in Appendix B.
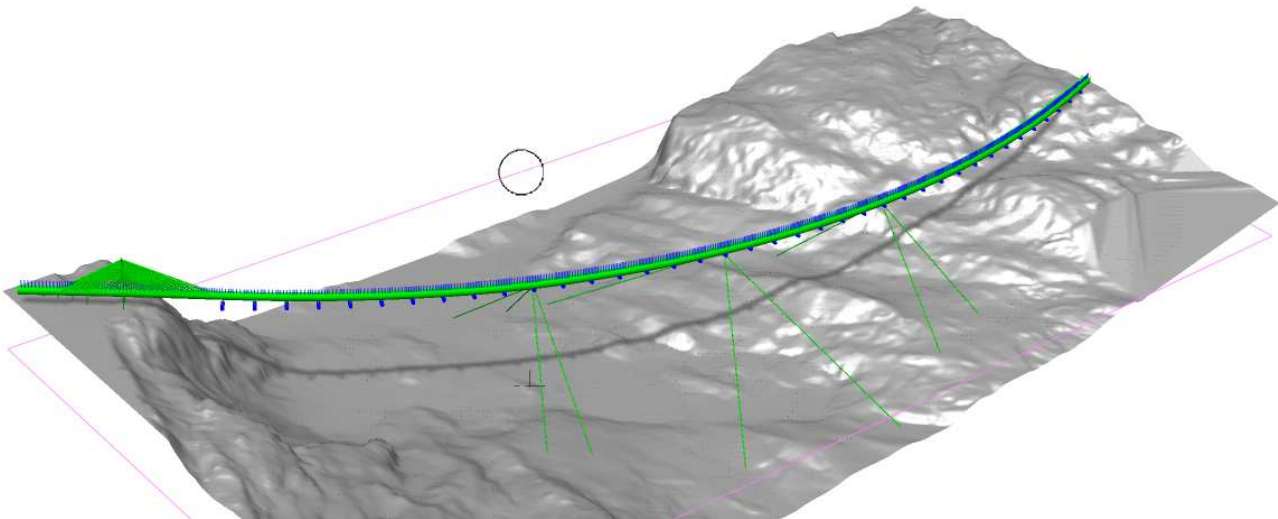
Figure 3-4   Bridge model in SIMA including Bjørnafjord seabed Surface.
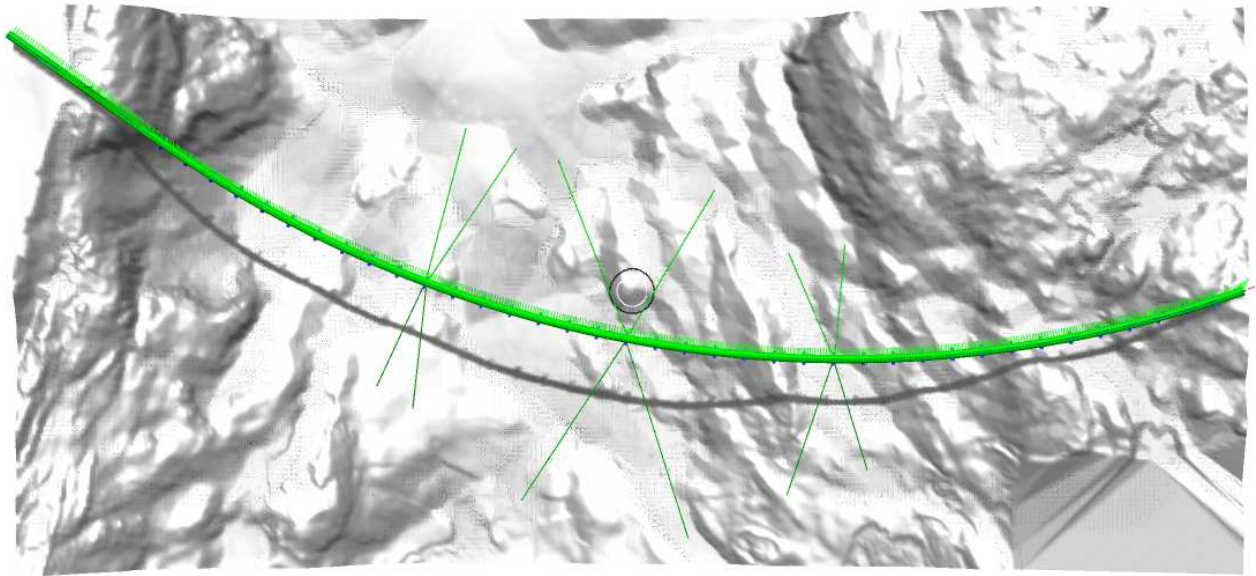
Figure 3-5 Bridge model seen from above, South end is on the left hand side.
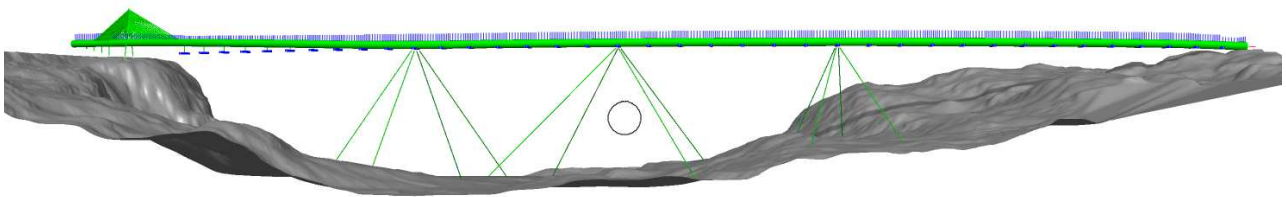
Figure 3-6 Bridge model as seen from East. Note that Bjørnafjord elevation above mean sea level is not represented. The bottom of the columns in axes 1B, 1C, 1D and 1E and the bottom of the high bridge tower are fixed.
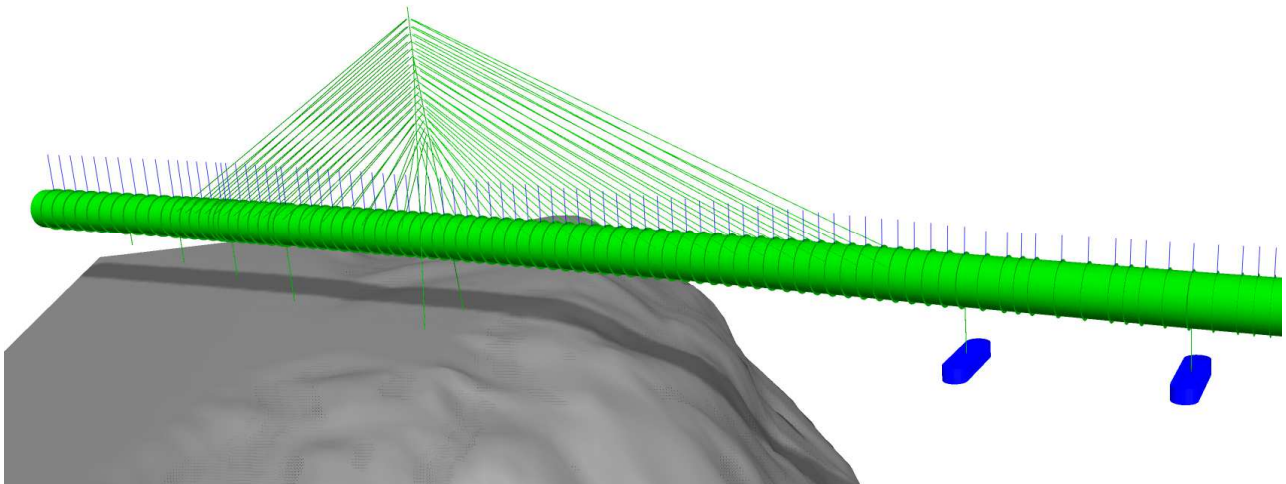
Figure 3-7 View of the "high bridge".

3.2.3 Materials

The mechanical properties of the structural members in the finite element model are defined based on the material properties listed in Table 3-2:

Table 3-2   Material properties

Material	E [MPa]	G [MPa]	ρ[kN/m3]
Structural Steel	210000	80770	77
Concrete	29760	12400	26
Stay cables	195000	-	77·1.2=92.4

3.2.4 Bridge girder properties

3.2.4.1 General

The bridge girder consists in four traffic lanes each 3.5 metres wide and a 3 metres foot path and bicycle trail. In addition, 1.5 metres shoulder is kept on both sides of the girder. Figure 3-8 shows the distribution of the different lanes on the bridge girder, with the foot path and bicycle trail lane on the right of the figure.
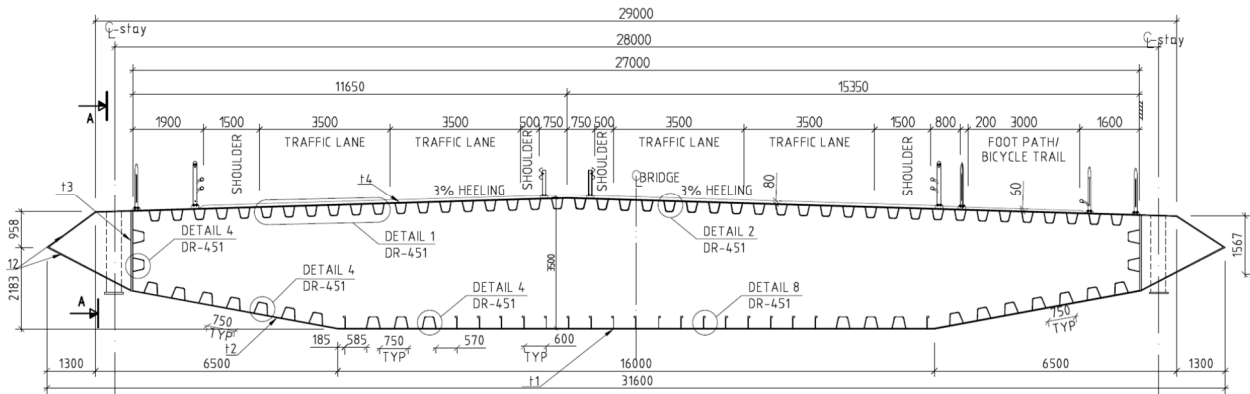
Figure 3-8   Bridge girder cross-section /2/.

3.2.4.2 Mass and stiffness properties

The bridge girder is modelled as a single beam. Figure 3-9 shows how the cross-sections are distributed in the bridge /3/, as:

- C1: Concrete box girder, connected between abutment south and column 1E. Properties are received from designer /3/ and summarised in Table 3-3;

- H1&H2: Steel box girder, connected between column 1E and cable T218. Properties are calculated based on drawing and information described in SBJ-32-C5-AMC-22-DR-103 /1/, see Table 3-3.

S1_H&S1: Typical cross sections above column. S1_H is from Axis 3 to 8, and S1 is from Axis 9-40. Properties are calculated based on drawing and information described in SBJ-32-C5-AMC-22-DR-404 for S1_H and SBJ-32-C5-AMC-22-DR-434 for S1 /1/, see Table 3-4   Mechanical section properties from Axes 3 to 40.Table 3-4.

- T1_H&T1: Typical cross section at transition. T1_H is from Axis 3 to 8, and T1 is from Axis 9-40. Properties are calculated based on drawing and information described in SBJ-32-C5-AMC-22-DR-403 for T1_H and SBJ-32-C5-AMC-22-DR-433 for T1 /1/, see Table 3-4.

- F1_H&F1: Typical cross section at midspan. F1_H is from Axis 3 to 8, and F1 is from Axis 9-40. Properties are calculated based on drawing and information described in SBJ-32-C5-AMC-22-DR-402 for F1_H and SBJ-32-C5-AMC-22-DR-432 for F1 /1/, see Table 3-4.
- B1, B2, B3, B4 and B5: End of bridge girder at abutment north. Properties are calculated based on drawing and information described in SBJ-32-C5-AMC-22-DR-462 /1/, see Table 3-5.

The bridge girder section properties have been derived from the Nauticus Hull software 'Cross Sections' or Autodesk Inventor and by hand calculations. Examples of modelled cross sections are shown in Figure 3-10 and Figure 3-11.
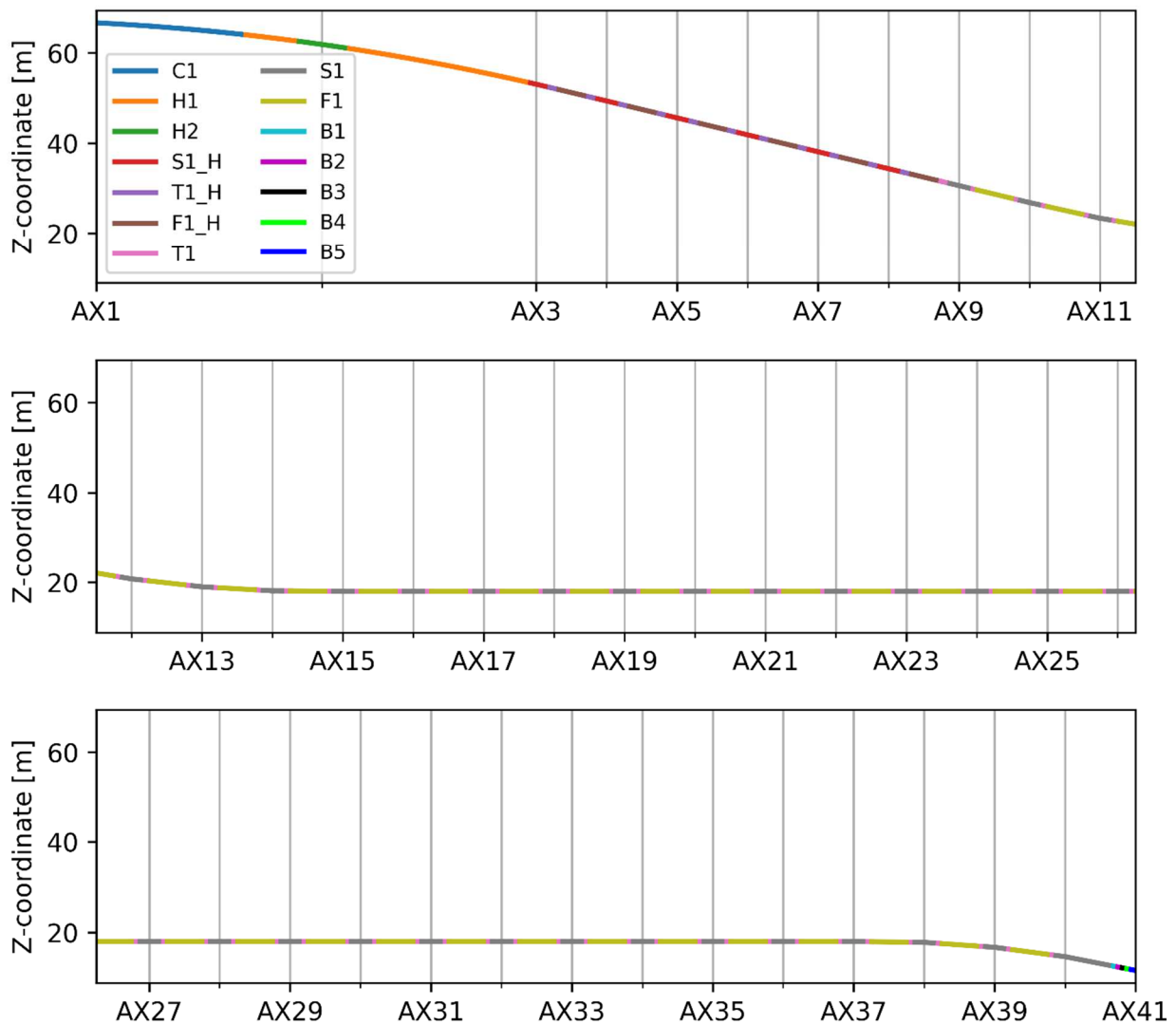
Figure 3-9   Distribution of girder cross-sections along the bridge.

Table 3-3 Mechanical section properties of C1, H1 and H2.

Magnitude	Unit	C1	H1	H2
Weight	ton/m	79.1	19	19
Area	m^2	27.951	1.309	1.651
Torsional inertia	m^4	135.400	6.274	9.103
Inertia around weak axis	m^4	40.5	2.575	3.413
Inertia around strong axis	m^4	2138	88.57	111.4
Axial stiffness, EA	kN	8.32E+08	2.75E+08	3.47E+08
Weak axis bending stiffness, EI_Y	kNm^2	1.21E+09	5.41E+08	7.17E+08
Strong axis bending stiffness, EI_Z	kNm^2	6.36E+10	1.86E+10	2.34E+10
Torsion stiffness, GI_X	kNm^2	1.68E+09	5.07E+08	7.35E+08
Gyration radius	m	8.828	8.639	8.618

Table 3-4 Mechanical section properties from Axes 3 to 40.

Magnitude	Unit	S1_H	S1	T1_H	T1	F1_H	F1
Weight	ton/m	19	19	19	19	19	19
Area	m^2	1.931	1.792	1.553	1.553	1.403	1.340
Torsional inertia	m^4	11.246	10.532	9.555	9.555	8.962	8.182
Inertia around weak axis*	m^4	4.793	4.462	4.039	4.039	3.632	3.408
Inertia around strong axis	m^4	125.7	112.7	103.2	103.2	93.14	88.29
Axial stiffness, EA	kN	4.06E+08	3.76E+08	3.26E+08	3.26E+08	2.95E+08	2.81E+08
Weak axis bending stiffness, EI_Y	kNm^2	1.01E+09	9.37E+08	8.48E+08	8.48E+08	7.63E+08	7.16E+08
Strong axis bending stiffness, EI_Z	kNm^2	2.64E+10	2.37E+10	2.17E+10	2.17E+10	1.96E+10	1.85E+10
Torsion stiffness, GI_X	kNm^2	9.08E+08	8.51E+08	7.72E+08	7.72E+08	7.24E+08	6.61E+08
Gyration radius	m	8.201	8.201	8.268	8.268	8.335	8.335

*) The moment of inertia was reduced by 5% due to shear lag effects, as described in section 3.2.4.3

Table 3-5 Mechanical properties of bridge end sections.

Magnitude	Unit	B1	B2	B3	B4	B5
Weight	ton/m	19	20.52	25.16	29	30.12
Area	m^2	1.972	2.187	2.403	2.618	2.833
Torsional inertia	m^4	15.368	15.344	15.319	15.295	15.270
Inertia around weak axis	m^4	5.445	5.860	6.276	6.691	7.106
Inertia around strong axis	m^4	140.600	190.525	240.450	290.375	340.300
Axial stiffness, EA	kN	4.14E+08	4.59E+08	5.05E+08	5.5E+08	5.95E+08
Weak axis bending stiffness, EI_Y	kNm^2	1.14E+09	1.23E+09	1.32E+09	1.41E+09	1.49E+09
Strong axis bending stiffness, EI_Z	kNm^2	2.95E+10	4E+10	5.05E+10	6.1E+10	7.15E+10
Torsion stiffness, GI_X	kNm^2	1.24E+09	1.24E+09	1.24E+09	1.24E+09	1.23E+09
Gyration radius	m	9.159	10.086	10.606	11.383	11.635
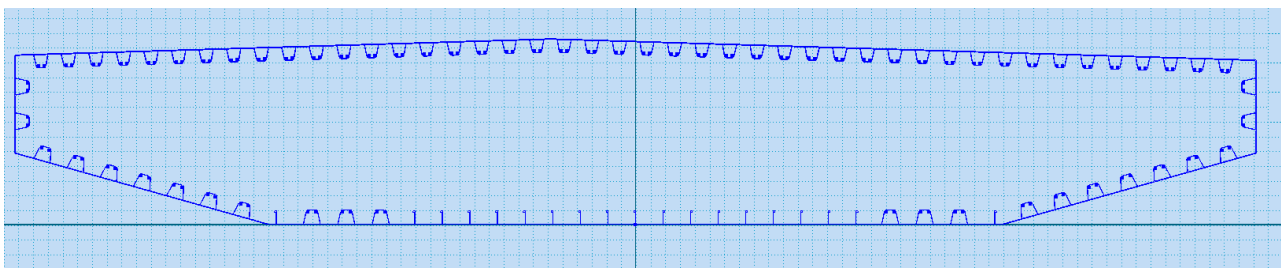
Figure 3-10 Midspan low bridge – modelled in Autodesk Inventor

Scale: 11200.   -8.0   -4.0   4.0   8.0   12.0
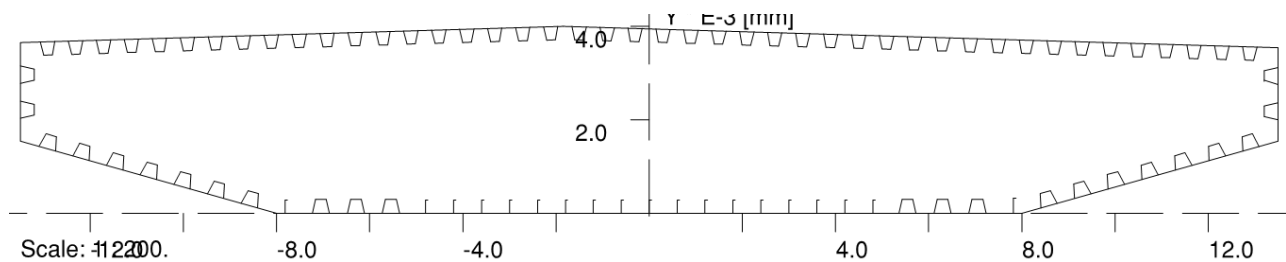
Figure 3-11 Midspan low bridge – modelled in Nauticus Hull

3.2.4.3 Girder stiffness modification due to shear lag effects

A study was performed to check whether inertias around weak axis were affected by shear lag effect/ normal stress distribution in the girder cross sections. An initial assumption was that the moment of inertia was reduced by 5%. This stiffness reduction was used in the global analyses for the high bridge and low bridge parts.

The study did however show that the effect was negligible for the investigated load cases. This was based on the comparison of a local beam model and a local shell model, as seen in Figure 3-12 and Figure 3-13 respectively. The assumption of 5% shear lag effect was made before the results from the local analyses were available, and is within normal uncertainty for a model, giving a small change in thee natural periods for the weak axis bending modes.
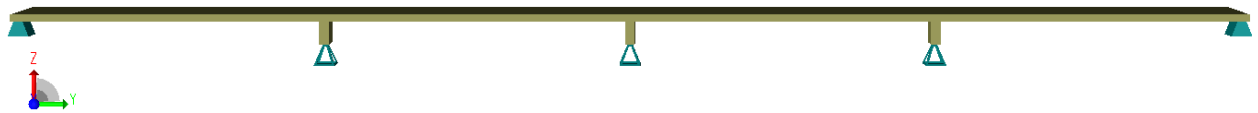
Figure 3-12   Local beam model of low bridge
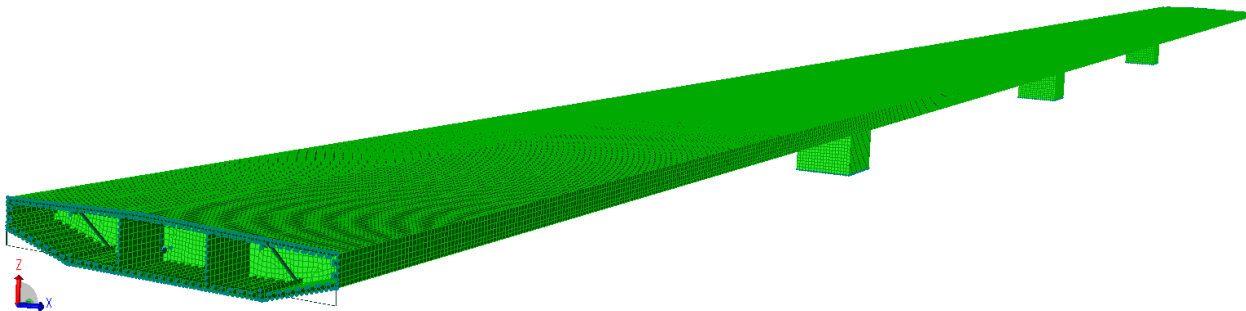
Figure 3-13   Local shell model of low bridge

The models represent the same segment of the low bridge which was modelled straight in the bridge longitudinal direction. Four bridge spans were modelled with symmetry conditions at each end. By controlling the vertical displacement of the three modelled columns sought deformation patterns were achieved. Two cases were investigated; a single and a double sine pattern. These are shown in Figure 3-14 and in Figure 3-15. By comparing reaction forces in the beam model with the shell model for the same load cases the stiffness difference was found. As can be seen in Table 3-6 and Table 3-7 the effect was found to be negligible. Support point numbering is shown in Figure 3-16. The effect of shear lag on fatigue is presented in Section 7.3.
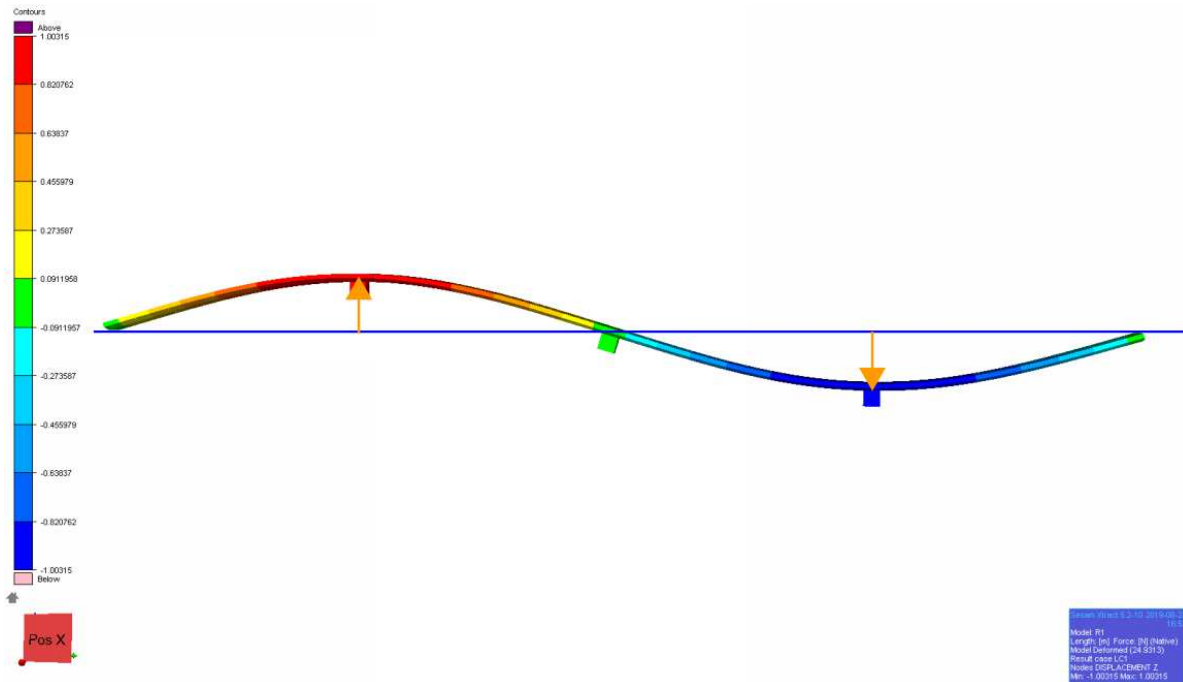
Figure 3-14   Vertical deformation of shell model – case 1
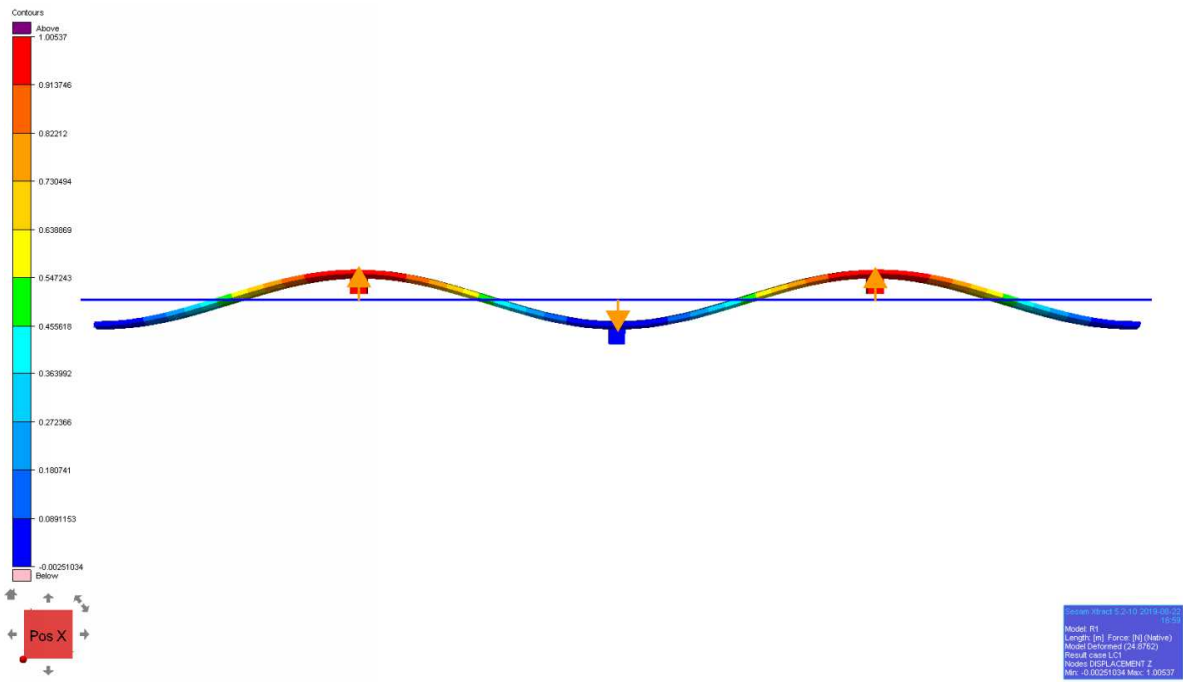
Figure 3-15   Vertical deformation of shell model – case 2
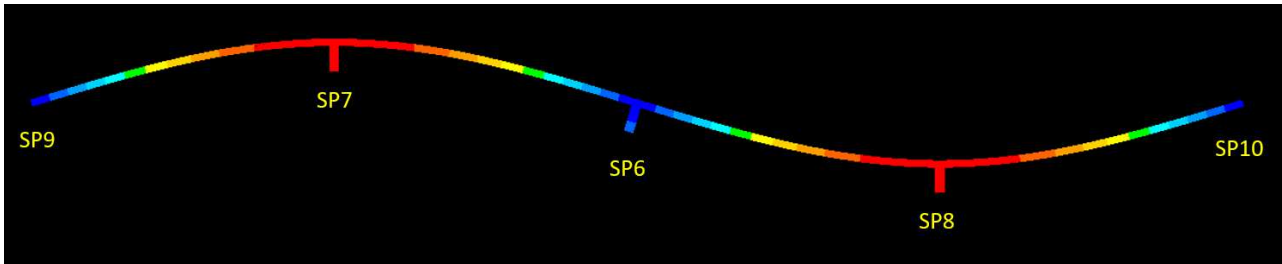
Figure 3-16 Support point numbering

Table 3-6 Comparison of beam and shell model reaction forces - case 1

Support	F_z [MN] – beam model	F_z [MN] – shell model	Stiffness comparison
Sp6	0.00	0.00	-
Sp7	2.55	2.56	100%
Sp8	-2.55	-2.56	100%
Sp9	-1.27	-1.28	100%
Sp10	1.27	1.28	100%

Table 3-7 Comparison of beam and shell model reaction forces - case 2

Support	F_z [MN] – beam model	F_z [MN] – shell model	Stiffness comparison
Sp6	-9.85	-9.78	99%
Sp7	9.85	9.76	99%
Sp8	9.85	9.76	99%
Sp9	-4.93	-4.87	99%
Sp10	-4.93	-4.87	99%

3.2.4.4 Aerodynamic properties

The aerodynamic properties are based on information provided in /4/. The wind load coefficients for the bridge girder in the high bridge and the low bridge are different due to the boundary effect of the sea surface. The coefficients without and with passing traffic are used for ultimate limit state and fatigue conditions, respectively.

The lift (CL), drag (CD) and moment (CM) coefficients are obtained by interpolation in Table 3-8 and Table 3-9 based on angle of attack (α). The same set of load coefficients is applied regardless of the Reynolds number (Re). The coefficients for other angles than 0 and 180 degrees have been established based on the derivatives of the coefficients up to rotations of 10 degrees. The forces and moment per unit length are defined per equation (1).

$$F_L = \frac{1}{2} C_L \rho_{air} \cdot c \cdot \left(V_{r,x}^2 + V_{r,y}^2 \right)$$
$$F_D = \frac{1}{2} C_D \rho_{air} \cdot c \cdot \left(V_{r,x}^2 + V_{r,y}^2 \right) \qquad (1)$$
$$M = \frac{1}{2} C_M \rho_{air} \cdot c^2 \cdot \left(V_{r,x}^2 + V_{r,y}^2 \right)$$

The lift, drag and moment are normalized on the foil chord length c. Bridge girder width is used as chord length for normalization.

Table 3-8 Aerodynamic properties of bridge girder in ULS/ALS conditions

Angle of attack (deg)	"High bridge"			"Floating bridge"		
	C_D [-]*	C_L [-]	C_M [-]	C_D [-]*	C_L [-]	C_M [-]
-180	0.076	0.378	0.019	0.092	0.378	0.019
-178.5	0.078	0.456	-0.007	0.094	0.456	-0.007
-177	0.084	0.579	-0.033	0.101	0.579	-0.033
-175	0.099	0.731	-0.069	0.119	0.731	-0.069
-172	0.142	0.941	-0.110	0.170	0.941	-0.110
-90	0.258	0.000	0.000	0.258	0.000	0.000
-8	0.142	-0.941	0.110	0.170	-0.941	0.110
-5	0.099	-0.731	0.069	0.119	-0.731	0.069
-3	0.084	-0.579	0.033	0.101	-0.579	0.033
-1.5	0.078	-0.456	0.007	0.094	-0.456	0.007
0	0.076	-0.378	-0.019	0.092	-0.378	-0.019
1.5	0.075	-0.286	-0.045	0.090	-0.286	-0.045
3	0.077	-0.186	-0.067	0.093	-0.186	-0.067
5	0.086	-0.073	-0.096	0.103	-0.073	-0.096
8	0.102	0.052	-0.125	0.122	0.052	-0.125
90	0.258	0.000	0.000	0.258	0.000	0.000
172	0.102	-0.052	0.125	0.122	-0.052	0.125
175	0.086	0.073	0.096	0.103	0.073	0.096
177	0.077	0.186	0.067	0.093	0.186	0.067
178.5	0.075	0.286	0.045	0.090	0.286	0.045
180	0.076	0.378	0.019	0.092	0.378	0.019

*   The drag coefficients defined in /4/ are normalized on the girder height not the breadth. Therefore, they have been scaled in this table.

Table 3-9 Aerodynamic properties of bridge girder in FLS conditions

Angle of attack (deg)	"High bridge"			"Floating bridge"		
	C_D [-]*	C_L [-]	C_M [-]	C_D [-]*	C_L [-]	C_M [-]
-180	0.130	0.378	0.019	0.156	0.378	0.019
-178.5	0.133	0.456	-0.007	0.160	0.456	-0.007
-177	0.143	0.579	-0.033	0.172	0.579	-0.033
-175	0.168	0.731	-0.069	0.202	0.731	-0.069
-172	0.241	0.941	-0.110	0.289	0.941	-0.110
-90	0.258	0.000	0.000	0.258	0.000	0.000
-8	0.241	-0.941	0.110	0.289	-0.941	0.110
-5	0.168	-0.731	0.069	0.202	-0.731	0.069
-3	0.143	-0.579	0.033	0.172	-0.579	0.033
-1.5	0.133	-0.456	0.007	0.160	-0.456	0.007
0	0.130	-0.378	-0.019	0.156	-0.378	-0.019
1.5	0.128	-0.286	-0.045	0.154	-0.286	-0.045
3	0.131	-0.186	-0.067	0.157	-0.186	-0.067
5	0.146	-0.073	-0.096	0.175	-0.073	-0.096
8	0.173	0.052	-0.125	0.208	0.052	-0.125
90	0.258	0.000	0.000	0.258	0.000	0.000
172	0.173	-0.052	0.125	0.208	-0.052	0.125
175	0.146	0.073	0.096	0.175	0.073	0.096
177	0.131	0.186	0.067	0.157	0.186	0.067
178.5	0.128	0.286	0.045	0.154	0.286	0.045
180	0.130	0.378	0.019	0.156	0.378	0.019

*   The drag coefficients defined in /4/ are normalized on the girder height not the breadth. Therefore, they have been scaled in this table.

3.2.5 Stay cable properties

3.2.5.1 General

The "high bridge" is supported by 18 pairs of stay cables at each side of the tower.

3.2.5.2 Mass and stiffness properties

The mechanical properties of the stay cables are presented in Table 3-10. The cable identification numbers are explained in Figure 3-17. The adjacent cables on East and West side of bridge girder form a cable pair. The cross-sectional properties are identical for both cables in a pair.

The cables are modelled bar elements without any bending stiffness.

Detail input for stay cable fatigue assessment is presented in Table 3-11.

The coordinates of the cable connection points are described in detail in Appendix B.
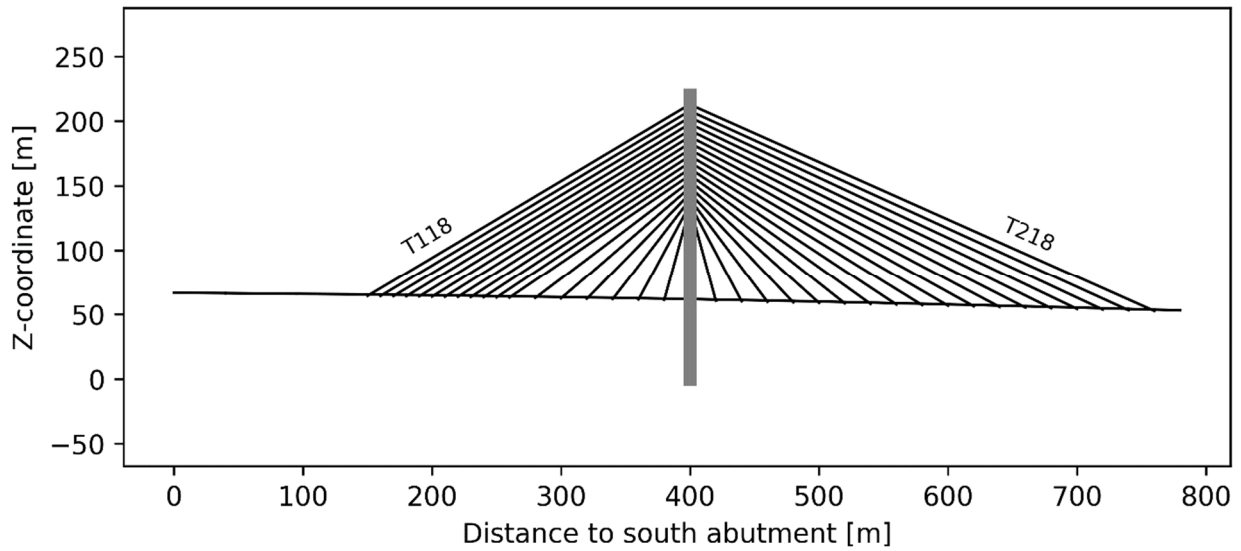
Figure 3-17 Stay cable identification numbering. Tendon pairs numbered 1xx are attached to the high bridge south and 2xx are in the northern side.

Table 3-10 Cross-sectional properties of stay cables in "high bridge". Tendons 1xx are the back span cable pairs, and 2xx are the front span cable pairs /3/.

Cable pair number	Mass [ton/m]	Axial stiffness [kN]	Streched length [m]	Unstreched length [m]	Cross section area [mm^2]
T118	0.0234	2.02E+06	288.917	288.137	34636
T117	0.0225	2.02E+06	277.813	277.066	34636
T116	0.0216	2.02E+06	266.713	265.979	34636
T115	0.0201	1.96E+06	255.618	254.917	34636
T114	0.0181	1.84E+06	244.531	243.863	34636
T113	0.0164	1.76E+06	233.459	232.827	28353
T112	0.0157	1.76E+06	222.392	221.792	28353
T111	0.0141	1.67E+06	211.336	210.766	28353
T110	0.0127	1.58E+06	200.288	199.752	25447
T109	0.0113	1.49E+06	189.250	188.740	25447
T108	0.0100	1.40E+06	178.226	177.751	25447
T107	0.0092	1.37E+06	167.216	166.768	25447
T106	0.0071	1.20E+06	148.226	147.882	17671
T105	0.0058	1.11E+06	129.720	129.402	17671
T104	0.0045	9.95E+05	111.936	111.646	17671
T103	0.0034	8.78E+05	95.278	95.028	15394
T102	0.0026	8.19E+05	80.448	80.254	15394
T101	0.0021	7.61E+05	68.636	68.461	15394
T201	0.0021	7.61E+05	69.307	69.127	15394
T202	0.0027	8.19E+05	81.675	81.460	15394
T203	0.0034	8.78E+05	96.943	96.697	15394
T204	0.0045	9.95E+05	113.950	113.648	17671
T205	0.0059	1.11E+06	132.029	131.680	21382
T206	0.0073	1.20E+06	150.795	150.394	21382
T207	0.0094	1.37E+06	170.023	169.595	25447
T208	0.0107	1.40E+06	189.573	189.090	25447
T209	0.0125	1.49E+06	209.355	208.822	25447
T210	0.0145	1.58E+06	229.311	228.709	25447
T211	0.0167	1.67E+06	249.399	248.746	25447
T212	0.0190	1.76E+06	269.590	268.886	28353
T213	0.0204	1.76E+06	289.864	289.083	28353
T214	0.0230	1.84E+06	310.206	309.383	28353
T215	0.0260	1.96E+06	330.610	329.723	34636
T216	0.0284	2.02E+06	351.059	350.110	34636
T217	0.0301	2.02E+06	371.547	370.531	34636
T218	0.0318	2.02E+06	392.051	390.968	34636

Table 3-11 Stay cable details to be assessed for fatigue /16/.

Magnitude	Unit	Stay cable
Cross-sectional area	mm^2	See Table 3-10
SCF	-	1.0
$loga_1$ (fatigue parameter)	-	15.0054
m_1 (fatigue parameter)	-	4.0
m_2 (fatigue parameter)	-	6.0
Fatigue position	-	Cable end points
Hotspot	-	Nominal stress from cable tension
DFF	-	2.5

3.2.5.3 Aerodynamic properties

Wind loads on the stay cables are modelled as Morison-like drag loads defined as per (2). ρ_{air} is the density of air, D is the diameter and v is the wind velocity. A drag coefficient, C_D, of 0.8 is applied to all the tendons.

$$\vec{F_D} = \frac{1}{2} C_D \rho_{air} \cdot D \cdot |\vec{v}| \cdot \vec{v} \qquad (2)$$

3.2.6 Tower properties

3.2.6.1 General

The "high bridge" tower is divided in three different elements:

- The two legs, defined from the tower foundation to the tower crown.

- The tower top, modelled from the crown to the very top of the tower.

3.2.6.2 Mass and stiffness properties

The tower legs are discretized in 24 sections. Applied mechanical properties for the different cross-sections are presented in Table 3-12 to Table 3-17.

Table 3-12   Tower leg cross-sectional properties. Numbered from tower bottom.

Magnitude	Unit	Section 1	Section 2	Section 3	Section 4
Weight	ton/m	115.36	135.22	76.46	79.39
Area	m^2	43.52	51.02	28.85	29.95
Torsional inertia	m^4	202.38	311.38	266.10	315.21
Inertia around weak axis	m^4	359.34	406.94	290.19	301.93
Inertia around strong axis	m^4	43.52	51.02	28.85	29.95
Axial stiffness, EA	kN	1.30E+09	1.52E+09	8.60E+08	8.93E+08
Weak axis bending stiffness, EI_Y	kNm^2	1.07E+10	1.21E+10	8.65E+09	9.00E+09
Strong axis bending stiffness, EI_Z	kNm^2	1.30E+09	1.52E+09	8.60E+08	8.93E+08
Torsion stiffness, GI_X	kNm^2	2.51E+09	3.87E+09	3.30E+09	3.91E+09
Gyration radius	m	3.15	3.21	3.81	4.03

Table 3-13   Tower leg cross-sectional properties. Numbered from tower bottom.

Magnitude	Unit	Section 5	Section 6	Section 7	Section 8
Weight	ton/m	82.37	85.41	88.51	91.66
Area	m^2	31.08	32.23	33.40	34.58
Torsional inertia	m^4	370.83	433.50	503.80	582.32
Inertia around weak axis	m^4	308.42	310.24	307.97	302.14
Inertia around strong axis	m^4	31.08	32.23	33.40	34.58
Axial stiffness, EA	kN	9.26E+08	9.60E+08	9.95E+08	1.03E+09
Weak axis bending stiffness, EI_Y	kNm^2	9.19E+09	9.25E+09	9.18E+09	9.00E+09
Strong axis bending stiffness, EI_Z	kNm^2	9.26E+08	9.60E+08	9.95E+08	1.03E+09
Torsion stiffness, GI_X	kNm^2	4.60E+09	5.38E+09	6.26E+09	7.23E+09
Gyration radius	m	4.26	4.48	4.71	4.94

Table 3-14   Tower leg cross-sectional properties. Numbered from tower bottom.

Magnitude	Unit	Section 9	Section 10	Section 11	Section 12
Weight	ton/m	46.96	44.11	41.36	38.69
Area	m^2	17.72	16.64	15.60	14.60
Torsional inertia	m^4	115.62	107.93	100.64	93.73
Inertia around weak axis	m^4	147.68	131.97	117.39	103.90
Inertia around strong axis	m^4	17.72	16.64	15.60	14.60
Axial stiffness, EA	kN	5.28E+08	4.96E+08	4.65E+08	4.35E+08
Weak axis bending stiffness, EI_Y	kNm^2	4.40E+09	3.93E+09	3.50E+09	3.10E+09
Strong axis bending stiffness, EI_Z	kNm^2	5.28E+08	4.96E+08	4.65E+08	4.35E+08
Torsion stiffness, GI_X	kNm^2	1.44E+09	1.34E+09	1.25E+09	1.16E+09
Gyration radius	m	3.30	3.25	3.21	3.16

Table 3-15   Tower leg cross-sectional properties. Numbered from tower bottom.

Magnitude	Unit	Section 13	Section 14	Section 15	Section 16
Weight	ton/m	36.97	36.15	35.33	34.52
Area	m^2	13.95	13.64	13.33	13.03
Torsional inertia	m^4	89.25	86.98	84.75	82.56
Inertia around weak axis	m^4	95.05	90.16	85.43	80.85
Inertia around strong axis	m^4	13.95	13.64	13.33	13.03
Axial stiffness, EA	kN	4.16E+08	4.06E+08	3.97E+08	3.88E+08
Weak axis bending stiffness, EI_Y	kNm^2	2.83E+09	2.69E+09	2.55E+09	2.41E+09
Strong axis bending stiffness, EI_Z	kNm^2	4.16E+08	4.06E+08	3.97E+08	3.88E+08
Torsion stiffness, GI_X	kNm^2	1.11E+09	1.08E+09	1.05E+09	1.03E+09
Gyration radius	m	3.12	3.09	3.07	3.04

Table 3-16 Tower leg cross-sectional properties. Numbered from tower bottom.

Magnitude	Unit	Section 17	Section 18	Section 19	Section 20
Weight	ton/m	33.73	32.94	32.16	31.39
Area	m^2	12.73	12.43	12.13	11.84
Torsional inertia	m^4	80.42	78.32	76.26	74.24
Inertia around weak axis	m^4	76.43	72.16	68.04	64.07
Inertia around strong axis	m^4	12.73	12.43	12.13	11.84
Axial stiffness, EA	kN	3.79E+08	3.70E+08	3.62E+08	3.53E+08
Weak axis bending stiffness, EI_Y	kNm^2	2.28E+09	2.15E+09	2.03E+09	1.91E+09
Strong axis bending stiffness, EI_Z	kNm^2	3.79E+08	3.70E+08	3.62E+08	3.53E+08
Torsion stiffness, GI_X	kNm^2	9.99E+08	9.72E+08	9.47E+08	9.22E+08
Gyration radius	m	3.02	2.99	2.96	2.94

Table 3-17 Tower leg cross-sectional properties. Numbered from tower bottom.

Magnitude	Unit	Section 21	Section 22	Section 23	Section 24
Weight	ton/m	30.63	29.88	29.14	28.40
Area	m^2	11.56	11.27	10.99	10.72
Torsional inertia	m^4	72.26	70.32	68.42	66.56
Inertia around weak axis	m^4	60.25	56.58	53.05	49.66
Inertia around strong axis	m^4	11.56	11.27	10.99	10.72
Axial stiffness, EA	kN	3.44E+08	3.36E+08	3.28E+08	3.19E+08
Weak axis bending stiffness, EI_Y	kNm^2	1.80E+09	1.69E+09	1.58E+09	1.48E+09
Strong axis bending stiffness, EI_Z	kNm^2	3.44E+08	3.36E+08	3.28E+08	3.19E+08
Torsion stiffness, GI_X	kNm^2	8.97E+08	8.73E+08	8.50E+08	8.26E+08
Gyration radius	m	2.91	2.88	2.86	2.83

Table 3-18 and Table 3-19 presents the mechanical properties of the tower top sections.

Table 3-18 Tower leg cross-sectional properties. Numbered from tower crown.

Magnitude	Unit	Section 1	Section 2	Section 3	Section 4
Weight	ton/m	41.84	37.63	33.65	29.89
Area	m^2	15.79	14.20	12.70	11.28
Torsional inertia	m^4	170.43	129.31	96.12	69.77
Inertia around weak axis	m^4	81.72	69.59	58.45	48.25
Inertia around strong axis	m^4	15.79	14.20	12.70	11.28
Axial stiffness, EA	kN	4.70E+08	4.23E+08	3.78E+08	3.36E+08
Weak axis bending stiffness, EI_Y	kNm^2	2.44E+09	2.07E+09	1.74E+09	1.44E+09
Strong axis bending stiffness, EI_Z	kNm^2	4.70E+08	4.23E+08	3.78E+08	3.36E+08
Torsion stiffness, GI_X	kNm^2	2.12E+09	1.61E+09	1.19E+09	8.66E+08
Gyration radius	m	4.04	3.70	3.37	3.04

Table 3-19 Tower leg cross-sectional properties. Numbered from tower crown.

Magnitude	Unit	Section 5	Section 6	Section 7	Section 8
Weight	ton/m	26.36	23.04	21.00	20.07
Area	m^2	9.94	8.69	7.92	7.57
Torsional inertia	m^4	49.25	33.63	25.70	22.55
Inertia around weak axis	m^4	38.94	30.48	25.42	23.19
Inertia around strong axis	m^4	9.94	8.69	7.92	7.57
Axial stiffness, EA	kN	2.96E+08	2.59E+08	2.36E+08	2.26E+08
Weak axis bending stiffness, EI_Y	kNm^2	1.16E+09	9.08E+08	7.58E+08	6.91E+08
Strong axis bending stiffness, EI_Z	kNm^2	2.96E+08	2.59E+08	2.36E+08	2.26E+08
Torsion stiffness, GI_X	kNm^2	6.12E+08	4.18E+08	3.19E+08	2.80E+08
Gyration radius	m	2.71	2.39	2.18	2.09

3.2.6.3 Aerodynamic properties

The aerodynamic coefficients for the tower are defined as Morison drag loads based on the coefficients included in Table 3-20.

The aerodynamic coefficients are scaled to compensate for the wind profile as described in Section 3.3.5.

Table 3-20 Aerodynamic coefficients for the "high bridge" tower

Element	Drag coefficient	Lift coefficient	Length [m]	Breadth [m]
Tower leg – Section 1	1.52	2.50	4.10	9.94
Tower leg – Section 2	1.72	2.47	5.47	9.83
Tower leg – Section 3	1.95	2.38	6.84	9.69
Tower leg – Section 4	2.15	2.25	8.80	9.53
Tower leg – Section 5	2.28	2.11	10.76	9.37
Tower leg – Section 6	2.37	1.97	12.72	9.21
Tower leg – Section 7	2.43	1.83	14.67	9.05
Tower leg – Section 8	2.50	1.57	19.17	8.87
Tower leg – Section 9	1.64	2.49	4.41	8.54
Tower leg – Section 10	1.72	2.47	4.50	8.11
Tower leg – Section 11	1.79	2.44	4.58	7.71
Tower leg – Section 12	1.86	2.42	4.67	7.31
Tower leg – Section 13	1.90	2.40	4.72	7.06
Tower leg – Section 14	1.92	2.39	4.74	6.94
Tower leg – Section 15	1.94	2.38	4.77	6.83
Tower leg – Section 16	1.96	2.37	4.79	6.72
Tower leg – Section 17	1.98	2.36	4.81	6.60
Tower leg – Section 18	2.00	2.35	4.84	6.49
Tower leg – Section 19	2.01	2.34	4.86	6.38
Tower leg – Section 20	2.03	2.33	4.89	6.26
Tower leg – Section 21	2.05	2.32	4.91	6.15
Tower leg – Section 22	2.22	2.18	6.22	6.03
Tower leg – Section 23	2.18	2.22	5.70	5.92
Tower leg – Section 24	2.13	2.26	5.18	5.81
Tower top – Section 1	2.43	1.82	9.32	5.69
Tower top – Section 2	2.40	1.91	8.29	5.58
Tower top – Section 3	2.35	2.00	7.25	5.47
Tower top – Section 4	2.28	2.10	6.21	5.35
Tower top – Section 5	2.19	2.21	5.18	5.24
Tower top – Section 6	2.06	2.32	4.14	5.13
Tower top – Section 7	1.93	2.39	3.47	5.05
Tower top – Section 8	1.85	2.42	3.16	5.02

3.2.7 Column properties

3.2.7.1 General

The 38 columns in the bridge are all built in steel. The columns cross-sections with dimensions are presented in Figure 3-18 and Figure 3-19.
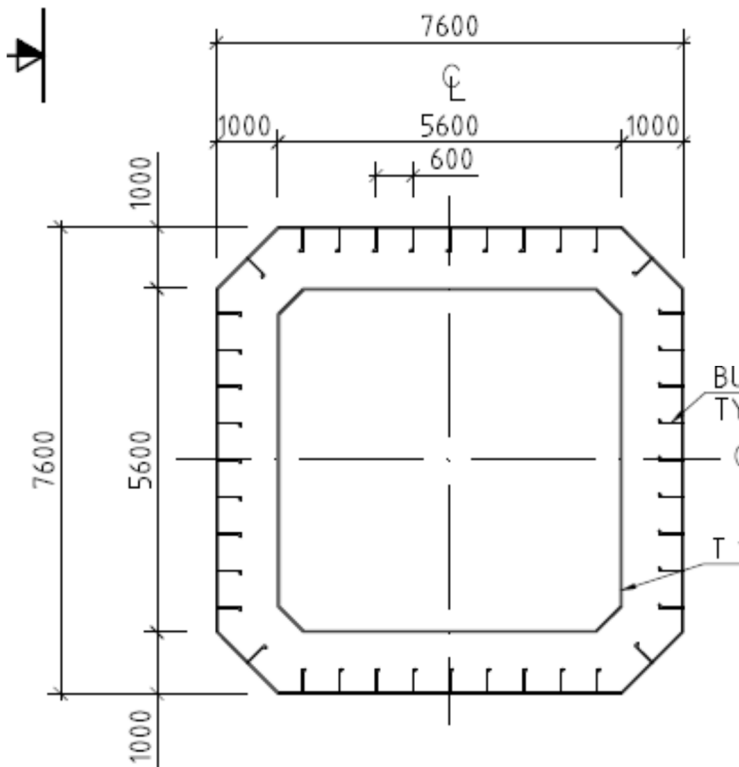
Figure 3-18 Columns cross-section, Axis 3-8. SBJ-33-C5-AMC-22-DR-471 /1/.
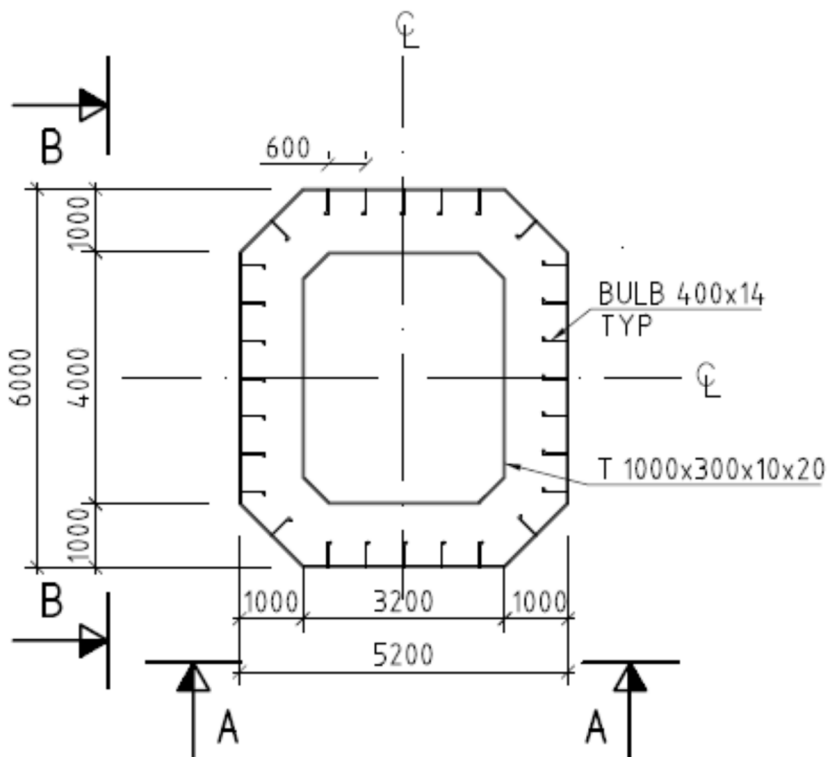
Figure 3-19 Columns cross-section, Axis 9-40. SBJ-33-C5-AMC-22-DR-481 /1/.

3.2.7.2 Mass and stiffness properties

The steel columns can be subdivided in 2 different types. Column mechanical properties are presented in Table 3-21.

Table 3-21   Column cross-sectional properties.

Magnitude	Unit	Axes 3-8	Axes 9-40
Weight	ton/m	8.98	6.42
Area	m^2	7.91	5.65
Torsional inertia	m^4	112.40	44.26
Inertia around weak axis	m^4	71.32	29.34
Inertia around strong axis	m^4	7.91	5.65
Axial stiffness, EA	kN	2.36E+08	1.68E+08
Weak axis bending stiffness, EI_Y	kNm^2	2.13E+09	8.74E+08
Strong axis bending stiffness, EI_Z	kNm^2	2.36E+08	1.68E+08
Torsion stiffness, GI_X	kNm^2	1.40E+09	5.50E+08
Gyration radius	m	4.25	3.07

3.2.7.3 Aerodynamic properties

Wind loads in the columns are modelled as Morison drag loads with a drag coefficient of 2.2 in the column's longitudinal and transversal directions.

As described in Section 3.3.5, the drag coefficients for each column are scaled down to compensate for the larger wind velocity for the length of the columns laying below the input wind field.

3.2.8 Pontoon properties

3.2.8.1 General

There are 38 pontoons in the floating section of the bridge. Based on their dimensions, 2 different types of pontoons can be defined. Table 3-22 contains the dimensions of all the different types of pontoons.

A 3D model of the pontoon is included in Figure 3-20.

Table 3-22   Pontoon dimensions

Type	Axes	Length [m]	Width [m]	Draft [m]	Freeboard [m]
Type1	General	53	14.9	5	3.5
Type2	13, 20 and 27	53	14.9	7.5	3.5
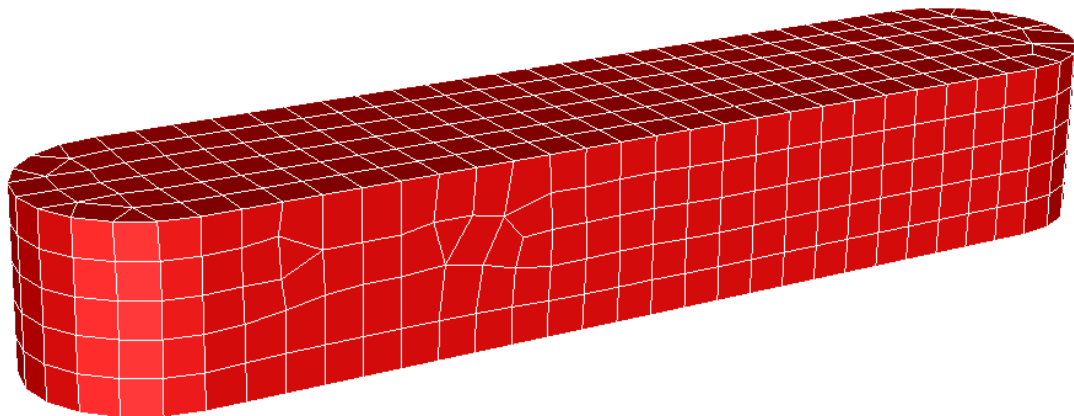
Figure 3-20   Pontoon panel model

3.2.8.2   Pontoon positions

The pontoons are positioned directly underneath the axes of the "floating bridge", i.e. axes 3-40. The positions and heading provided in Table 3-23 refer to the global model coordinate system, see Section 3.1.3. All the pontoons are initially located at the nominal draft on an even keel, i.e. with zero heel or list angles.

Table 3-23 Pontoon positions in the global model coordinate system

Axis	X (m)	Y (m)	Heading (deg)
3	-1944.27	817.24	55.0
4	-1840.96	746.88	56.5
5	-1735.92	679.12	57.9
6	-1629.22	614.01	59.3
7	-1520.93	551.59	60.8
8	-1411.11	491.89	62.2
9	-1299.83	434.96	63.6
10	-1187.16	380.82	65.1
11	-1073.18	329.52	66.5
12	-957.95	281.08	67.9
13	-841.54	235.54	69.4
14	-724.03	192.93	70.8
15	-605.50	153.26	72.2
16	-486.01	116.57	73.6
17	-365.64	82.88	75.1
18	-244.46	52.21	76.5
19	-122.56	24.58	77.9
20	0.00	0.00	79.4
21	123.13	-21.51	80.8
22	246.76	-39.93	82.2
23	370.82	-55.25	83.7
24	495.22	-67.47	85.1
25	619.88	-76.58	86.5
26	744.73	-82.56	88.0
27	869.70	-85.43	89.4
28	994.69	-85.17	90.8
29	1119.65	-81.78	92.3
30	1244.47	-75.27	93.7
31	1369.10	-65.65	95.1
32	1493.44	-52.91	96.6
33	1617.43	-37.07	98.0
34	1740.99	-18.13	99.4
35	1864.03	3.89	100.9
36	1986.48	28.98	102.3
37	2108.27	57.12	103.7
38	2229.32	88.30	105.2
39	2349.54	122.49	106.6
40	2468.88	159.68	108.0

3.2.8.3 Hydrostatic and mass data

Table 3-24 presents the main hydrostatic results for each of the pontoon types. Note that all the included properties are exclusively dependent on the outer geometry of the pontoons.

In a free-floating vessel, the metacentric height (GM) is the key parameter on initial stability. However, in these analyses, the weight and the buoyancy of the SIMO pontoon bodies are not balance. The weight of the column and the bridge girder is applied as a force acting at pontoon's deck.

For a floating body, the restoring moment for a certain heel angle θ can be calculated as:

$$Moment = (\nabla \cdot \rho \cdot g \cdot (KB + BM) - M \cdot g \cdot KG) \cdot \theta \qquad (3)$$

where ∇ is the displaced volume, ρ is water density, g is gravity acceleration and M is the mass of the structure plus its ballast. KB is the distance between the keel and the centre of buoyancy of the body and BM is the distance from the centre of buoyancy to the metacentre, i.e. the point where the buoyancy force vector intersects the centreline of the vessel. It should be noted that the location of the metacentre differs between roll and pitch.

Out of the three components of (3), the mass term is applied as follows:

- Pontoon and ballast mass is represented by a vertical force acting at pontoon's centre of gravity.

- The weight of the bridge girder and the column is a force applied at the pontoon's deck level.

- Mooring lines loads are applied at the fairleads.º

The KB term represents the buoyancy force, which is explicitly modelled as a vertical force acting at pontoon's centre of buoyancy.

The BM term is the only one included as roll and pitch stiffness of the pontoons, denoted as C44 and C55 in Table 3-25.

Table 3-24   Pontoons hydrostatic results

Type	Displacement [ton]	Water plane area [m2]	Center of buoyancy vertical position [m]	BMT [m]	BML [m]
Type1	3803.0	741.9	-2.50	3.48	41.86
Type2	5704.7	741.9	-3.75	2.32	27.91
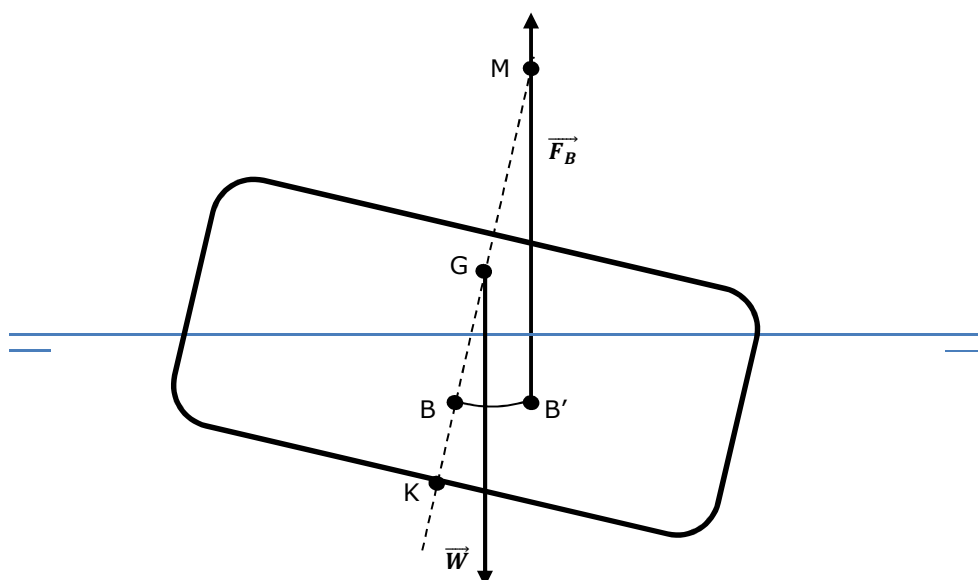
Figure 3-21   Initial stability of floating vessels. After heeling, the centre of buoyancy B moves to B' and the force pair produced by the weight ($\vec{W}$) and the buoyancy ($\vec{F_B}$) result in a restoring moment as long as the metacentre (M) is over the centre of gravity (G).

The resultant mass and hydrostatic model are given in Table 3-25.

Table 3-25   Pontoons hydrostatic and mass data

Axis	Mass [ton]	KG [m]	Ixx [t·m2]	Iyy [t·m2]	Izz [t·m2]	C44 [kN·m]	C55 [kN·m]	Buoyancy [ton]
3	2277	2.04	71097	396330	377582	1.30E+05	1.56E+06	3803.0
4	714	3.58	37138	265501	263224	1.30E+05	1.56E+06	3803.0
5	1185	3.54	40051	275484	271536	1.30E+05	1.56E+06	3803.0
6	1089	3.85	37035	264620	262268	1.30E+05	1.56E+06	3803.0
7	1161	3.61	39320	272840	269277	1.30E+05	1.56E+06	3803.0
8	1183	3.55	51338	410799	418116	1.30E+05	1.56E+06	3803.0
9	1280	3.29	43020	286311	280816	1.30E+05	1.56E+06	3803.0
10	1302	3.24	43696	288795	282951	1.30E+05	1.56E+06	3803.0
11	1326	3.18	44415	291446	285232	1.30E+05	1.56E+06	3803.0
12	1343	3.14	44931	293353	286875	1.30E+05	1.56E+06	3803.0
13	3256	2.86	167273	658909	595956	1.30E+05	1.56E+06	5704.7
14	1360	3.11	45461	295316	288567	1.30E+05	1.56E+06	3803.0
15	1361	3.11	45480	295384	288626	1.30E+05	1.56E+06	3803.0
16	1361	3.11	55557	415567	418765	1.30E+05	1.56E+06	3803.0
17	1361	3.11	45482	295392	288633	1.30E+05	1.56E+06	3803.0
18	1361	3.11	45483	295397	288637	1.30E+05	1.56E+06	3803.0
19	1361	3.11	45480	295387	288628	1.30E+05	1.56E+06	3803.0
20	3262	2.85	167608	659793	596605	1.30E+05	1.56E+06	5704.7
21	1361	3.11	45480	295387	288628	1.30E+05	1.56E+06	3803.0
22	1361	3.11	45483	295396	288636	1.30E+05	1.56E+06	3803.0
23	1361	3.11	45482	295393	288633	1.30E+05	1.56E+06	3803.0
24	1361	3.11	55555	415563	418762	1.30E+05	1.56E+06	3803.0
25	1361	3.11	45482	295395	288635	1.30E+05	1.56E+06	3803.0
26	1361	3.11	45480	295387	288629	1.30E+05	1.56E+06	3803.0
27	3262	2.85	167607	659790	596602	1.30E+05	1.56E+06	5704.7
28	1361	3.11	45480	295387	288628	1.30E+05	1.56E+06	3803.0
29	1361	3.11	45483	295396	288636	1.30E+05	1.56E+06	3803.0
30	1361	3.11	45482	295394	288634	1.30E+05	1.56E+06	3803.0
31	1361	3.11	45482	295395	288635	1.30E+05	1.56E+06	3803.0
32	1361	3.11	45483	295396	288636	1.30E+05	1.56E+06	3803.0
33	1361	3.11	45482	295393	288633	1.30E+05	1.56E+06	3803.0
34	1361	3.11	45484	295402	288641	1.30E+05	1.56E+06	3803.0
35	1360	3.11	45476	295372	288615	1.30E+05	1.56E+06	3803.0
36	1361	3.10	45502	295468	288698	1.30E+05	1.56E+06	3803.0
37	1358	3.11	45414	295141	288416	1.30E+05	1.56E+06	3803.0
38	1370	3.09	45754	296401	289503	1.30E+05	1.56E+06	3803.0
39	1342	3.15	44916	293297	286827	1.30E+05	1.56E+06	3803.0
40	1453	2.92	48250	305719	297559	1.30E+05	1.56E+06	3803.0

3.2.8.4   Hydrodynamic data

The wave excitation forces, 2nd order wave drift forces, added mass and potential damping are computed in frequency domain by WADAM. An example of the panel models is given in Figure 3-20.

The wave drift forces are influenced by the magnitude of the 1st order wave induced motions of the pontoons. Based on the experience of previous phases, drift forces are computed based on fully fixed pontoons. Only the horizontal drift forces are computed.

Added mass, potential damping, first order wave excitation forces and moments, second order wave drift forces and moments are documented in more detail in Appendix C.

3.2.8.5   Current load

Current load is computed based on the drag coefficient of a rectangle with round corners. The load on longitudinal and transversal directions is then calculated as follows:

$$F_{curr,x}(\alpha) = \frac{1}{2}\rho C_{D,x} TB \frac{2 \cdot cos\alpha}{1 + cos^2\alpha} v_{curr}^2 \tag{4}$$

$$F_{curr,y}(\alpha) = \frac{1}{2}\rho C_{D,y} TL \frac{2 \cdot sin\alpha}{1 + sin^2\alpha} v_{curr}^2 \tag{5}$$

where α is the relative current heading angle, ρ is seawater density, T is the draft, B is the breadth and L is the pontoon length.

Table 3-26   Pontoon's quadratic current drag coefficients

Type	Drag coefficient	
	Longitudinal direction, $C_{D,x}$	**Transversal direction, $C_{D,y}$**
Type1	0.36	1.62
Type2	0.36	1.62

3.2.8.6   Wind load

Wind loads are calculated in a similar manner as the current load, except using the projected area over the sea. The wind drag coefficients are also the same as the current coefficient.

$$F_{wind,x}(\alpha) = \frac{1}{2}\rho C_{D,x} f B \frac{2 \cdot cos\alpha}{1 + cos^2\alpha} v_{wind}^2 \qquad (6)$$

$$F_{wind,y}(\alpha) = \frac{1}{2}\rho C_{D,y} f L \frac{2 \cdot sin\alpha}{1 + sin^2\alpha} v_{wind}^2 \qquad (7)$$

where f is the freeboard.

3.2.8.7   Mooring system

Pontoons 13, 20, and 27 are moored to the seabed with four lines each. The mooring lines are made up of chain and wire segments which are described in Table 3-27. Segment lengths are defined in Table 3-28. The drag coefficients for the mooring lines are based on DNVGL-OS-E301 /5/ and the used coefficients can be taken as upper limit for mooring design. This is also the value that has been used for design analyses.

Table 3-27   Mooring components mechanical and hydrodynamic properties without marine growth /6/ and /7/.

Magnitude	Unit	Top chain	Wire	Bottom chain
Type	-	Studless chain, R4	Sprial strand wire – SPR2 plus	Studless chain, R4
Nominal diameter	mm	147	124 mm	147
Sheating thickness	-	-	-	-
Outer diameter	mm	147	146*	147
Corrosion rate	mm/year	0.2	-	0.2
Design life	years	50	50	100
Corrosion allowance	mm	10	-	20
Weight in air	kg/m	432	82.2	432
Weight in water	kg/m	376	65.3	376
MBL (uncorroded)	kN	19089	15073	19089
MBL (corroded)*	kN	16992	-	14955
Cross-sectional area**	mm^2	33943	12076	33943
SCF	-	1.15***	1	1.15***
a_D (fatigue parameter)****	-	6.0e10	-	6.0e10
m (fatigue parameter)****	-	3.0	-	3.0
Axial stiffness	kN	1.73e6	1.45e6	1.73e6
Drag coefficient in longitudinal direction	-	1.15	0.1	1.15
Drag coefficient in transversal direction	-	2.4	1.2	2.4
Added mass coeff. in longitudinal direction	-	0	0	0
Added mass coeff. in transversal direction	-	1	1	1

*	Coating thickness is 11mm
**	For fatigue calculations. The area is based on a reduction in diameter of 50% of the corrosion allowance.
***	Used for the chain link in the fairlead due to out of plane bending, taken from DNVGL-OS-E301 /5/. For bottom, keep consistent with designer.
****	Fatigue life of wire is not considered here, thus capacity is not given in the table.

Table 3-28   Mooring lines segment length

Line number	Length [m]			Pretension [kN]
	Top chain	Wire*	Bottom chain	
1	50	555	100	1980
2	50	515	100	2000
3	50	719	100	2080
4	50	715	100	1930
5	50	877	100	2590
6	50	812	100	2280
7	50	831	100	2540
8	50	718	100	2630
9	50	467	100	2170
10	50	562	100	1690
11	50	480	100	2090
12	50	436	100	2040

*	Adjusted to keep a pretension close to the design value, see Figure 3-22.

The fairlead and anchor locations are extracted from /7/. Applied fairlead locations are listed in Table 3-29 and the anchor coordinates are included in Table 3-30.

Pretension comparison is presented in Figure 3-22.
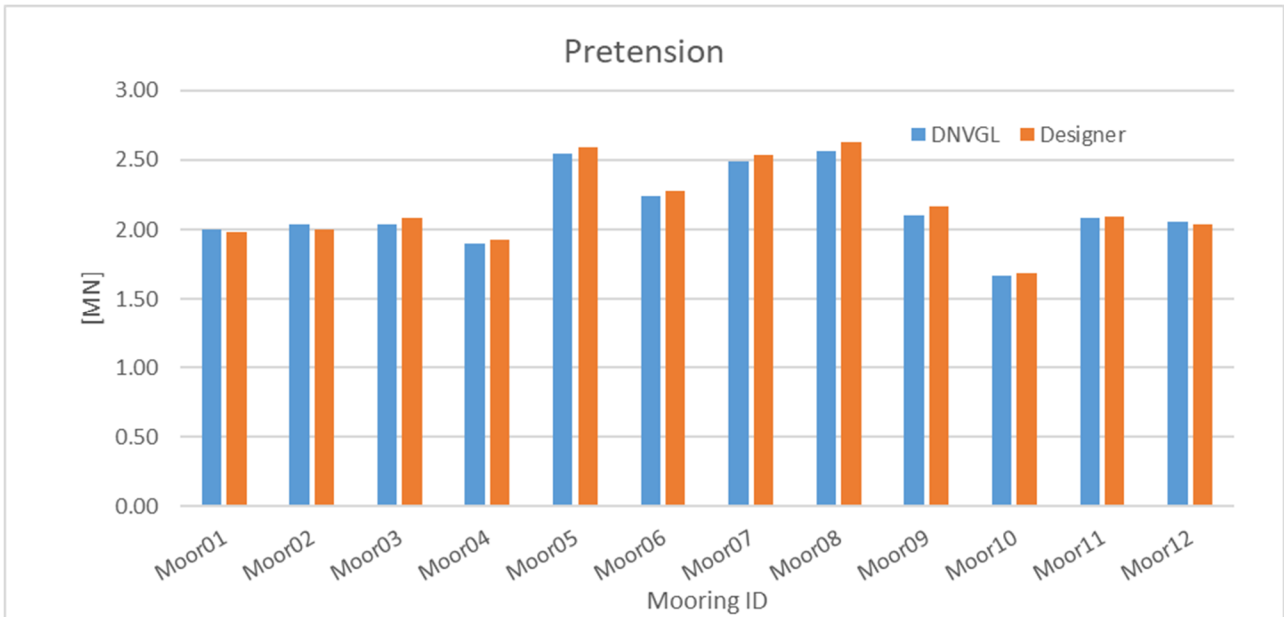
Figure 3-22   Pretensions applied by designer /7/ and DNVGL.

.

Table 3-29   Fairlead coordinates. Given in local pontoon coordinate system. Coordinates based on /7/ are included in parenthesis.

Fairlead number	X-location [m]*	Y-location [m]	Z-location [m]
Fairlead1	-24 (7)	-7 (-24)	-6
Fairlead2	-24 (-7)	7 (-24)	-6
Fairlead3	24 (-7)	7 (24)	-6
Fairlead4	24 (7)	-7 (24)	-6

Table 3-30   Mooring anchors location /7/.

Line number	Pontoon	Anchor X location [m]	Anchor Y location [m]	Anchor Z location [m]
1	Pontoon 13	-941.33	-312.37	-466.00
2	Pontoon 13	-1098.33	-216.37	-449.00
3	Pontoon 13	-714.33	915.63	-559.00
4	Pontoon 13	-494.33	825.63	-560.00
5	Pontoon 20	270.67	-886.37	-491.00
6	Pontoon 20	-462.33	-716.37	-491.00
7	Pontoon 20	-303.33	774.63	-560.00
8	Pontoon 20	385.67	640.63	-485.00
9	Pontoon 27	1048.67	-578.37	-367.00
10	Pontoon 27	700.67	-683.37	-388.00
11	Pontoon 27	710.67	365.63	-442.00
12	Pontoon 27	949.67	398.63	-360.00

3.2.9   Structural damping

Structural damping is applied using the stiffness and mass proportional Rayleigh damping which estimates the damping matrix as a coefficient $a1$ times the mass matrix and another coefficient $a2$ multiplied with the stiffness matrix (both geometric stiffness and material stiffness). /3/ defines the structural damping to be used for different sections, as shown in Table 3-31.

The $a1$ and $a2$ coefficients are calculated so the desired critical damping is achieved for oscillations with two periods. With the Rayleigh model, it is only possible to set the structural damping value at two frequencies. The resulting structural damping is lower than the target value in between those frequencies and larger outside that range. It will then vary for other oscillation periods. The calculation of $a1$ and $a2$ is done as follows:

$$a_1 = \frac{2\omega_1\omega_2}{\omega_2{}^2 - \omega_1{}^2}(\lambda_1\omega_2 - \lambda_2\omega_1) \tag{8}$$

$$a_2 = \frac{2(\lambda_2\omega_2 - \lambda_1\omega_1)}{\omega_2{}^2 - \omega_1{}^2} \tag{9}$$

where ω_1 and ω_2 are the angular frequencies at which the structural damping is defined, i.e. corresponding to RDp1 and RDp2 given in Table 3-31; λ_1 and λ_2 are the values of the critical damping at those frequencies.

Table 3-31 Structural damping values for different sections.

Sections	Rayleigh damping ratio	Rayleigh damping period 1 (RDp1 [s])	Rayleigh damping period 2 (RDp2 [s])	$a1$	$a2$
Main girder section	0.005	2	70	0.00087	0.0031
Girder section at abutment North	0.005	2	120	0.00052	0.0031
Girder section at abutment South	0.005	2	70	0.00087	0.0031
Back columns	0.008	2	70	0.0014	0.0050
Columns	0.005	2	70	0.00087	0.0031
Cable	0.002	1	20	0.0012	0.00061
Tower	0.008	1	20	0.0048	0.0024
Mooring	0.005	2	70	0.00087	0.0031

3.3 Environmental data

3.3.1 General

This section summarizes the metocean model included in /11/. The applied environmental conditions for each of the analyses is afterwards detailed in the relevant section for the analyses.

3.3.2 Wind waves

The wind generated wave conditions with the largest significant wave height for different return periods are included in Table 3-32. This wind sea conditions correspond to the maximum value in 1 hour; they can be scaled to 3-hour maxima with the factors included in Table 3-33.

Table 3-32 Extreme wind sea conditions /11/.

Return period/ Heading	1 year Hs [m]	Tp [s]	10 years Hs [m]	Tp [s]	50 years Hs [m]	Tp [s]	100 years Hs [m]	Tp [s]	10000 years Hs [m]	Tp [s]
Omni	1.3	4.3	1.7	4.8	2.0	5.2	2.1	5.3	2.9	6.1
345°-15°	0.3	2.5	0.6	3.5	0.8	4.0	0.8	4.0	1.3	4.7
15°-45°	0.2	1.9	0.5	3.3	0.7	4.2	0.7	4.2	1.2	4.9
45°-75°	0.5	3.1	0.7	3.6	0.8	3.9	0.9	4.1	1.2	4.8
75°-105°	1.0	4.0	1.5	4.7	1.9	5.2	2.1	5.5	3.1	6.5
105°-135°	0.9	3.7	1.1	4.1	1.3	4.4	1.4	4.6	2.0	5.4
135°-165°	0.9	3.4	1.1	3.8	1.2	4.0	1.2	4.0	1.6	4.7
165°-195°	0.8	3.3	1.0	3.6	1.2	3.9	1.2	3.9	1.6	4.3
195°-225°	0.9	3.7	1.2	4.3	1.3	4.4	1.4	4.6	1.8	5.2
225°-255°	0.8	3.1	1.1	3.6	1.3	3.9	1.4	4.0	1.9	4.6
255°-285°	1.0	3.5	1.4	4.0	1.7	4.4	1.8	4.5	2.7	5.3
285°-315°	1.2	4.3	1.6	4.8	1.8	5.0	2.0	5.2	2.7	5.9
315°-345°	0.7	3.7	0.9	4.1	1.1	4.5	1.2	4.6	1.7	5.3

Table 3-33   Correction factor from 1-hour to 3-hour maximum wind sea significant wave height /11/.

Return period	Correction factor from 1-hour to 3-hour maximum Hs
1 year	0.917
10 years	0.934
50 years	0.942
100 years	0.945
10000 years	0.959

Suggested wind waves spectral parameters are included in Table 3-34.

Table 3-34   Wind wave spectral parameters according to the Metocean design basis /11/.

Parameter	Recommended value
Spectrum	JONSWAP with average spectral width (σ_a=0.07 and σ_b=0.09)
JONSWAP peakedness factor	Between 1.8 and 2.3
Spreading function exponent ($\cos^n$)	Between 3 and 8

3.3.3   Swell

The maximum swell significant wave height for different return periods is included in Table 3-35. The swell significant wave height shall be scaled for peak periods below 12 seconds as defined in Table 3-36. In addition, a factor of 0.917 shall be used to convert from the 1-hour to the 3-hour maximum swell significant wave height.

Table 3-35   Extreme swell conditions /11/.

Return period	1 year	10 years	50 years	100 years	10000 years
Significant wave height [m]	0.22	0.28	0.33	0.34	0.46

Table 3-36   Swell significant wave height scaling factor

Swell peak period [s]	Swell significant wave height scaling factor [-]
6	0.50
7	0.58
8	0.67
9	0.75
10	0.83
11	0.92
12	1.00
18	1.00
20	1.00

Suggested wind waves spectral parameters are included in Table 3-37.

Table 3-37   Swell spectral parameters according to the Metocean design basis /11/.

Parameter	Recommended value
Spectrum	JONSWAP with average spectral width (σ_a=0.07 and σ_b=0.09)
JONSWAP peakedness factor	Between 3 and 5
Spreading function exponent ($\cos^n$)	Between 10 and 20
Mean swell direction	Between 300 and 330 degrees

3.3.4   Wind

Extreme wind speeds for different return periods are specified in Table 3-38; they shall be scaled depending on the incoming direction with the factors included in Table 3-39.

Table 3-38   Extreme wind speeds according to the Metocean design basis /11/.

Return period	Maximum 1-hour average wind speed [m/s]	Maximum 3-hour average wind speed [m/s]
1 year	21.4	22.9
10 years	25.8	27.6
50 years	28.5	30.5
100 years	29.6	31.7
10000 years	35.9	38.4

Table 3-39 Extreme wind speed directional correction factor.

Direction	Reduction coefficient
345°-15°	0.7
15°-45°	0.7
45°-75°	0.7
75°-105°	0.85
105°-135°	0.85
135°-165°	0.85
165°-195°	0.85
195°-225°	0.85
225°-255°	0.9
255°-285°	1.0
285°-315°	1.0
315°-345°	1.0

The wind profile specified in the Metocean design basis /11/ is given as

$$V(z) = C_r(z) * C_{prob} * 24.3 \,, \tag{3-10}$$

where $V(z)$ is the 1-hour average wind speed at height z and

$$C_r(z) = k_T * \ln\left(\frac{z}{z_0}\right) \text{ and } C_{prob} = \left(\frac{1 - K*\ln(-\ln(1-p))}{1 - K*\ln(-\ln(0.98))}\right)^n \,, \tag{3-11}$$

where z_0=0.01, k_T=0.17, K=0.2, n=0.5 and p=1-exp($-1/T$) where T is the return period in years.

The turbulence intensity for winds from 0°-150° and 210°-360° of the along wind component I_u is set in accordance with the Metocean design basis to

$$I_u = \frac{k_{tt}}{\ln\left(\frac{z}{z_0}\right)} \tag{3-12}$$

where k_{tt}=1.0, z_0=0.01 and z is the height above sea level. As the mean wind speed $V(z)$ also is proportional to $\ln(z/z_0)$, the standard deviation σ_u of the wind component within a stationary time period is constant with height, i.e.

$$\sigma_u = I_u * v_m = k_{tt}k_T C_{prob} * 24.3 = 4.29 \, m/s \; (for \; 100 \; year \; return \; period) \tag{3-13}$$

The standard deviation given in the Metocean design basis is assumed here to be representative for a stationary 10 minutes period. Since the analyses of the floating bridge will be performed on 3-hour periods, the 3-hour long wind fields will contain fluctuation at a larger range of frequencies (i.e. the wind field will contain also slower fluctuations). To maintain the energy level contained in the higher frequencies, it is necessary to increase the standard deviation of the wind time series. The required scaling factor is found by the ratio between the integral of the frequency spectrum in the frequency range f=[1/3hour, *inf*] and the range f=[1/10min, *inf*]:

$$\sigma_{u,3hr} = \sigma_{u,10\,min} \times \frac{\sqrt{\int_{f=\frac{1}{3hr}}^{\infty} S_i}}{\sqrt{\int_{f=\frac{1}{10min}}^{\infty} S_i}} \tag{3-14}$$

where S_i is the power spectral density, see below. For the P50 spectrum specified in the MDB, the factor is found to be 1.024, resulting in a 3-hour standard deviation of $\sigma_{u,3hr} = 4.39 \, m/s$. The effect of this correction is considered to be minor.

The turbulence intensity for winds from 150°-210° is high on the southern side of the fjord before becoming more steady during the travel across the fjord. In the Metocean design basis, the turbulence intensity is specified as given in Table 3-40. It is further stated that linear interpolation can be used between 50 m and 200 m above sea level.

Table 3-40   Turbulence intensities for southerly winds (coming from 150°-210°)

Sector/Height above sea level	Turbulence Intensity, I_u
10 m - 50 m	Linearly decreasing from 30% at southern tower to 17% in the north
200 m	15%

In TurbSim, the wind field is generated in three dimensions: a two-dimensional plane (y,z) and a time dimension. The third spatial dimension is, when the wind field is imported in Sima, taken as the time dimension with a one-to-one conversion based on the mean wind speed. This implies that a variation in turbulence intensity along the wind direction is not possible to model with the present modelling tool. As a conservative approach, the wind along the bridge is therefore modelled with a constant turbulence intensity along the bridge corresponding to the largest turbulence intensity (30% at 50 m height). The standard deviation of the *u*-component is constant with height and across the wind field in the present analyses.

Regardless of wind direction, the transverse and vertical turbulence components I_v and I_w are set (in accordance with the Metocean design basis) to

$$\begin{bmatrix} I_v \\ I_w \end{bmatrix} = \begin{bmatrix} 0.84 \\ 0.60 \end{bmatrix} I_u \tag{3-15}$$

The one-point frequency spectra $S_i(n)$ for all wind components are specified in the Metocean design basis as

$$\frac{nS_i}{\sigma_i^2} = \frac{A_i \hat{n}_i}{(1 + 1.5 A_i \hat{n}_i)^{5/3}} \quad \text{for} \quad i = u, v, w, \tag{3-16}$$

where A_i is the spectral density coefficient, σ_i is the standard deviation of the wind component and

$$\hat{n}_i = \frac{n\,^x L_i}{V(z)} \tag{3-17}$$

where *n* is the frequency and $^x L_i$ is an integral length scale parameter. The different parameters in this specification are given at 50 m above ground level in Table 3-41. In an e-mail from SVV /22/, it was clarified that the spectral density coefficients (A_i's) were obtained through fitting to the observed data keeping the integral length scale parameters from N400. In other words, to best represent the spectral properties observed at site, the P10/P50/P90 value of the spectral density coefficients should be applied together with the integral length scales from N400.

In equation (5.2) of N400 /xx/, a vertical variation in the integral length scale is indicated. In a clarification from SVV /22/ it was stated that this height dependency should be considered also at this site. This leads to the following height dependent expression for $\hat{n}_i$:

$$\hat{n}_i = n \frac{L_{1,i} \left(\frac{z}{z_1}\right)^{0.3}}{V_c \ln\left(\frac{z}{z_0}\right)} \tag{3-18}$$

where $L_{1,I}$ is a the reference length scale for component *i,* in accordance with N400, z_1=10 m, z_0=0.01 m, and V_c is a constant found from the wind profile (see eq. (3-10)). With these values, a factor of 1.23 between $\hat{n}_i(z = 15\,m)$ and $\hat{n}_i(z = 50\,m)$ is obtained as an example. This height dependency is not possible

to model in TurbSim. In the present work a reference height of 50 m is selected and used in the analyses, as this is the height at which site-specific wind data has been evaluated. The height dependency of the spectrum is negligible compared to the statistical variations of the spectral coefficients: the difference between P10 and P90 corresponds to a factor of 4.

In conclusion, the P50 values of A_i have been applied for the present analyses. The integral length scales have been set equal to the values listed in N400 (and replicated in Table 3-41 below.)

Table 3-41 Parameters for the definition of turbulence spectra and coherence functions, as specified in ref. /22/(which was a correction to /11).

Parameter	N400	P10	P50	P90
^xL_u	162 m	108 m	232 m	586 m
^xL_v	40.5 m	50 m	141 m	472 m
^xL_w	13.5 m	21 m	40 m	81 m
^yL_u	54.0 m	X	X	X
^yL_v	40.5 m	X	X	X
^yL_w	9.0 m	X	X	X
^zL_u	32.4 m	X	X	X
^zL_v	13.5 m	X	X	X
^zL_w	9.0 m	X	X	X
A_u	6.8	3.9	7.3	16.3
A_v	9.4	5.6	13.3	32.5
A_w	9.4	7.7	12.3	18.2
C_{uy}	10.0	6.4	8.0	10.8
C_{uz}	10.0	8.3	11.5	17.6
C_{vy}	6.5	3.0	3.8	4.9
C_{vz}	6.5	6.0	8.8	16.5
C_{wy}	6.5	4.5	5.8	8.3
C_{wz}	3.0	2.8	3.7	5.7

The **normalized co-spectra** $S_{i1,i2}$ (for $i=u,v,w$) between points 1 and 2 separated in the (y,z)-plane (normal to the main wind direction) is specified in the Metocean design basis as

$$\frac{RE[S_{i_1 i_2}(n, \Delta s_j]}{\sqrt{S_{i_1}(n)S_{i_2}(n)}} = exp\left(-C_{ij}\frac{n\Delta s_j}{V(z)}\right) \text{, for } i_1, i_2 = u,v,w \text{ and } j = y,z, \tag{3-19}$$

where Δs_j is the horizontal or vertical distance between the points. Values for C_{ij} are given in Table 3-41. $V(z)$ is assumed by DNV GL to be the mean wind speed averaged at the two points.

The P10 values for C_{ij} in Table 3-41 have been selected here, as these give a more coherent wind field than the larger values. This is assumed to give a higher global response than less coherent wind fields.

Eq. (3-19) is an exponential Davenport coherence function, where it can be noted that none of the six C_{ij} values are equal. In TurbSim, it is not possible to specify different coherence for vertical and horizontal separations. For the floating part of the bridge, the horizontal coherence is more important than the vertical coherence. Therefore, the vertical coherence coefficients are in practice set equal to the horizontal ones, i.e. $C_{uz}=C_{uy}=6.4$, $C_{vz}=C_{vy}=3.0$, and $C_{wz}=C_{wy}=4.5$.

In TurbSim, a more general expression than eq. (3-19) is implemented. The "IEC Coherence" model, which is applied here, is given as

$$\frac{RE[S_{i_1 i_2}(n, \Delta s]}{\sqrt{S_{i_1}(n) S_{i_2}(n)}} = exp\left(-a_i \sqrt{\left(\frac{n \Delta s}{\overline{V}_{hub}}\right)^2 + (b_i \Delta s)^2}\right) \text{, for i} = u, v, w \, . \tag{3-20}$$

where $\overline{V}_{hub}$ is the mean wind velocity at "hub height", which in practice is the height of the middle of the defined wind field. This value is therefore not varying across the wind field, in contrast to the coherence function defined in eq. (3-19). In the wind field applied in the present analyses, the $\overline{V}_{hub}$ is evaluated at a height of 42.5 m, which leads to a slight increase in the coherence for most of the bridge girder. However, this effect is small compared to the variation in coherence represented by the P10 and P90 values in Table 3-41. Another limitation in the TurbSim implementation is that it is not possible to set b_i to zero. Hence, it is set as low as possible in the present analyses (b_i=0.00001). As can be seen in Figure 3-23, the effect of this is negligible.
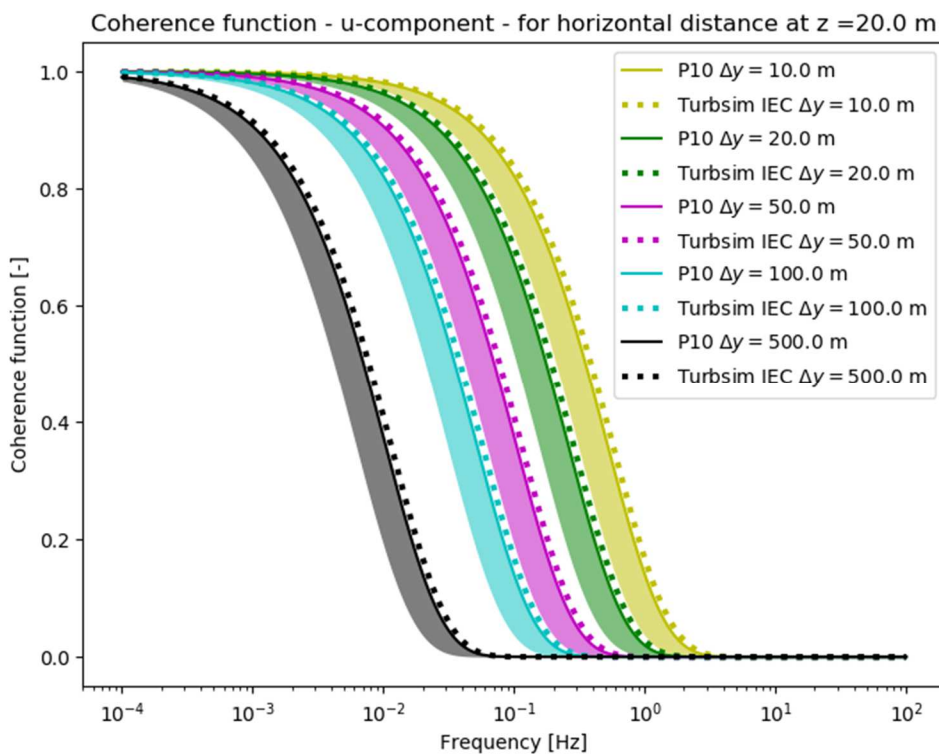
Figure 3-23: Coherence function for *u*-component, for horizontal separations (Δy). The shadowed areas represent P10 to P90 values as given in the Metocean design basis /11/.

3.3.5   Wind profile in SIMO-RIFLEX

The turbulent wind model in SIMO-RIFLEX is calculated in Turbsim for a mesh of points prioritizing the bridge girder. Due to the size of the bridge it is required to limit the size of the turbulent wind field. The columns, the pontoons and the stay cables lay partially or totally outside that mesh. In those cases, it is the wind velocity at the closest mesh boundary that is used in SIMO-RIFLEX as shown in the wind profile in Figure 3-24.

In order to avoid an under- or over-prediction of wind loads, the wind load coefficients in those elements which are outside the defined wind field are scaled to match the expected resultant wind load.

Wind profiles comparison
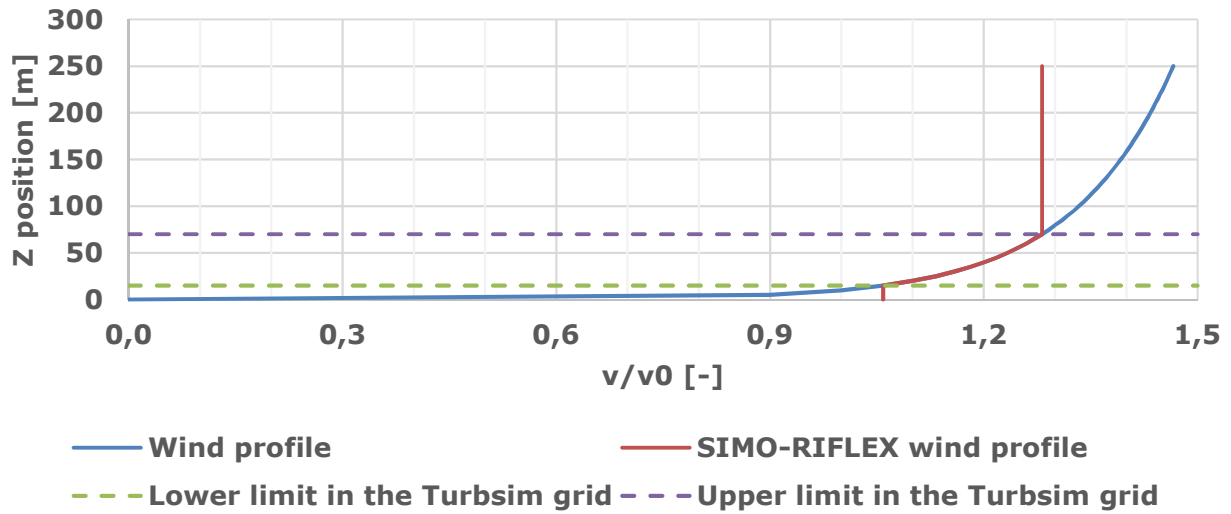
Figure 3-24 Wind profile in SIMO-RIFLEX coupled analyses

3.3.6 Current

The maximum current velocities at different locations in the fjord are included in Table 3-42.

The current velocity is assumed constant and uniform in the water column.

Table 3-42 Extreme current velocity at different locations in Bjørnafjord /11/, see **Figure 3-25**

Return period	Depth [m]	Current velocity [m/s]				
		S1	S2	S3	S4	Average
10 years	1.5	1.49	1.45	1.27	1.30	1.38
	5	1.26	1.55	1.26	1.55	
	10	1.23	1.18	1.08	1.14	
	15	0.96	0.99	1.11	1.29	
50 years	1.5	1.68	1.63	1.46	1.54	1.58
	5	1.45	1.85	1.51	1.94	
	10	1.39	1.34	1.24	1.38	
	15	1.15	1.14	1.31	1.54	
100 years	1.5	1.76	1.71	1.54	1.64	1.66
	5	1.53	1.97	1.62	2.11	
	10	1.46	1.40	1.31	1.48	
	15	1.23	1.21	1.39	1.65	
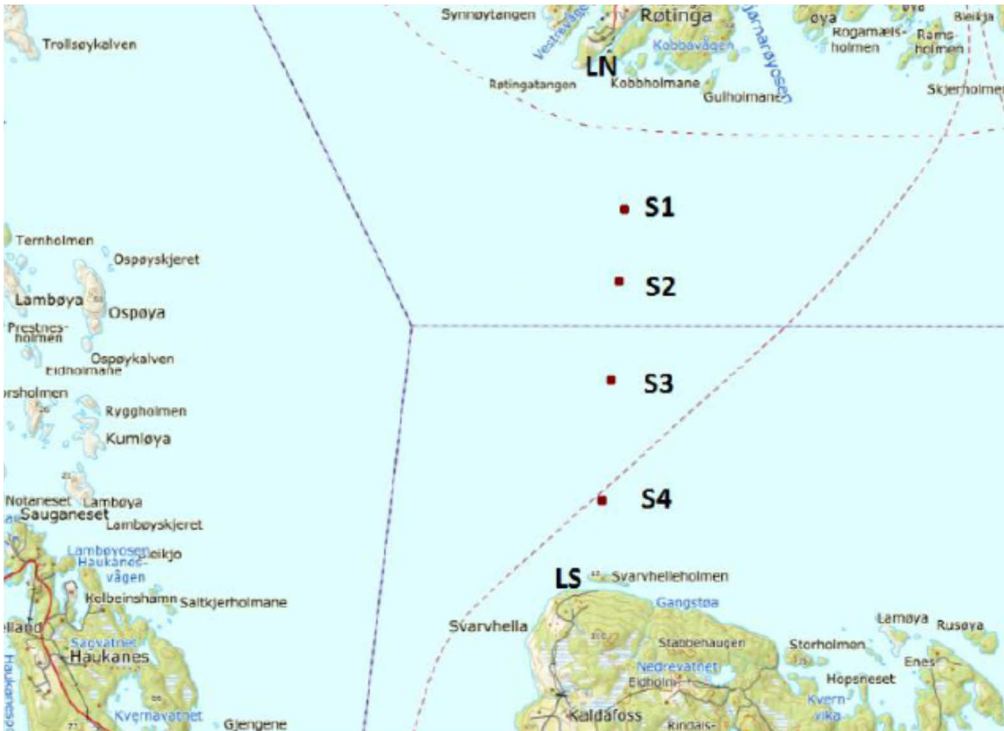
Figure 3-25   Location of the current measurement stations, from /11/**.**

3.3.7   Tidal variations

The water level variation is defined a combination of an astronomical component and the effect of atmospheric sources. Table 3-43 summarizes the different astronomical extreme tidal amplitudes. The extreme water levels for different return periods are included in Table 3-44. The atmospherical component can be calculated as the difference between the extreme levels and the MSL.

Table 3-43   Tidal amplitudes /11/.

Component	Amplitude [m]
Lowest Astronomical Tide (LAT)	0.00
Mean Low Water (MLW)	0.39
Mean Sea Level (MSL)	0.77
Mean high water (MHW)	1.15
Highest Astronomical Tide (HAT)	1.53
NN 1954	0.88
NN 2000	0.97

Table 3-44   Extreme water level for different return periods /11/.

Return period	Highest water level [m]	Lowest water level [m]
1 years	1.81	-0.20
10 years	1.97	-0.30
100 years	2.10	-0.50
10000 years	2.50	-0.65

The mean water level shall be increased by 0.74 metres due to climate change where this is unfavourable.

3.3.8 Temperature loads

Table 3-45   Extreme temperatures for different return periods

Return period	Minimum temperature [deg]	Maximum temperature [deg]
1 years	-7	25
10 years	-12	29
100 years	-15	32
10000 years	-17	33

3.3.9 Environmental load combinations

Table 3-46 presents the return period for each of the environmental effects for the applicable environmental load combinations, as defined in /12/.

Table 3-46   Return period for each component for the environmental load combinations

Return period	Wind	Waves		Current	Sea level	
		Wind sea	Swell		Astonomical	Atmospheric surge
1 years	1	1	1	1	HAT	1
10 years	10	10	1	10	HAT	10
	1	1	10	1	HAT	1
100 years	100	100	10	100	HAT	100
	10	10	100	10	HAT	10
10000 years	10000	10000	100	10000	MSL	10000
	100	100	10000	100	MSL	100

3.3.10 Fatigue conditions

The Metocean design basis /11/ includes wind sea scatter diagrams for different sectors and an omni-directional scatter diagram. A relation between wind speed and significant wave height is also specified for each sector. Wind sea from East shall not be combined with swell.

The load cases for fatigue analyses are generated according to the following procedure:

- The sea states outside the 210-330 degrees sector are included with their probabilities as defined in the wind waves scatter diagrams.

- The wind wave sea states in the 210-330 degrees sector shall be combined with swell. Both the wind sea and swell conditions in the scatter diagrams are sorted by decreasing probability of occurrence. The wind sea and swell conditions are combined pairwise in this decreasing probability order. The following considerations are made:

  o If wind sea probability is larger than swell probability, the sea state is split in two: one with swell and with the swell case probability; and one with wind sea only with the remaining probability.

  o If swell probability is larger than wind sea probability, the wind sea probability is assigned. This happens for 70 sea states, all of them with a low probability. Only 0.34% of the swell probability is lost by this procedure.

  o Swell direction is randomly selected in the 300-330 degrees range.

  o Swell conditions with less than 3 cm significant wave height are discarded.

- Current speed is set to zero. This is a conservative assumption, as the main effect of current is damping.

It should be noted that this combination of wind sea and swell will be somewhat random.

A total of 580 load cases are established for the fatigue analyses. The complete list of sea states for the fatigue analyses is included in Appendix D.

3.3.11 Marine fouling

Marine fouling, also referred to as marine growth, is not considered in the analysis.

4 METHOD DESCRIPTION

4.1 Time domain simulations

4.1.1 General

Time domain simulations have been performed with a net duration of 3 hours when the initial 1200 seconds are removed before further processing. Output from the simulations are time series of sectional loads (axial force, shear forces, bending moments and torque) at selected elements in the global model and motions at the pontoons and at the bridge girder at each axis.

For ULS/ALS code checks envelopes of 3-hour P90 extreme values along the bridge loads will be provided, hence information about concurrency between the different sectional loads will not be used and the most onerous combinations must be applied.

For FLS code checks time series of stress resultant will be calculated based on mechanical transfer functions and time series of sectional loads as input. The stress time series will then be used for fatigue calculations through rainflow-counting, using appropriate SN curves for the actual details.

4.1.2 Fitting statistical distribution to samples of extreme load effects

30 simulations with randomized wind and wave field for each 100-year environmental condition were run.

Before further processing, the permanent/functional component (self-weight) was removed.

For each load effect, e.g. axial force, the largest value from each of the 30 repetitions was found, resultimg in an extreme value sample of size 30.

Then a generic Gumbel distribution, c.f. equation (21), is fitted to the extreme value samples using equations (22) and (23).

$$F(x_e; 3hr) = \exp\left(-\exp\left[-\frac{x_e - \mu}{\beta}\right]\right) \tag{21}$$

where:

   x_e = 3-hour extreme value [kN]

   μ = Gumbel location parameter [kN]

   β = Gumbel scale parameter [kN]

$$\beta = \frac{\sqrt{6}}{\pi} \cdot S_{Xe} \tag{22}$$

$$\mu = \overline{x_e} - 0.57722 \cdot \beta \tag{23}$$

where:

   $\overline{x_e}$ = Extreme value sample mean

   S_{Xe} = Extreme value sample (unbiased) standard deviation

The estimate the 100-year load effect as the 0.90 fractile of the fitted Gumbel distribution.

Note the following relations:

Expected 3 hour maximum = $\overline{x_e}$. Corresponds to 0.57 fractile (43% probability of exceedance).

Most Probable 3-hour Maximum (MPM) = α. Corresponds to 0.37 fractile (63% probability of exceedance).

Examples of Gumbel extreme value distributions are shown in Figure 4-1.
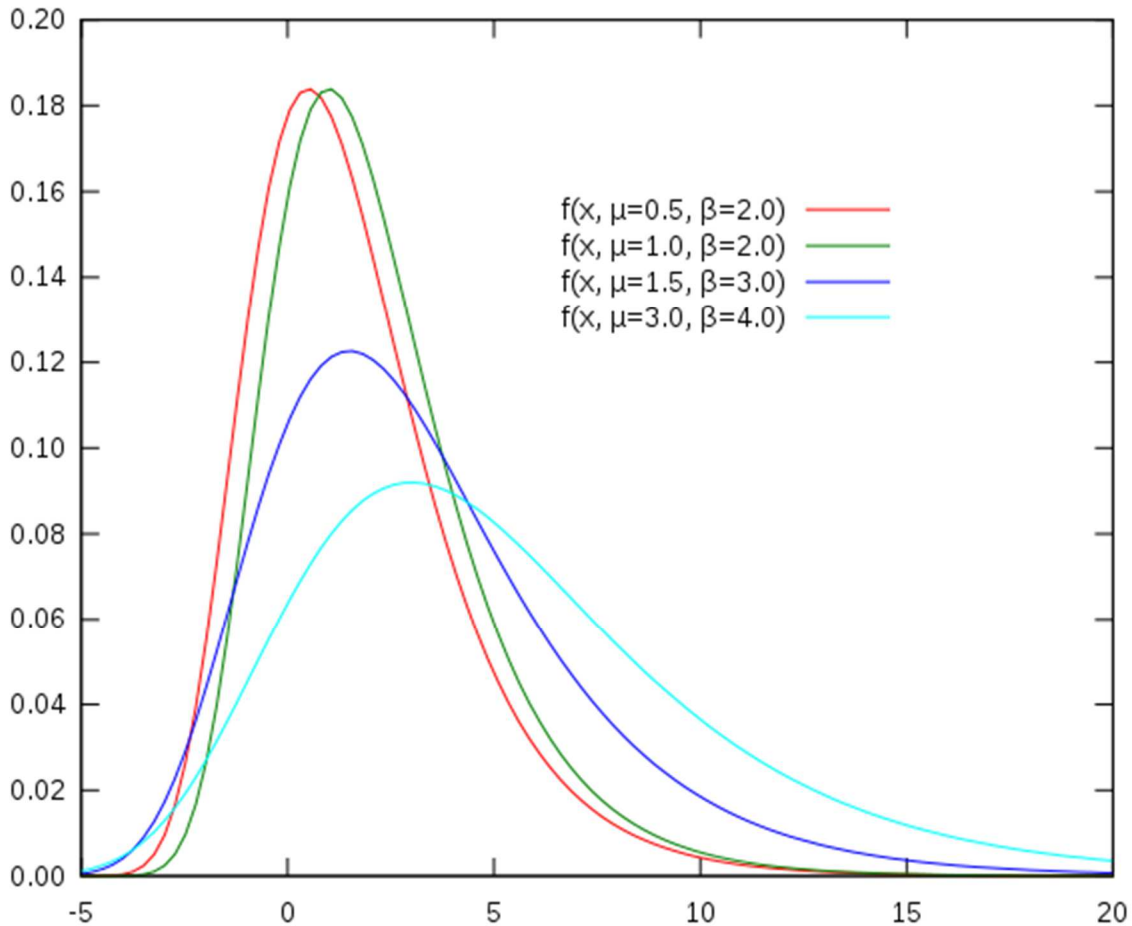
Figure 4-1 Gumbel probability distributions with different location parameter (μ), and different scale parameter (β).

4.1.3 Estimating the characteristic load effects

The exact 100-year load effect can only be found trough a proper long-term analysis accounting for both the variability in the short-term environmental conditions and the long-term variability of the climate parameters defining the short-term environmental conditions e.g. HS. For marine structures, DNV GL typically apply the 0.9 fractile (10% probability of exceedance) in the extreme value distribution of largest 3-hour maximum based on 100-year environmental conditions as an estimate of the 100-year load effect. Calibration with long-term calculations may prove other fractiles to be more precise estimates, but a priory this is not known.

4.1.4 Calculation of stresses

For extraction of normal and shear stresses from the model; stress transfer factors have been established for the bridge cross sections. For each cross section, factors have been derived for eight selected points for responses in all six degrees of freedom. The locations of the selected points are shown in Figure 4-2. As can be seen; stresses were calculated for all knuckle points in the outer plating as well as in bottom plating at bridge girder centre line. The stress transfer factors for the typical low

bridge midspan are listed in Table 4-1. The signing of the stress factors was based on combinations of forces and moments assuring that the resulting stress is given the right signing. For normal stress; tension was defined as positive. The stress transfer factors for other cross sections are listed in Appendix E. It should be noted that the stresses were based on the lesser plate thickness in the knuckle points.
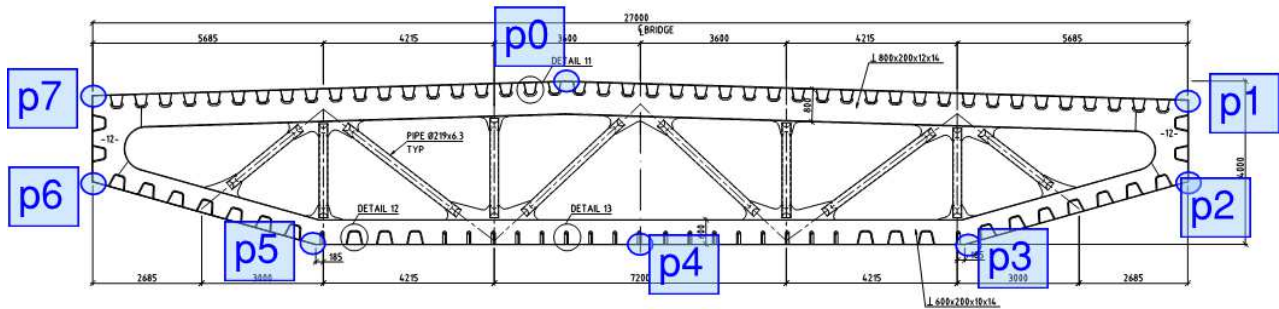
Figure 4-2   Selected points for stress transfer factor calculations

Table 4-1   Midspan low bridge – Stress factors

Position	C_{xA} [m^{-2}]	C_{xMS} [m^{-3}]	C_{xMw} [m^{-3}]	$C_{\tau z}$ [m^{-2}]	$C_{\tau y}$ [m^{-2}]	$C_{\tau M}$ [m^{-3}]
Point 0	0.75	-0.02	-0.46	0.00	1.69	0.33
Point 1	0.75	0.16	-0.33	10.02	0.00	0.44
Point 2	0.75	0.16	0.23	11.58	0.00	0.44
Point 3	0.75	0.09	0.66	0.00	1.46	-0.44
Point 4	0.75	0.00	0.66	0.00	2.11	-0.44
Point 5	0.75	-0.09	0.66	0.00	1.46	-0.44
Point 6	0.75	-0.15	0.23	11.58	0.00	-0.44
Point 7	0.75	-0.15	-0.36	10.02	0.00	-0.44

The axial and shear stresses at check point i are calculated as:

$$\sigma_x = C_{xA} * P_A + C_{xiMs} * M_S + C_{xiMw} * M_w$$

$$\tau_{xy} = C_{\tau iy} * Q_y + C_{\tau iz} * Q_z + C_{\tau iM} * M_{tor}$$

Where:

P_A – axial load (positive when tension)

M_S – Strong axis moment (positive when tension in negative y-axis – east side)

M_W – Weak axis moment (positive when tension in negative z-axis - bottom flange)

M_{tor} – torsional moment (positive when rotation is clockwise in x-direction)

C_{xA}	Stress factor axial
C_{xMs}	Stress factor strong axis bending
C_{xMw}	Stress factor weal axis bending
$C_{\tau z}$	Stress factor vertical shear
$C_{\tau y}$	Stress factor horizontal shear
$C_{\tau M}$	Stress factor torsional moment

4.1.5 Calculation of stress cycles for FLS analyses

An internal rainflow-counting algorithm is used to estimate the number of cycles for each of the stress ranges in the FLS analysis.

4.2 Applied software

The software suite consisting of SIMO /8/, RIFLEX /9/ and SIMA /10/ from SINTEF Ocean is applied for the static and dynamic load effect calculations. The software suite is validated trough decades of application to offshore, subsea and maritime problems. The following program versions have been used for these analyses:

- SIMO 4.12.3

- RIFLEX 4.12.3

- SIMA 3.6-01

TurbSim version 2.00.07 /21/ has been applied to simulate three component wind fields in a three-dimensional domain. TurbSim is developed by the federal National Renewable Energy Laboratory (NREL) in US, and is used extensively for load and response analyses of wind turbines within the wind energy industry. Output from TurbSim is read directly by SIMO/RIFLEX and SIMA.

5 GLOBAL ANALYSIS RESULTS

5.1 General

Load effect calculations are performed based on the information in Section 3.

The results from the eigen value calculations are documented in Section 5.2.

The static load effects such as permanent loads are documented in Section 5.3.

The dynamic load effects from environmental loading are documented in Section 5.4.

Mooring line loads in extreme and fatigue conditions are reported in Section 5.5.

Calculated loads are compared against designer's analyses in Section 5.6.

The static configuration of the bridge under permanent loads is not completely as designed. The bridge girder presents small deviations from its straight shape due to the difficulty of adjusting mooring line pretension to accurately match both design line tension and shape. In addition, deformations due to self-weight weak axis bending moment are not compensated in the analysis.

Permanent loads are subtracted from the rest of static and dynamic loads and stresses.

5.2 Natural periods and modes

In the design analyses, ref. /14/, eigen modes were calculated by Orcaflex where the mooring lines were modelled by linear springs. The eigen modes calculated in SIMA were calculated for the full model of the bridge, including also mooring lines and tendons. These calculations will therefore include several modes that are not included in the Orcaflex calculations. In the present version of SIMA it was only possible to calculate eigen values with frequency independent added mass. Therefore 7 different calculations were done, each with constant added mass for the pontoons based on period 5 seconds to 35 seconds in steps of 5 seconds. The resulting eigen period for a specific mode is then taken from the analyses with the period for added mass that is closest to actual natural period.

Table 5-1   Calculated the first 10 transverse natural periods

Mode	Natural periods
1st transverse mode	55.56
2nd transverse mode	44.84
3rd transverse mode	31.35
4th transverse mode	21.69
5th transverse mode	17.15
6th transverse mode	13.61
7th transverse mode	12.76
8th transverse mode	10.31
9th transverse mode	9.31
10th transverse mode	8.52
1st vertical mode	6.91

5.3 Static load effects

5.3.1 General

Static load cases are presented in this section. Environmental and traffic loads are not considered in this analyses.

Permanent loads and deformations due to self-weight, buoyancy and mooring and stay cables pretension are presented in Section 5.3.2. It shall be noted that these permanent loads are subtracted from all the other load cases results presented in this report, both static and dynamic.

5.3.2 Permanent loads

Loads distribution along the bridge girder under the permanent loads are presented in Figure 5-1 to Figure 5-6, while the static configuration of the bridge and tower are presented in **Figure 5-7** and Figure 5-8.
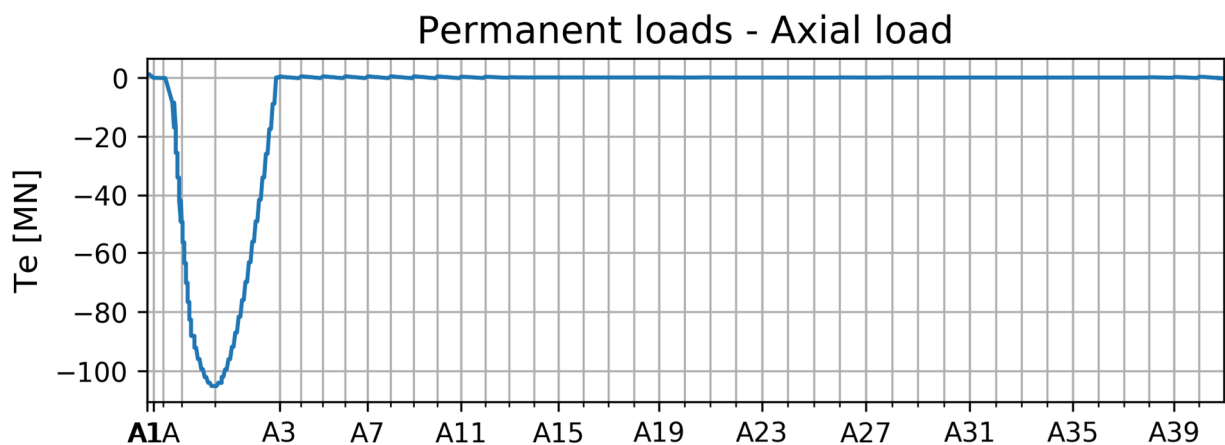
Figure 5-1   Axial loads in bridge girder under permanent loads.
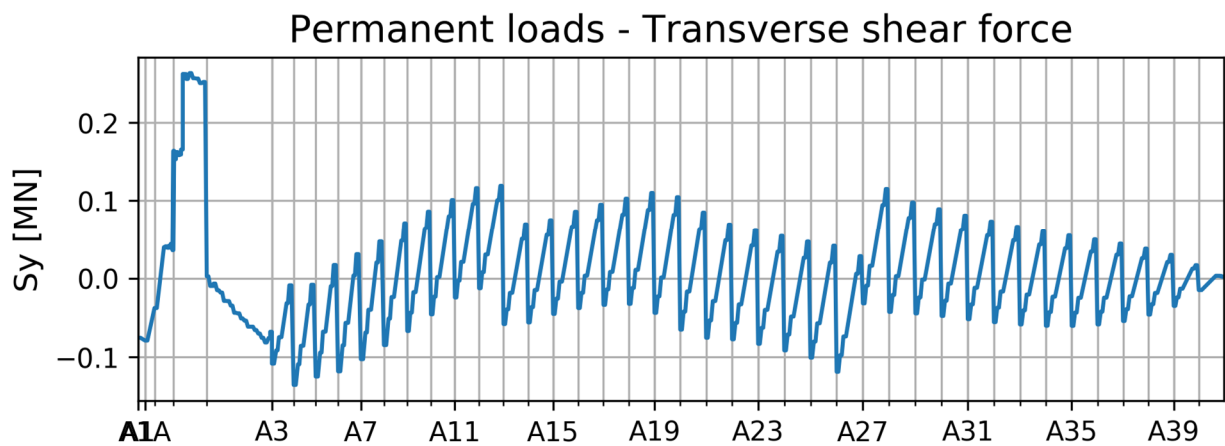
Figure 5-2   Transverse shear force in bridge girder under permanent loads.

Permanent loads - Vertical shear force
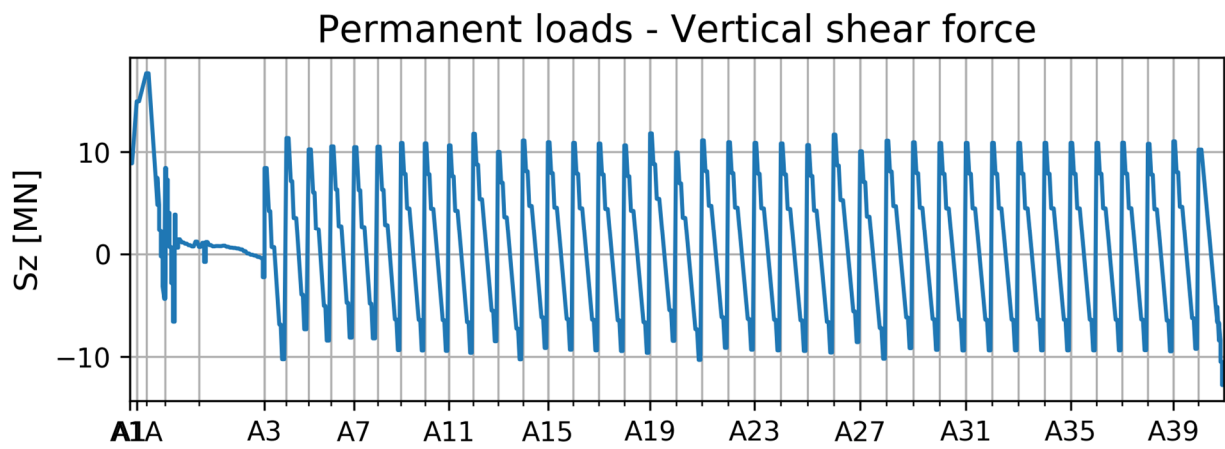
Figure 5-3 Vertical shear force in bridge girder under permanent loads.

Permanent loads - Weak axis moment
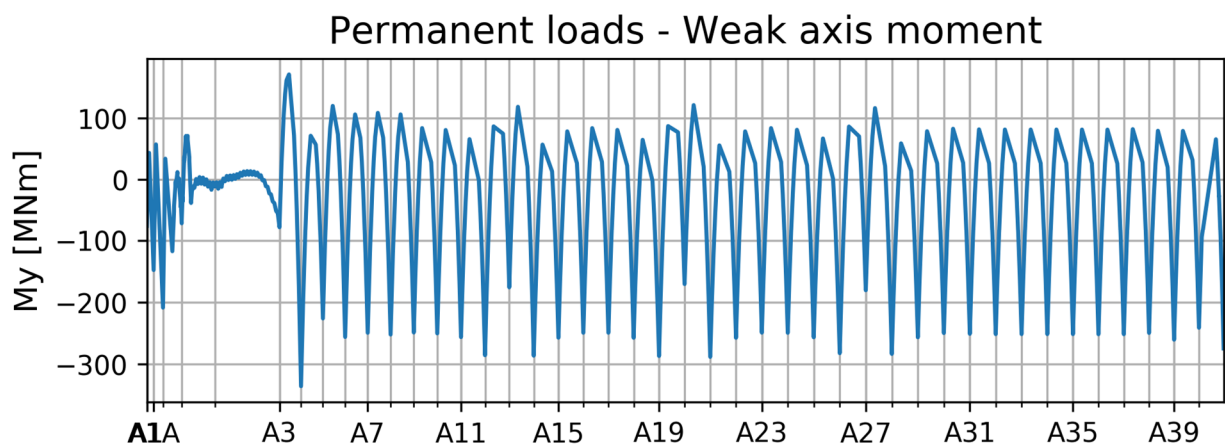
Figure 5-4 Weak axis moment in bridge girder under permanent loads.

Permanent loads - Strong axis moment
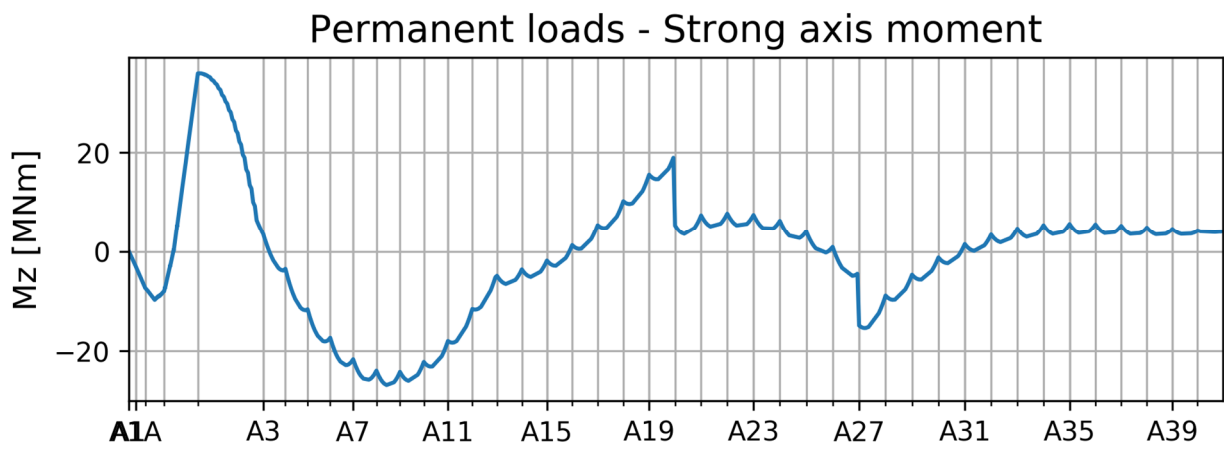
Figure 5-5   Strong axis moment in bridge girder under permanent loads.

Permanent loads - Torsional moment
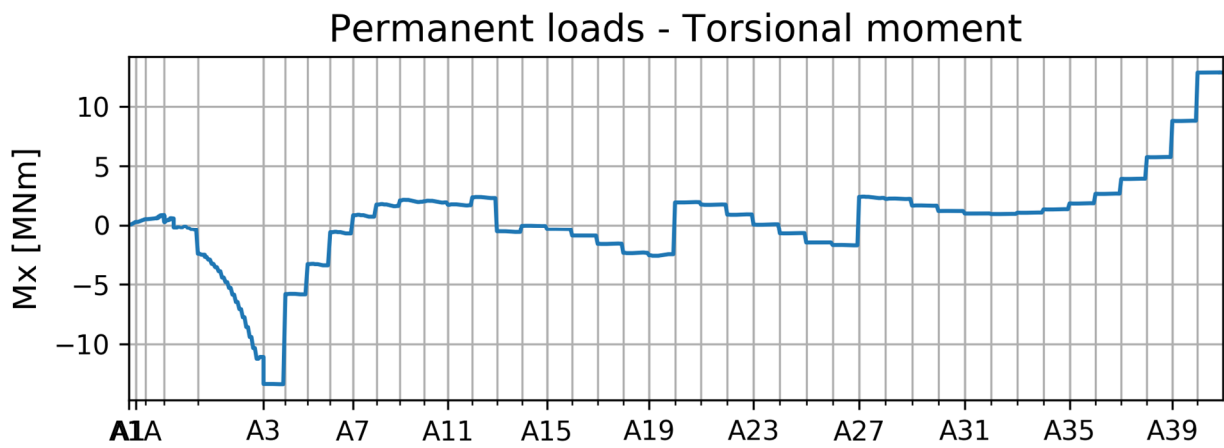
Figure 5-6   Torsional moment in bridge girder under permanent loads.
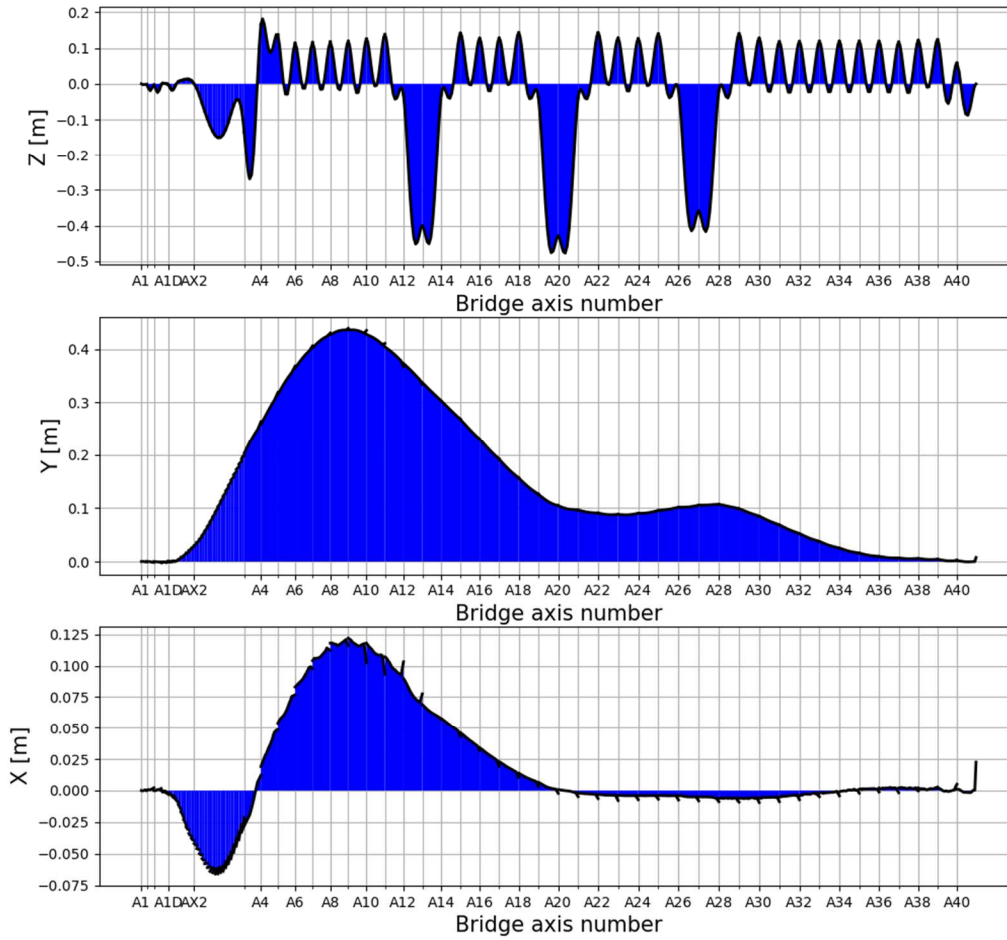
Figure 5-7   Deformed shape of the bridge girder under permanent loads

Permanent loads - Tower deformation
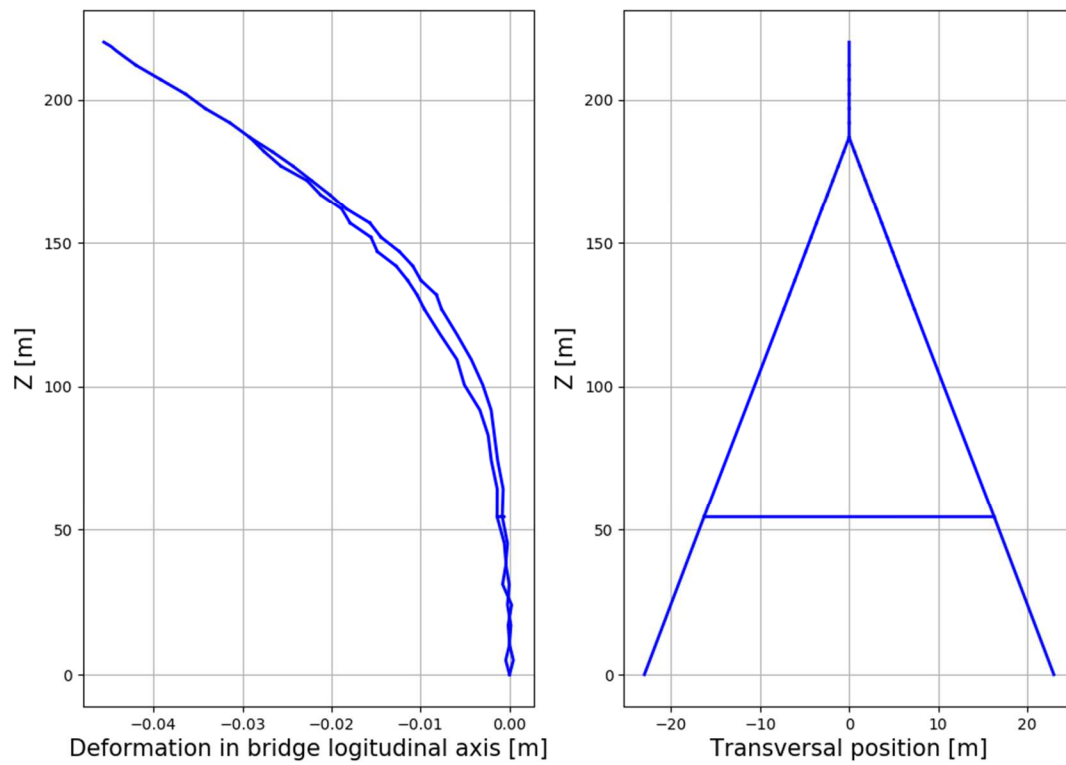
Figure 5-8   Deformed shape of the stay cable bridge tower under permanent loads

5.3.3 Temperature loads

The effect of temperature oscillations is studied by modifying the unstressed bridge girder length. A positive 10 degrees difference is expected to produce a 0.012% expansion of the bridge girder.

Both positive and negative temperature variations are studied, although its effect is very linear.

The most significant effects of a temperature change are the strong axis bending moment, the transverse shear force and the torsional moment, as shown below.

Temp plus 10deg - Vertical shear force
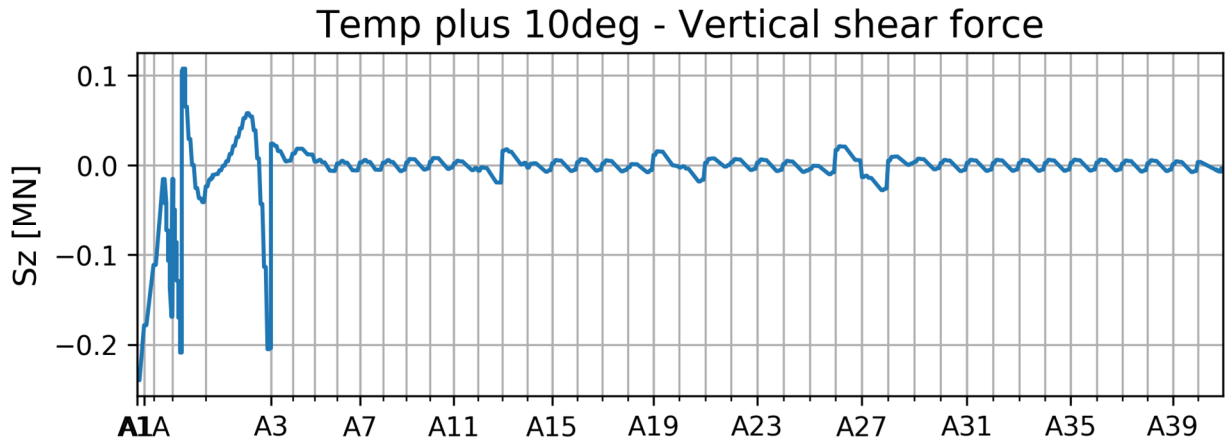
Figure 5-9   Vertical shear force in bridge girder under temperature loads

Temp plus 10deg - Strong axis moment
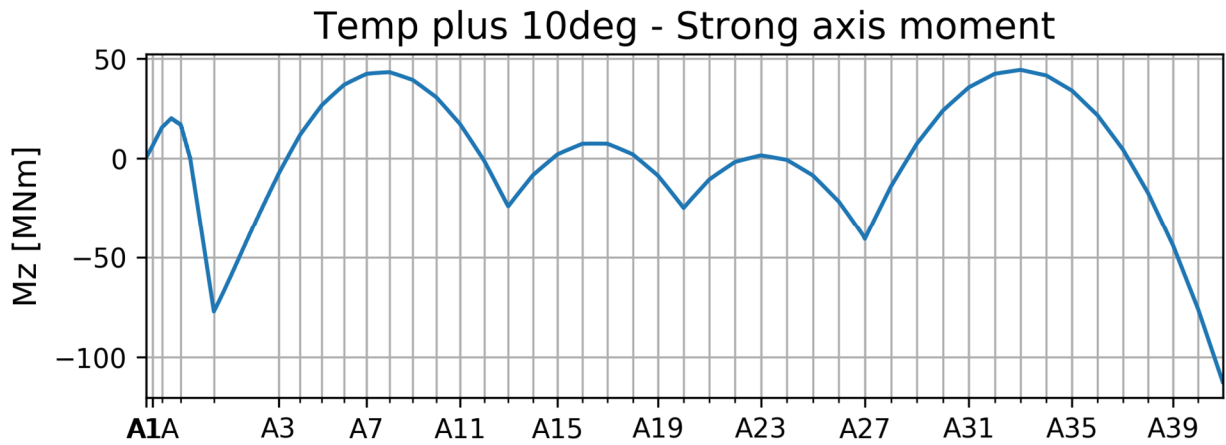
Figure 5-10   Strong axis moment in bridge girder under temperature loads

Temp plus 10deg - Torsional moment
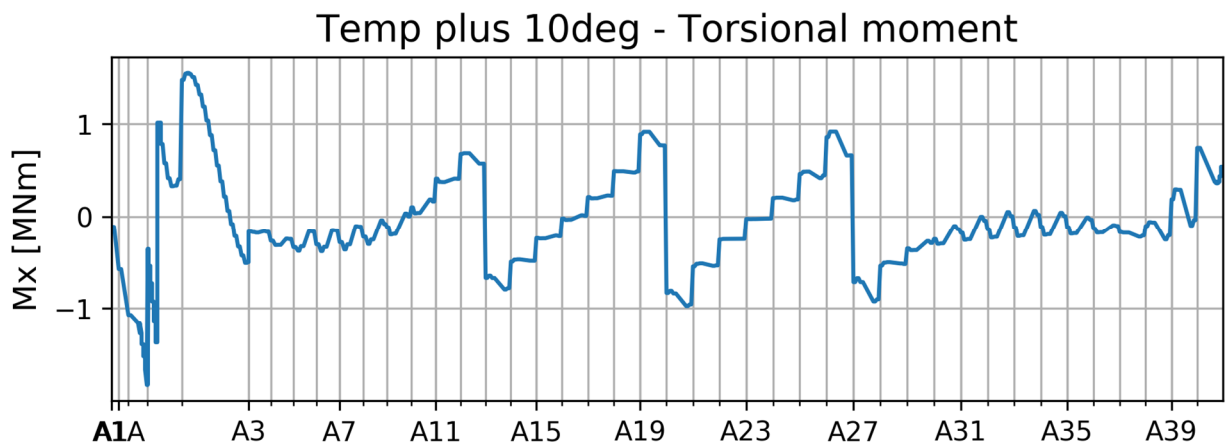
Figure 5-11   Torsional moment in bridge girder under temperature loads.

5.3.4 Tidal loads

The loads induced by a 1-metre variation of the water level are studied in this section. The results for a decrease in the water level show a linear response. The following figures summarize the main loads due to water level variations.
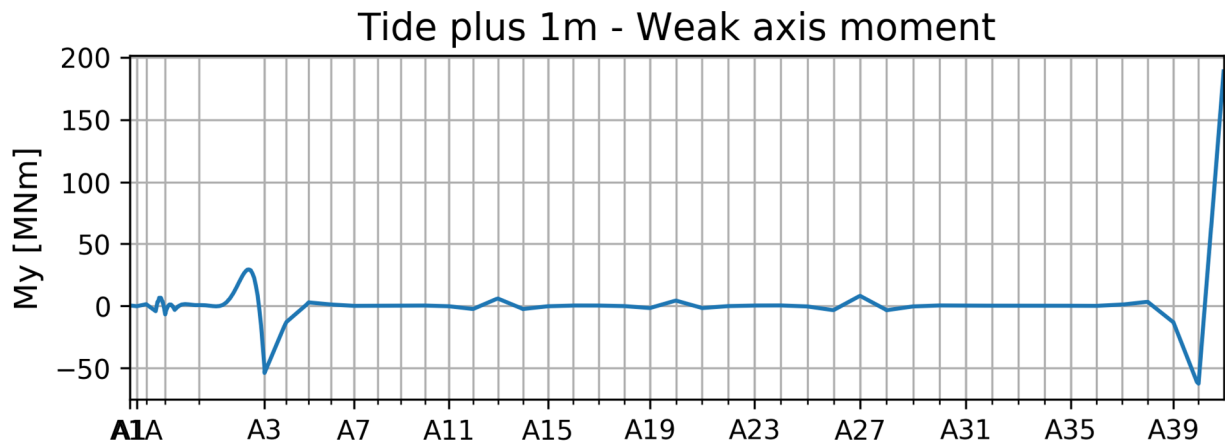
Figure 5-12   Weak axis moment in bridge girder under tide variations
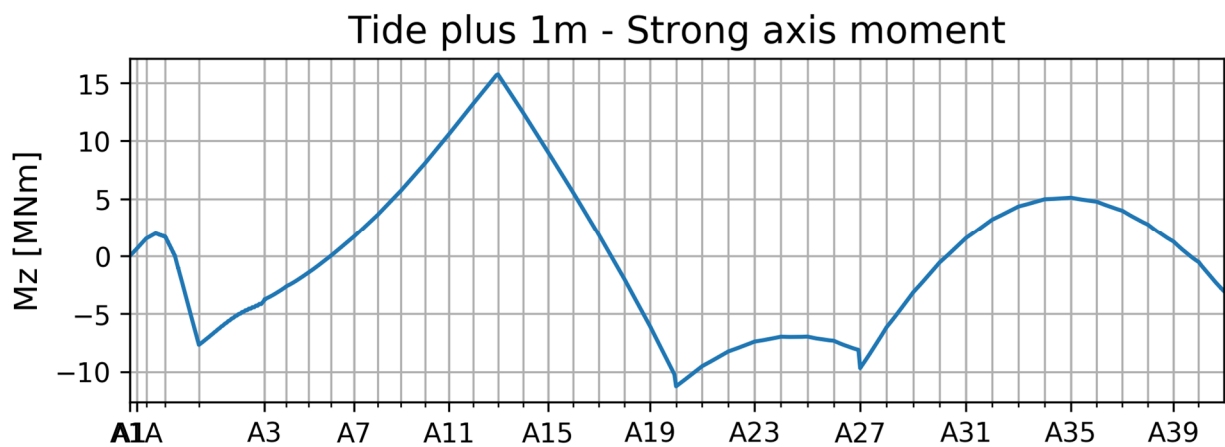
Figure 5-13   Strong axis moment in bridge girder under tide variations
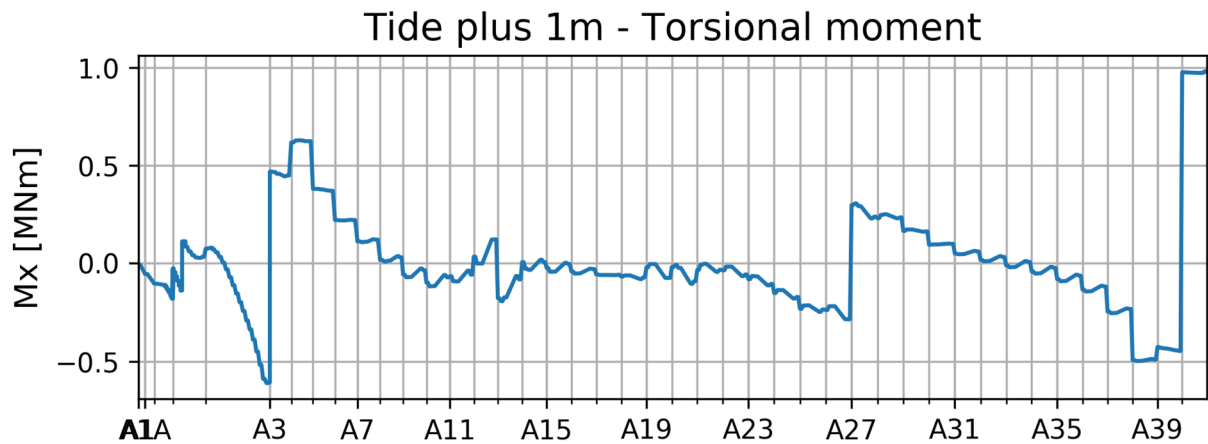
Figure 5-14 Torsional moment in bridge girder under tide variations

5.4 Environmental load effects

5.4.1 General

Wave-, wind- and current loading is calculated simultaneously based on the SIMO-RIFLEX coupled analysis model. An initial screening analysis is performed for a reduced number of wave- and wind realizations to identify the governing conditions. The 1-, 100- and 10000-year loads are calculated for those governing conditions, assuming they do not vary across return periods.

The sea states are denoted by the following notation: *XXXyy_ZZZ*, where:

- *XXX* corresponds to the return period: *1*, *100* or *10000*.

- *yy* identifies the dominating wave component: *wa* for wind waves or *sw* for swell.

- *ZZZ* corresponds to the wind-, wind waves- and current incoming direction in degrees.

5.4.2 100-years return period conditions screening analyses

A screening analysis is performed for all the directions using 5 wave realizations to estimate the 90% fractile maximum of the different loads and stresses. Both wind wave dominating- and swell dominating load cases are tested. A summary of the analysis parameters is included in Table 5-2 and the applied sea states are presented in Table 5-3..

Table 5-2 Analysis parameters for the 100-years return period conditions screening analysis

Analysis parameter	Value
Wind-, wind waves- and current headings	From 0 to 330 degrees every 30 degrees
Effective analysis duration (after transient effects)	10800 seconds
Number of wave-, wind realizations	5

Table 5-3 Environmental conditions for the 100-years return period conditions screening analysis

Case id	Wind waves			Swell			Wind		Current	
	Hs [m]	Tp [s]	Dir. [deg]	Hs [m]	Tp [s]	Dir. [deg]	Velocity [m/s]	Dir. [deg]	Velocity [m/s]	Dir. [deg]
ULS_100wa_000	0.76	4.00	0				22.2	0	0.80	0
ULS_100wa_030	0.66	4.20	30				22.2	30	0.88	30
ULS_100wa_060	0.85	4.10	60				22.2	60	0.97	60
ULS_100wa_090	1.98	5.50	90				26.9	90	1.08	90
ULS_100wa_120	1.32	4.60	120				26.9	120	0.81	120
ULS_100wa_150	1.13	4.00	150				26.9	150	0.90	150
ULS_100wa_180	1.13	3.90	180				26.9	180	1.34	180
ULS_100wa_210	1.32	4.60	210	0.26	12	320	26.9	210	1.53	210
ULS_100wa_240	1.32	4.00	240	0.26	12	320	28.5	240	1.46	240
ULS_100wa_270	1.70	4.50	270	0.26	12	320	31.7	270	1.13	270
ULS_100wa_300	1.89	5.20	300	0.26	12	320	31.7	300	0.91	300
ULS_100wa_330	1.13	4.60	330	0.26	12	320	31.7	330	0.80	330
ULS_100sw_210	1.12	4.30	210	0.31	12	320	23.5	210	1.26	210
ULS_100sw_240	1.03	3.60	240	0.31	12	320	24.8	240	1.21	240
ULS_100sw_270	1.31	4.00	270	0.31	12	320	27.6	270	0.94	270
ULS_100sw_300	1.49	4.80	300	0.31	12	320	27.6	300	0.76	300
ULS_100sw_330	0.84	4.10	330	0.31	12	320	27.6	330	0.66	330

The selection of the governing sea states is based on the conditions resulting on the envelope of the combined stresses at all the knuckle points in the cross sections along the bridge girder, as defined in Figure 4-2. As an example, Figure 5-15 shows the combined stress at Point 2, while Figure 5-16 shows the same results for the selected governing conditions.
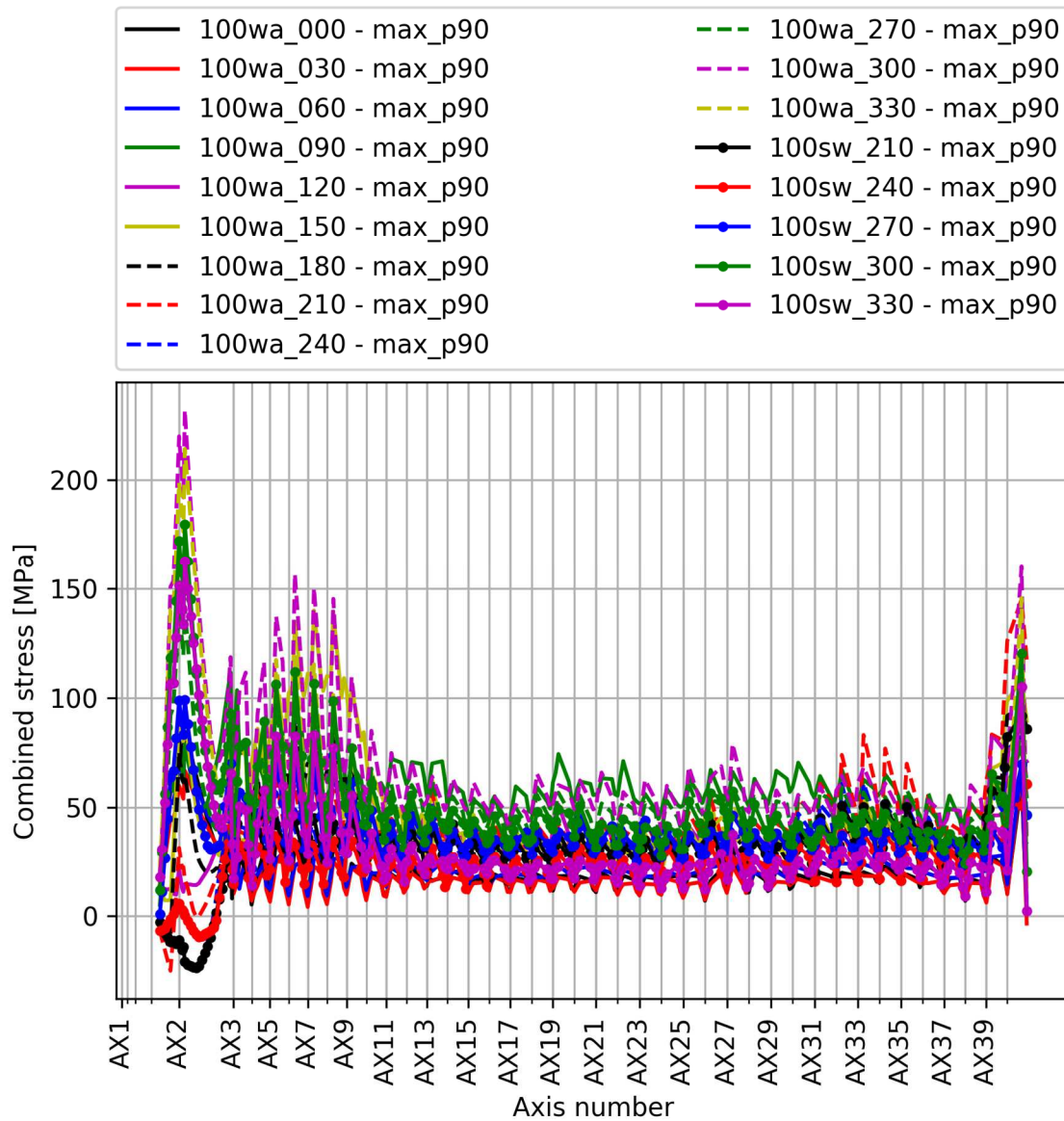
Figure 5-15 Combined stress at Point 2 based on the 100-years return period condition screening analysis
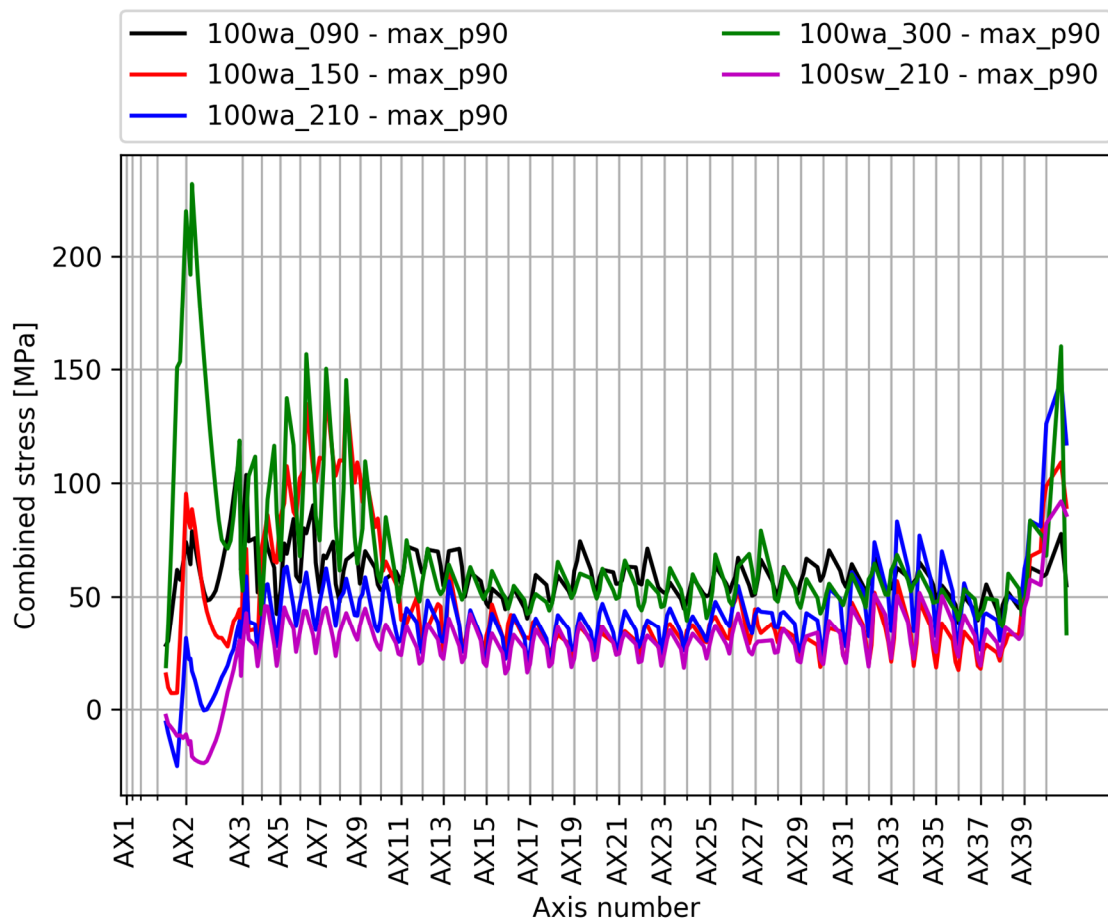
Figure 5-16   Combined stress at Point 2 based on the 100-years return period condition governing conditions

5.4.3   100-years return period conditions analysis of the governing conditions

The 90% fractile loads and stresses are calculated based on 30 different wave- and wind- realizations, as indicated in Table 5-4. The five governing sea states are presented in Table 5-5.

Table 5-4   Analysis parameters for the 100-years return period conditions analysis

Analysis parameter	Value
Wind-, wind waves- and current headings	Wind wave dominating: 90, 150, 210, 300 degrees Swell dominating:210 degrees
Effective analysis duration (after transient effects)	10800 seconds
Number of wave-, wind realizations	30

Table 5-5 Environmental conditions for the 100-years return period conditions analysis

Case id	Wind waves			Swell			Wind		Current	
	Hs [m]	Tp [s]	Dir. [deg]	Hs [m]	Tp [s]	Dir. [deg]	Velocity [m/s]	Dir. [deg]	Velocity [m/s]	Dir. [deg]
100wa_090	1.98	5.50	90				26.9	90	1.08	90
100wa_150	1.13	4.00	150				26.9	150	0.90	150
100wa_210	1.32	4.60	210	0.26	12	320	26.9	210	1.53	210
100wa_300	1.89	5.20	300	0.26	12	320	31.7	300	0.91	300
100sw_210	1.12	4.30	210	0.31	12	320	23.5	210	1.26	210

Figure 5-17includes the 100-years return period combined stress at Point 2 in the bridge girder. There are minor differences between these results and those shown in Figure 5-16.
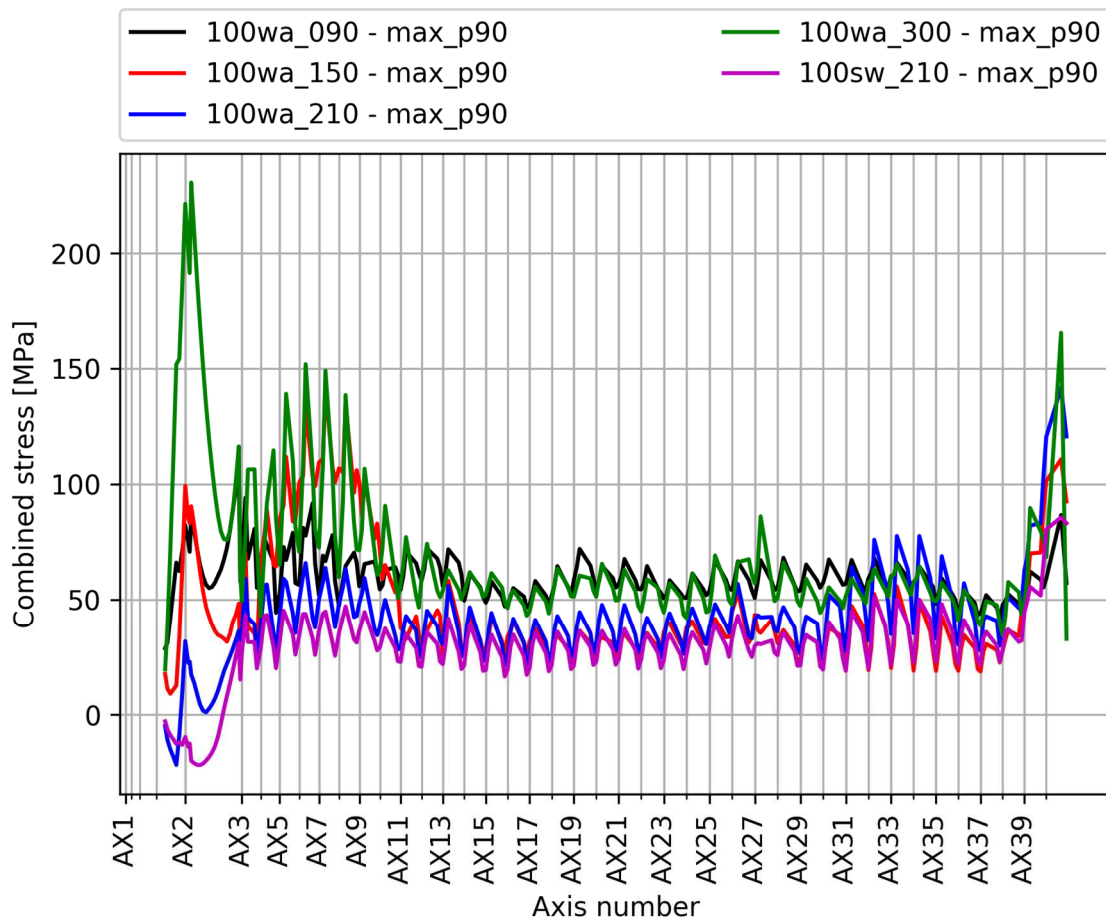
Figure 5-17 Combined stress at Point 2 in the governing 100-years conditions

The environmental load effects for the different 100-year sea states listed in Table 5-5 are presented in the following figures. Permanent loads are subtracted, isolating the effect of dynamic loads.
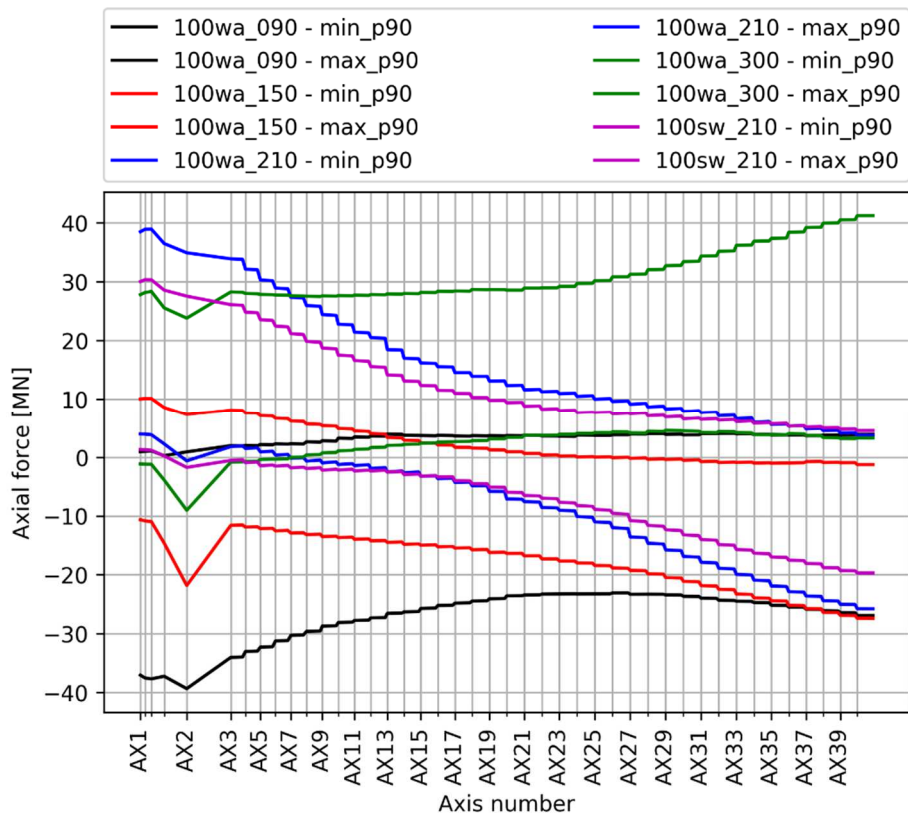
Figure 5-18   Axial force for the 100-year return period load cases
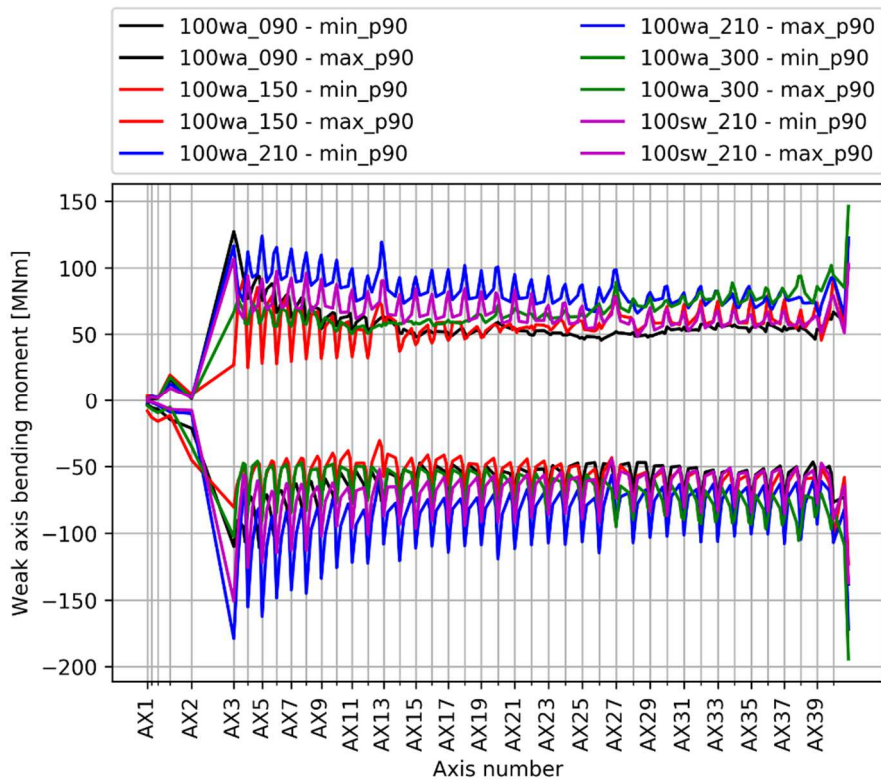
Figure 5-19   Weak axis bending moment for the 100-year return period load cases
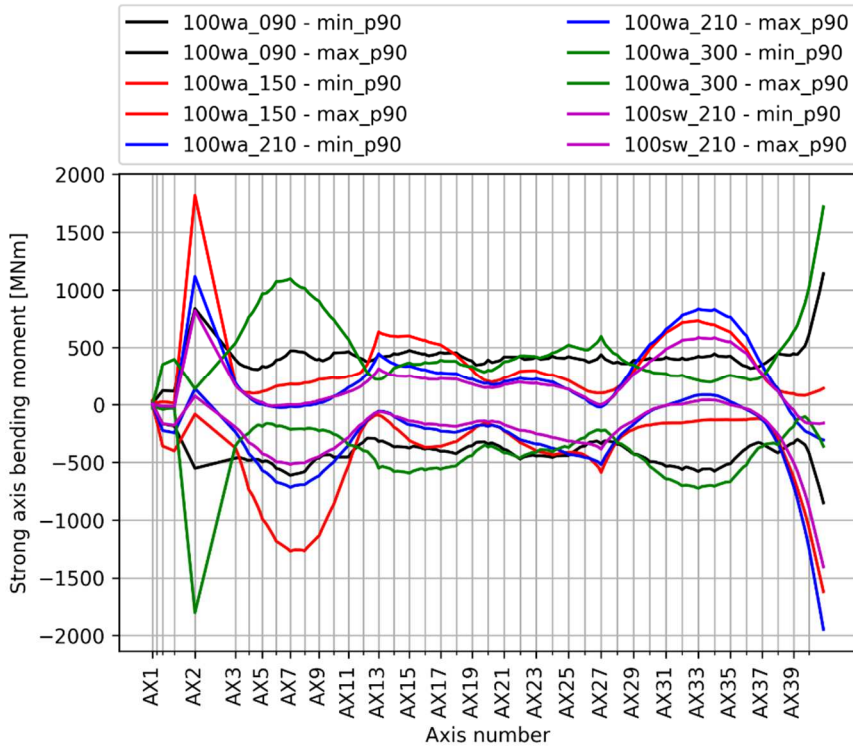
Figure 5-20   Strong axis bending moment for the 100-year return period load cases
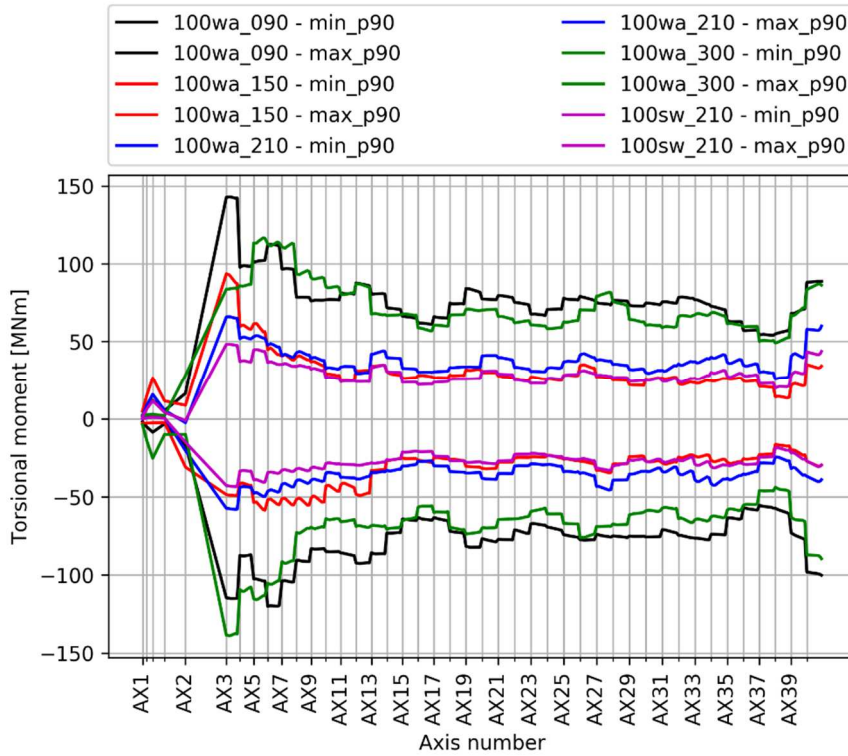
Figure 5-21   Torsional moment for the 100-year return period load cases
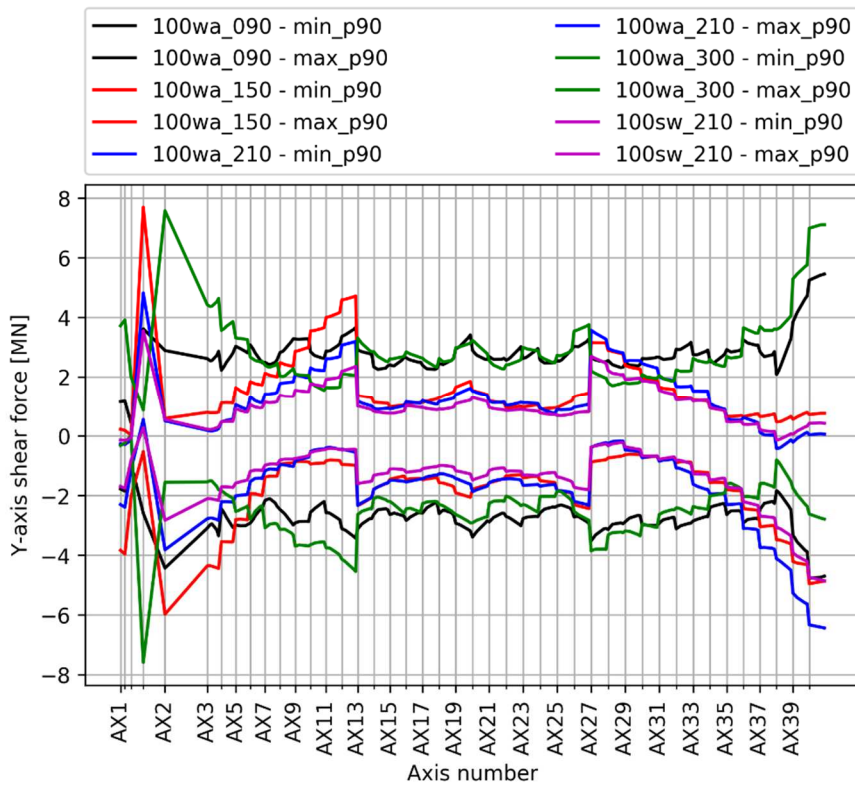
Figure 5-22   Transverse shear force for the 100-year return period load cases
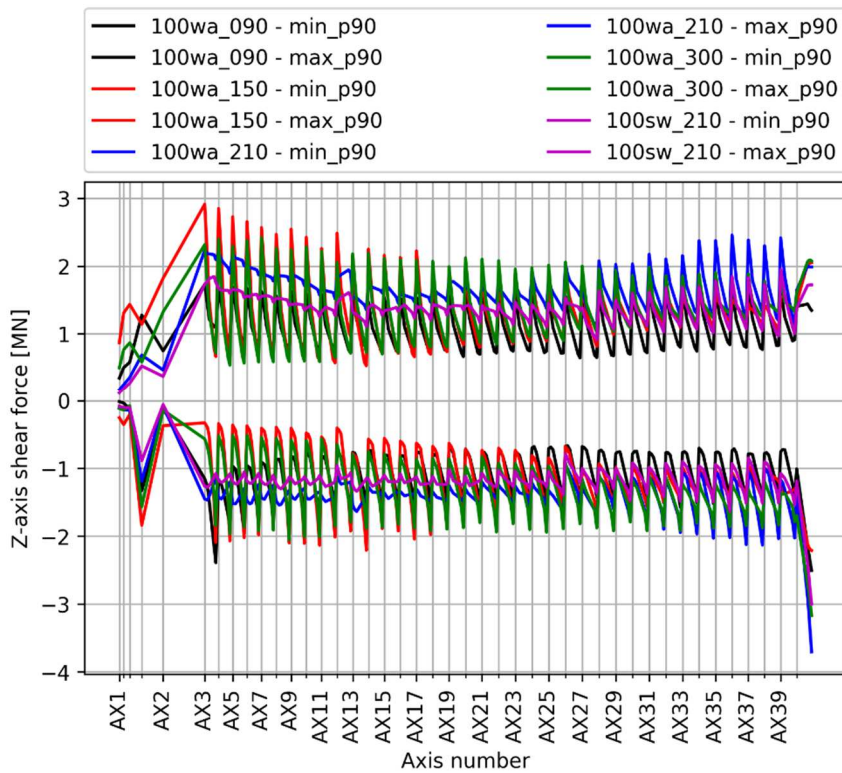
Figure 5-23   Vertical shear force for the 100-year return period load cases

5.4.4 1-year return period conditions analysis of the governing conditions

The analysis of the 1-year return period conditions is equivalent to the 100-years return period conditions analysis. However, as indicated in Table 5-7, only four conditions are analysed, since the swell dominating sea state in 210 degrees direction becomes the same as the *1wa_210* case.

Figure 5-24 presents the results for the combined stress at Point 3 for comparison against the 100-years return period results.

Table 5-6   Analysis parameters for the 1-year return period conditions analysis

Analysis parameter	Value
Wind-, wind waves- and current headings	90, 150, 210, 300 degrees
Effective analysis duration (after transient effects)	10800 seconds
Number of wave-, wind realizations	30

Table 5-7   Environmental conditions for the 1-year return period conditions analysis

Case id	Wind waves			Swell			Wind		Current	
	Hs [m]	Tp [s]	Dir. [deg]	Hs [m]	Tp [s]	Dir. [deg]	Velocity [m/s]	Dir. [deg]	Velocity [m/s]	Dir. [deg]
1wa_090	0.92	4.00	90				19.5	90	0.69	90
1wa_150	0.83	3.40	150				19.5	150	0.57	150
1wa_210	0.83	3.70	210	0.20	12	320	19.5	210	0.98	210
1wa_300	1.10	4.30	300	0.20	12	320	22.9	300	0.58	300
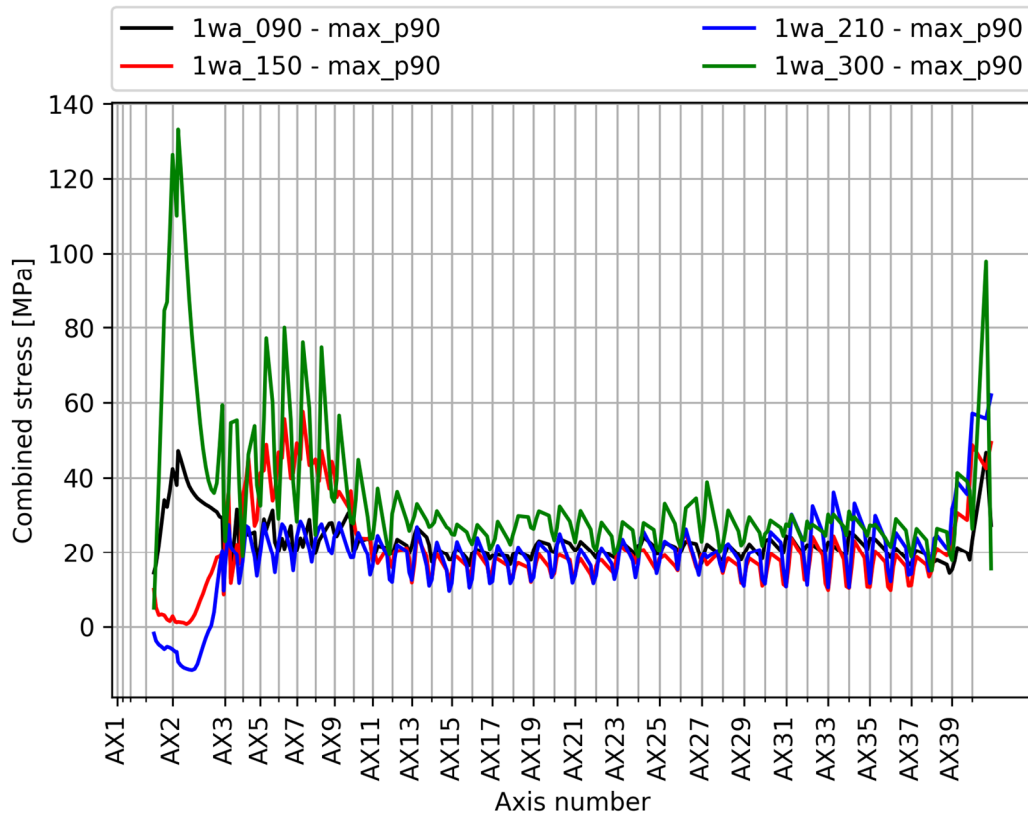
Figure 5-24   Combined stress at Point 2 in the governing 1-year conditions.

5.4.5 10000-years return period conditions analysis of the governing conditions

The analysis of the 10000-years conditions is carried out for the same governing conditions as selected above, with the same analysis parameters as the 1- and 100-years return period analyses, see Table 5-8. The analysed sea states are given in Table 5-9.

The combined stresses for Point 2 are presented in Figure 5-25.

Table 5-8 Analysis parameters for the 10000-years return period conditions analysis

Analysis parameter	Value
Wind-, wind waves- and current headings	Wind wave dominating: 90, 150, 210, 300 degrees Swell dominating:210 degrees
Effective analysis duration (after transient effects)	10800 seconds
Number of wave-, wind realizations	30

Table 5-9 Environmental conditions for the 10000-years return period conditions analysis

Case id	Wind waves			Swell			Wind		Current	
	Hs [m]	Tp [s]	Dir. [deg]	Hs [m]	Tp [s]	Dir. [deg]	Velocity [m/s]	Dir. [deg]	Velocity [m/s]	Dir. [deg]
10000wa_090	2.97	6.50	90				32.6	90	1.47	90
10000wa_150	1.53	4.70	150				32.6	150	1.22	150
10000wa_210	1.73	5.20	210	0.31	12	320	32.6	210	2.07	210
10000wa_300	2.59	5.90	300	0.31	12	320	38.4	300	1.24	300
10000sw_210	1.32	4.60	210	0.42	12	320	26.9	210	1.53	210
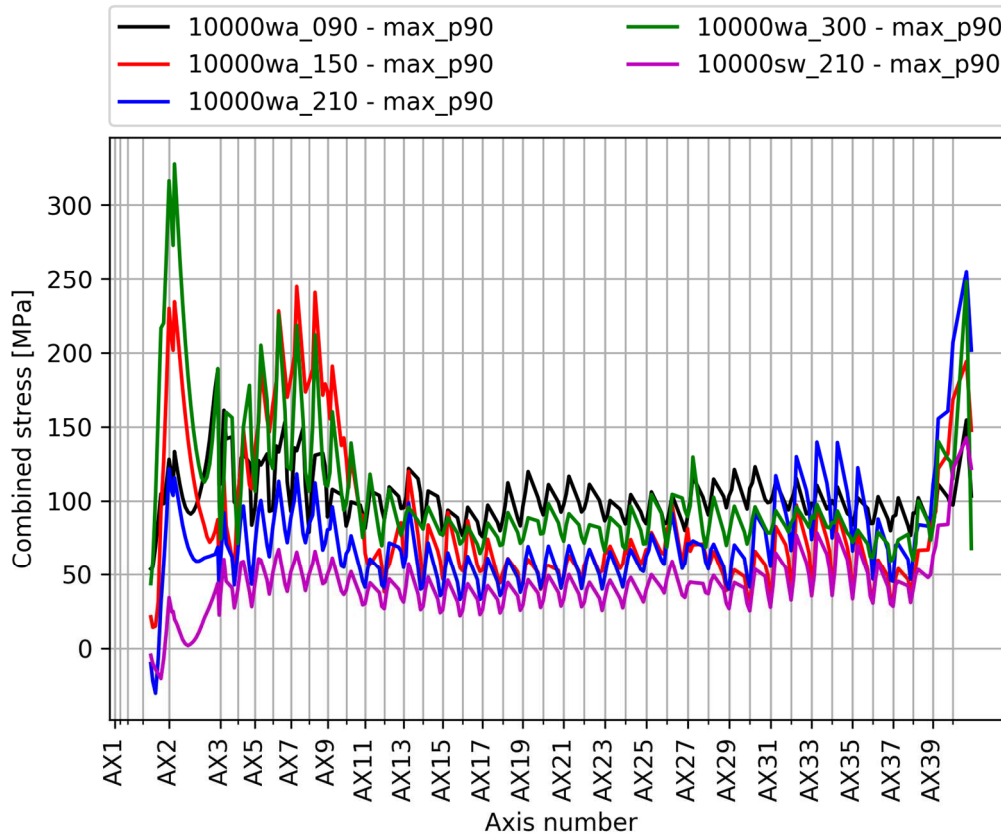
Figure 5-25   Combined stress at Point 2 in the governing 10000-years conditions.

5.4.6 Sensitivity analyses

5.4.6.1 General

A series of sensitivity analyses are performed with two objectives: to validate some of the assumptions made in the independent analyses; and to gain knowledge on the dynamic behaviour of the curved bridge concept.

5.4.6.2 Wind waves peak period

A sensitivity analysis on the wave peak period is run for the governing conditions. Reported results are based on 5 different wave realizations. Table 5-10 and Table 5-11 present the basis for the analysis.

In general, longer peak periods have a large impact on girder stresses. Those sea conditions excite some longer torsional and horizontal bending eigen modes around 7 seconds. Then, the stresses are increased by up to 50%. However, it should be noted that the 100-years return period Hs-Tp contour is not applied, so the results are too conservative.

Figure 5-26 and Figure 5-27 show the effect of the wind wave period on the combined stress at Point 2 for two incoming wave directions.

Table 5-10   Analysis parameters for the 100-years return period conditions analysis

Analysis parameter	Value
Wind-, wind waves- and current headings	Wind wave dominating: 90, 150, 210, 300 degrees Swell dominating:210 degrees
Effective analysis duration (after transient effects)	10800 seconds
Number of wave-, wind realizations	5

Table 5-11   Environmental conditions for the 100-years return period conditions analysis

Case id	Wind waves			Swell			Wind		Current	
	Hs [m]	Tp [s]	Dir. [deg]	Hs [m]	Tp [s]	Dir. [deg]	Velocity [m/s]	Dir. [deg]	Veloci ty [m/s]	Dir. [deg]
100wa_090_tp4.68	1.98	4.68	90	0.001	5.00	0	26.9	90	1.08	90
100wa_090_tp4.95	1.98	4.95	90	0.001	5.00	0	26.9	90	1.08	90
100wa_090_tp6.05	1.98	6.05	90	0.001	5.00	0	26.9	90	1.08	90
100wa_090_tp6.60	1.98	6.60	90	0.001	5.00	0	26.9	90	1.08	90
100wa_150_tp3.40	1.13	3.40	150	0.001	5.00	0	26.9	150	0.90	150
100wa_150_tp3.60	1.13	3.60	150	0.001	5.00	0	26.9	150	0.90	150
100wa_150_tp4.40	1.13	4.40	150	0.001	5.00	0	26.9	150	0.90	150
100wa_150_tp4.80	1.13	4.80	150	0.001	5.00	0	26.9	150	0.90	150
100wa_210_tp3.91	1.32	3.91	210	0.257	12.00	320	26.9	210	1.53	210
100wa_210_tp4.14	1.32	4.14	210	0.257	12.00	320	26.9	210	1.53	210
100wa_210_tp5.06	1.32	5.06	210	0.257	12.00	320	26.9	210	1.53	210
100wa_210_tp5.52	1.32	5.52	210	0.257	12.00	320	26.9	210	1.53	210
100wa_300_tp4.42	1.89	4.42	300	0.257	12.00	320	31.7	300	0.91	300
100wa_300_tp4.68	1.89	4.68	300	0.257	12.00	320	31.7	300	0.91	300
100wa_300_tp5.72	1.89	5.72	300	0.257	12.00	320	31.7	300	0.91	300
100wa_300_tp6.24	1.89	6.24	300	0.257	12.00	320	31.7	300	0.91	300
100sw_210_tp3.66	1.12	3.66	210	0.312	12.00	320	23.5	210	1.26	210
100sw_210_tp3.87	1.12	3.87	210	0.312	12.00	320	23.5	210	1.26	210
100sw_210_tp4.73	1.12	4.73	210	0.312	12.00	320	23.5	210	1.26	210
100sw_210_tp5.16	1.12	5.16	210	0.312	12.00	320	23.5	210	1.26	210
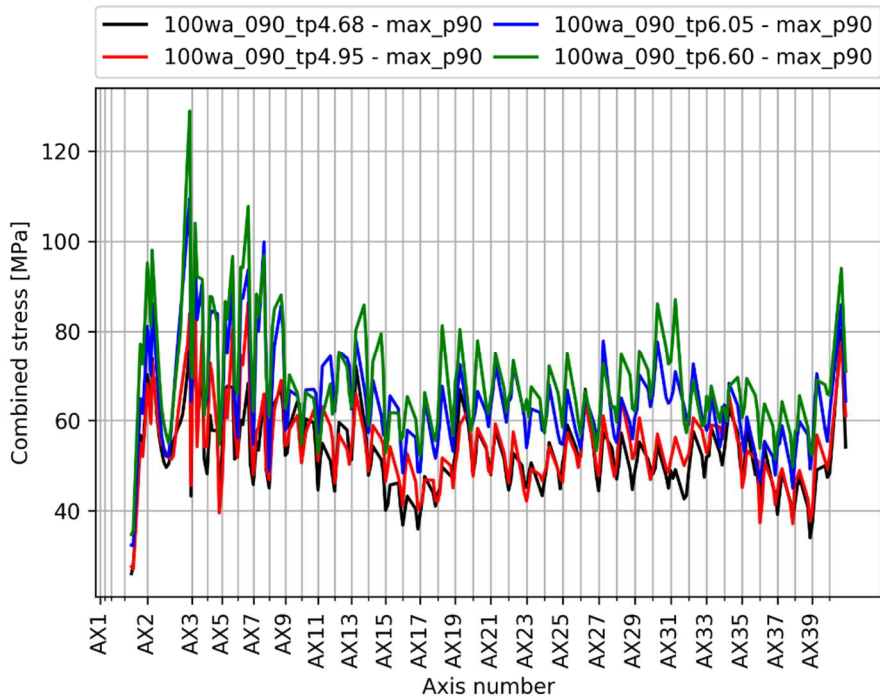
Figure 5-26   Combined stress at Point 2 for the 90 degrees sea states
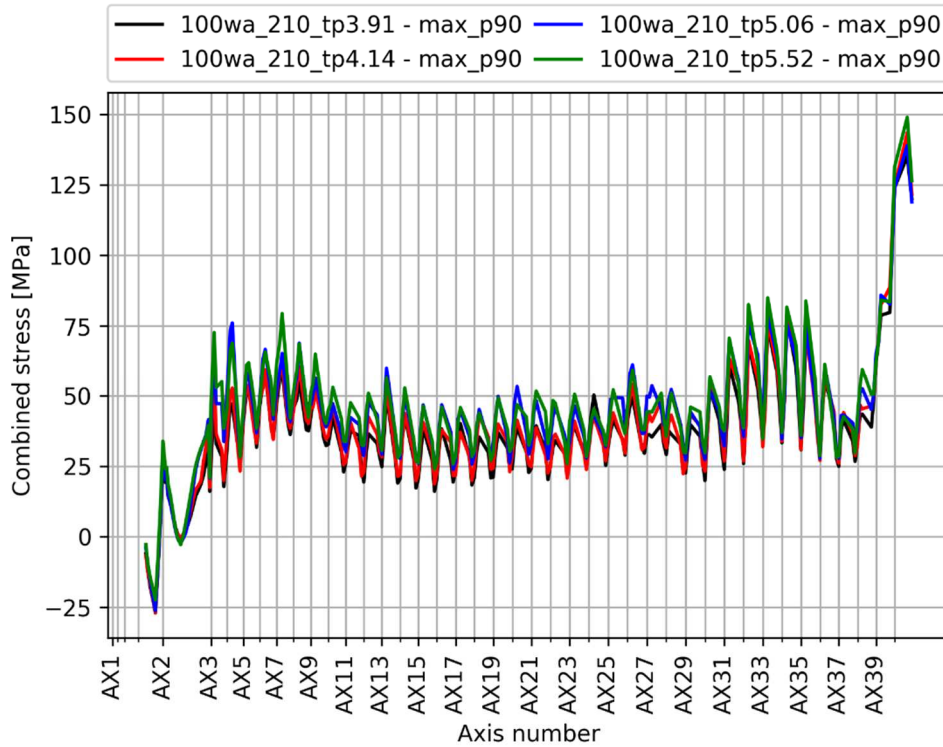
Figure 5-27   Combined stress at Point 2 for the 210 degrees sea states

5.4.6.3 Swell peak period

The influence of the swell peak period on the bridge girder stresses is evaluated. The Metocean design basis /11/ defines a set of scaling factors for the swell significant wave height depending on the peak period, included in Table 3-36. Table 5-13 summarizes all the environmental conditions analysed as per Table 5-12.

As shown in Figure 5-28, there is little impact of swell peak period on the combined stress for Point 2.

Table 5-12   Analysis parameters for the 100-years return period conditions analysis

Analysis parameter	Value
Wind-, wind waves- and current headings	Swell dominating:210 degrees
Effective analysis duration (after transient effects)	10800 seconds
Number of wave-, wind realizations	5

Table 5-13   Environmental conditions for the 100-years return period conditions analysis

Case id	Wind waves			Swell			Wind		Current	
	Hs [m]	Tp [s]	Dir. [deg]	Hs [m]	Tp [s]	Dir. [deg]	Velocity [m/s]	Dir. [deg]	Velocity [m/s]	Dir. [deg]
100sw_210_tp6	1.12	4.30	210	0.16	6.00	320	23.5	210	1.26	210
100sw_210_tp7	1.12	4.30	210	0.18	7.00	320	23.5	210	1.26	210
100sw_210_tp8	1.12	4.30	210	0.21	8.00	320	23.5	210	1.26	210
100sw_210_tp9	1.12	4.30	210	0.23	9.00	320	23.5	210	1.26	210
100sw_210_tp10	1.12	4.30	210	0.26	10.00	320	23.5	210	1.26	210
100sw_210_tp11	1.12	4.30	210	0.29	11.00	320	23.5	210	1.26	210
100sw_210	1.12	4.30	210	0.31	12.00	320	23.5	210	1.26	210
100sw_210_tp18	1.12	4.30	210	0.31	18.00	320	23.5	210	1.26	210
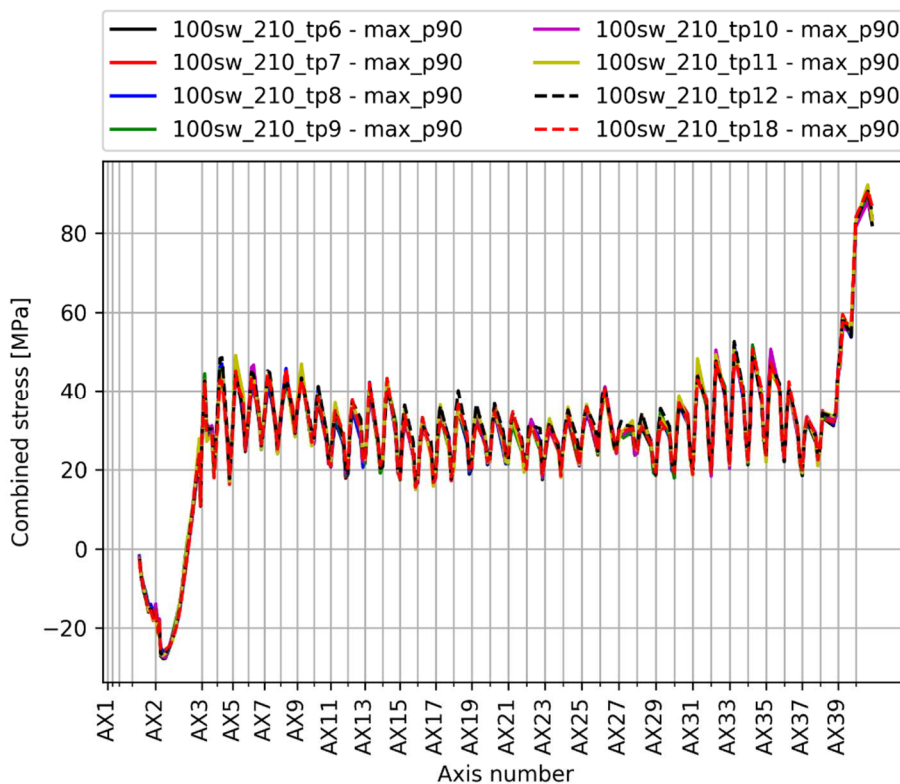
Figure 5-28   Combined stress at Point 2 for the swell peak period sensitivity analysis

5.4.6.4 Relative contribution of environmental loads

The relative importance of each of the environmental load contributions is examined in this section. The following figures present how wind-, current-, swell- and wind waves- loads compared to the resultant load from the 100-years return period analysis.

As it can be observed in the figures, wind waves are the main contributor to weak axis bending and torsional moments, while wind is the main source of strong axis bending moment. Current damping is expected to contribute more than the drag forces current may produce.
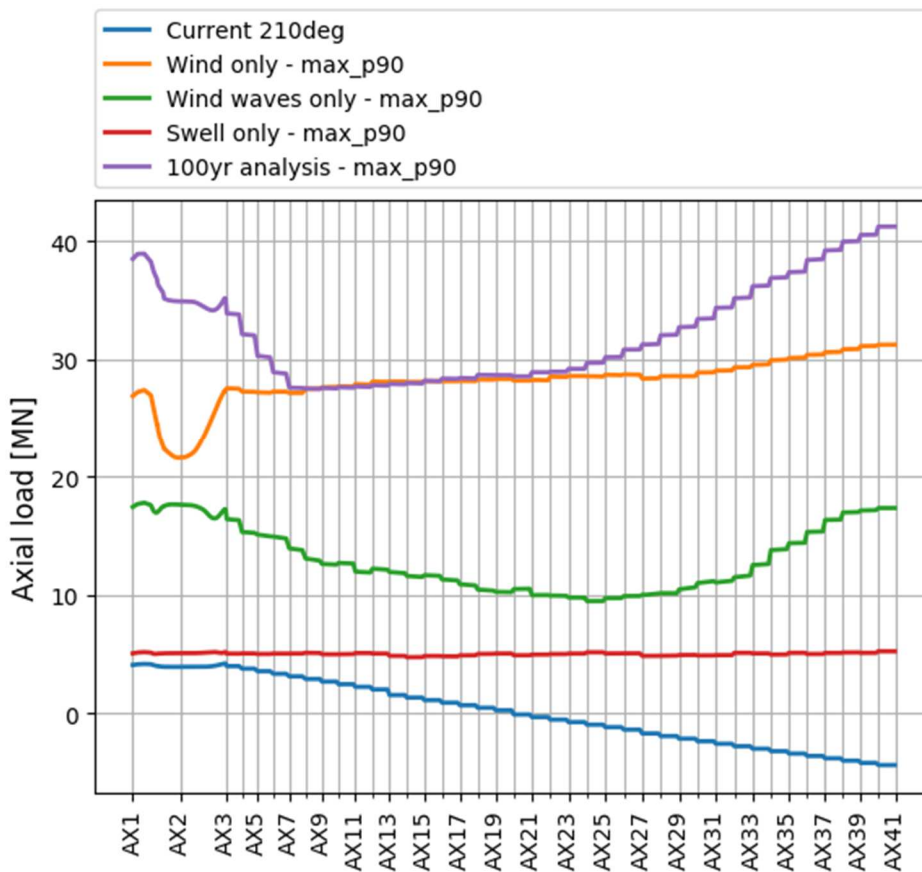
Figure 5-29 Axial force from the 100-years return period environment
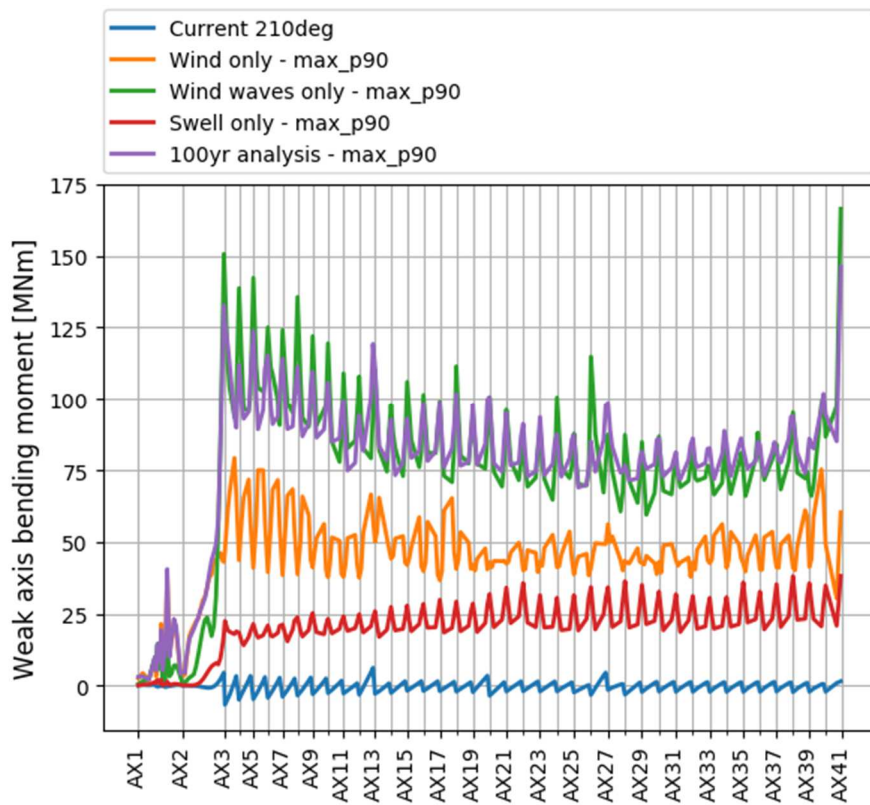
Figure 5-30   Weak axis bending moment from the 100-years return period environment
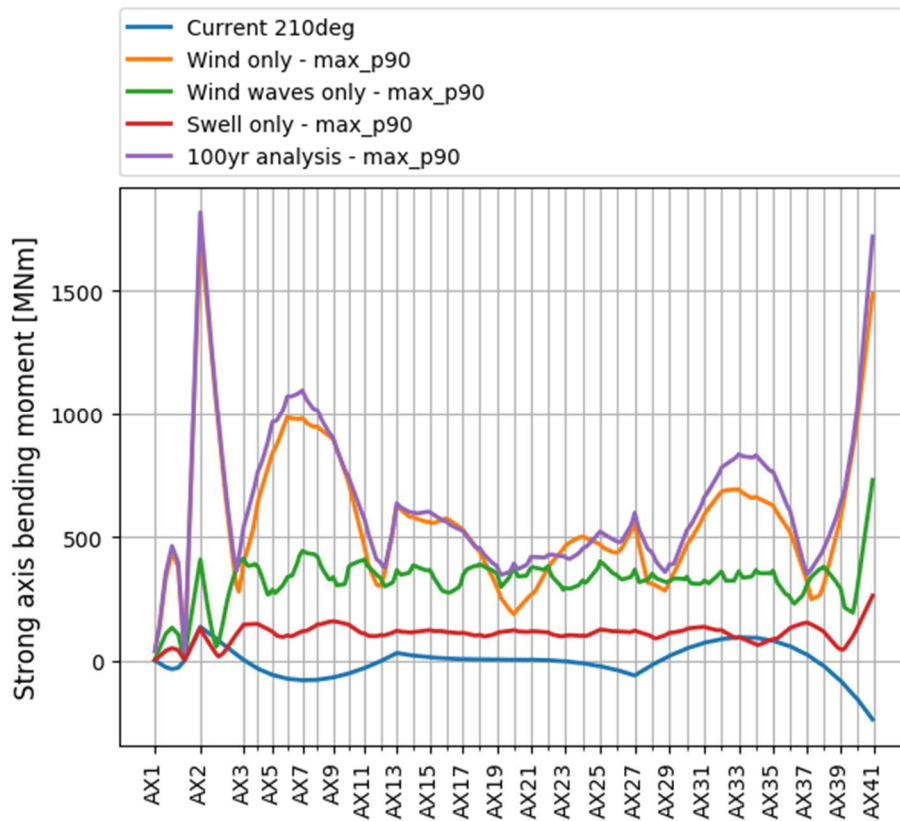
Figure 5-31   Strong axis bending moment from the 100-years return period environment
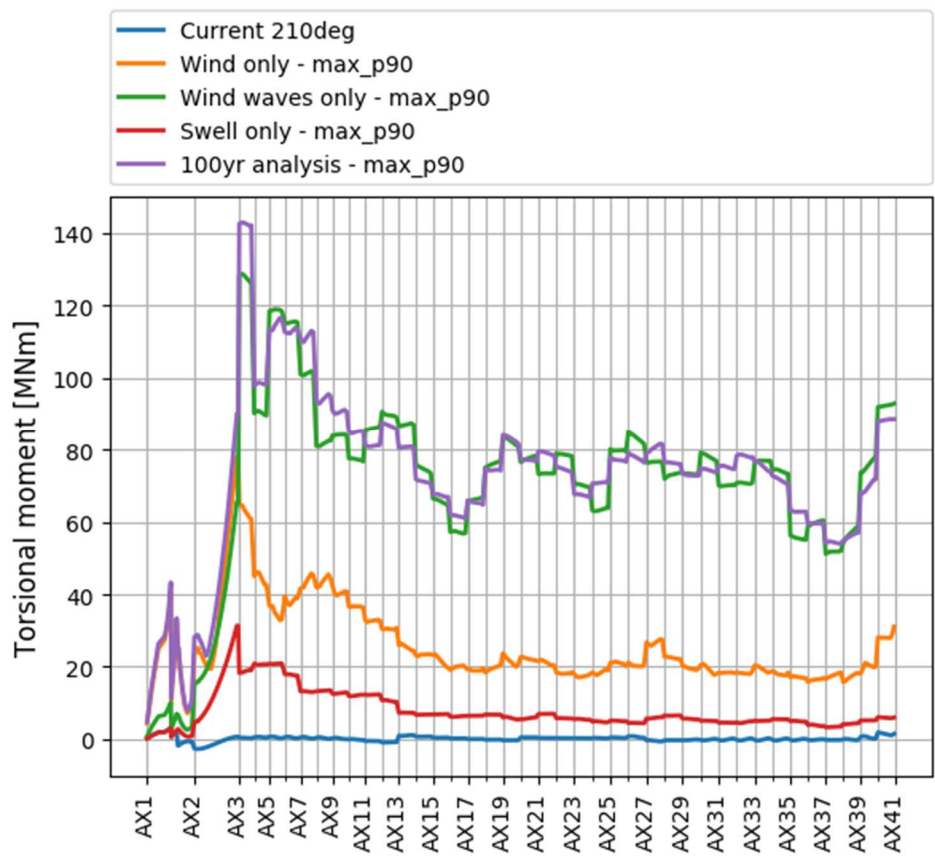
Figure 5-32   Torsional moment from the 100-years return period environment

5.5 Mooring line loads

5.5.1 ULS condition

Maximum 100-year return period line tensions are presented in Figure 5-33 for both the screening and the governing condition analyses. As it can be observed, the governing conditions for the bridge girder are also the critical conditions for the mooring system.

Maximum 100-year return period line tensions for top chain and bottom chain are calculated and compared with maximum tensions from designer /7/, see Figure 5-34 and Figure 5-35. Maximum loaded lines are line 9. The maximum line tension is 5.81 MN at top and 5.53 MN on the bottom. The safety factors are 2.93 and 2.71 correspondingly, which is above the required 2.2.
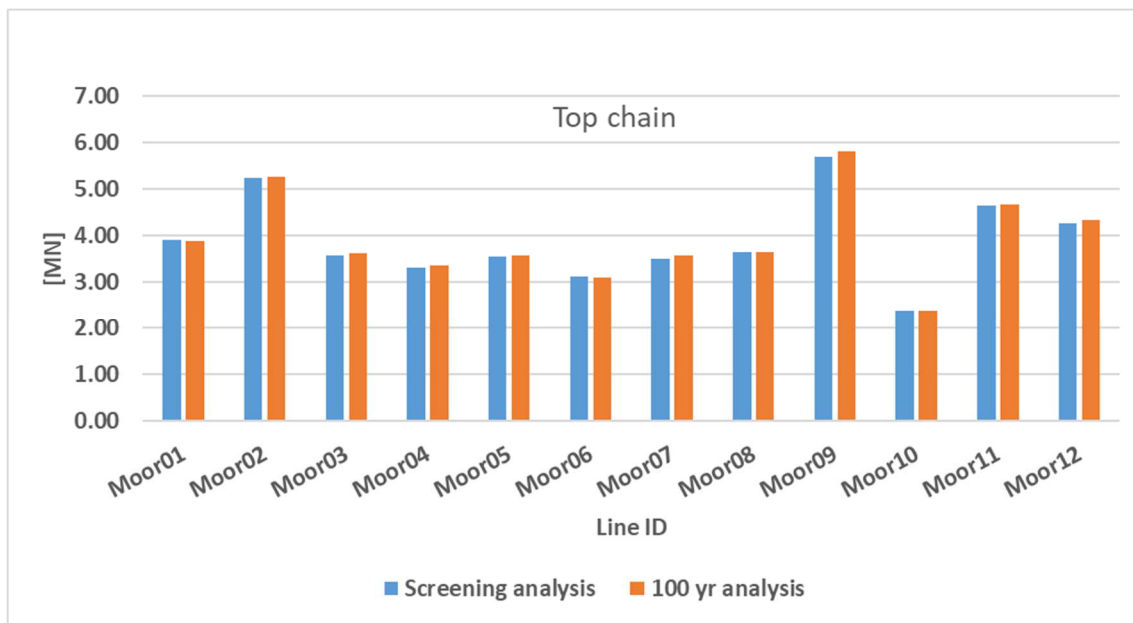
Figure 5-33   Line tension for the 100-year return period conditions
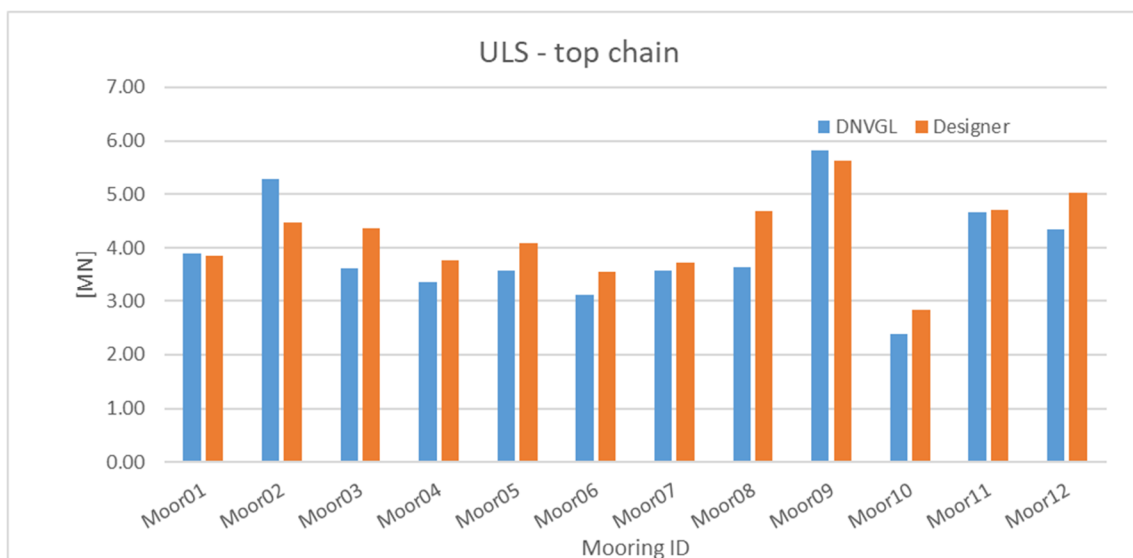
Figure 5-34   Top chain line tension for the 100-year return period conditions calculated by designer and DNVGL.
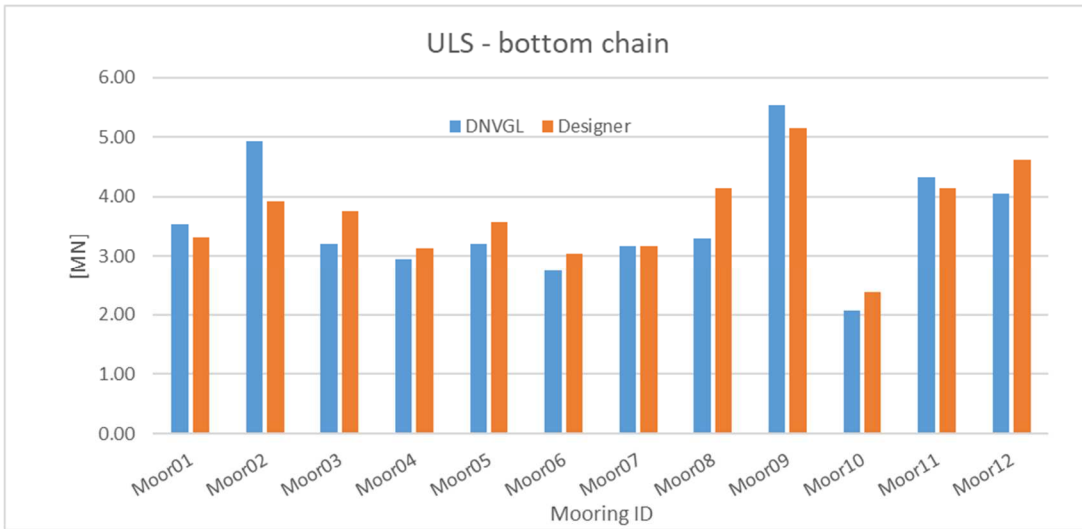
Figure 5-35   Bottom chain line tension for the 100-year return period conditions calculated by designer and DNVGL.

The effect of temperature and water level variations is included in the safety factor calculation by combining the different load cases with the load factors in Table 5-14. It is for later discussion how temperature loads should be included in this calculation.

Maximum mooring tensions under different combined load conditions are shown in Figure 5-36. The maximum line tension is 6.51 MN at top and 6.23 MN on the bottom at line 9. The safety factors are 2.61 and 2.41 correspondingly, which is above the required 2.2.

Table 5-14   Load factors for mooring line load combinations

Load	Load factor
Permanent loads	1.0
Environmental loads without traffic	1.0
Temperature	0.84
Water level variation	1.0
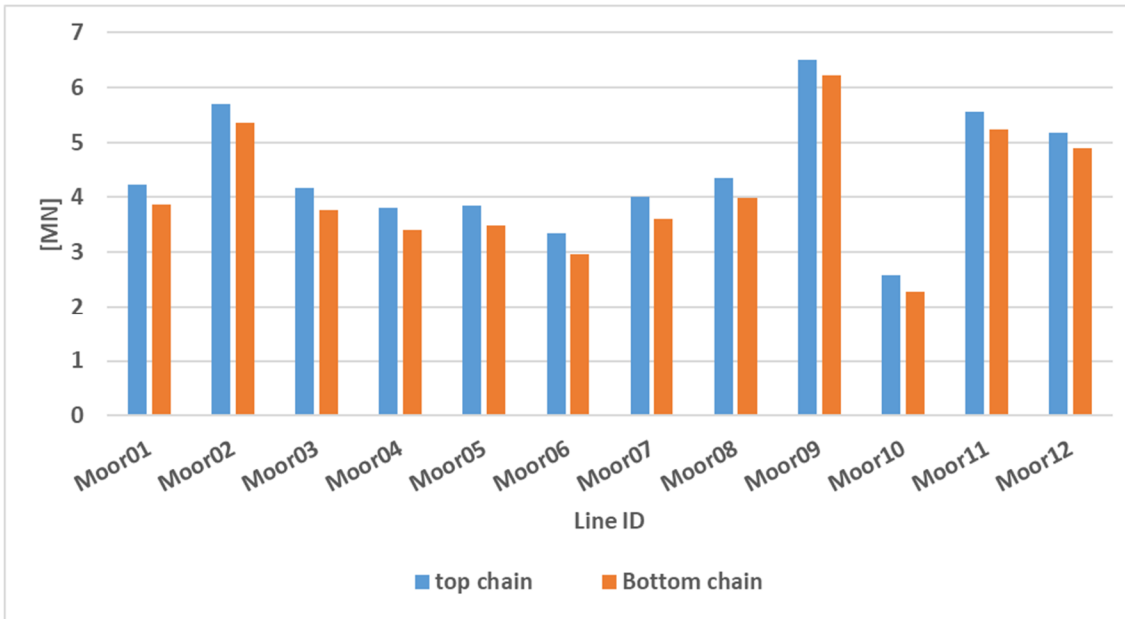
Figure 5-36 Mooring tensions under combined load conditions.

5.5.2 FLS condition

Fatigue analyses of top chain and bottom chain of all mooring lines were performed with the global analysis model. Calculated axial forces are divided by the cross-sectional area of the chain to obtain the fatigue stress. The number of loading cycles for each fatigue stress range is calculated using the rain-flow counting method. A single-slope SN curve is applied as given in DNVGL-OS-E301 /5/.

The initial diameter of top chain is 147 mm, and corrosion allowance is 20 mm. Fatigue calculations uses chain dimensions at mid-life, 142 mm for top chain and 137 mm for bottom chain /7/.

Calculated fatigue life is presented in Figure 5-37 and Table 5-15. As shown in the figure, the line most exposed to fatigue damage is mooring line 2, at top and bottom, with a calculated fatigue life of 524 and 424 years. The design specification requires a design fatigue factor of 10 and an operational fatigue life of 50 years for top chain and 100 years for bottom chain. Simulation results show that fatigue of the top chains fulfil the design's specification, while for bottom chains, more fatigue life is required.

Note that the calculated fatigue life at line 2 by designer is 1200 years and 1000 years for top and bottom chains /16/, which is around 2.3 times larger than the fatigue life presented here. Possible reasons:

- Wind. It is stated that wind is not included in designer's calculation, see /6/ and /16/.

- Current. Current is not considered in the independent analysis. As investigated in Section 5.6.4, current induced damping will reduce the system dynamics, indicating that the independent analysis falls to the conservative side.
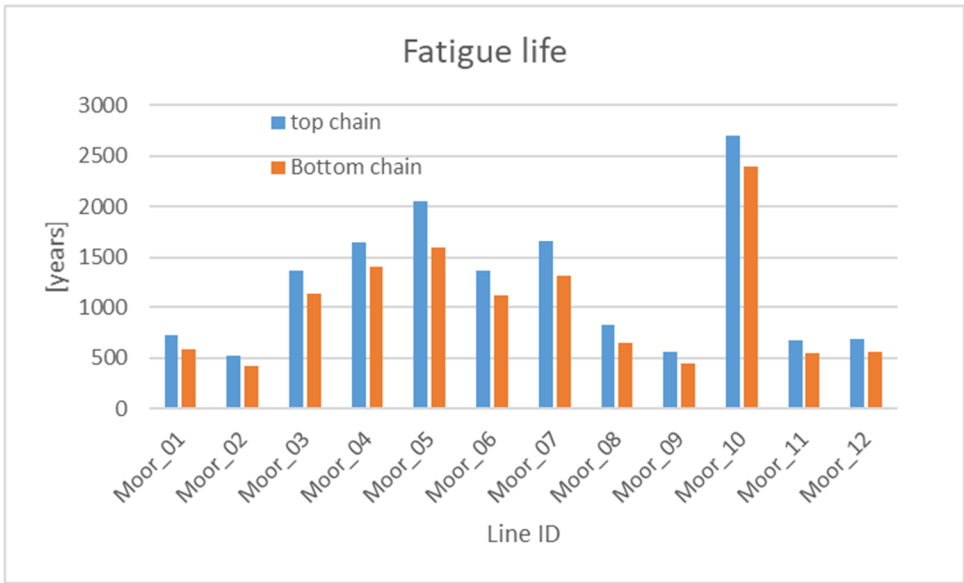
Figure 5-37   Fatigue life of mooring line segments, no DFF is included.

Table 5-15   Obtained and required fatigue life for mooring lines.

Line ID	Top chain		Bottom chain	
	Calculated fatigue life [years]	Required [years]	Calculated fatigue life [years]	Required [years]
Moor_01	721	500	589	1000
Moor_02	524		424	
Moor_03	1365		1137	
Moor_04	1644		1408	
Moor_05	2051		1595	
Moor_06	1367		1118	
Moor_07	1665		1312	
Moor_08	823		648	
Moor_09	554		448	
Moor_10	2698		2391	
Moor_11	673		545	
Moor_12	690		559	

5.6 Comparison against designer's analysis

5.6.1 Natural periods and modes

Comparison of natural periods is presented in Table 5-16 and Figure 5-38. The agreement between the two calculations is good.

Table 5-16   Comparison of the first 10 transverse natural periods

Mode	Designer – Orcaflex /14/	DNVGL – SIMO-Riflex
1st transverse mode	56.29	55.56
2nd transverse mode	43.19	44.84
3rd transverse mode	31.03	31.35
4th transverse mode	21.42	21.69
5th transverse mode	17.07	17.15
6th transverse mode	13.44	13.61
7th transverse mode	12.75	12.76
8th transverse mode	10.28	10.31
9th transverse mode	9.48	9.31
1^{0th} transverse mode	8.36	8.52
1st vertical mode	6.91	6.89
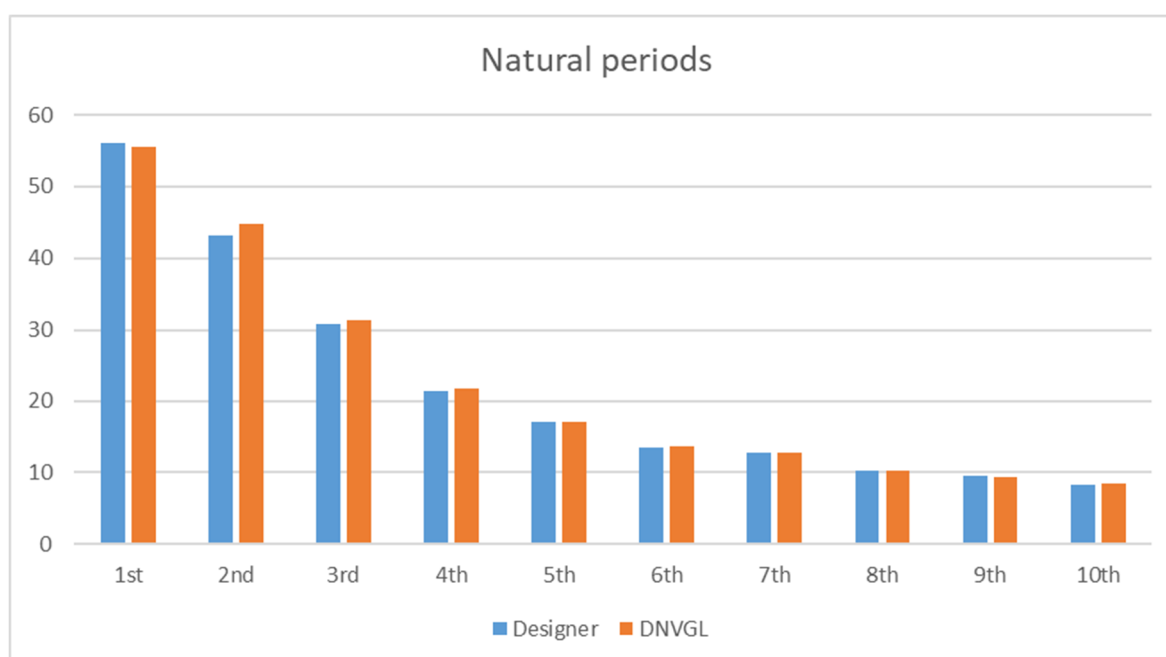
Figure 5-38   Transverse eigen-periods comparison. First 10 modes.

5.6.2 Permanent loads

Loads distribution along the bridge girder together with designer's results are presented here. Comparisons show that:

- Axial loads compared quite well. Minimum loads occur at Axis2, with a magnitude around 100 MN;

- Variations of vertical shear loads are quite similar, indicating a good agreement of gravity and buoyancy distributions.

- Similar variations of weak axis moment are found. The designer uses an opposition sign definition.

- The differences observed in strong axis moment is believed due to the mooring line tensions;

- Torsion and transverse shear are small.
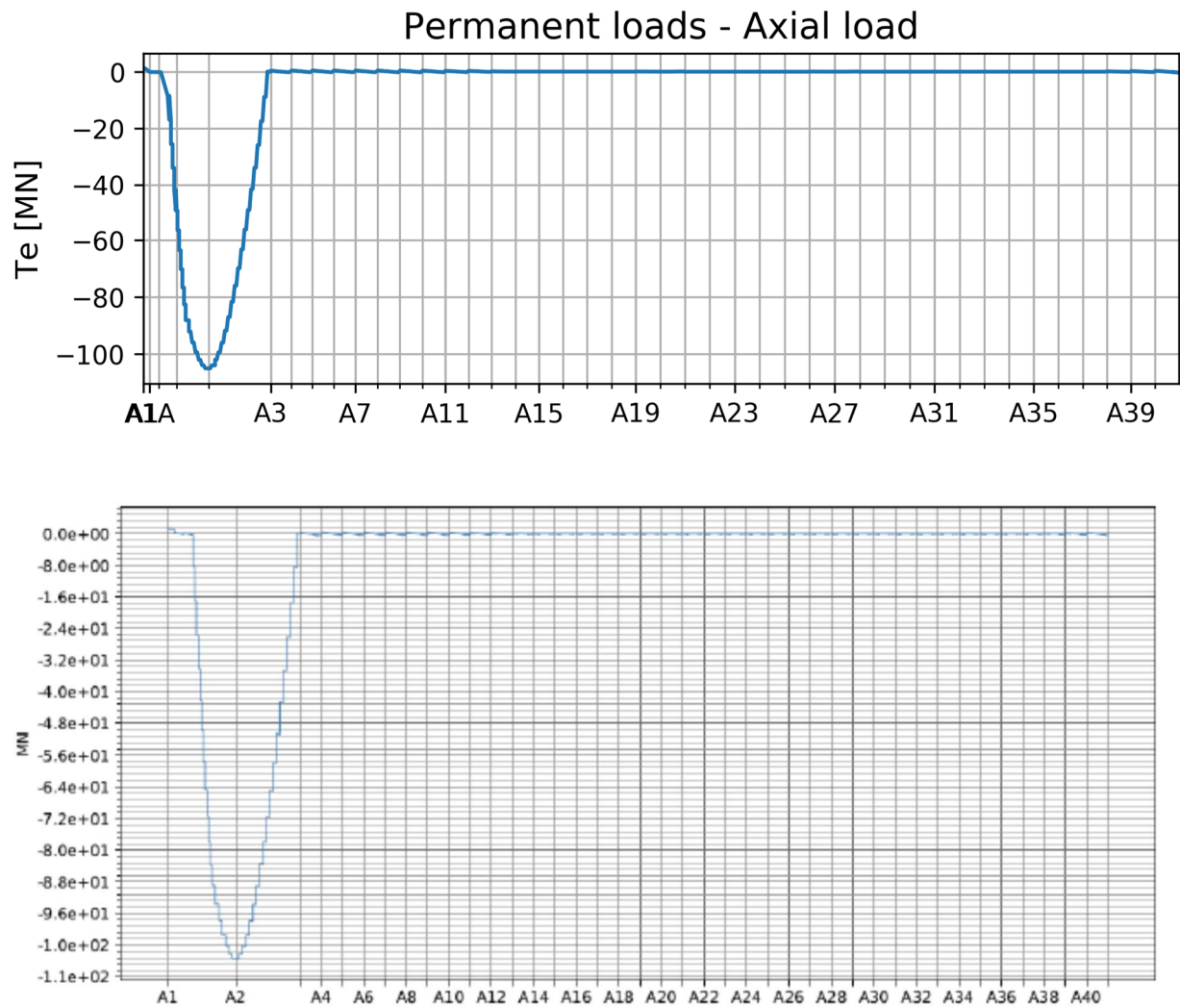
Figure 5-39 Axial loads in bridge girder under permanent loads. Top – DNVGL, bottom - Designer/15/.
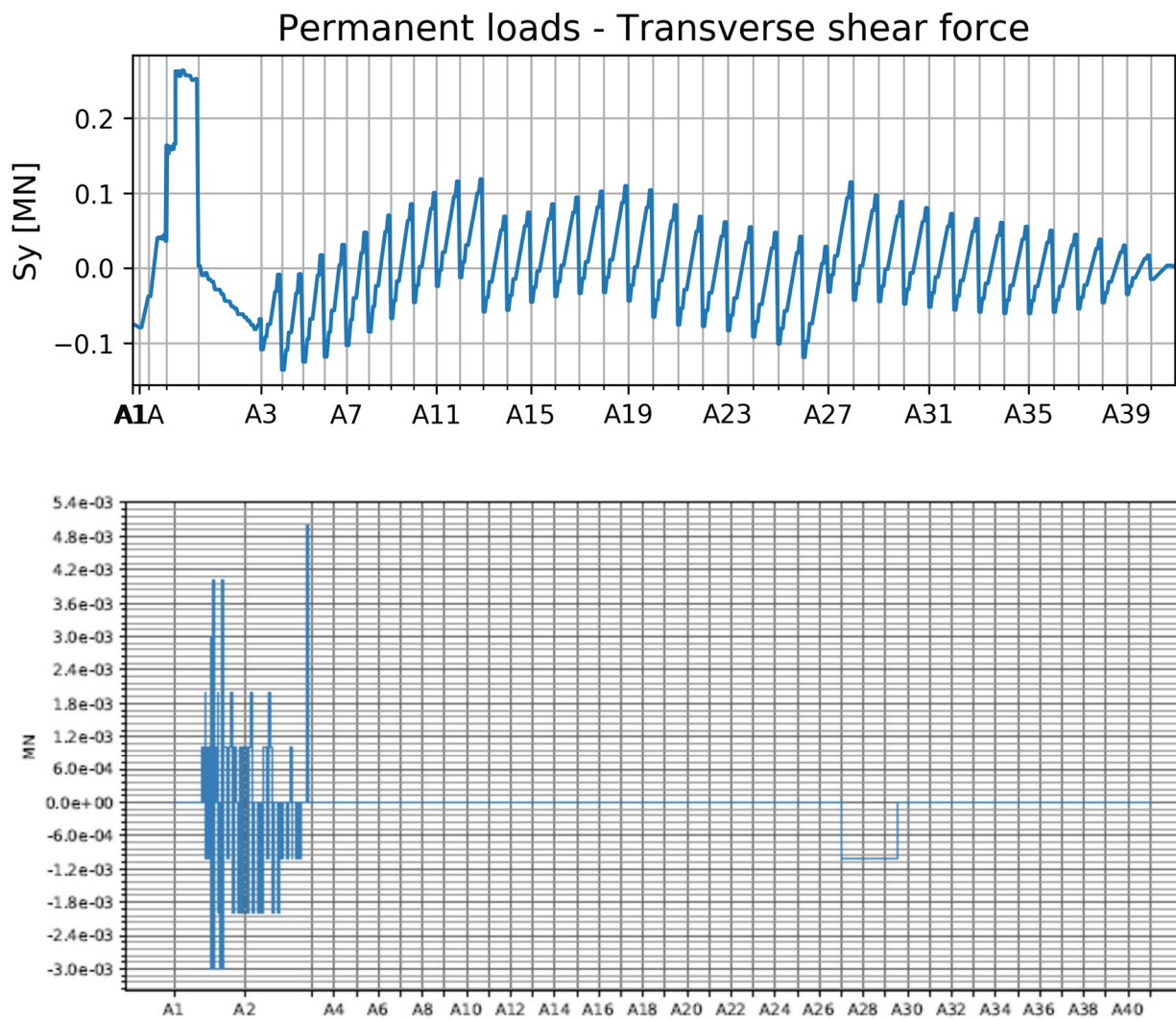
Figure 5-40   Transverse shear force in bridge girder under permanent loads. Top – DNVGL, bottom - Designer/15/.
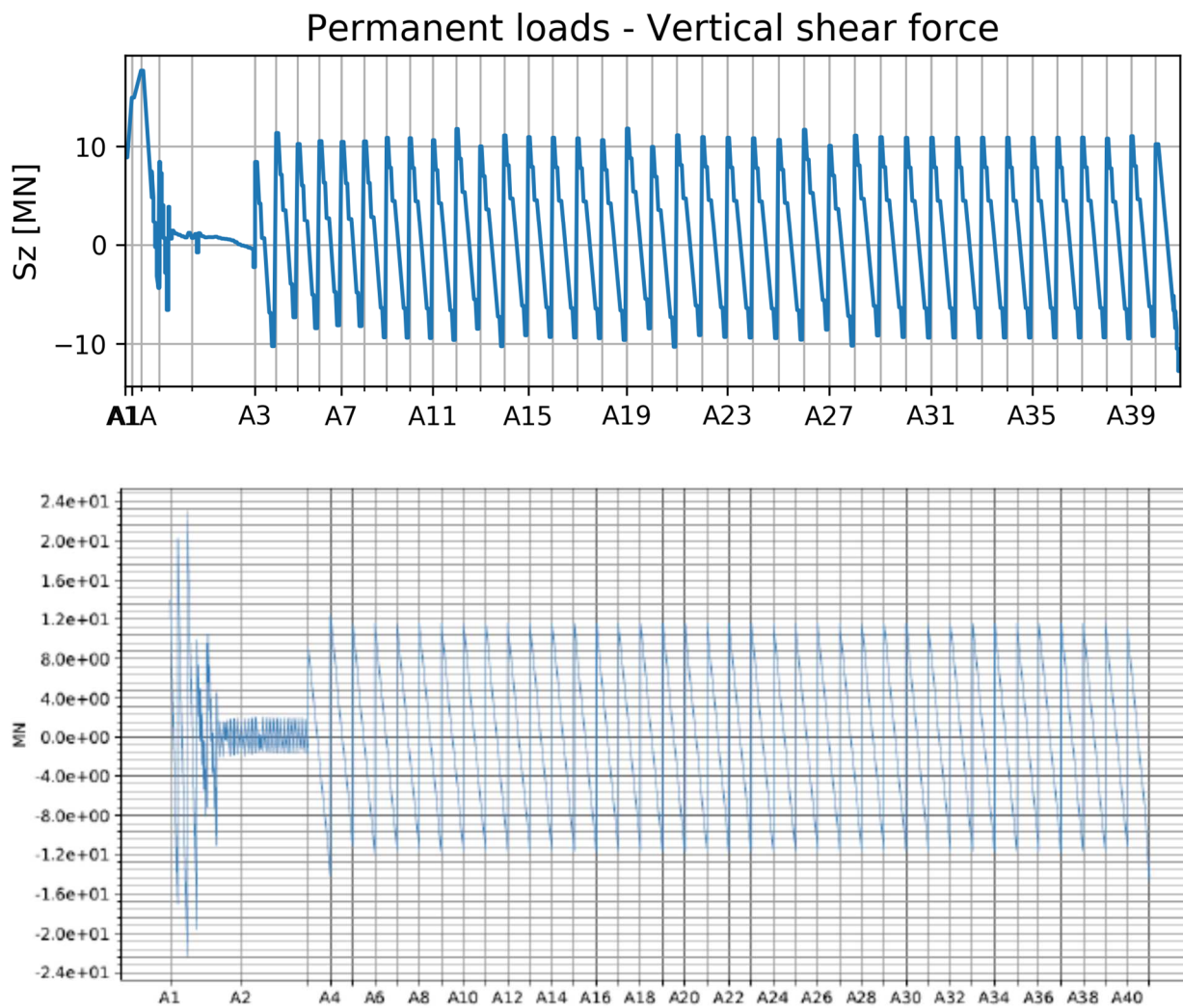
Figure 5-41   Vertical shear force in bridge girder under permanent loads. Top – DNVGL, bottom - Designer/15/.
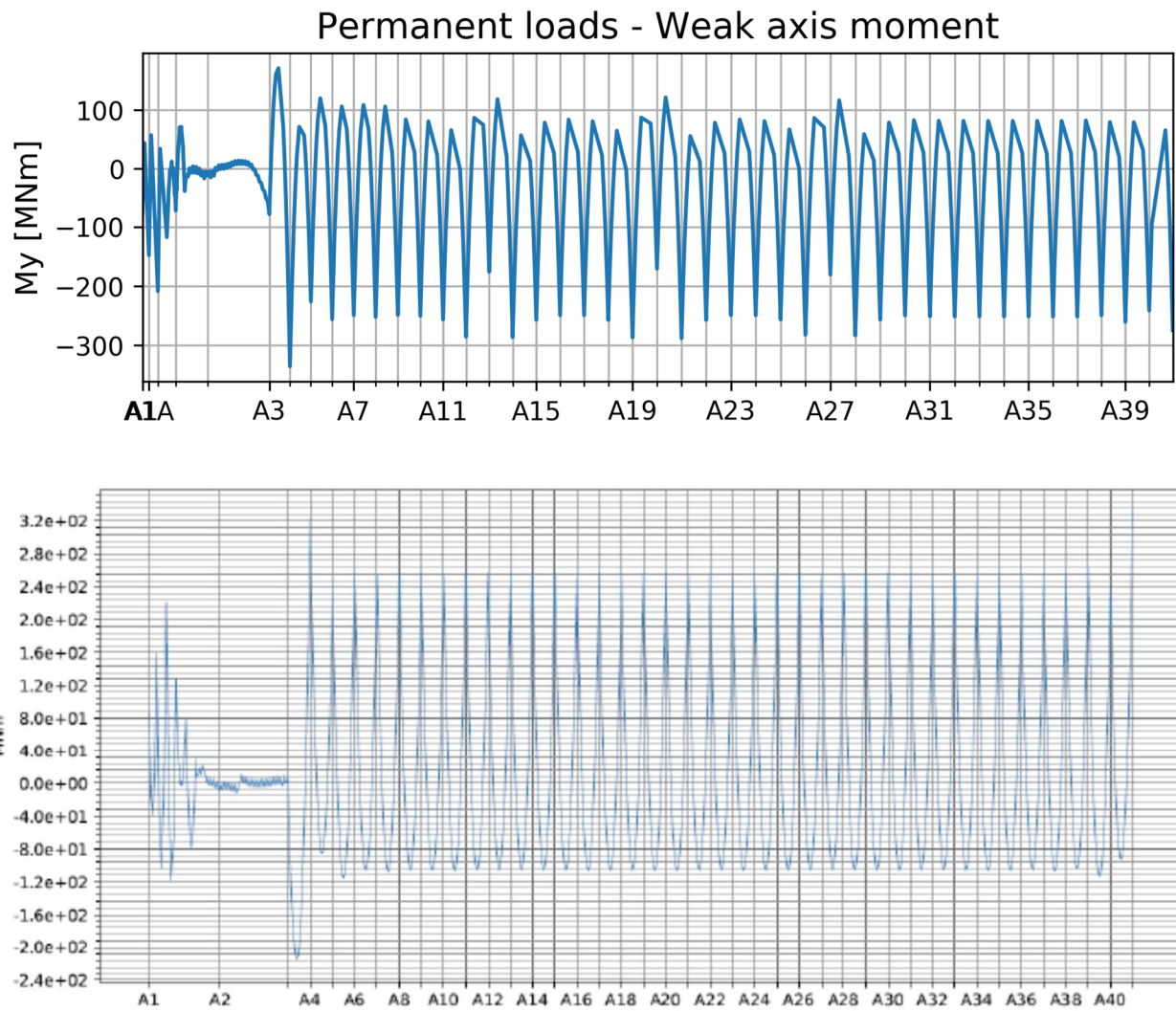
Figure 5-42   Weak axis moment in bridge girder under permanent loads. Top – DNVGL, bottom - Designer/15/.
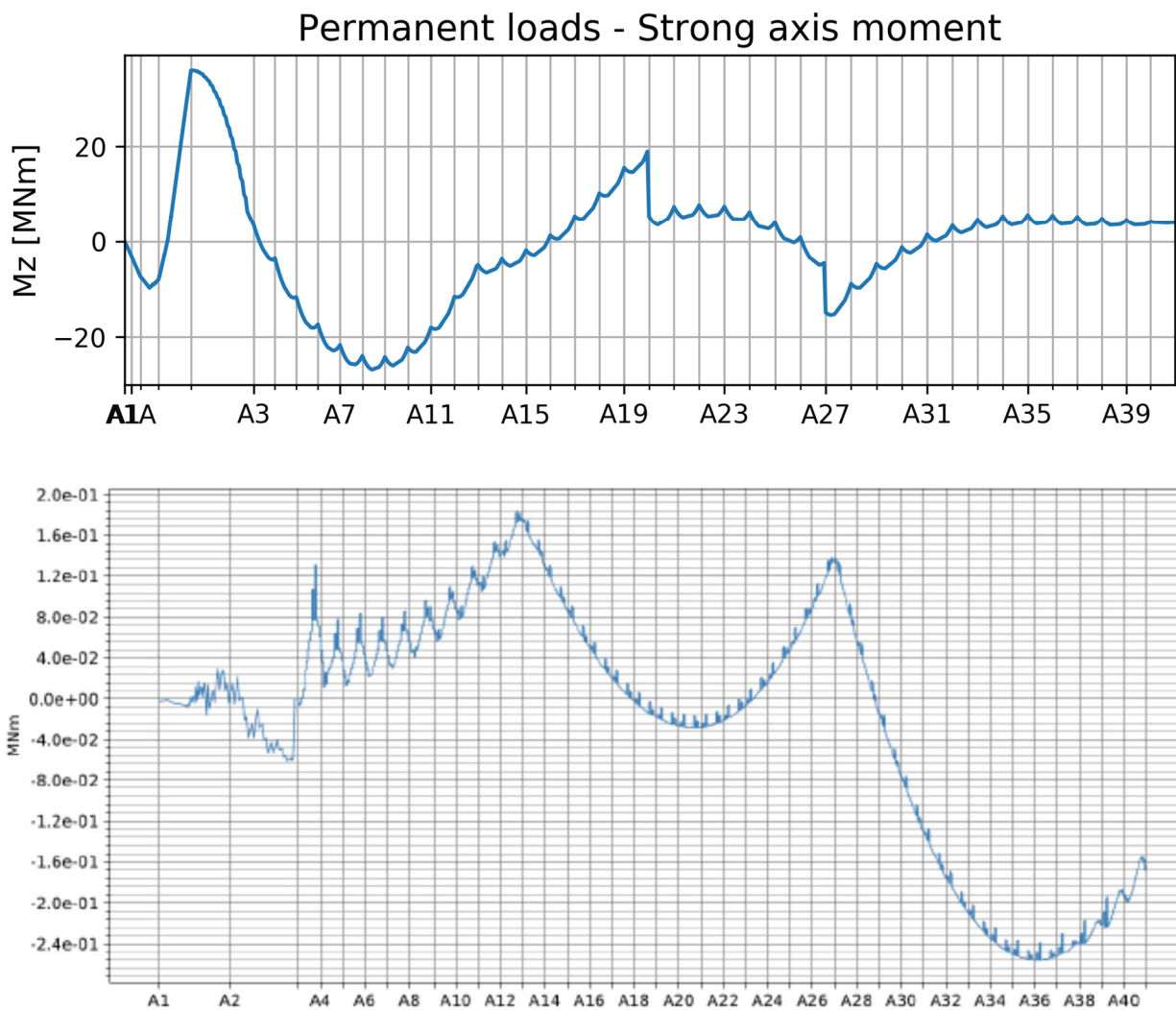
Figure 5-43   Strong axis moment in bridge girder under permanent loads. Top – DNVGL, bottom - Designer/15/.
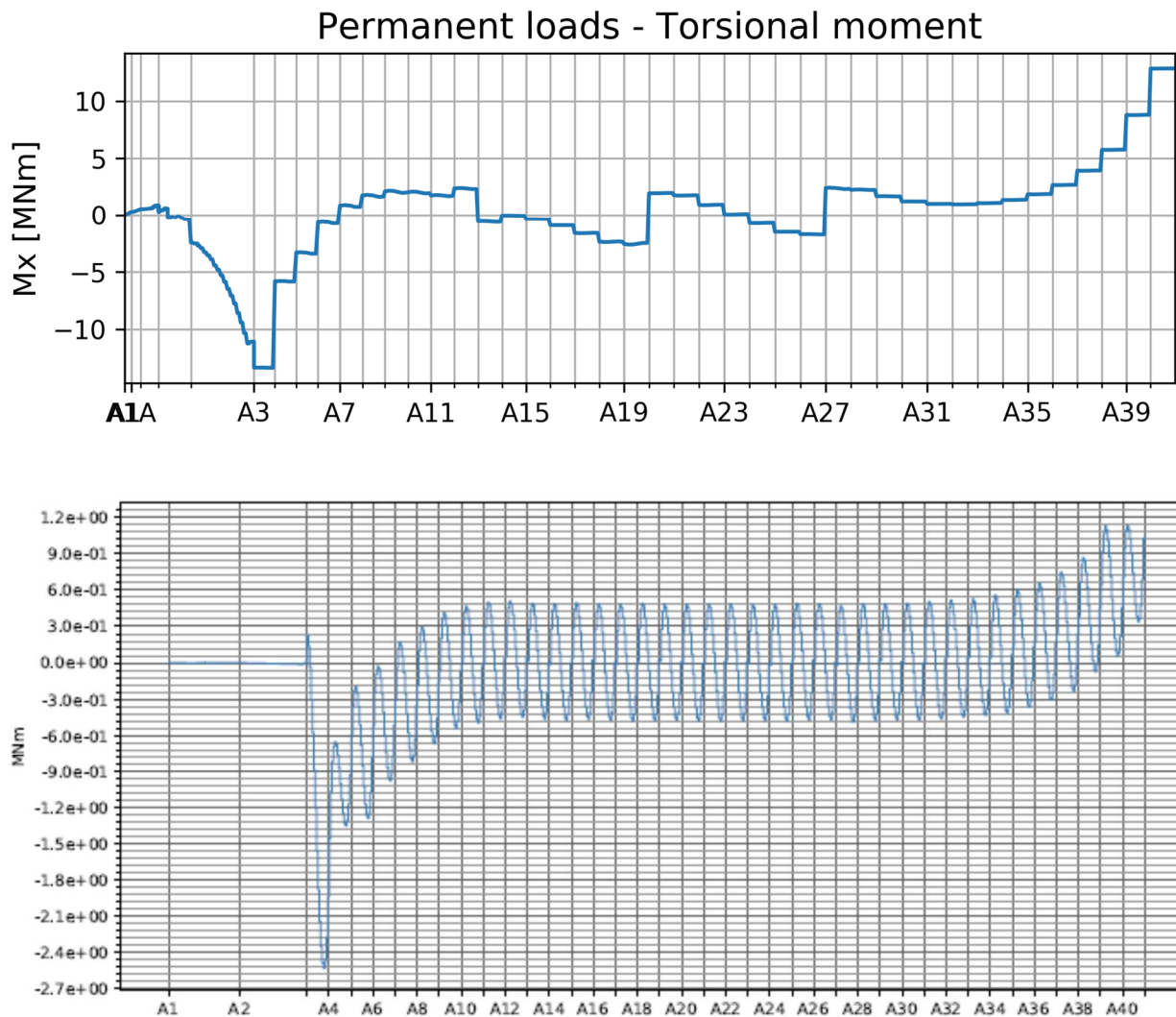
Figure 5-44 Torsional moment in bridge girder under permanent loads. Top – DNVGL, bottom - Designer/15/.

5.6.3 Dynamic loads

Permanent loads, tide, temperature and 100-year environmental loads combined with the load factors given in Table 6-1 are compared with the design analysis loads, see Figure 5-45 - Figure 5-50. Comparison shows that:

- Axial loads, torsional moment and shear forces agree well with forces calculated by designer.

- Similar variations are found for weak axis bending moment. Designer uses opposite sign definition.

- Larger strong axis bending moment is calculated by DNVGL at Axis 2. More investigations were performed in Section 5.6.4.
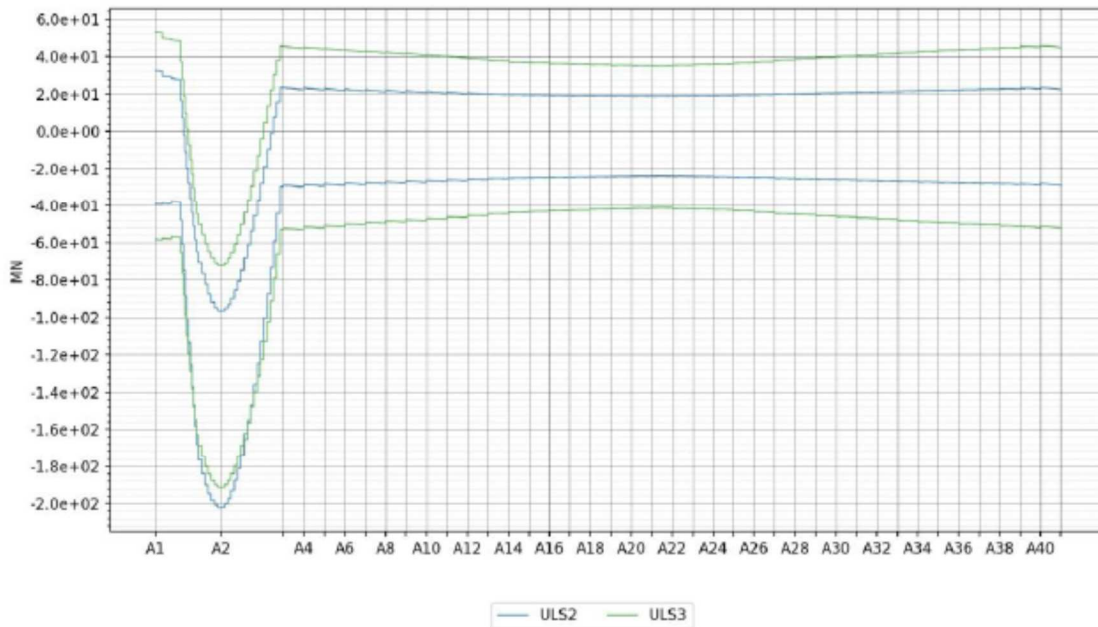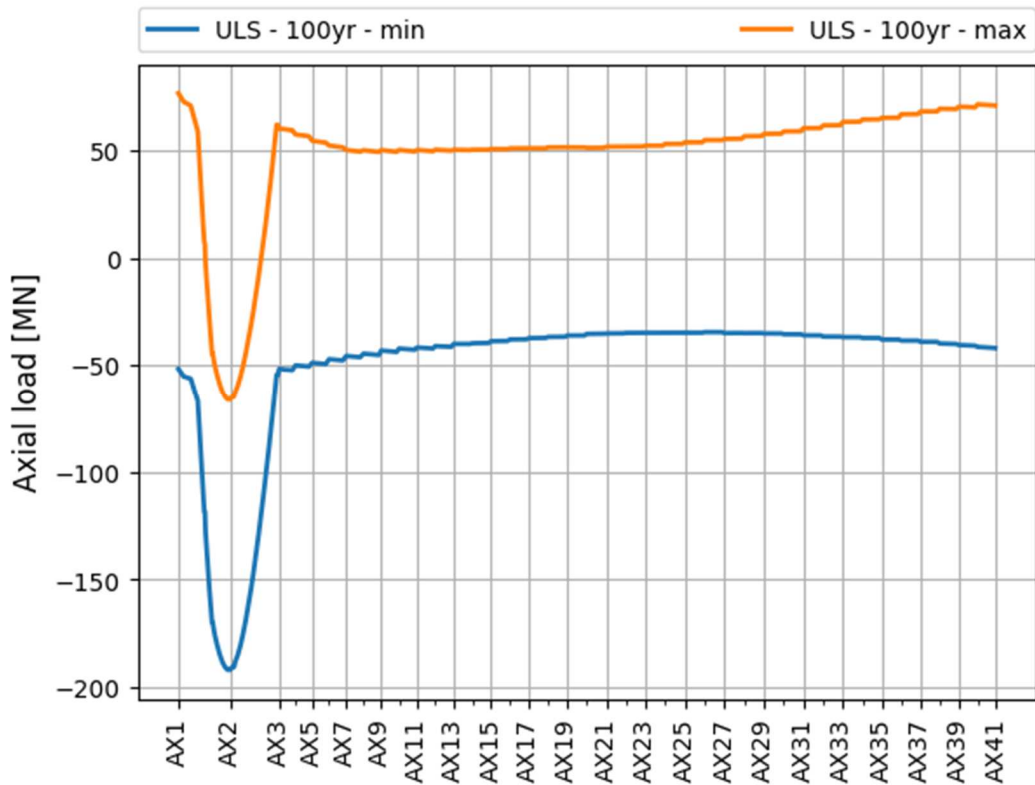
Figure 6-2 Bridge girder axial force – ULS for K12_07.

Figure 5-45 Axial force. Top – DNVGL, bottom – Designer /20/**. ULS3 presented by designer corresponds to the ULS case with 100 year environmental conditions.**
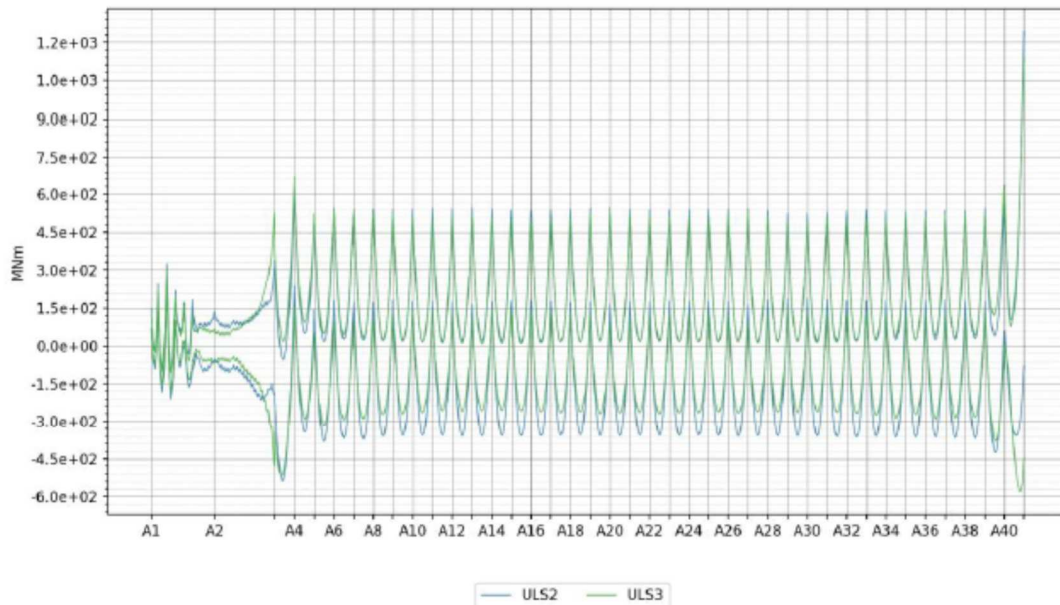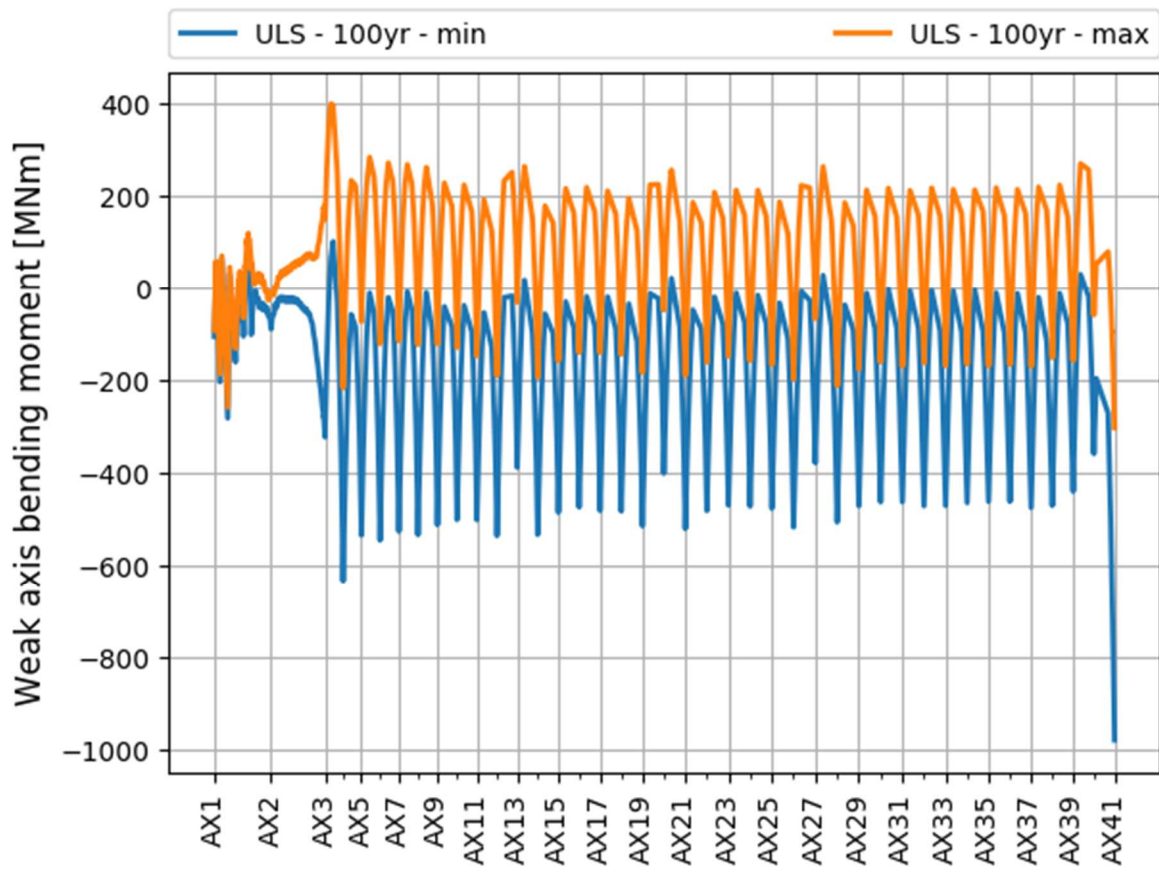
Figure 6-4 Bridge girder bending moment about weak axis – ULS for K12_07.

Figure 5-46 **Weak axis bending moment. Top – DNVGL, bottom – Designer** /20/**. ULS3 presented by designer corresponds to the ULS case with 100 year environmental conditions.**
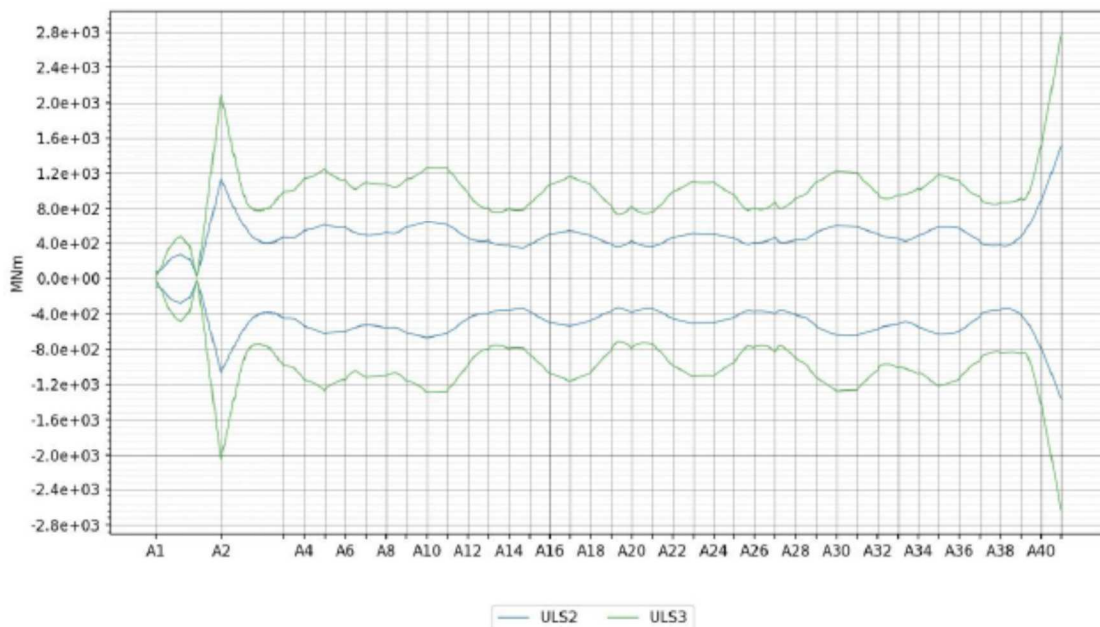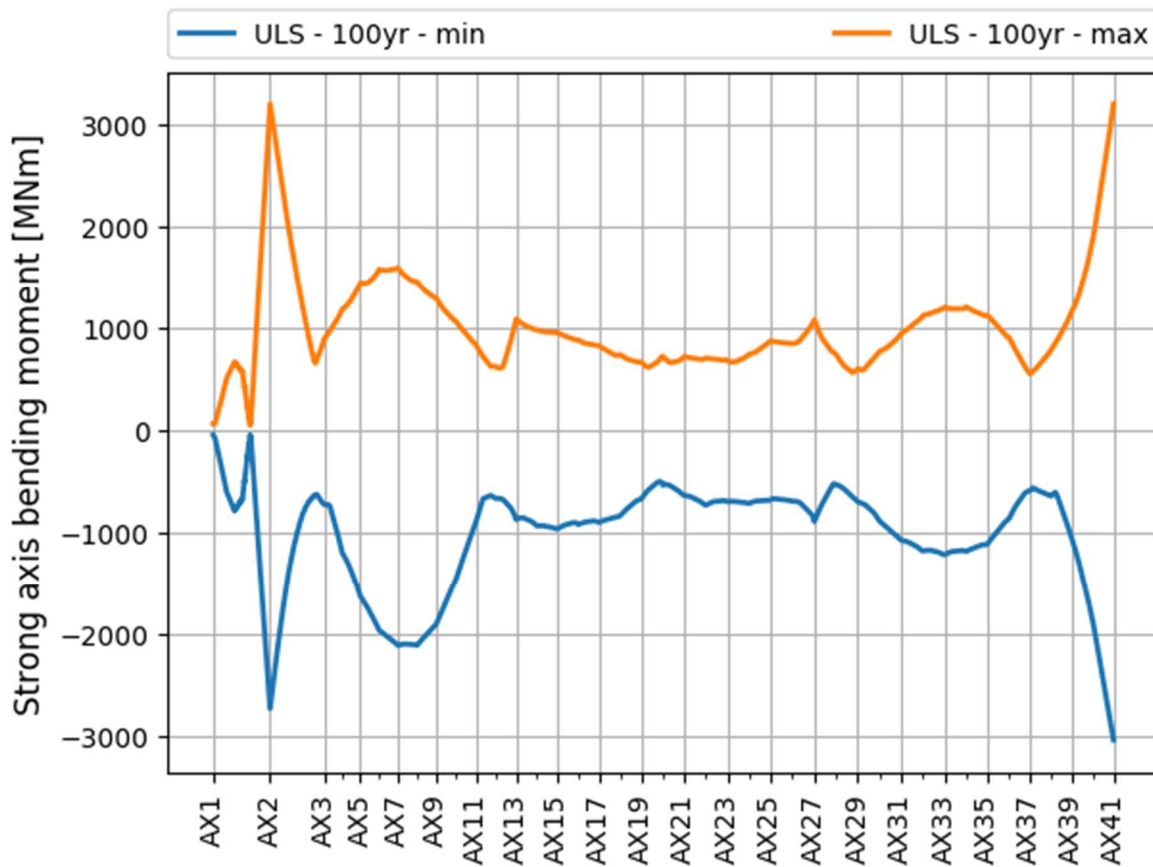
Figure 6-3 Bridge girder bending moment about strong axis – ULS for K12_07.

Figure 5-47   Strong axis bending moment. Top – DNVGL, bottom – Designer /20/. ULS3 presented by designer corresponds to the ULS case with 100 year environmental conditions.
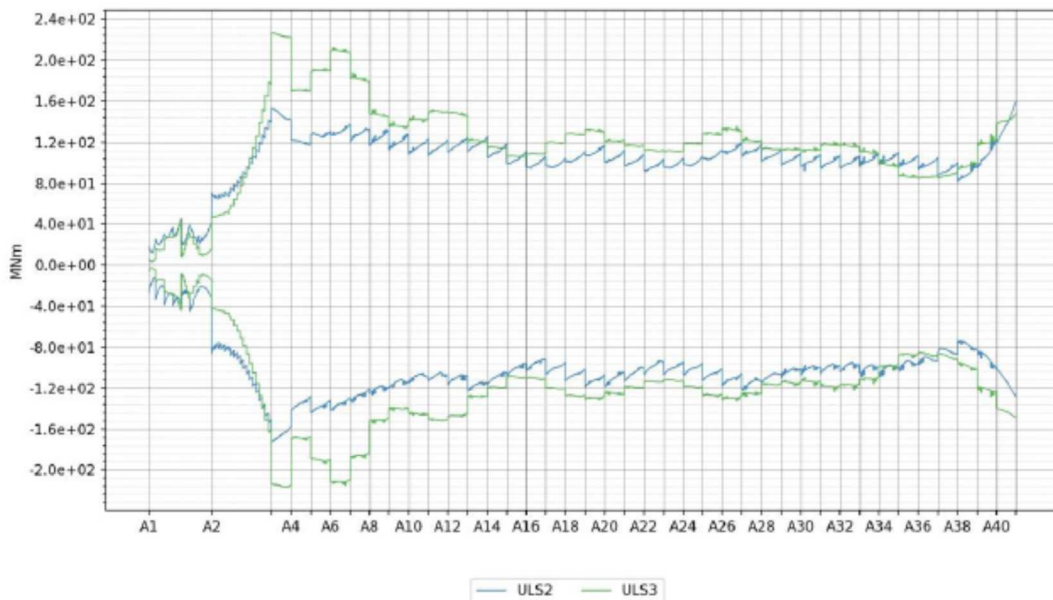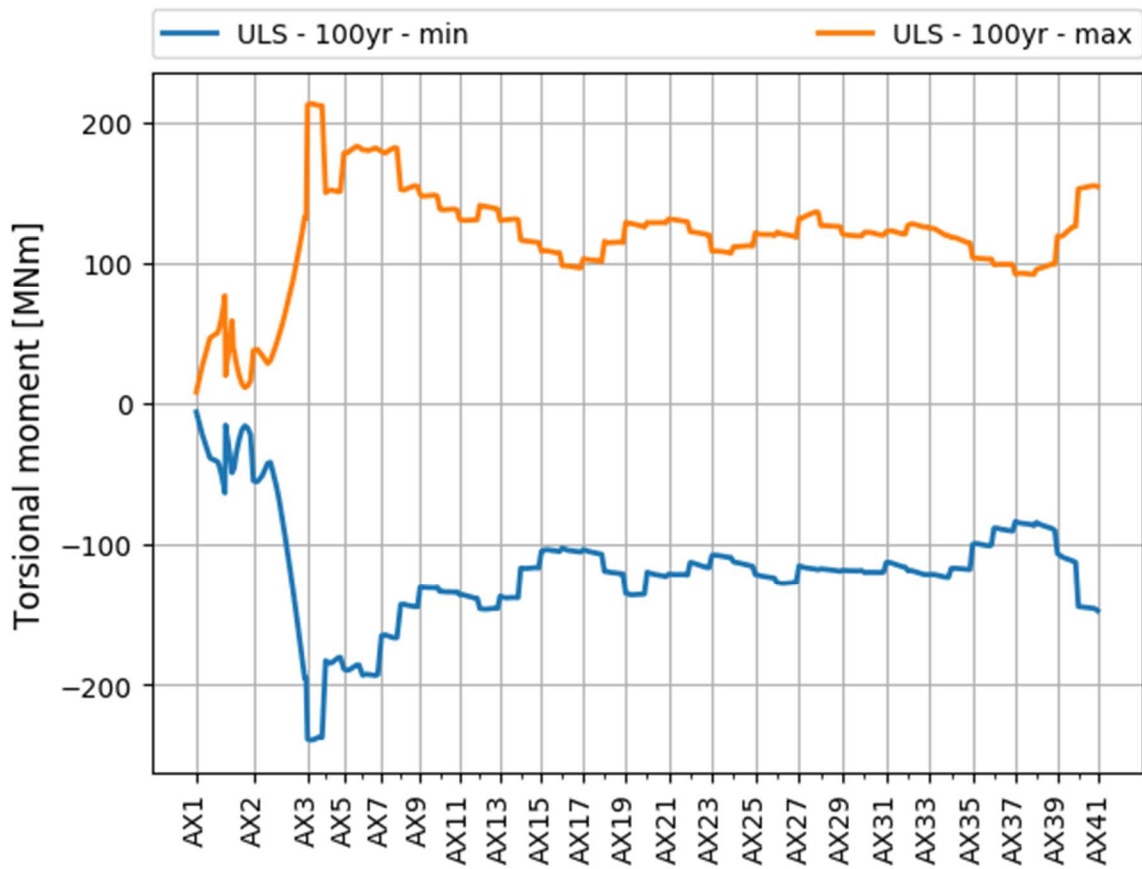
Figure 6-5 Bridge girder torsional moment – ULS for K12_07.

Figure 5-48 Torsional moment. Top – DNVGL, bottom – Designer /20/**. ULS3 presented by designer corresponds to the ULS case with 100 year environmental conditions.**
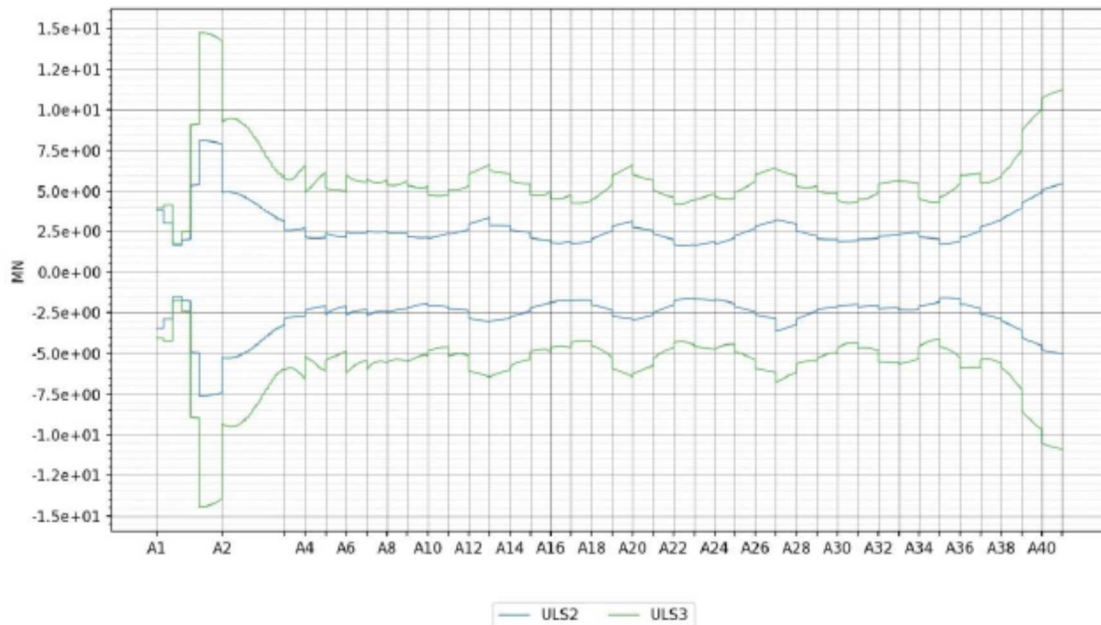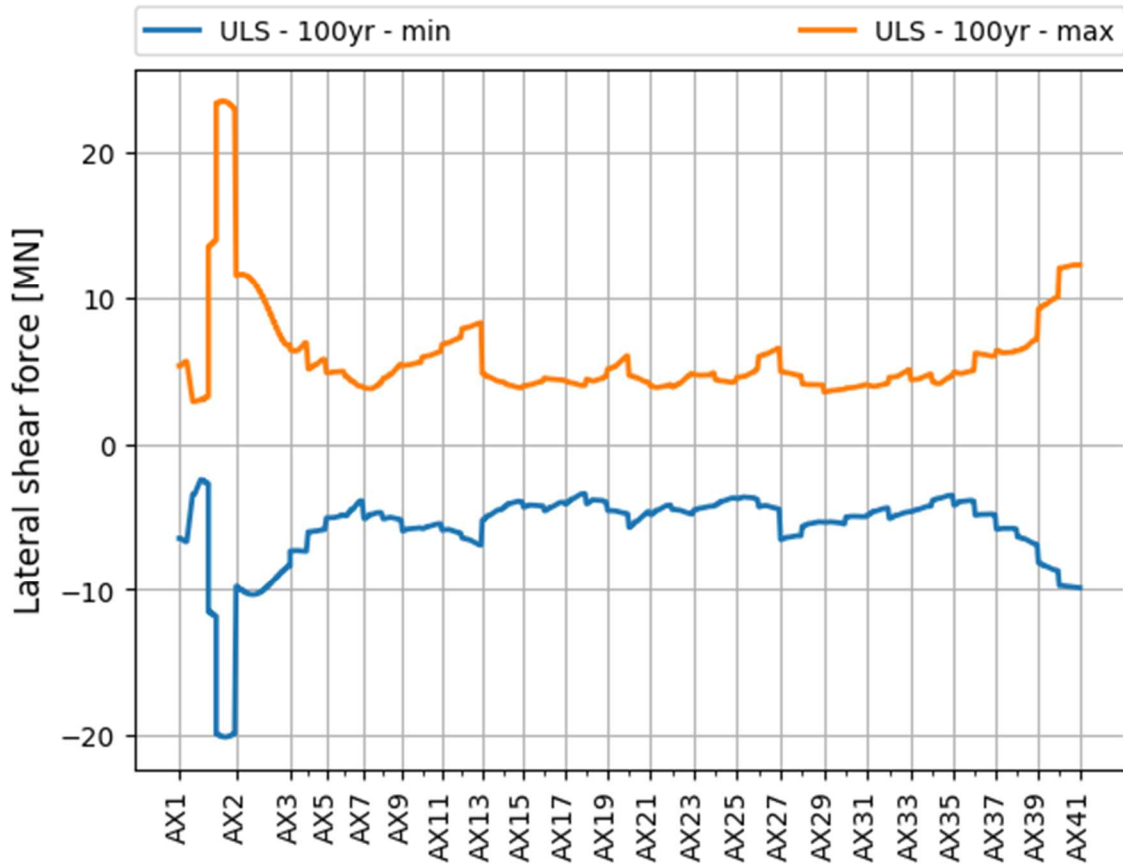
Figure 6-7 Bridge girder transverse shear force – ULS for K12_07.

Figure 5-49   Transverse shear force. Top – DNVGL, bottom – Designer /20/**. ULS3 presented by designer corresponds to the ULS case with 100 year environmental conditions.**
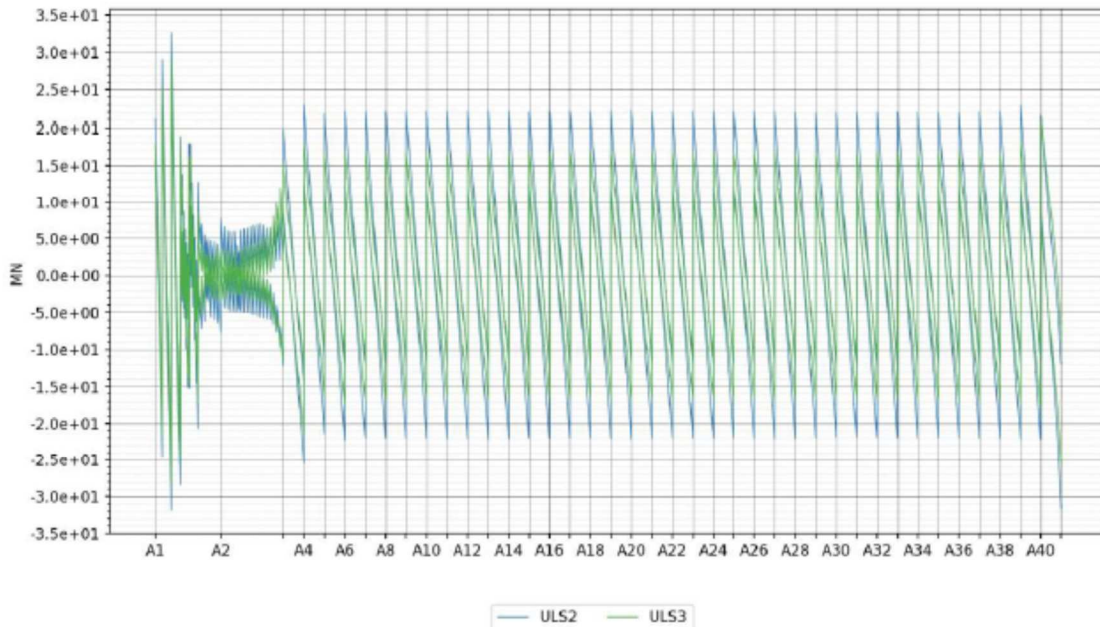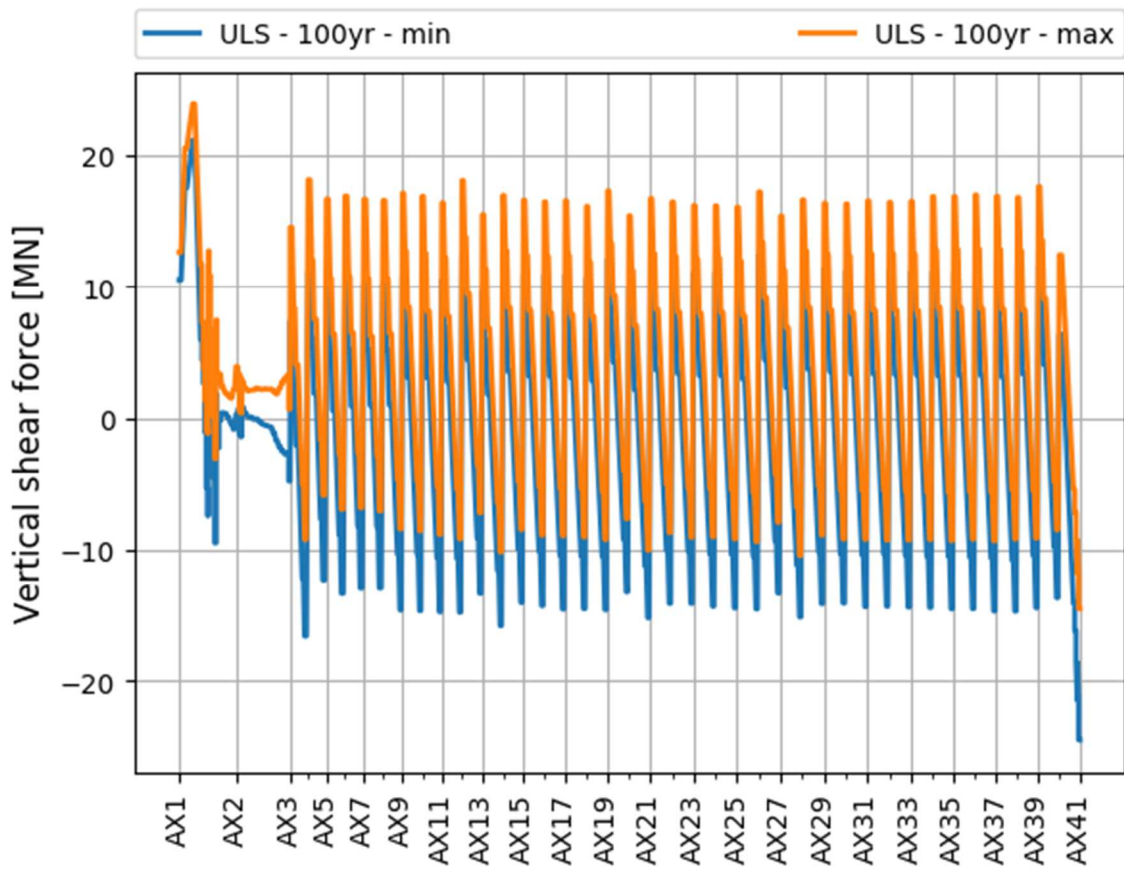
Figure 6-6 Bridge girder vertical shear force – ULS for K12_07.

Figure 5-50   Vertical shear force. Top – DNVGL, bottom – Designer /20/**. ULS3 presented by designer corresponds to the ULS case with 100 year environmental conditions.**

5.6.4 Dynamic loads using designer's environmental input

To investigate the large differences of strong axis bending moment at Axis 2, as shown in Figure 5-47, a series of simulations were performed using designer's specified environmental parameters, as shown in Table 5-17. Strong axis bending moment along the girder is presented and compared with the designer's calculation, as presented in Figure 5-51. It can be seen that bending moments at abutment north agree to each other quite well, while at Axis 2, a lower bending moments are calculated by DNVGL, which is mainly caused by the wave-induced motions of pontoon 3. A sensitivity analysis was performed by reducing the current velocity from 1.7 m/s to 0.5 m/s, i.e., by reducing the quadratic damping on the pontoons thus the motions. Corresponding strong axis bending moments are presented in Figure 5-52. It can be seen that with different applied current velocities, bending moments at abutment north are at same level, indicating that main contribution at this position is from the wind. At tower support position, Axis 2, the bending moment is influenced by the neighbour pontoon motions, thus the applied waves, current and model damping.

Comparing the strong axis bending moments calculated using the specified governing condition given in Table 5-5, the designer may miss some critical ULS conditions.

Table 5-17   Environmental conditions for the 100-year return period conditions specified by the designer /15/

Case id	Wind waves			Swell			Wind		Current	
	Hs [m]	Tp [s]	Dir. [deg]	Hs [m]	Tp [s]	Dir. [deg]	Velocity [m/s]	Dir. [deg]	Velocity [m/s]	Dir. [deg]
LC1	1.40	4.60	195	0.34	17.25	300	25.2*	280*	1.7	280*
LC2	1.40	4.60	195	0.34	13.25	300	25.2*	280*	1.7	280*
LC3	2.00	5.20	315	0.34	17.25	300	25.2*	280*	1.7	280*
LC4	2.00	5.20	315	0.001	5	300	25.2*	280*	1.7	280*
LC5	2.10	5.50	75	0.001	5	300	21.5**	90**	1.7	100**
LC6	2.10	5.50	105	0.001	5	300	21.5**	90**	1.7	100**

*   a velocity of 24.8 m/s and direction of 270 deg are applied.
**   a velocity of 19.5 m/s and direction of 90 deg are applied.
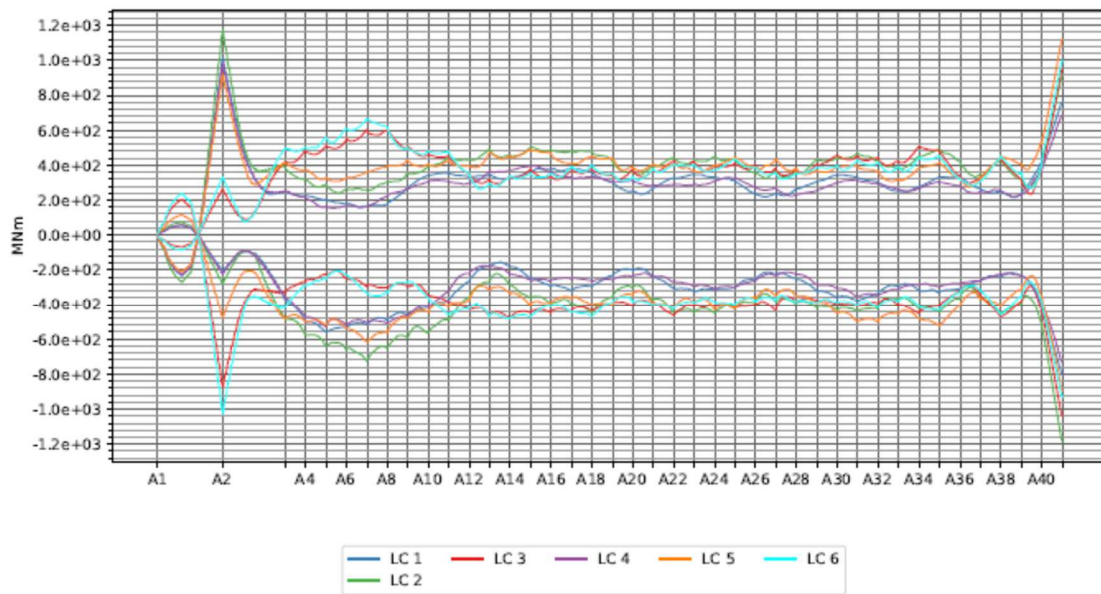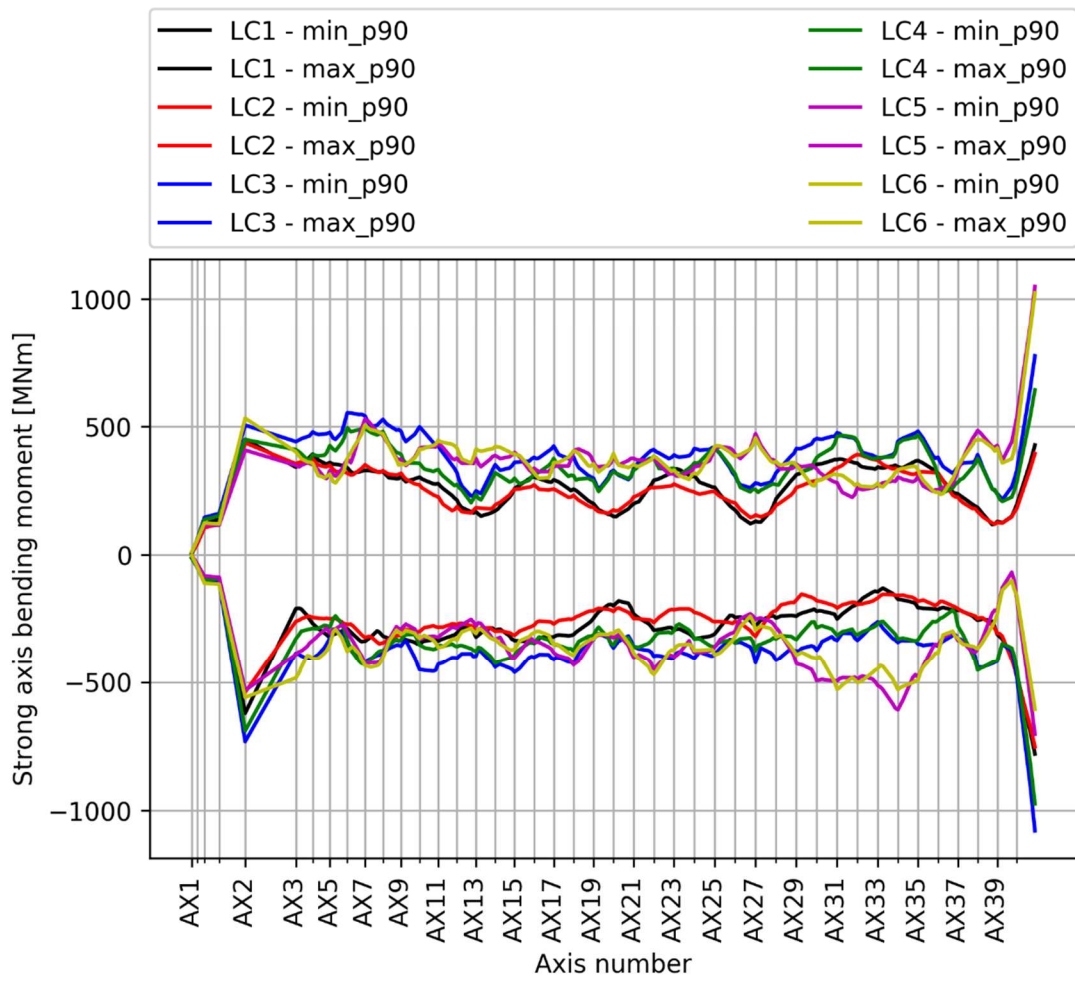
Figure 5-51   Strong axis bending moment. Top – DNVGL, bottom – Designer /15/.
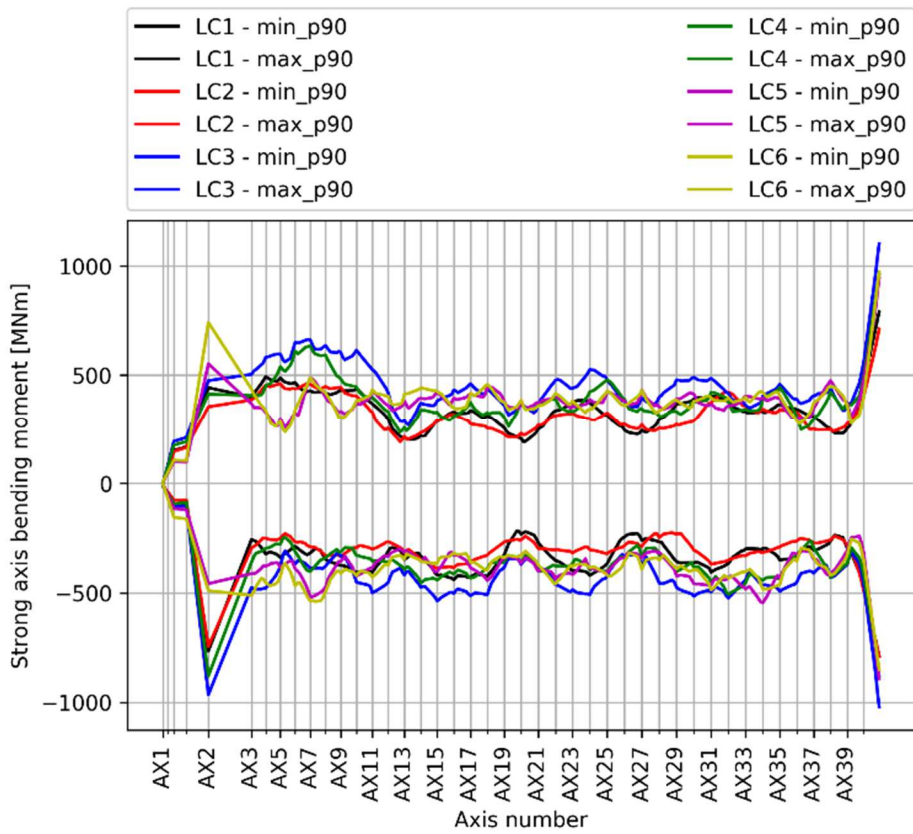
Figure 5-52   Strong axis bending moment under a current velocity of 0.5 m/s.

6 CAPACITY CHECKS FOR THE ULTIMATE LIMIT STATES

6.1 General

The ULS checks are carried out for the case without traffic on the bridge and with 100-years return period for the environmental loads. Other ULS cases that shall be checked as specified in the design basis /11/ are not covered by the independent global analyses and hence not covered by the capacity checks.

The capacity checks are simplified to only check the von-Mises stress from the global beam model. Normal and shear stresses are calculated for selected points in the cross-section which make it possible to assess if buckling capacity is exceeded.

6.2 Assumptions

The following assumptions are made:

- The extreme combined stresses from the different load effects are added without taking into account the non-linearity of the combined stress formulation.

6.3 Load and material factors

The capacity in ordinary ultimate limit state (STR) is checked for the case with dominant 100-years return period environmental condition. The load factors given in Table 6-1 are used.

Table 6-1   Load factors

Load	Load factor
Permanent loads	1.2
Environmental loads without traffic	1.6
Temperature	0.84
Water level variation	1.6

Based on the requirements in the Design Basis for Bjørnafjorden /11/, the material factors given in Table 6-2 are used.

Table 6-2   Material factors

Limit state	Material factor
Ultimate strength	1.1

6.4 Calculation of ULS stresses

The stresses are in the following calculated at selected points in the cross-section. Normal-, shear- and combined (von-Mises equivalent stress) stresses are presented for positions along the bridge. The yield stress is taken as 420 MPa for all section making the design stress 420/1.1 = 382 MPa.
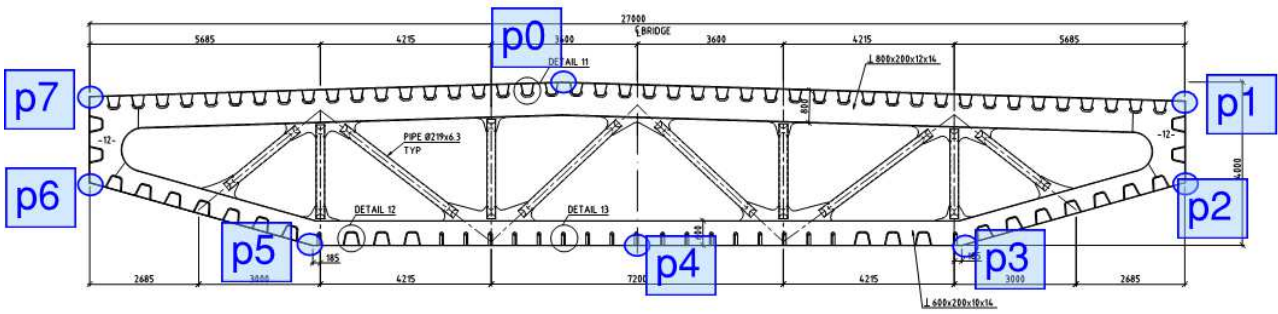
Figure 6-1   Stress point locations
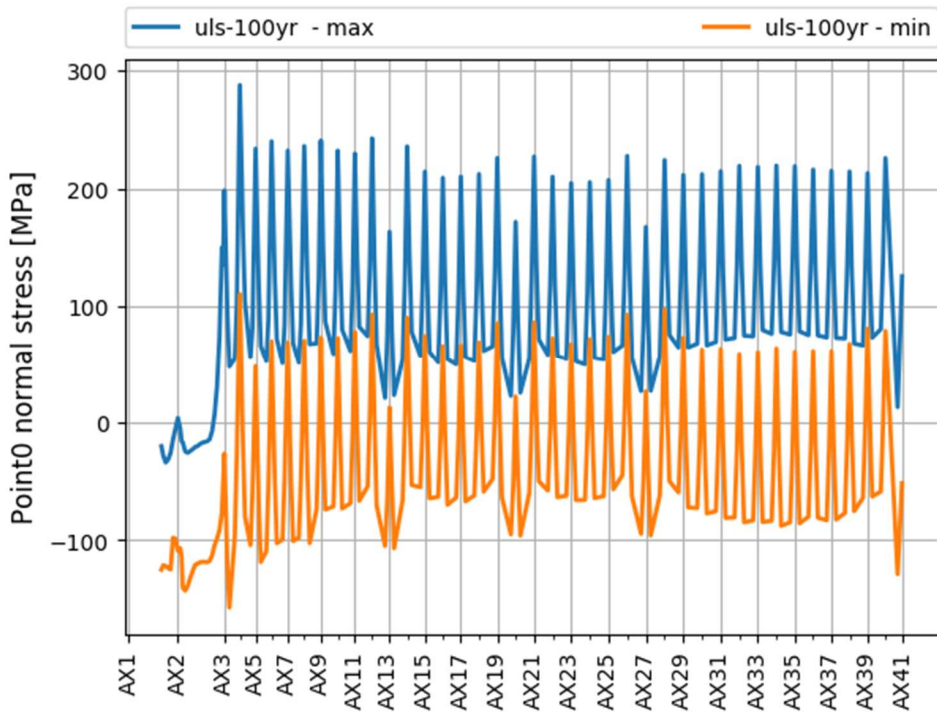
Figure 6-2   Normal stress at point 0
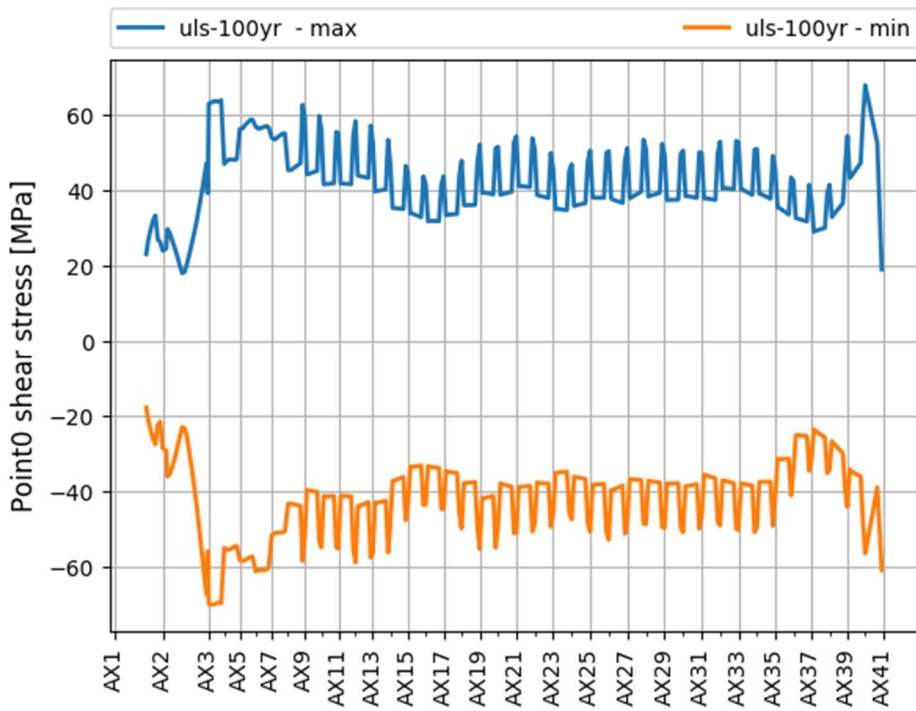
Figure 6-3   Shear stress at point 0
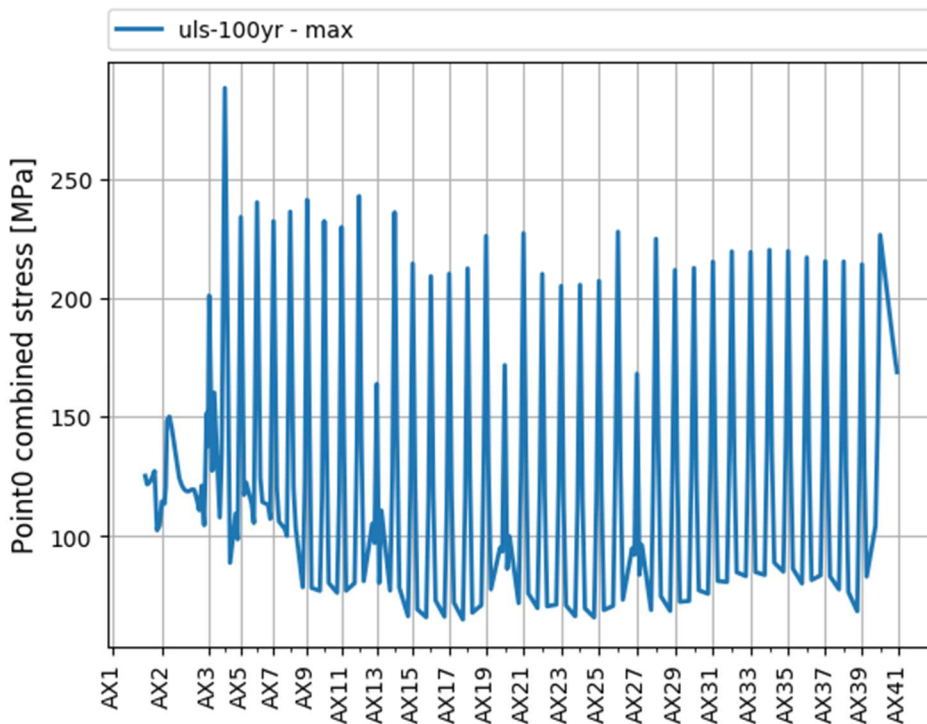
Figure 6-4   Combined stress at point 0
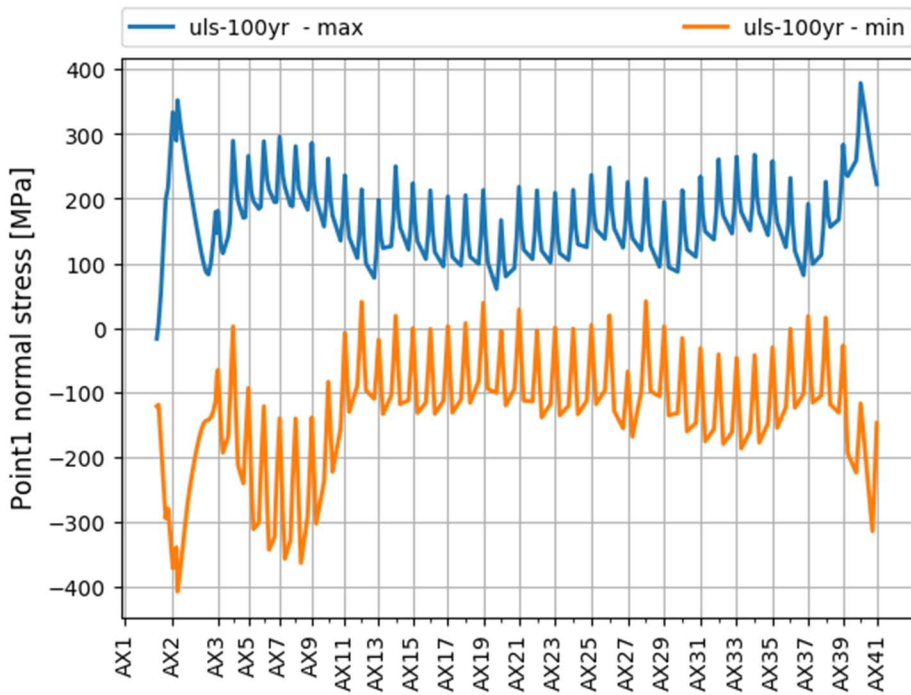
Figure 6-5   Normal stress at point 1
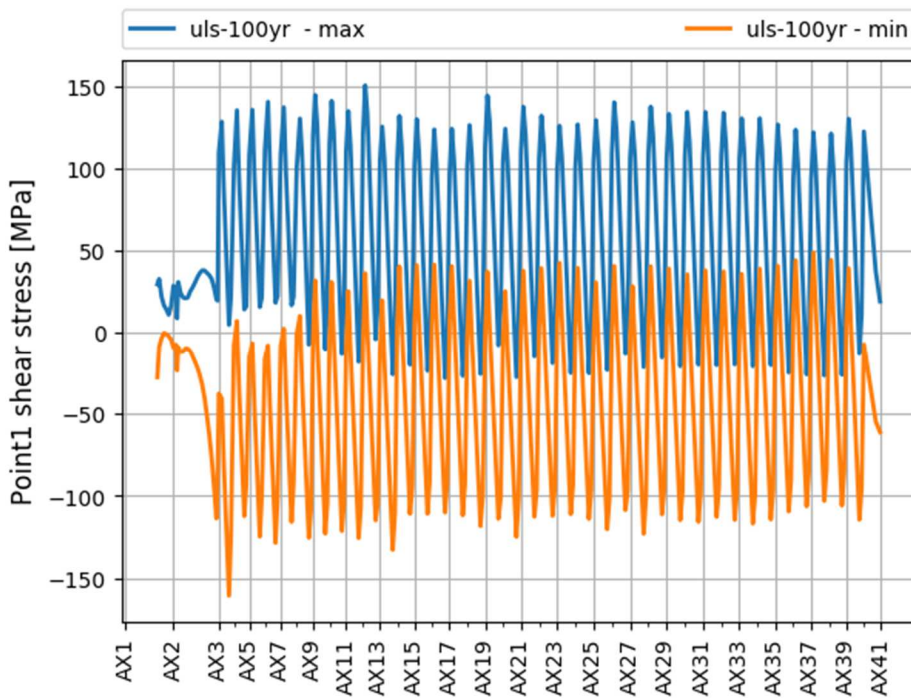
Figure 6-6   Shear stress at point 1
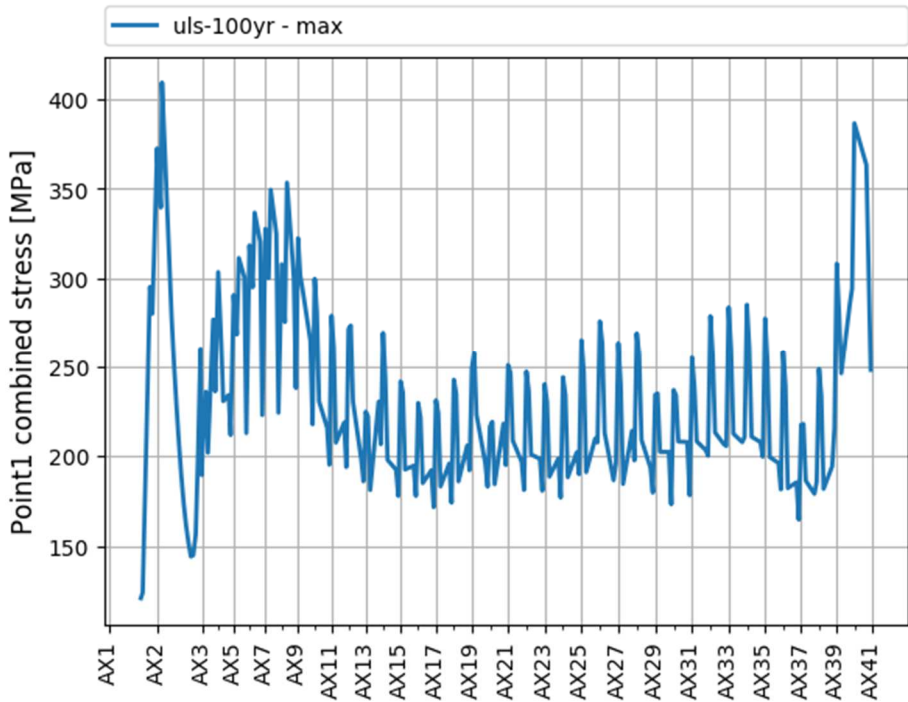
Figure 6-7   Combined stress at point 1
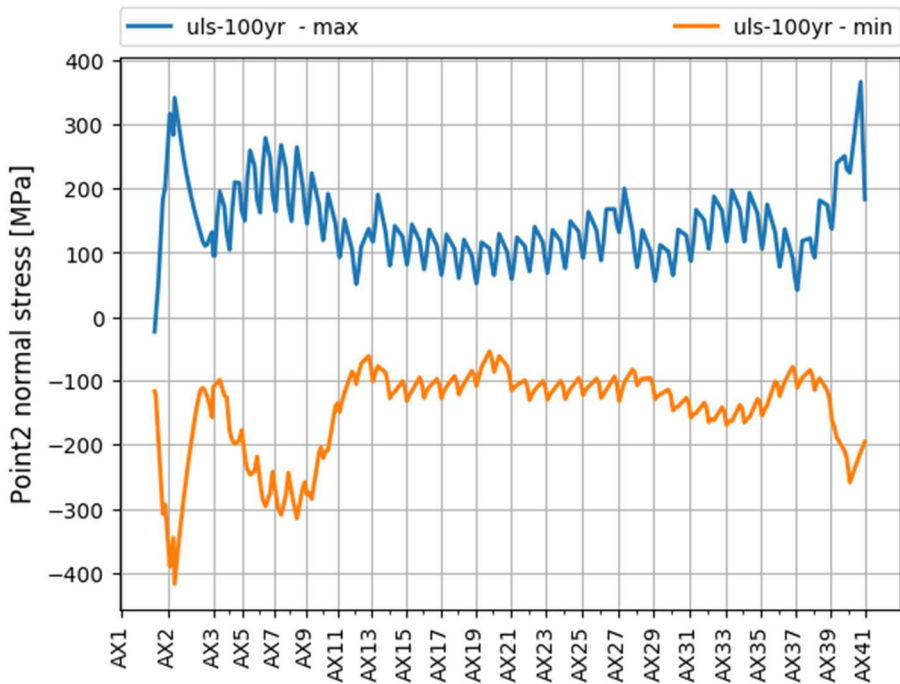
Figure 6-8   Normal stress at point 2
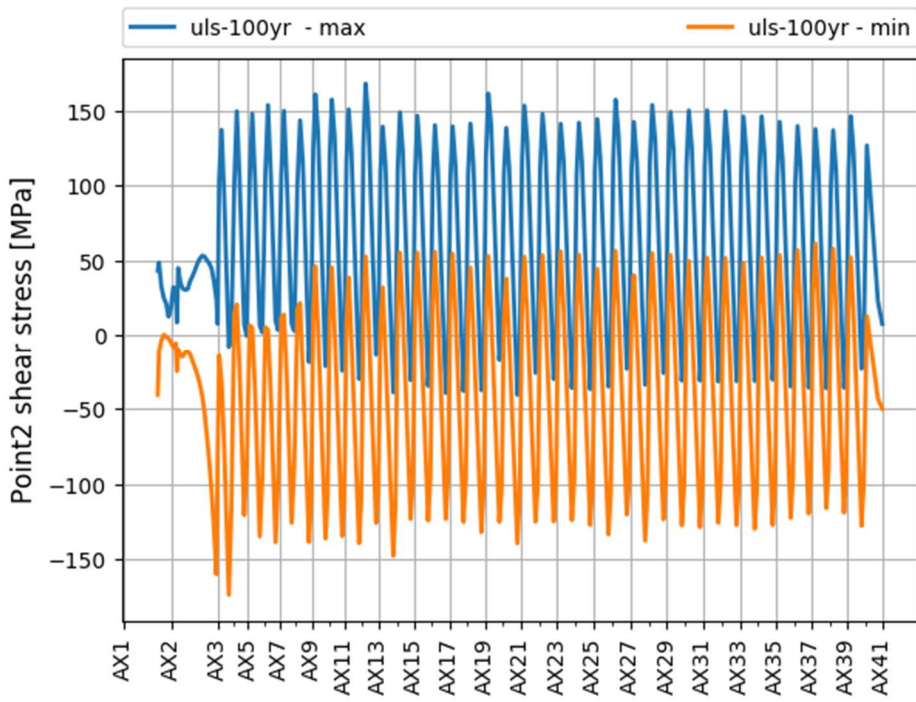
Figure 6-9   Shear stress at point 2
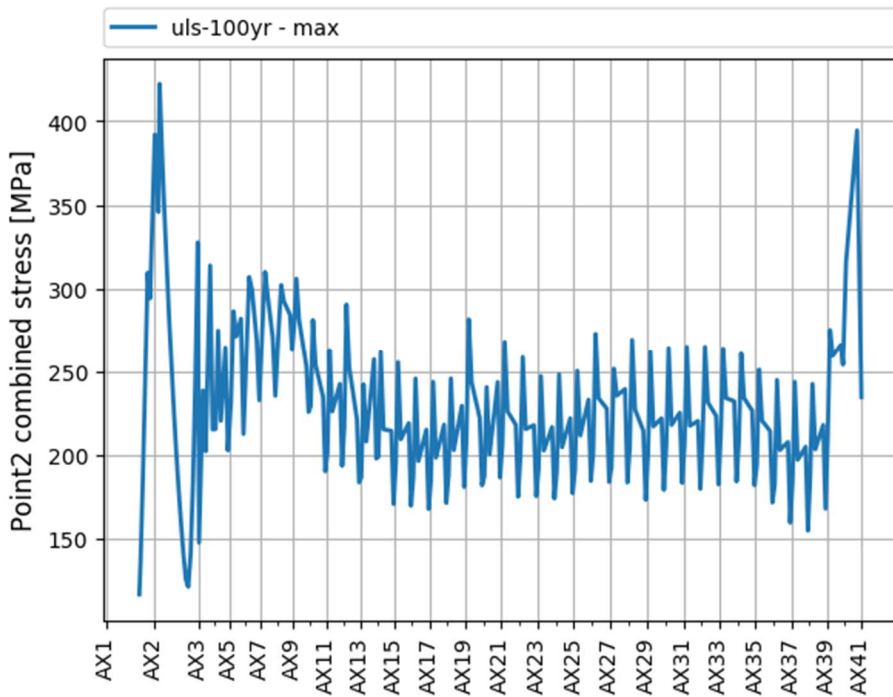
Figure 6-10   Combined stress at point 2
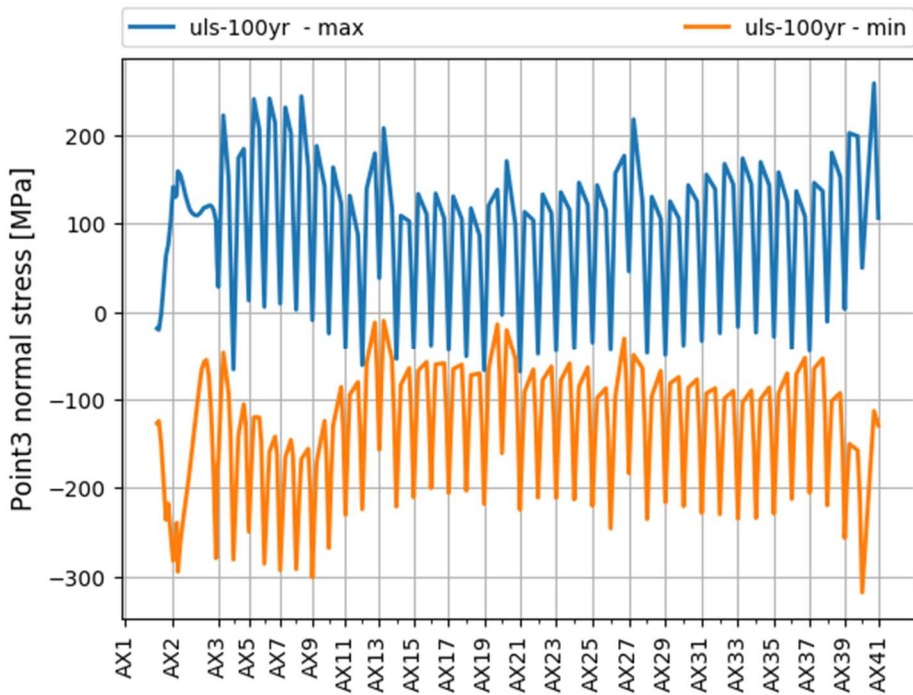
Figure 6-11 Normal stress at point 3
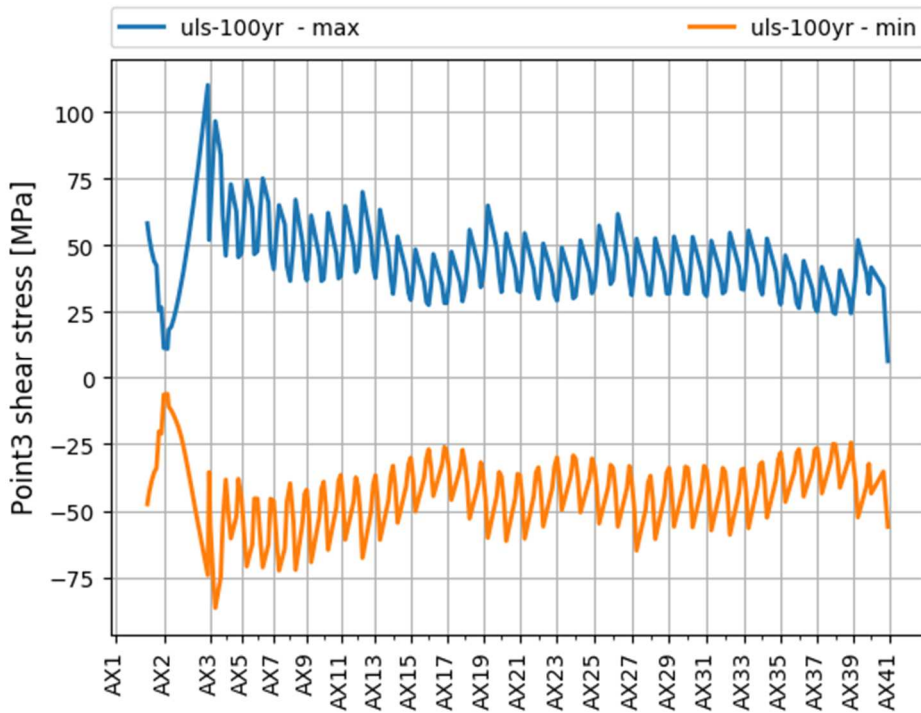
Figure 6-12 Shear stress at point 3
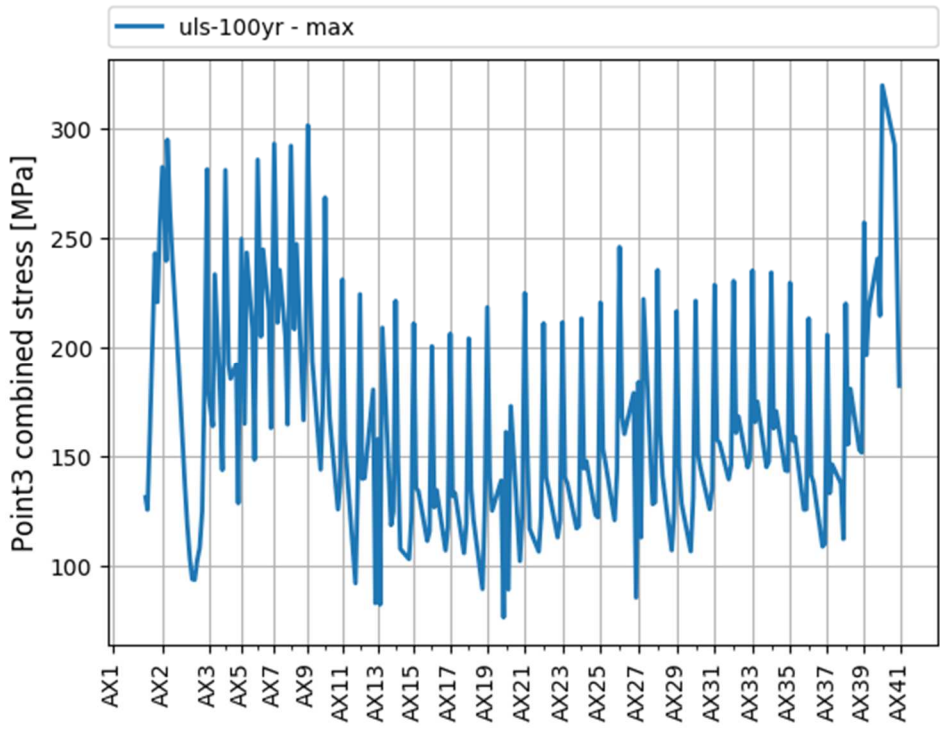
Figure 6-13   Combined stress at point 3
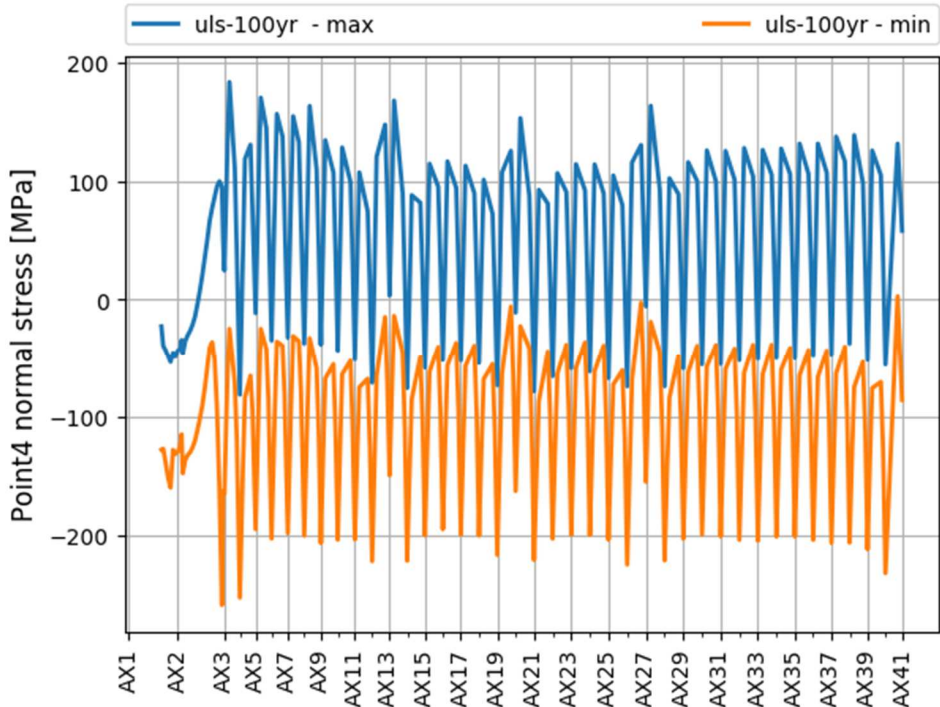
Figure 6-14   Normal stress at point 4
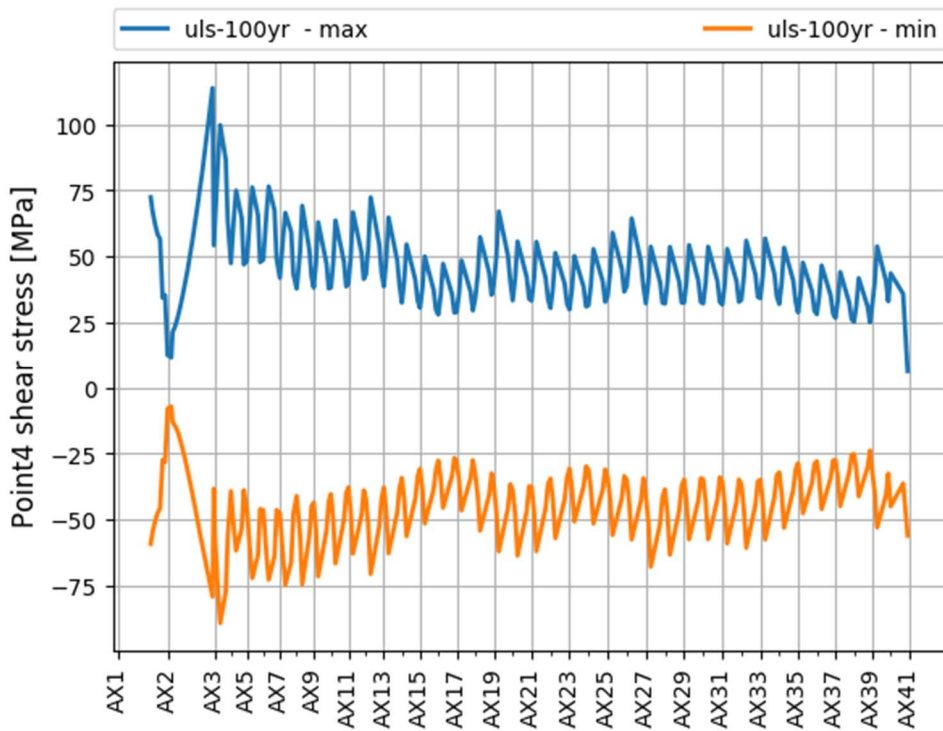
Figure 6-15   Shear stress at point 4
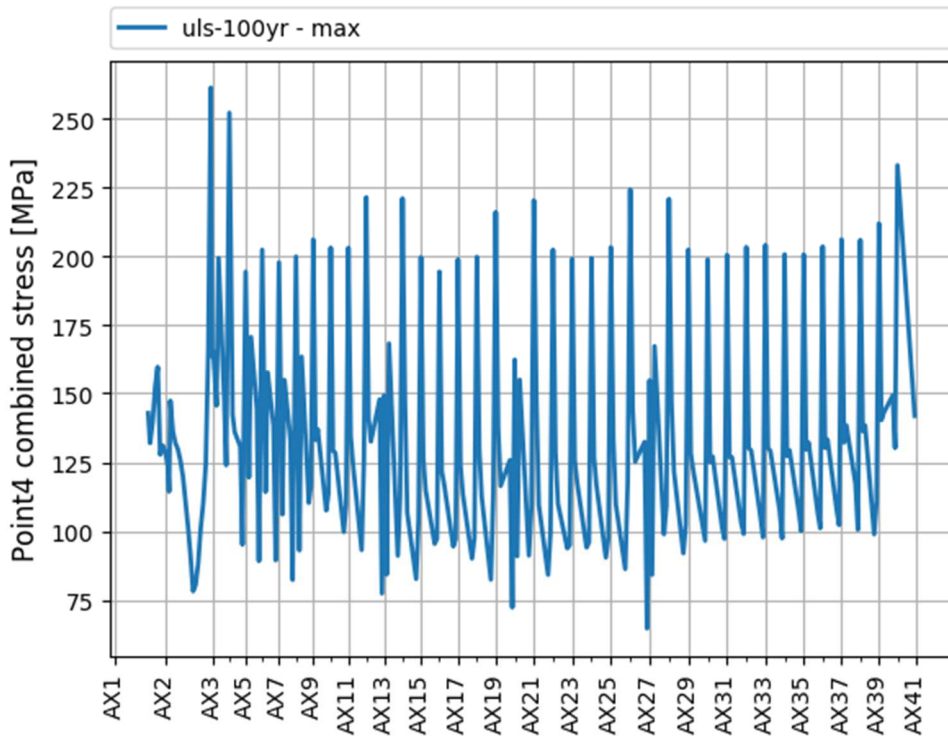
Figure 6-16   Combined stress at point 4
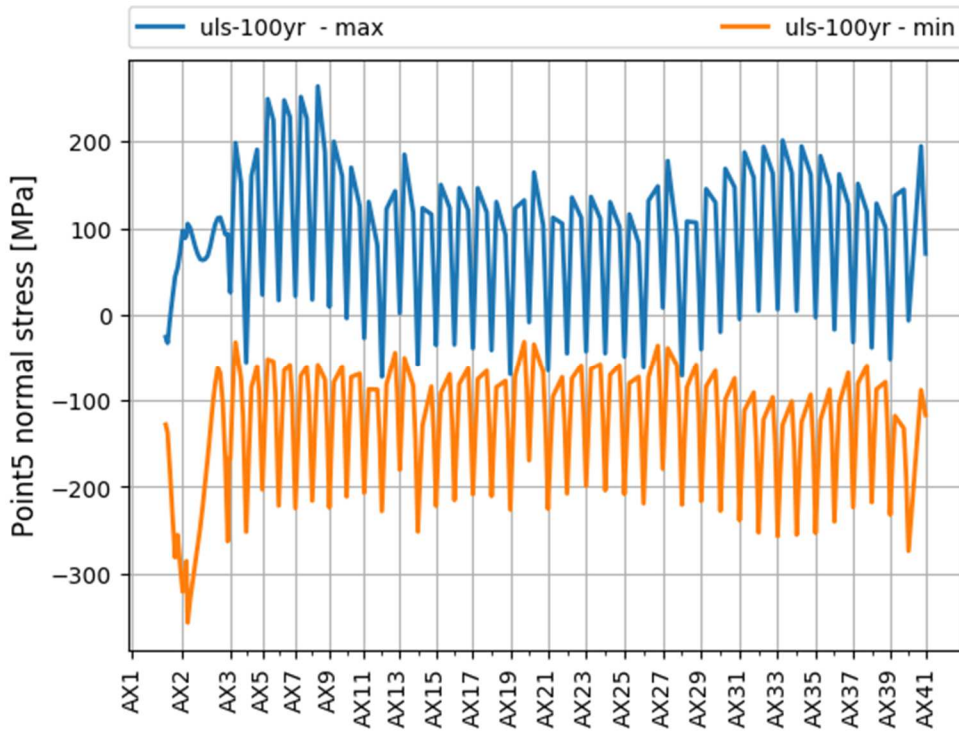
Figure 6-17   Normal stress at point 5
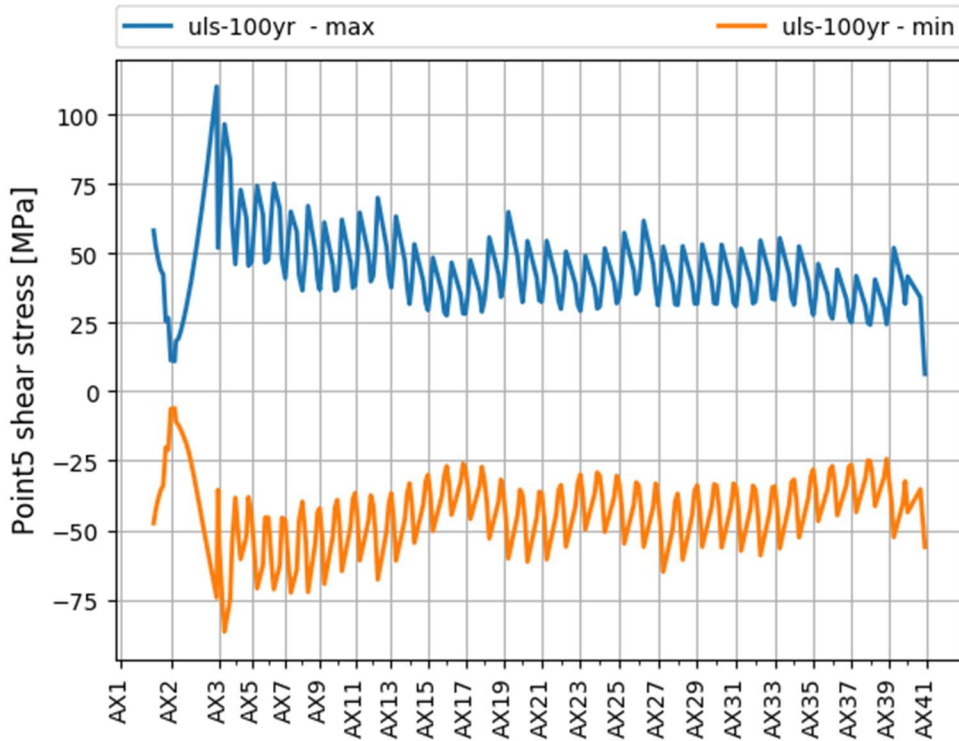
Figure 6-18   Shear stress at point 5
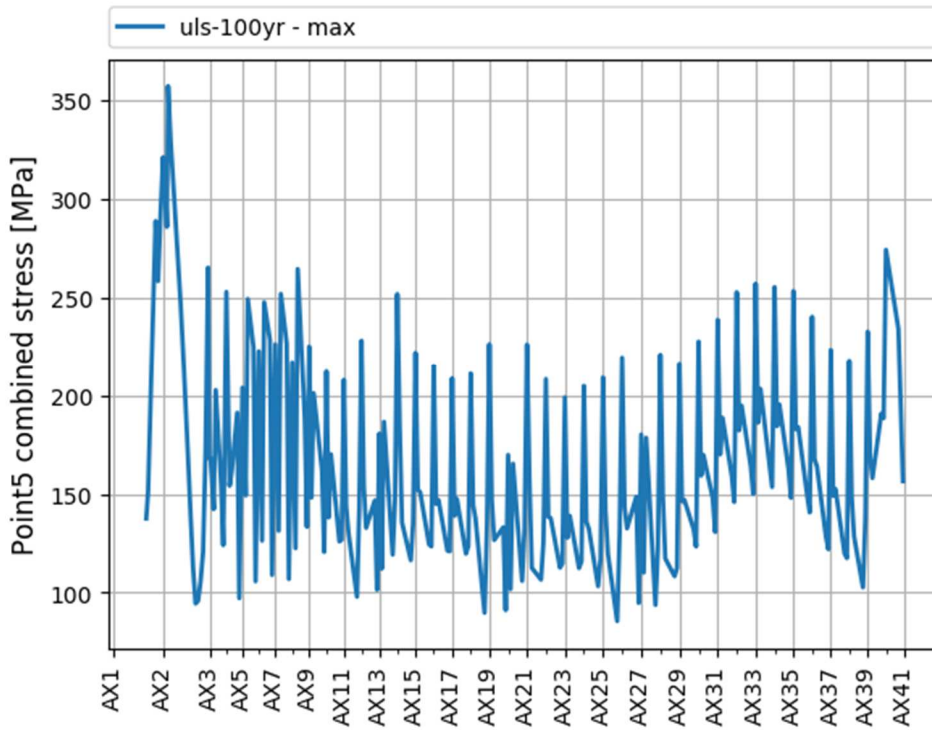
Figure 6-19   Combined stress at point 5
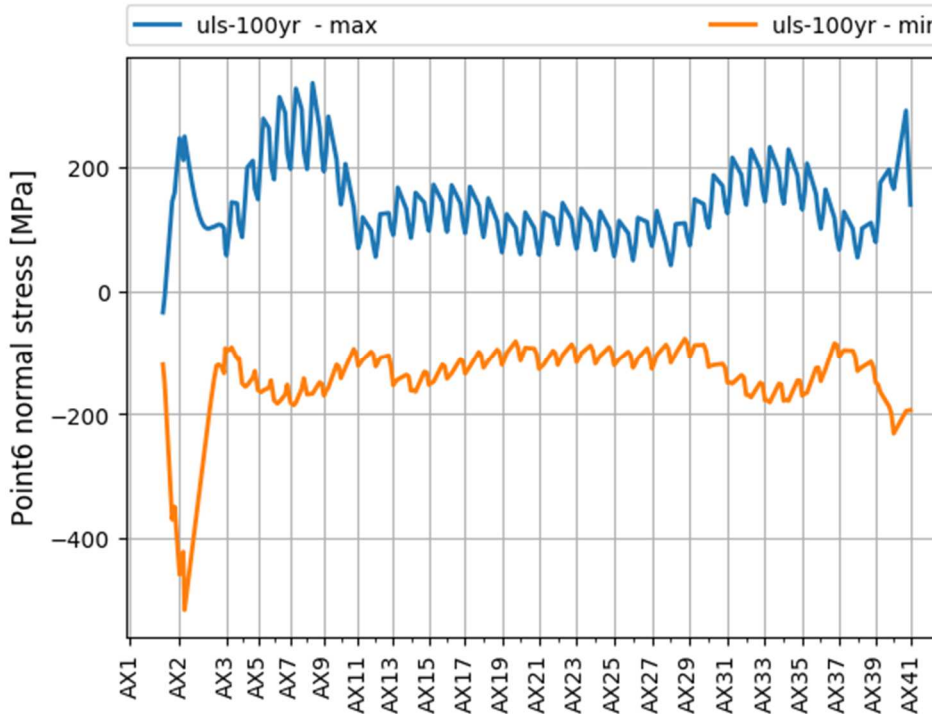
Figure 6-20   Normal stress at point 6
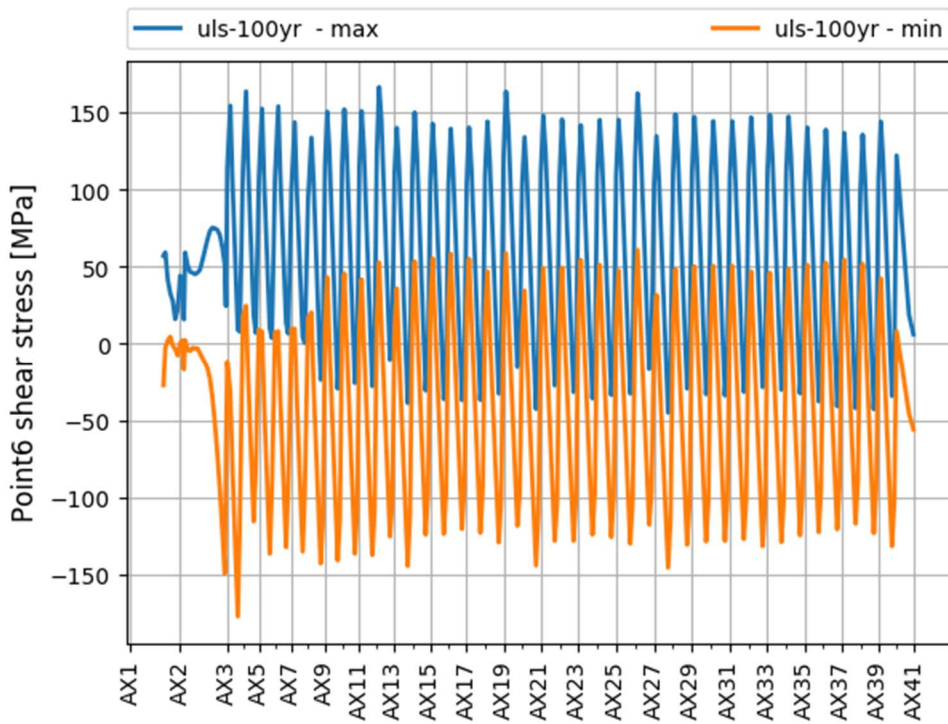
Figure 6-21   Shear stress at point 0
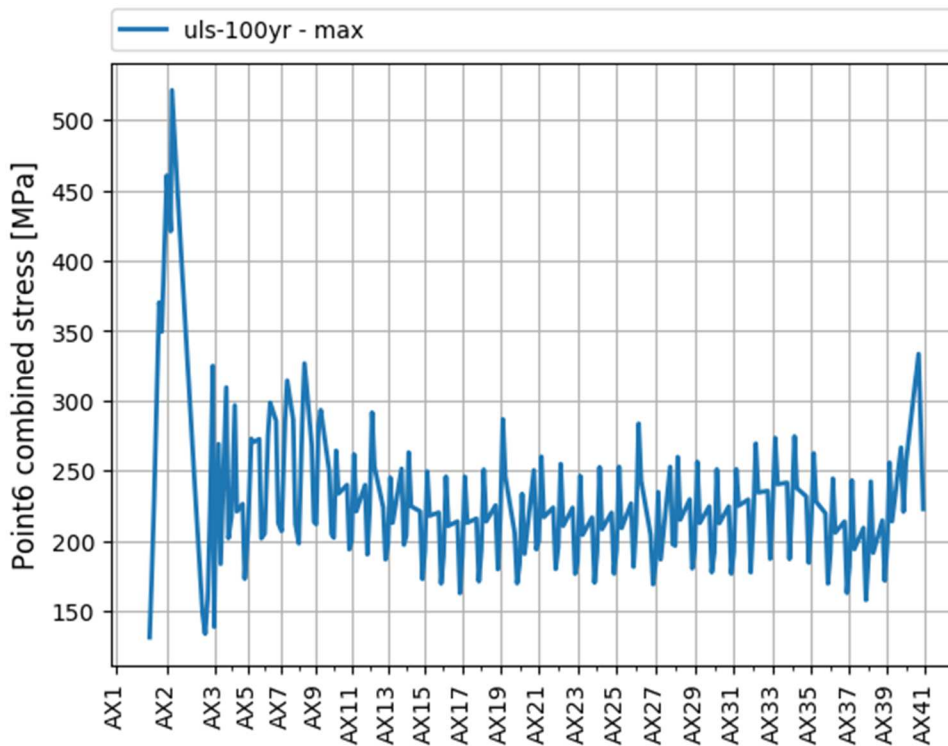
Figure 6-22   Combined stress at point 6
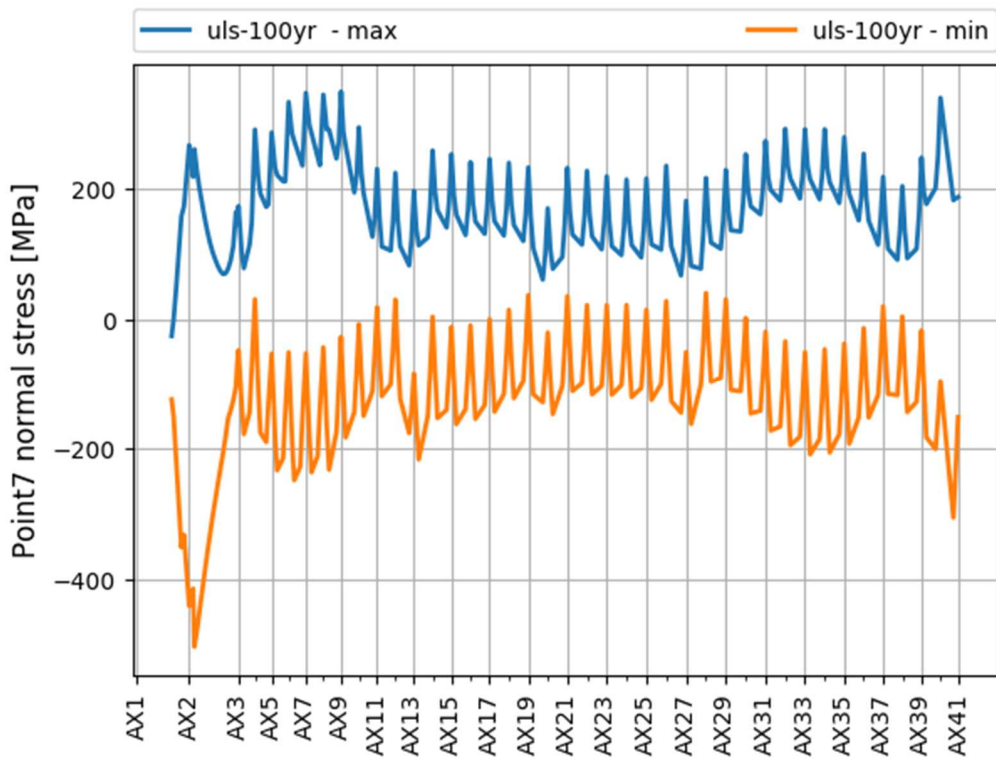
Figure 6-23   Normal stress at point 7
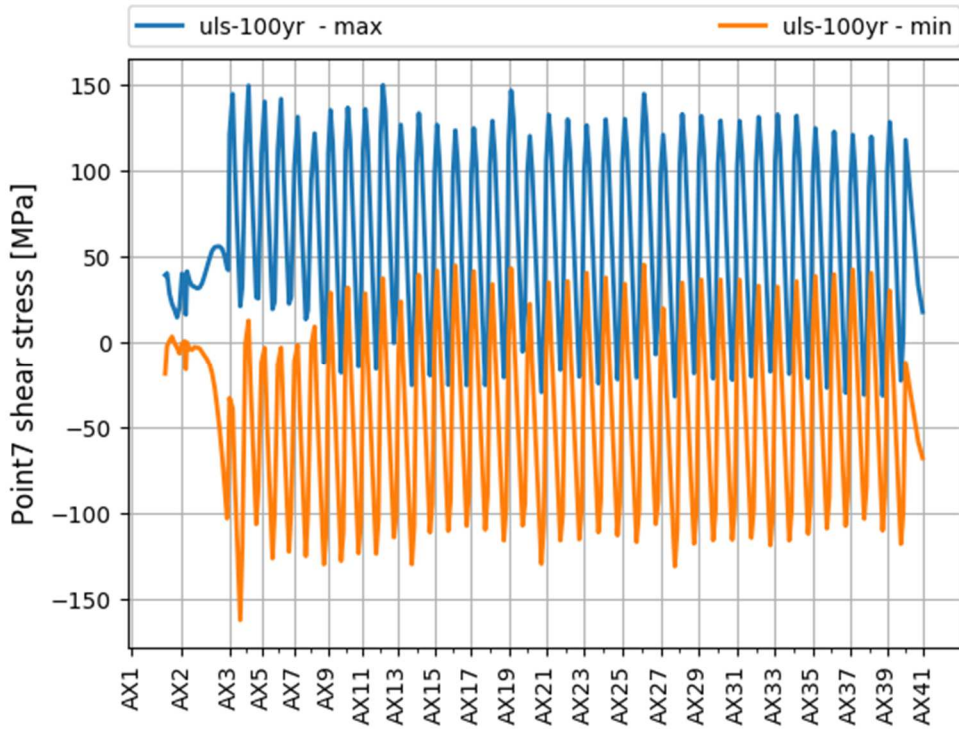
Figure 6-24   Shear stress at point 7
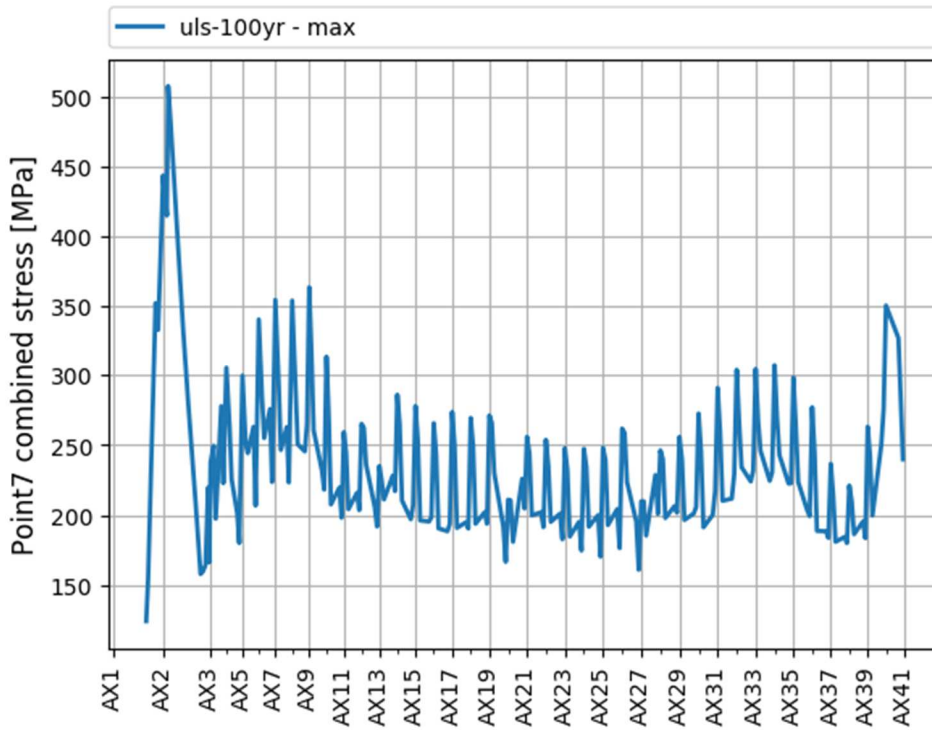
Figure 6-25   Combined stress at point 7
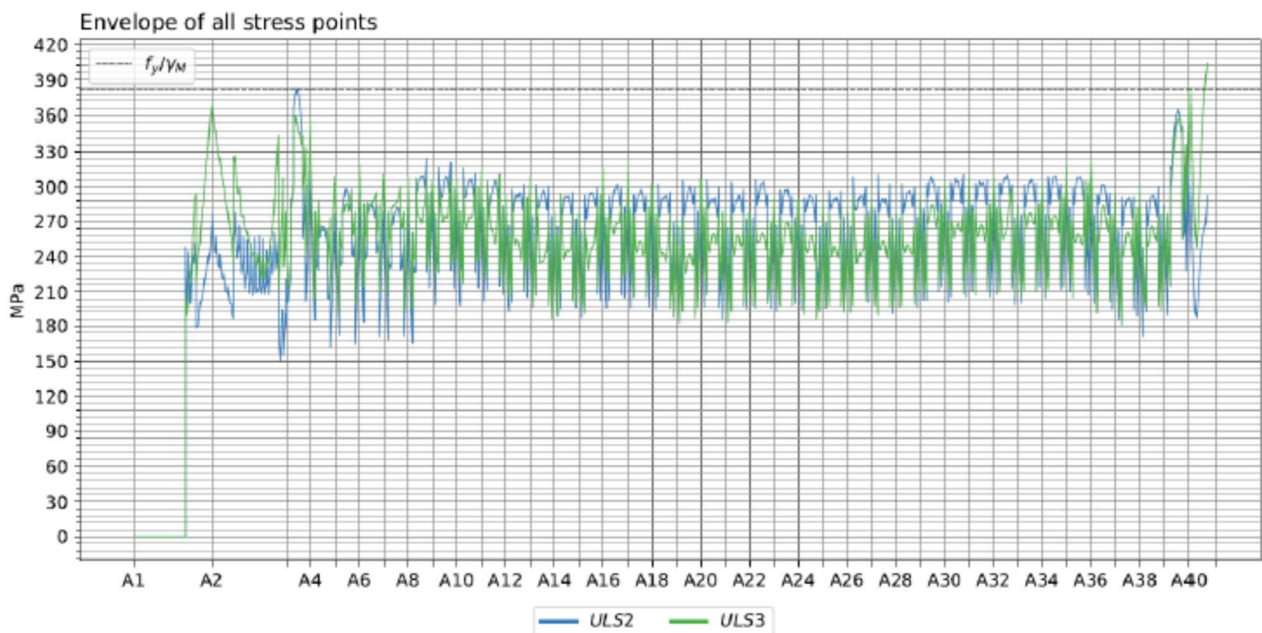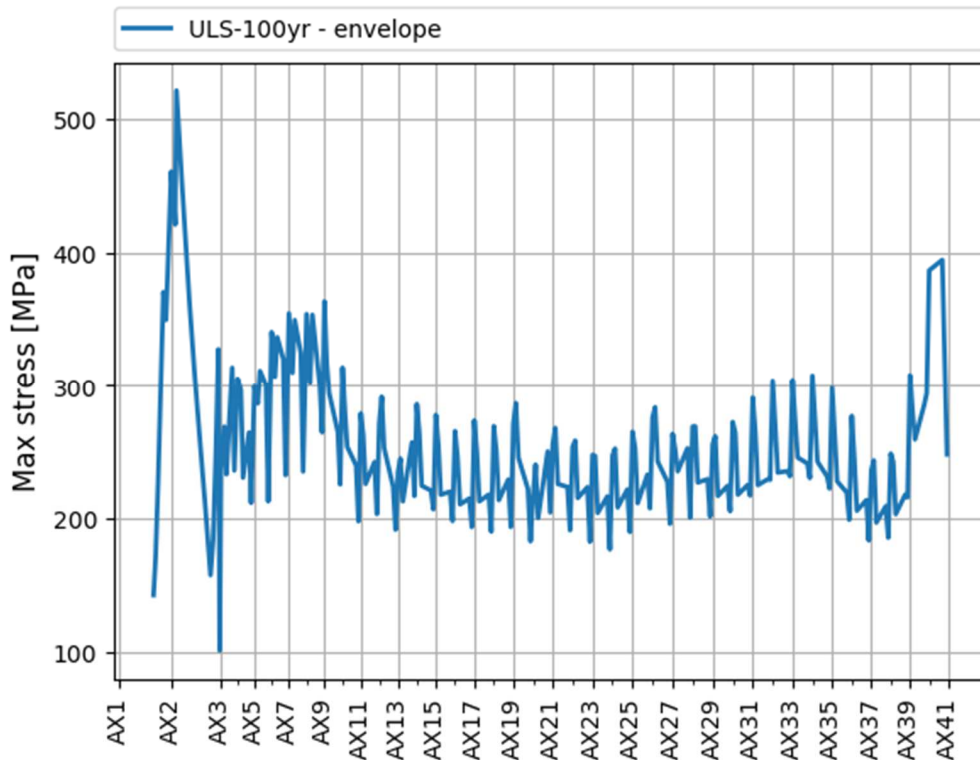
Figure 6-26   Maximum von Mises stresses along the bridge. Top – DNVGL, bottom – Designer /20/.

6.5 ULS Capacity checks

The maximum combined stresses in the box girder for the calculated points in the cross-section are presented in Figure 6-26. It can be seen that the cross-sections close to the abutment in the North and at axis 2 the combined stresses exceed the design stress. At these positions will also buckling of the

bridge stiffeners most likely fail. Reinforcements will be needed. For the remaining part of the bridge the capacity is judged to be adequate.

In Figure 6-26 is also shown designers results. The results from designer marked ULS 3 can be compared with the results from the independent analyses. It is seen that there is close correspondence with the exception of the cross-section at axis 2.

7 FATIGUE DAMAGE FROM ENVIRONMENTAL LOADS

7.1 General

The proposed concept for crossing of the Bjørnafjorden strait possesses several parts that need to be checked for fatigue. The bridge girder and pontoon columns are exposed to dynamic loads from waves, wind, tidal variation and traffic. The pontoons are exposed to variable load pressure and the high bridge and its cables are dynamically loaded. The independent analyses are directed to check that the bridge girder can be given satisfactory fatigue life as this is the dominating structural element and possible need for design changes here will have the largest impact on cost and schedule.

It should be realized that a floating bridge is considerably more exposed to fatigue loads than a conventional steel bridge girder with a steel orthotropic stiffened plate deck. Since the same structural detail may be exposed to dynamic loads from several sources, traditional considerations of suitable fatigue details may not be sufficient. In other words, as the bridge is exposed to much larger fatigue loads from environmental loads also the fatigue loading from traffic need to be treated more accurately.

The fatigue checks are made by analysing the fatigue from the wind and wave loads. The fatigue from traffic and tidal variations is not studied in this report.

The fatigue capacity of a structural detail will depend upon the local geometry and fabrication methods that will be determined at a later design phase. Consequently, the independent fatigue checks are focused on details where improvement will require changes that will impact the total cost or schedule.

It is presented results from screening based on results from the global beam analysis of the fatigue for a typical detail category that is assumed representative for normal details. Furthermore, the stress concentration due to shear lag and local strengthening elements are determined and an example of effect on the calculated fatigue life is given.

7.2 Results from screening of fatigue damage from wind and waves for the bridge girder

Screening of the fatigue damage of details in the bridge girder is made by analysing fatigue in typical details that will be present in the dominant cross-sections along the bridge. The damage is calculated at the selected points as shown in Figure 4-2. The results are in the screening presented for normal stresses neglecting possible contribution from shear stresses. Fatigue damage from shear stresses can be found in Appendix F.

The screening is made with the assumption of a typical detail that will be present at various positions along the bridge. The typical detail is selected as a buttweld assumed fabricated in accordance with NS-EN-1090-2 and a fabrication tolerance of 2 mm. A two-sided buttweld was assumed with a maximum thickness increase in plate thickness of 2 mm. Consequently, a stress concentration factor of 1.50 is applied for all the sections and the corresponding SN curve to be used is D curve according to DNVGL-RP-C203 /18/.

Rainflow counting is used to calculate the stress range distribution from time series of stresses from the global analysis. The fatigue damage is calculated separately for normal stresses and shear stresses. The reason is that combination of these stresses in a time domain analysis with a beam model is difficult.

In order to account for local stress-concentrations certain points are recalculated with stresses found from local analyses as shown in Section 7.3.5 More accurate analyses should be made by shell models as the design develops.

Figure 7-1 to Figure 7-8 show calculated fatigue lives induced by normal stress for axis 2 to 41 at the location points defined in Figure 4-2. Figure 7-9 present the envelope section fatigue life, i.e., minimum fatigue life of different locations, along the girder. As seen from the results, the most critical fatigue life is 482 years, occurs at axis 3, Section S1_H, Point 5. The details can be found in Appendix E.

The design fatigue factor is in the Design Basis given as 2.5 for details that can be inspected making the required design fatigue life to be 250 years for the details in the box girder. From the screening all sections of the bridge have sufficient fatigue capacity to deal with environmental dynamic stresses. However, fatigue from traffic and in the bridge ends also from tidal variations will add and reduce the margin. Local stress concentration need also to be accounted for see 7.3.5 and 7.3.6.
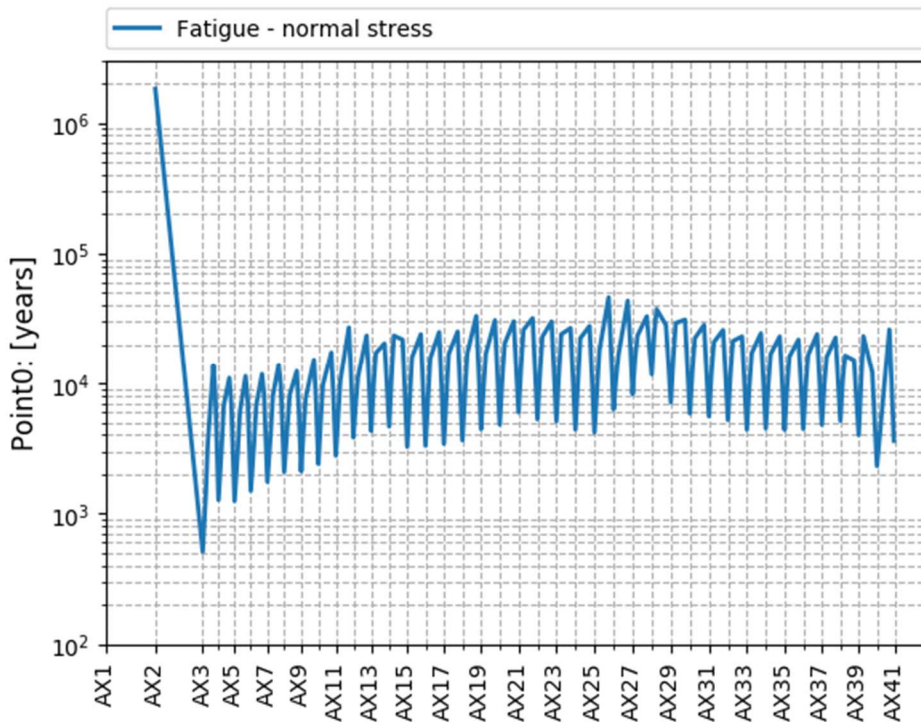
Figure 7-1   Fatigue life along bridge length for point no. 0. Normal stress is applied.
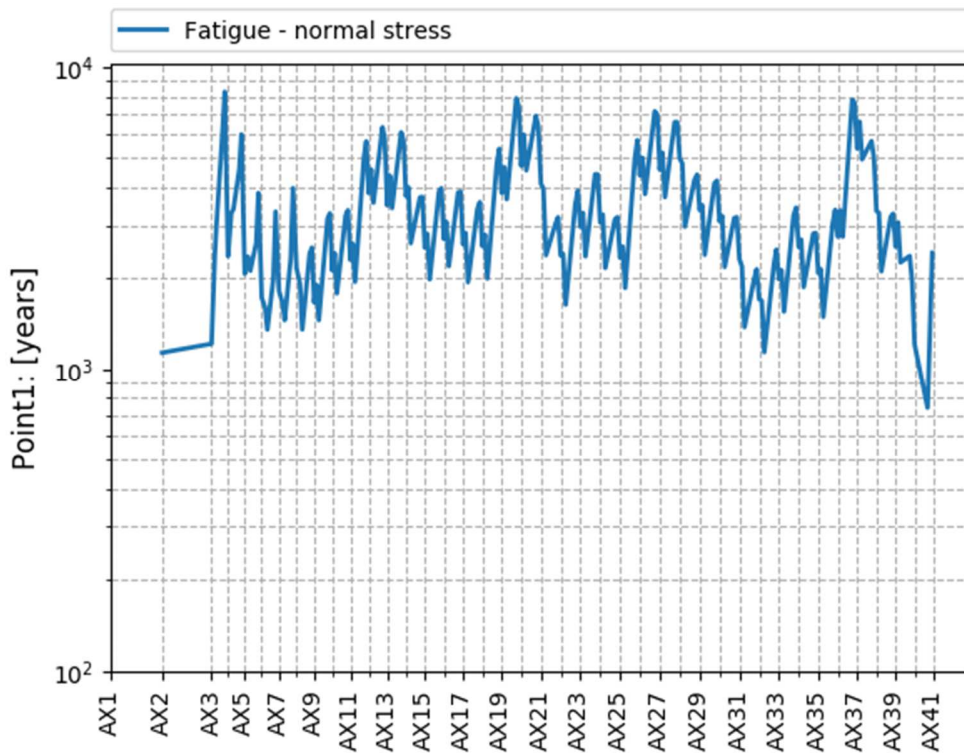
Figure 7-2   Fatigue life along bridge length for point no. 1. Normal stress is applied.
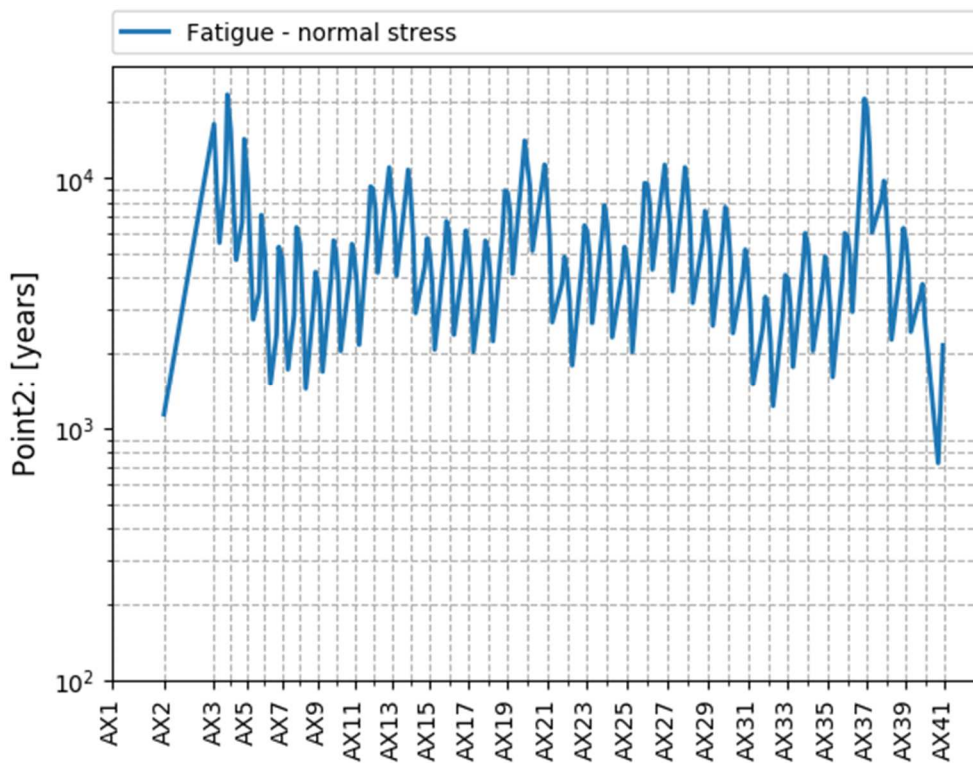
Figure 7-3   Fatigue life along bridge length for point no. 2. Normal stress is applied.
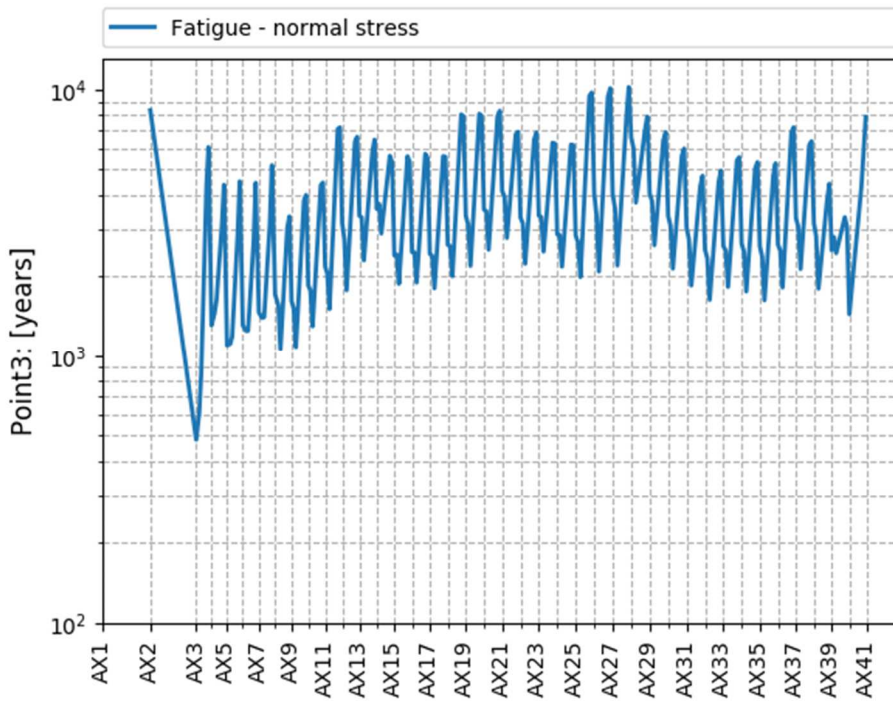
Figure 7-4   Fatigue life along bridge length for point no. 3. Normal stress is applied.
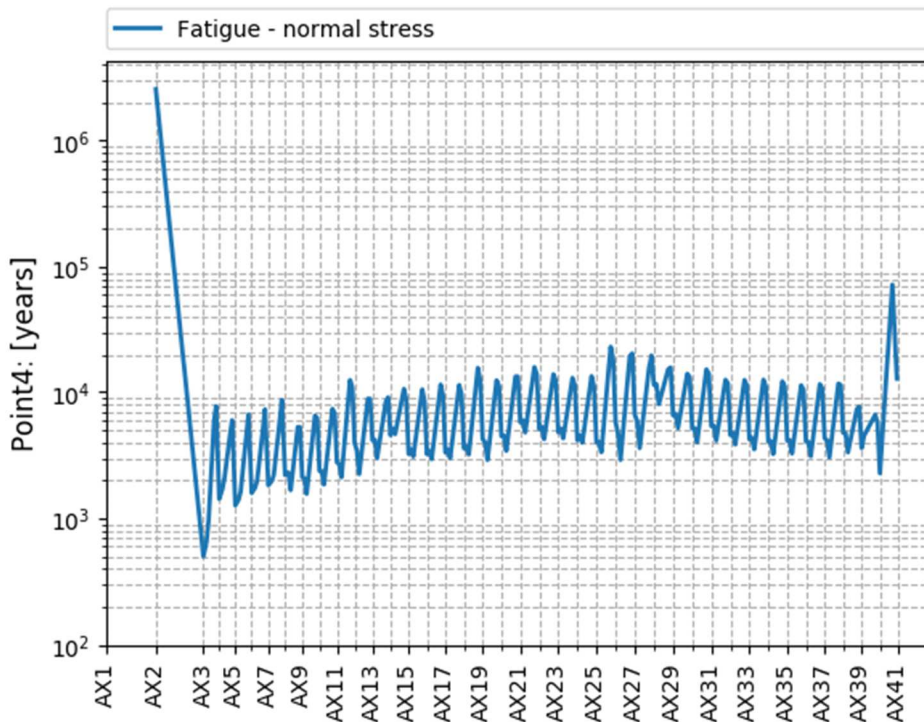
Figure 7-5   Fatigue life along bridge length for point no. 4. Normal stress is applied.
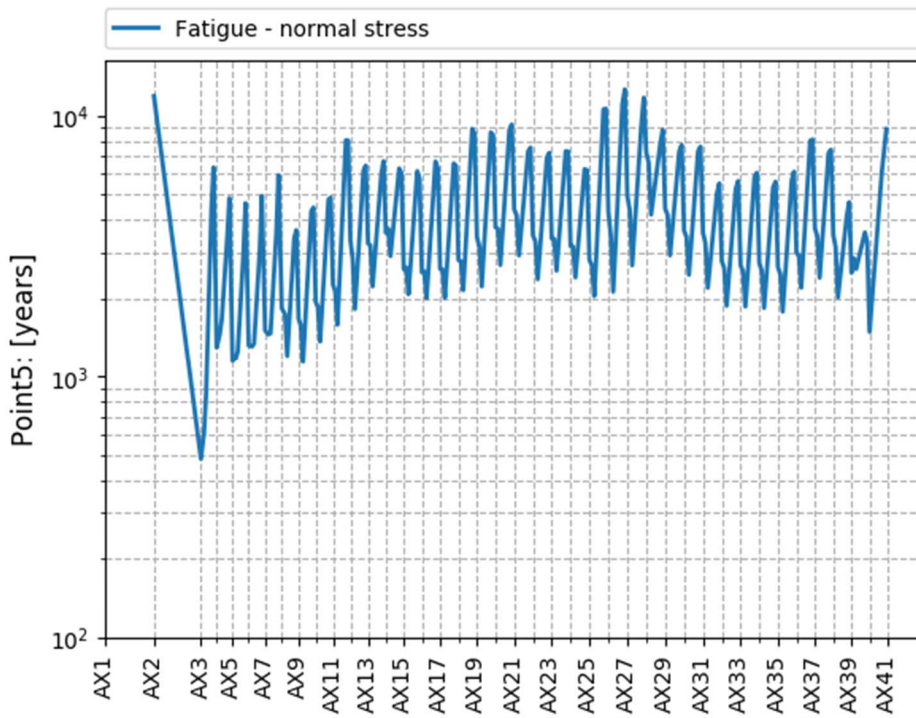
Figure 7-6 Fatigue life along bridge length for point no. 5. Normal stress is applied.
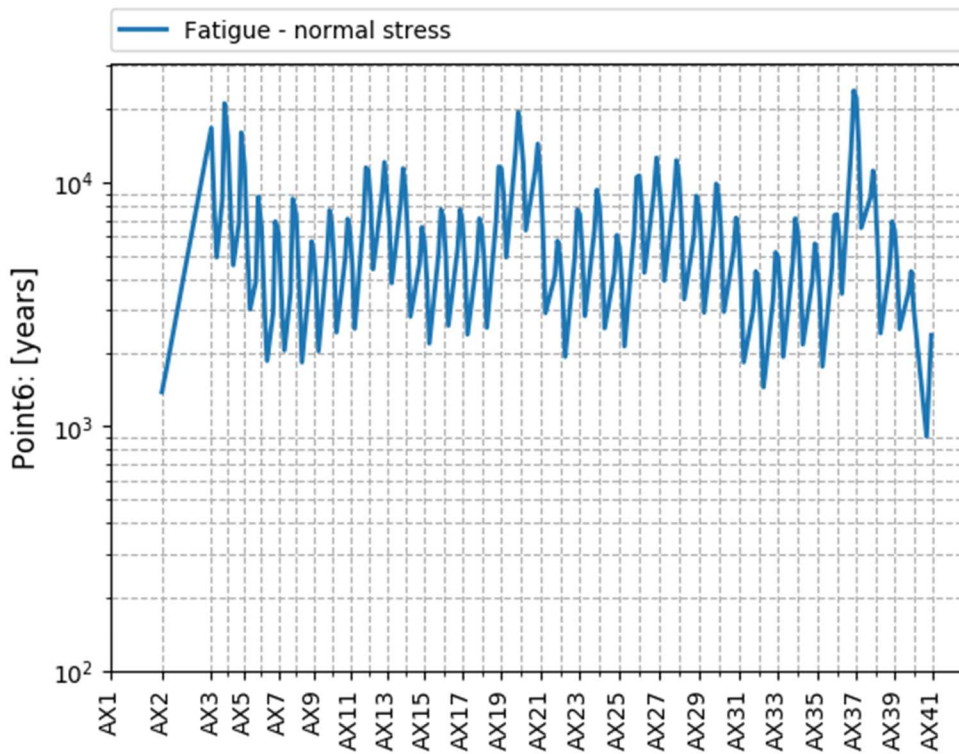
Figure 7-7 Fatigue life along bridge length for point no. 6. Normal stress is applied.
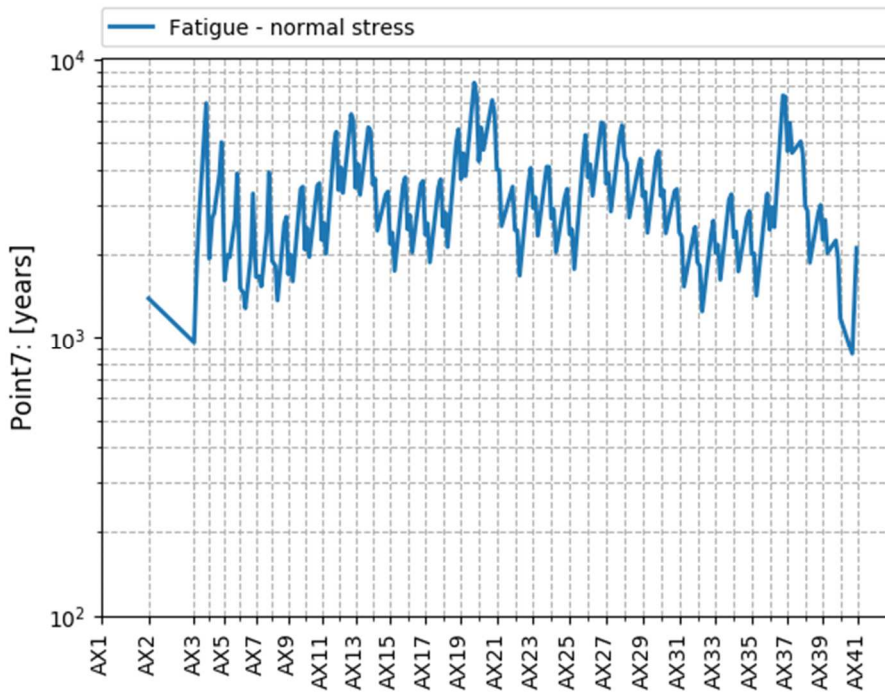
Figure 7-8   Fatigue life along bridge length for point no. 7. Normal stress is applied.
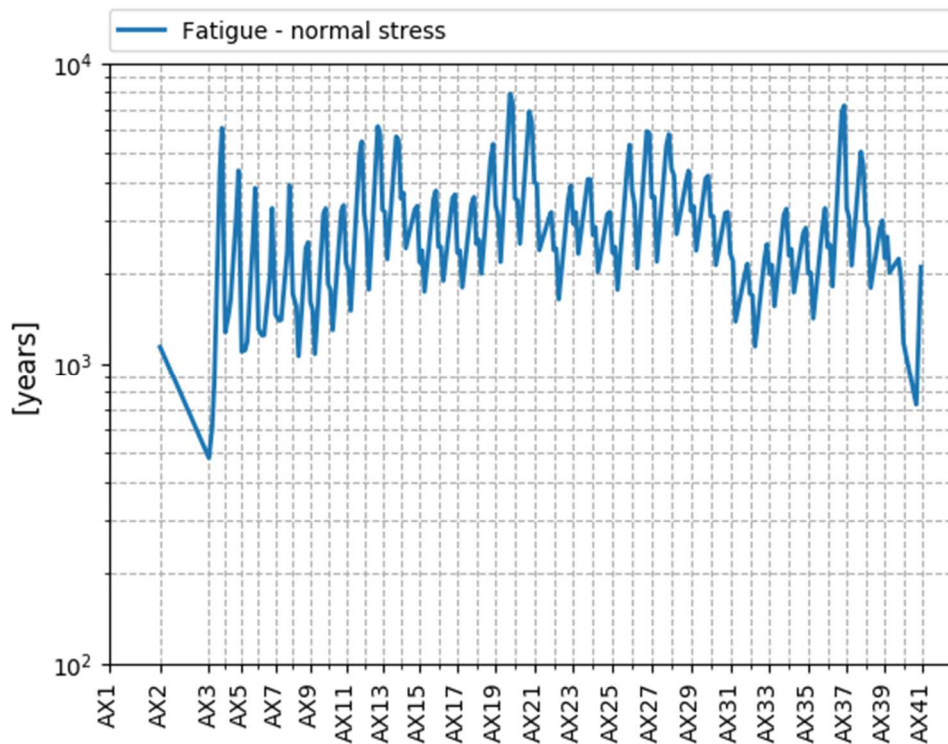
Figure 7-9   Envelope fatigue life along bridge length. Normal stress is applied.

7.3 Local stress concentrations in bridge girder due to shear lag and cross-sectional changes

7.3.1 General

The stresses used as basis for the fatigue calculations presented in 7.2 is based on beam theory. Due to the wide flange compared with the span length between pontoons shear lag effects may increase the stresses at certain points. Furthermore, the beam support is on the column in the middle of the cross-section and the cross section has internal bulkheads and longitudinal trusses that makes need to adjust the stresses that are found from beam theory. Therefore, a set of local analyses that compares results from beam theory with a detailed shell model of a selected part of the girder is made and stress concentration factors are determined

7.3.2 Selection of local models

In order to compare stresses from beam theory with a local model using shell elements a small part of the low bridge is studied. The model consists of 4 span of the girder and is simplified to be straight over this length. Then 4 load-cases are analysed both with a beam model with the same properties as in the global analysis and with a shell model where the cross-section details are modelled more accurately.

7.3.3 Description of the local models

A local shell model of the bridge is developed to:

1. Verify the stiffness of the global beam model.

2. Locate and examine local stress concentration factors (SCFs).

The shell model includes all longitudinal stiffeners, longitudinal diagonal trusses, transverse frames with diagonal beams, internal bulkheads above the column and simplified columns, see Figure 7-10 and Figure 7-11. The mesh density of the shell model is 0.4 m. The total length of the local model is 500 m, i.e. 4 spans of 125 m which is the distance between the pontoons. The origin of the models is in the middle of the bridge with y-axis in the longitudinal direction.
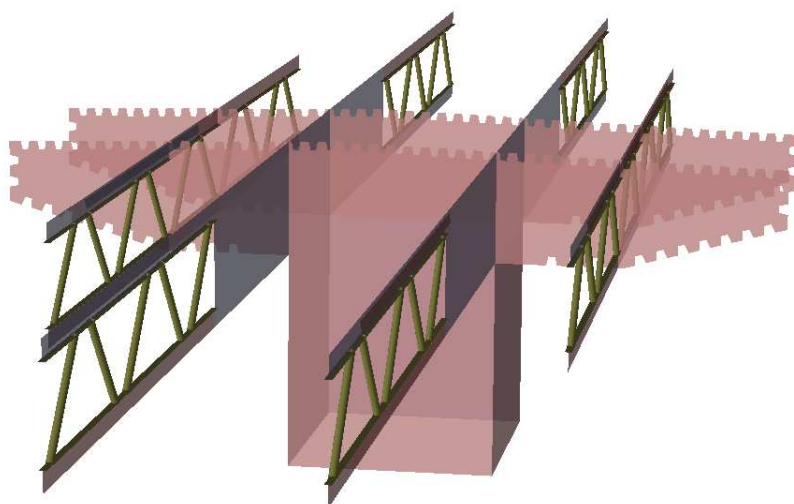
Figure 7-10   Transverse/longitudinal bulkheads and longitudinal trusses above columns
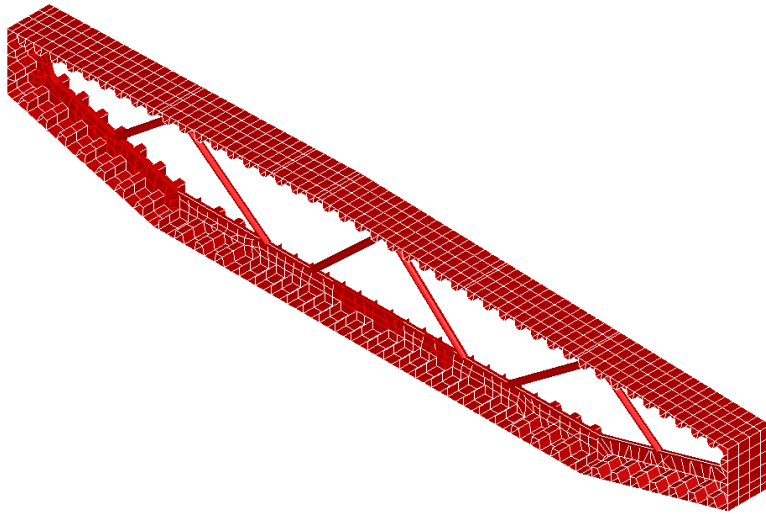
Figure 7-11 Typical transverse frame

The model is supported at five locations, at the bridge girder ends and at the bottom of the three columns, see FIGXX. Different boundary conditions are applied to the support points to achieve the desired deformation shapes.
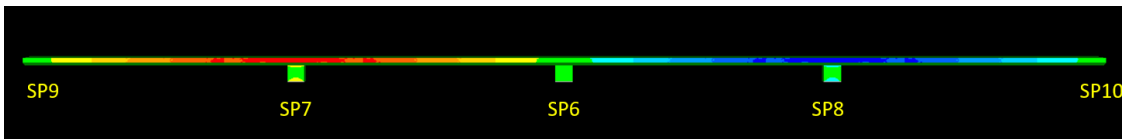
Figure 7-12 Side view showing support locations

Four load cases representing different bridge deformations are analyzed:

1. Bridge girder weak axis bending (1 sinus) around transverse x-axis, see Figure 7-13

2. Bridge girder weak axis bending (2 sinus) around transverse x-axis, see Figure 7-14

3. Bridge girder strong axis bending (½ sinus) around vertical z-axis, see Figure 7-15

4. Bridge girder strong axis bending (1 sinus) around vertical z-axis, see Figure 7-16
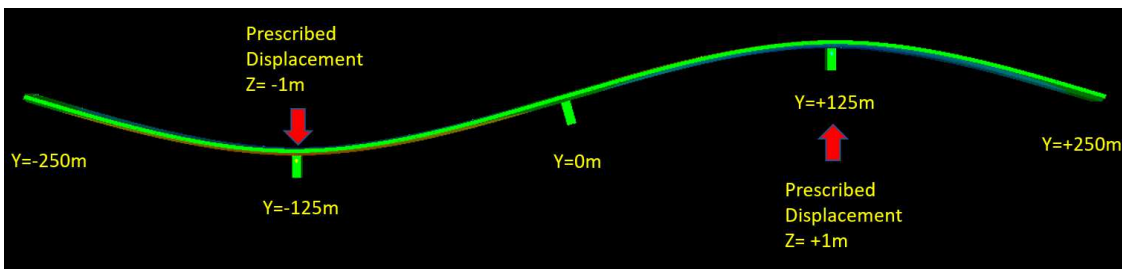
Figure 7-13 Side view 1 sinus
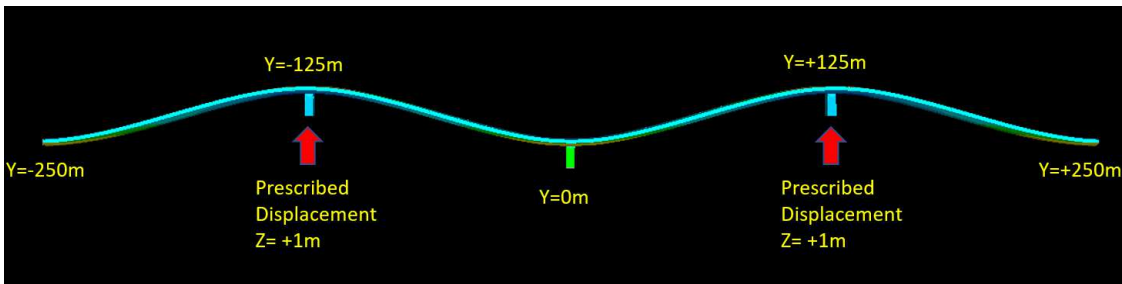
Figure 7-14   Side view 2 sinus
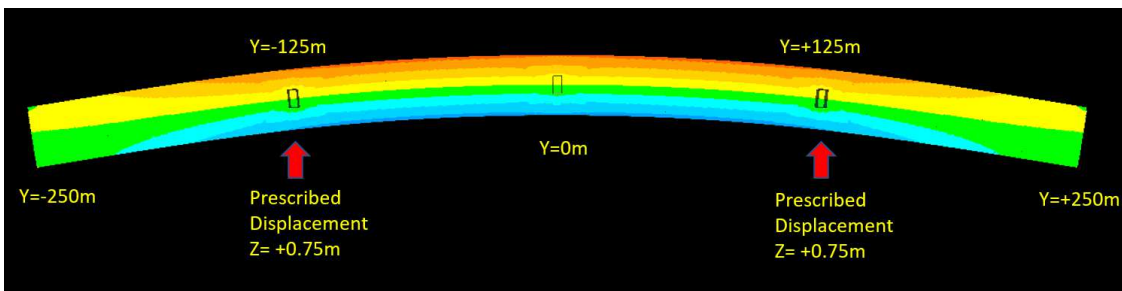
Figure 7-15   Top view ½ sinus
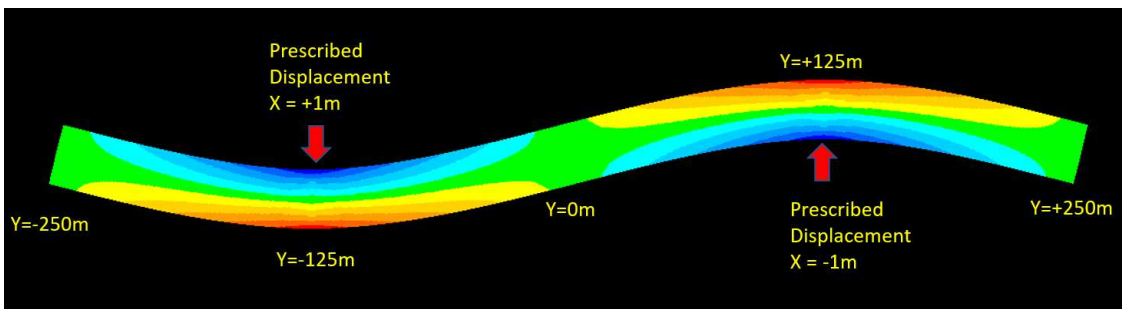
Figure 7-16   Top view 1 sinus

The same analysis is performed with a beam model with same dimensions and configurations as the shell model. The beam model has the same stiffness and properties as the global beam model.

The reaction forces at the support points are extracted for the beam models and the shell models. The difference in reaction forces between the beam and shell model shows the shear lag effect and is used to scale the calculated stresses in the beam model so that the stresses in both models are calculated for the same bending moment at the chosen cross section.

A spreadsheet has been developed to extract the stresses at eight different locations of the cross section of the bridge girder. The locations are shown in Figure 7-17.
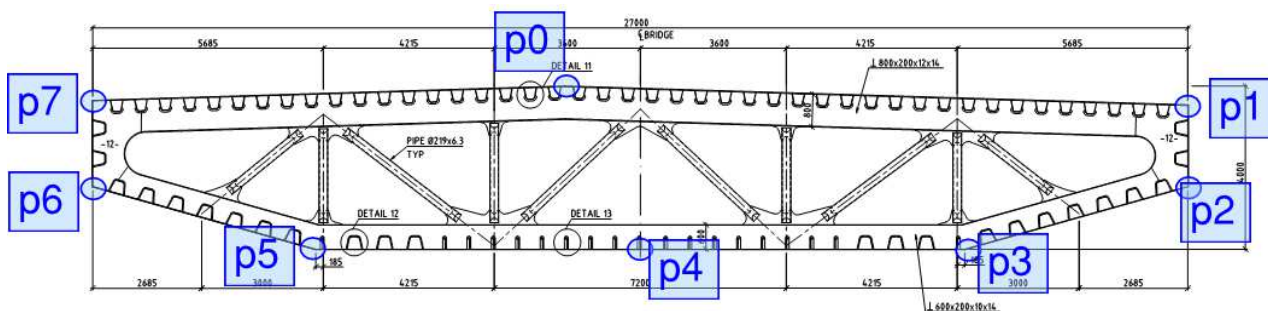
Figure 7-17 Stress point locations

From the shell analysis result file, the longitudinal element average D-stress (SIGMY) is exported. Only elements in the top and bottom plates are included. The exported listing contains longitudinal membrane stresses with associated coordinates for each element in the entire model. The listing is then imported in the spreadsheet and sorted on coordinates to easily present the stresses for any chosen cross section along the bridge girder.

From the beam model analysis result file, the weak/strong (MXY/MXZ) axis bending moment is extracted. The listing contains the moment and position along every meter of the bridge girder due to the 1 m mesh density. The moment is used to calculate the longitudinal stresses at the same cross section as for the shell model. Because the shell model and the beam model have different mesh density, the moment extracted from the beam model is interpolated to match the same longitudinal coordinate as the shell model.

The conclusion of this exercise shows that the highest local SCF's are found in the regions of the bridge girder above the columns at the intersection of longitudinal bulkheads and diagonals and top/bottom plates.

In order to study the effect of shear lag an assumption about the distance between zero moment locations have to be made. For weak axis bending the wave response spectrum is developed for the sea-states that contribute the most to fatigue damage. An example is shown in Figure 7-18. It is found that a large part of the fatigue damage is due to wave periods from 3.2 to 4.2 seconds.
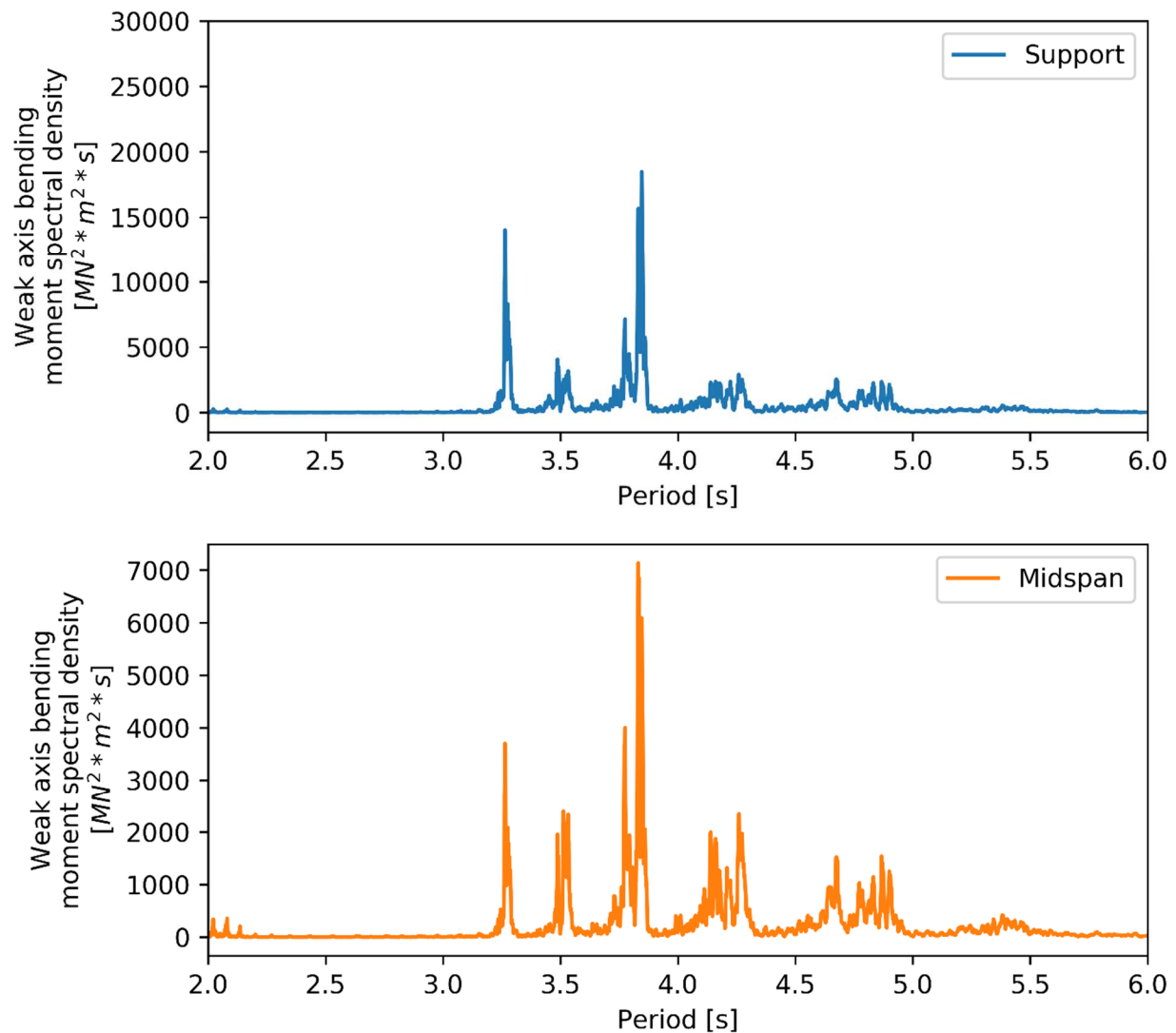
Figure 7-18   Weak axis response spectrum for the sea-state that contribute the most to fatigue for the middle part of the bridge.

The eigen modes for periods in this range were investigated and it was found that the distance between locations of zero weak axis moments where at the same distance as the span between pontoons. See Figure 7-19.
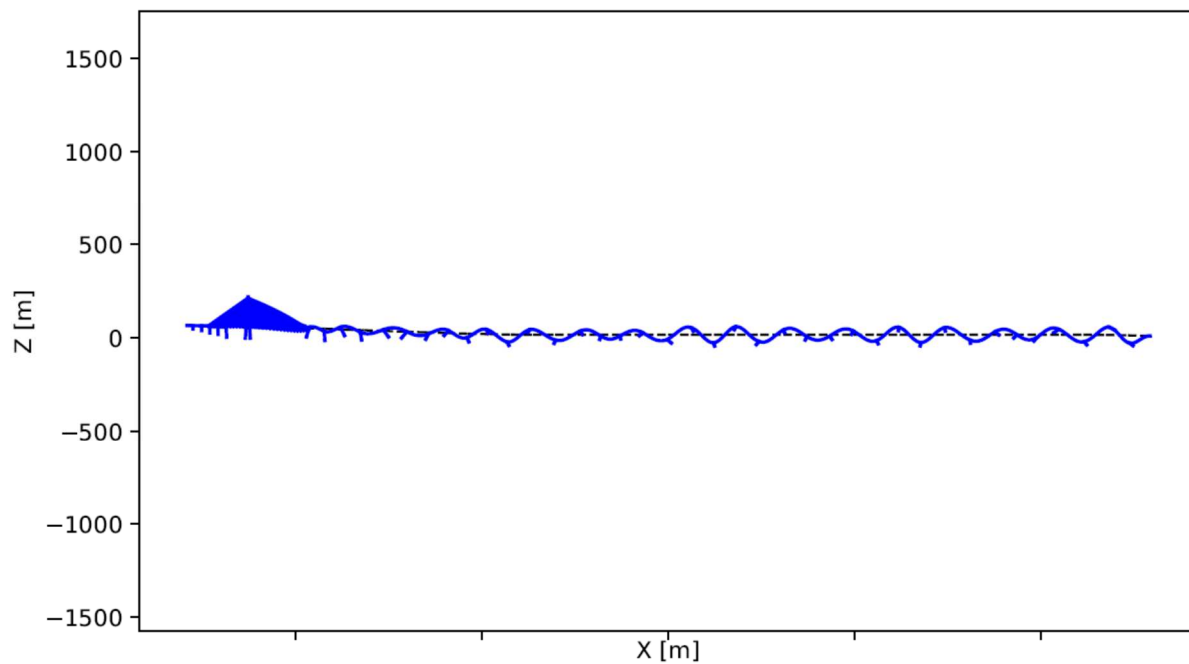
Figure 7-19   Plot of eigenmodes period 3.33 seconds showing example of mode shape with span length as distance between zero moments.

7.3.4 Comparison of beam model and shell model stresses

In the following the stresses are compared between stress calculated from the shell and the beam model for various positions along the bridge.

Figure 7-21 to Figure 7-25 shows results from weak axis bending with a 2 sinus deformation, see Figure 7-14

Figure 7-27 to Figure 7-31 shows results from strong axis bending with a 1/2 sinus deformation, see Figure 7-15
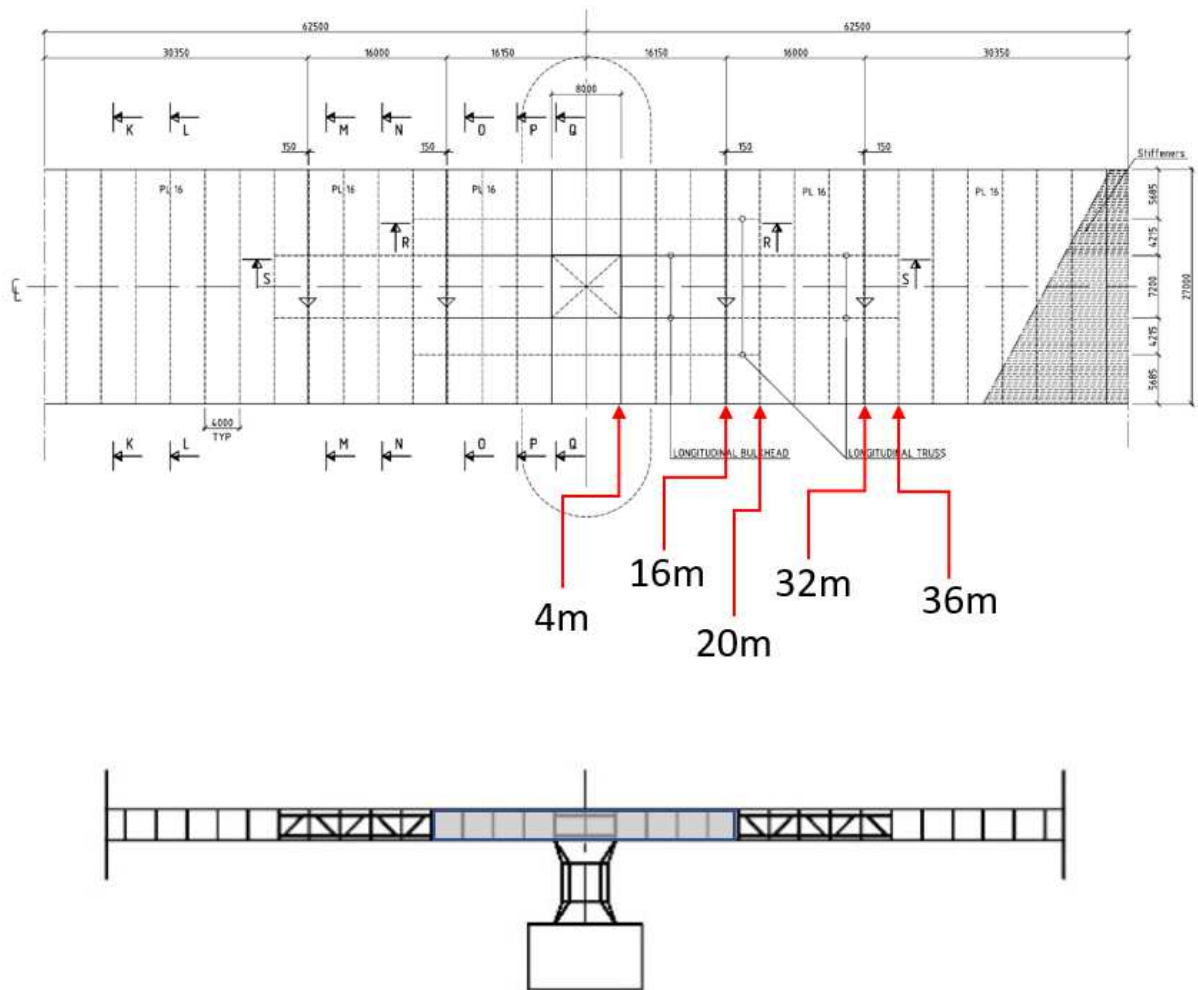
Figure 7-20 Typical positions for reported cross sections
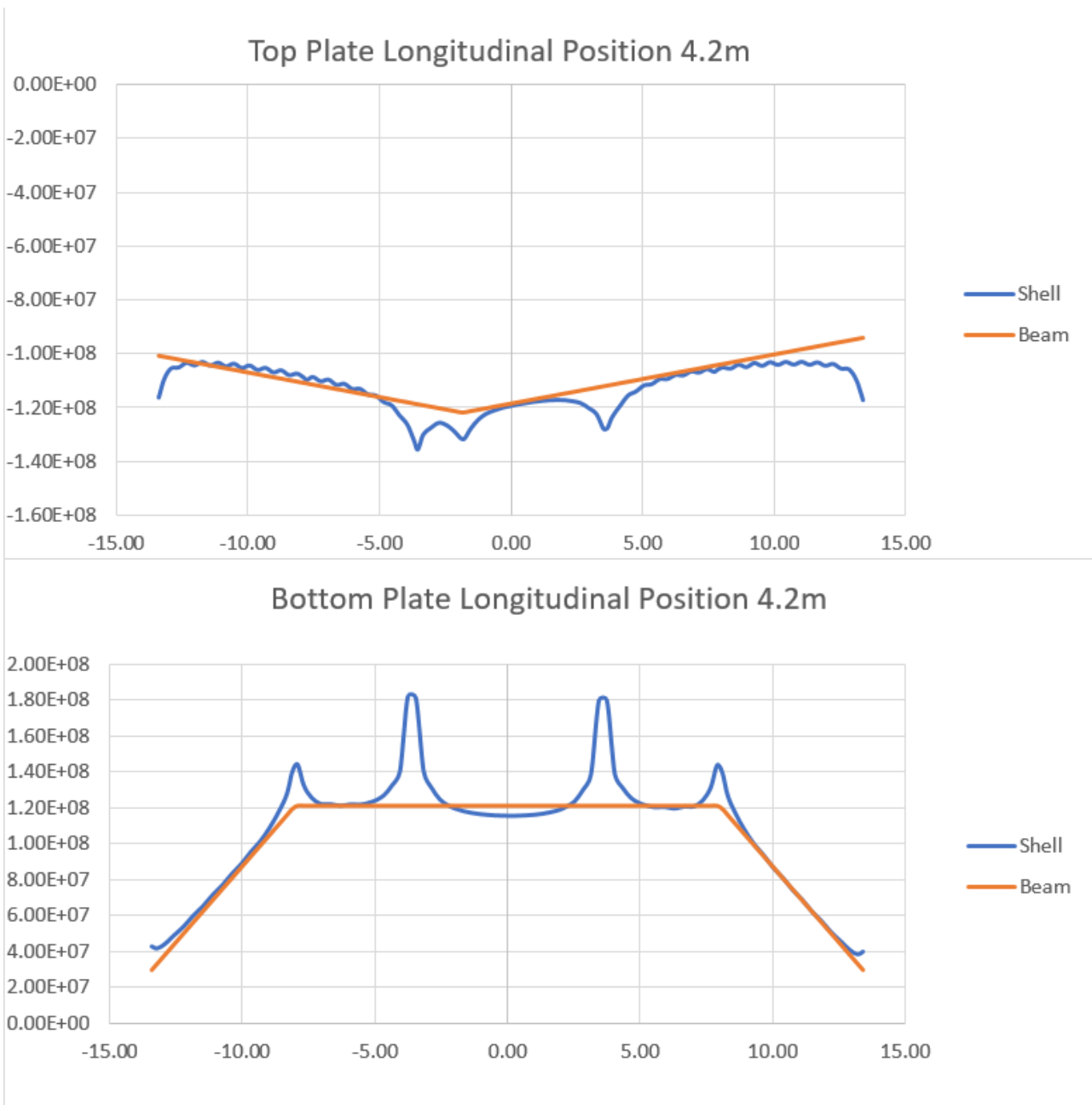
Figure 7-21   Stress comparison from weak axis bending at position 4,2 m

Figure 7-22   Stress comparison from weak axis bending at position 16,2 m
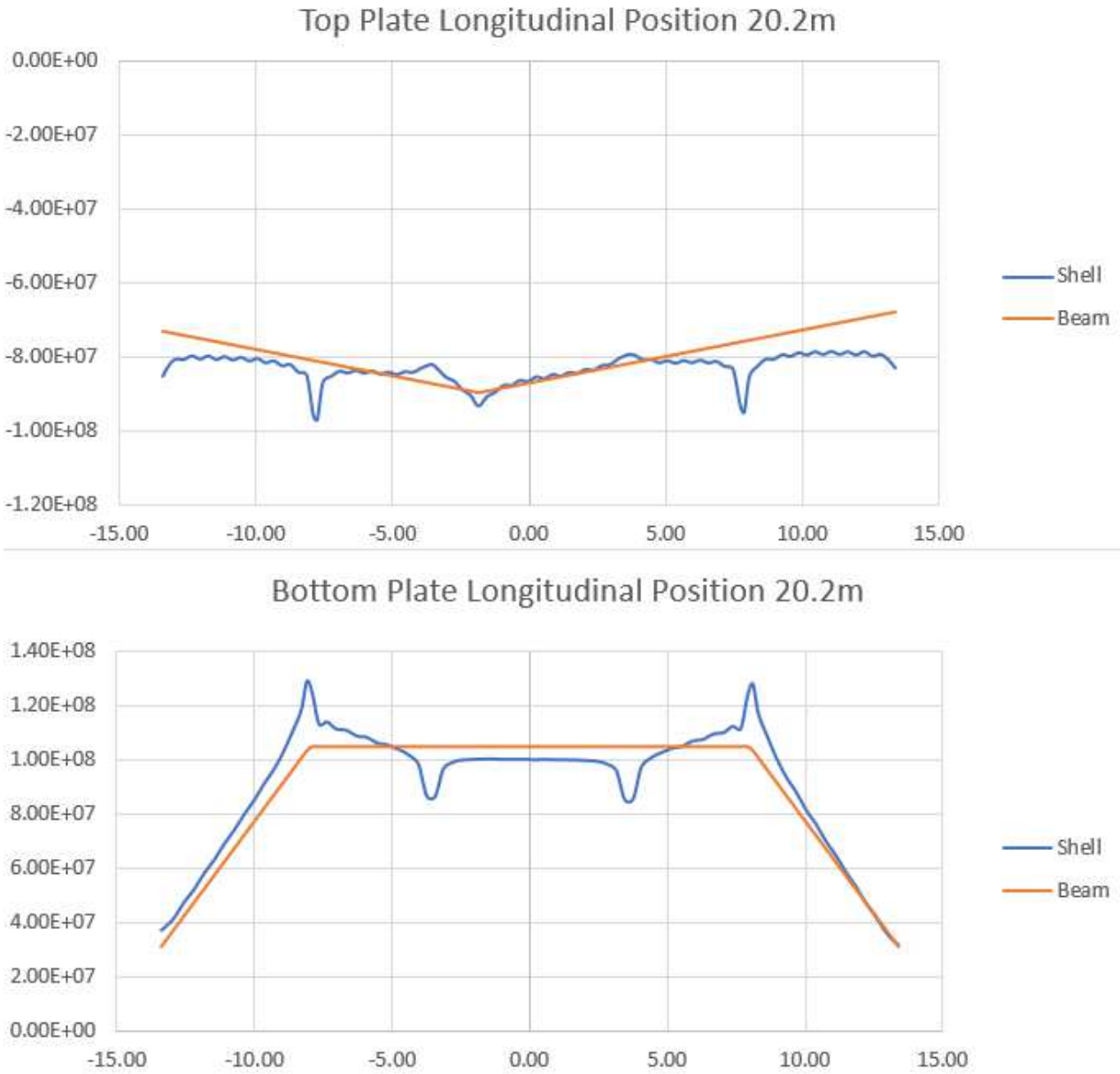
Figure 7-23   Stress comparison from weak axis bending at position 20,2 m

Top Plate Longitudinal Position 32.2m

Bottom Plate Longitudinal Position 32.2m

Figure 7-24   Stress comparison from weak axis bending at position 32,2 m

Figure 7-25 Stress comparison from weak axis bending at position 36,2 m
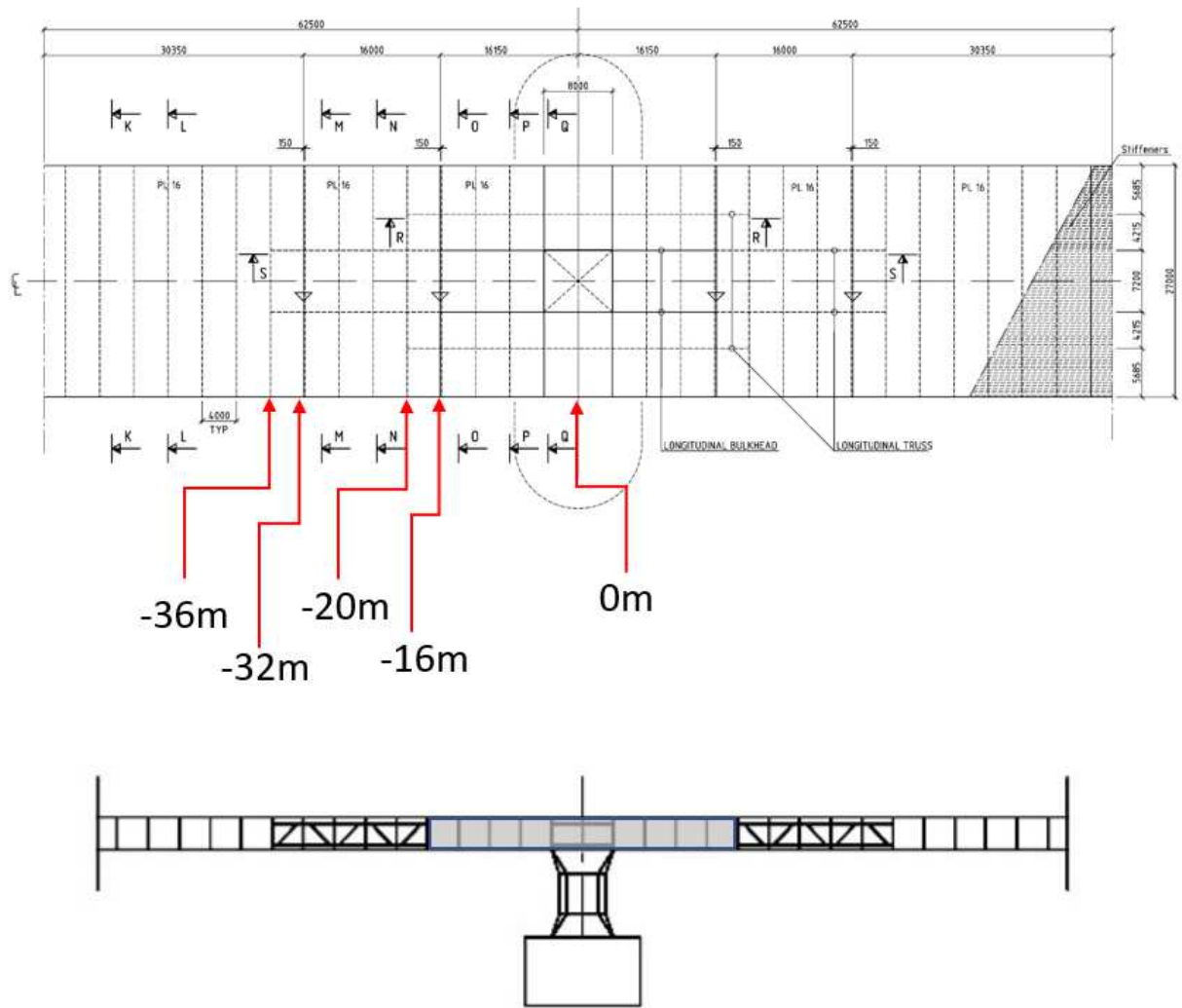
Figure 7-26   Typical positions for reported cross sections
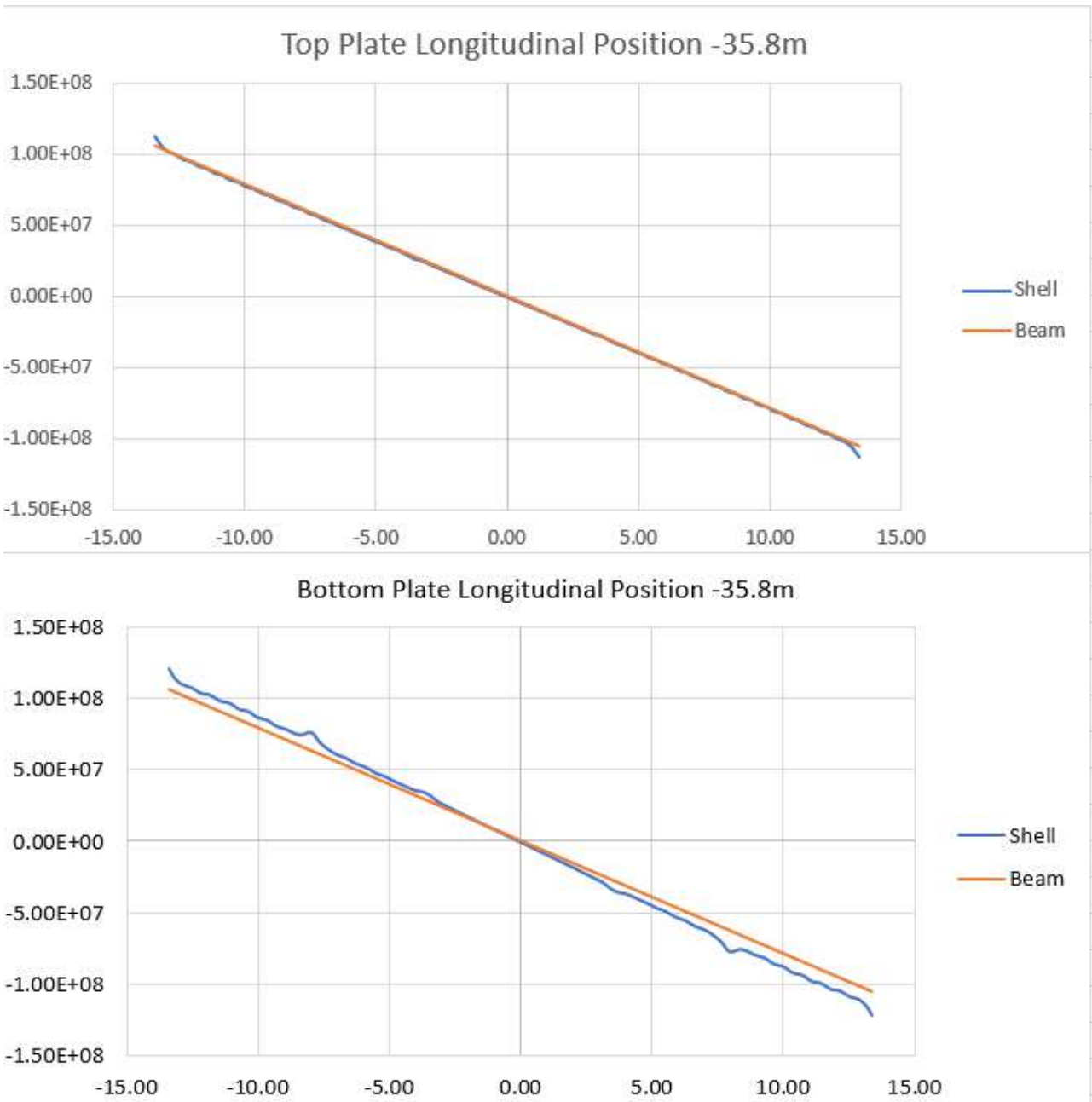
Figure 7-27   Stress comparison from strong axis bending at position -35,8 m
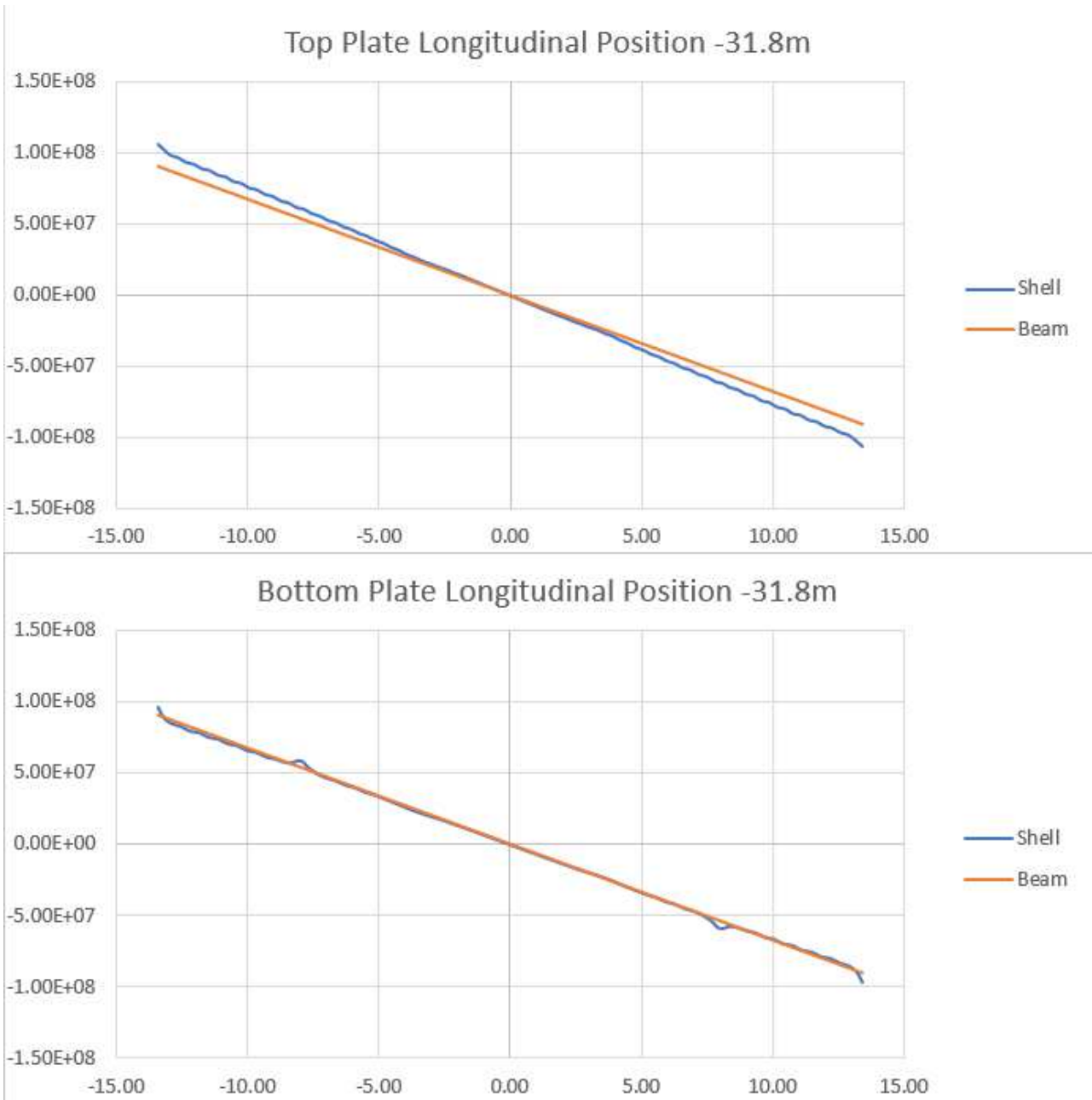
Figure 7-28 Stress comparison from strong axis bending at position -31,8 m
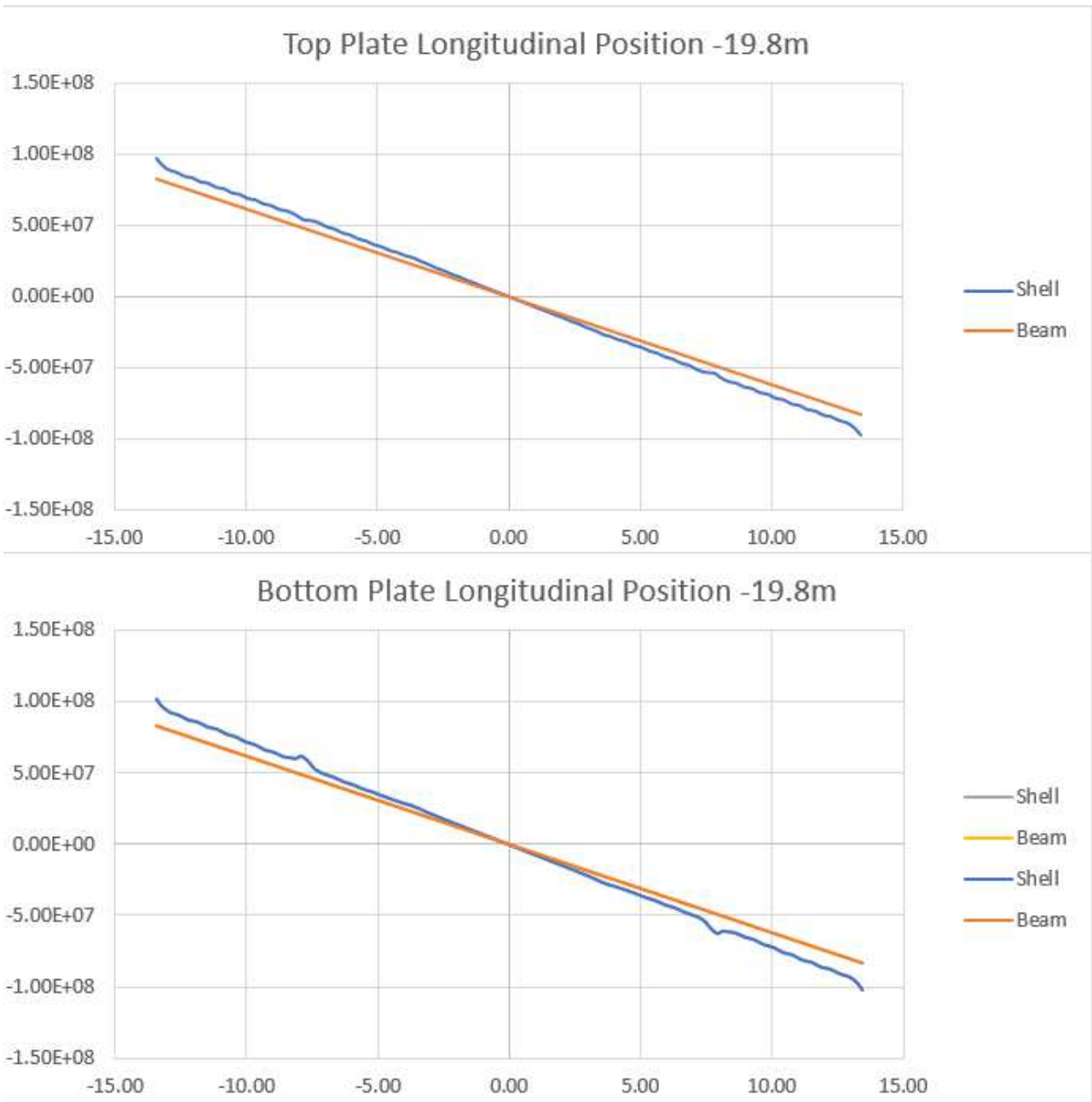
Figure 7-29   Stress comparison from strong axis bending at position -19,8 m

Top Plate Longitudinal Position -15.8m

Bottom Plate Longitudinal Position -15.8m
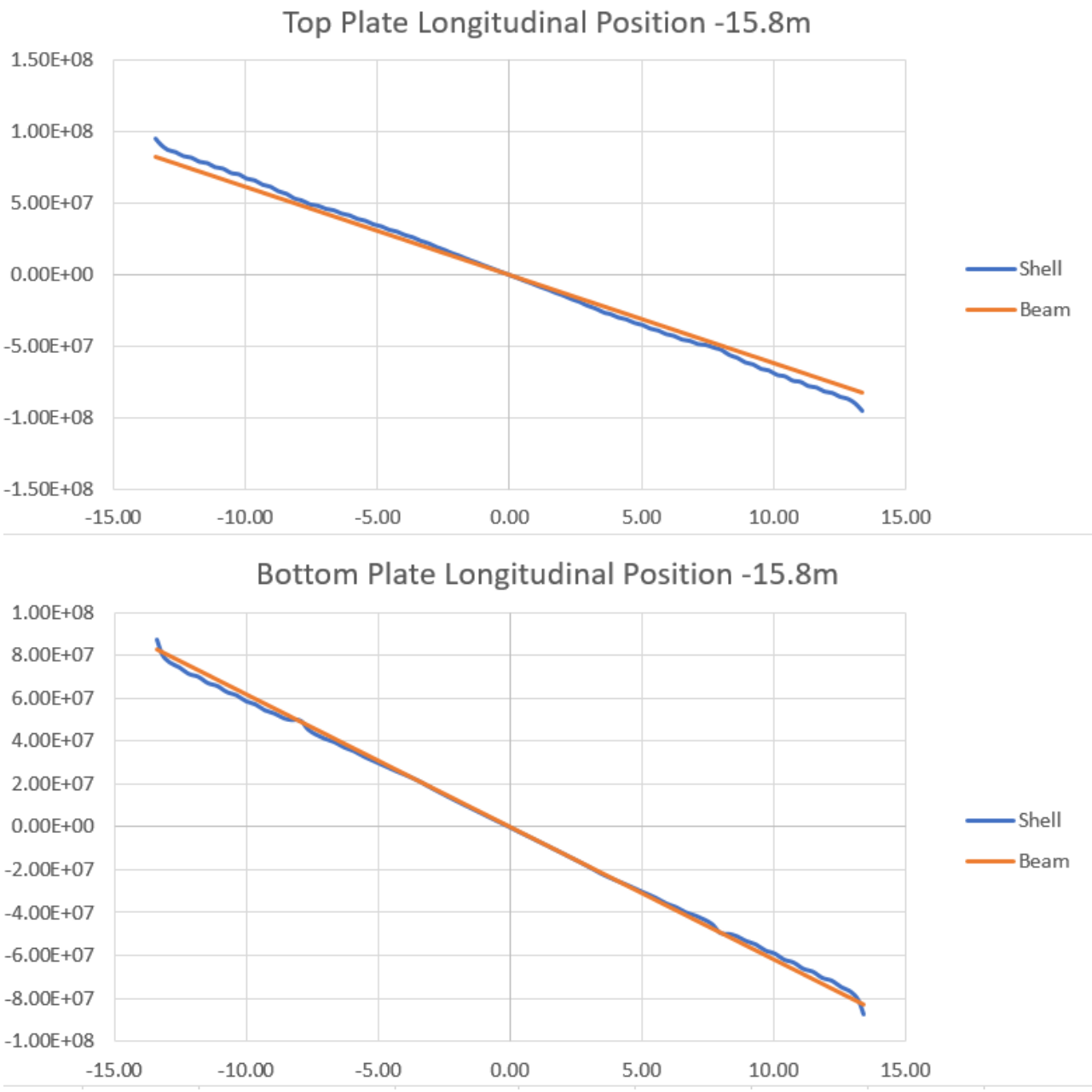
Figure 7-30   Stress comparison from strong axis bending at position -15,8 m
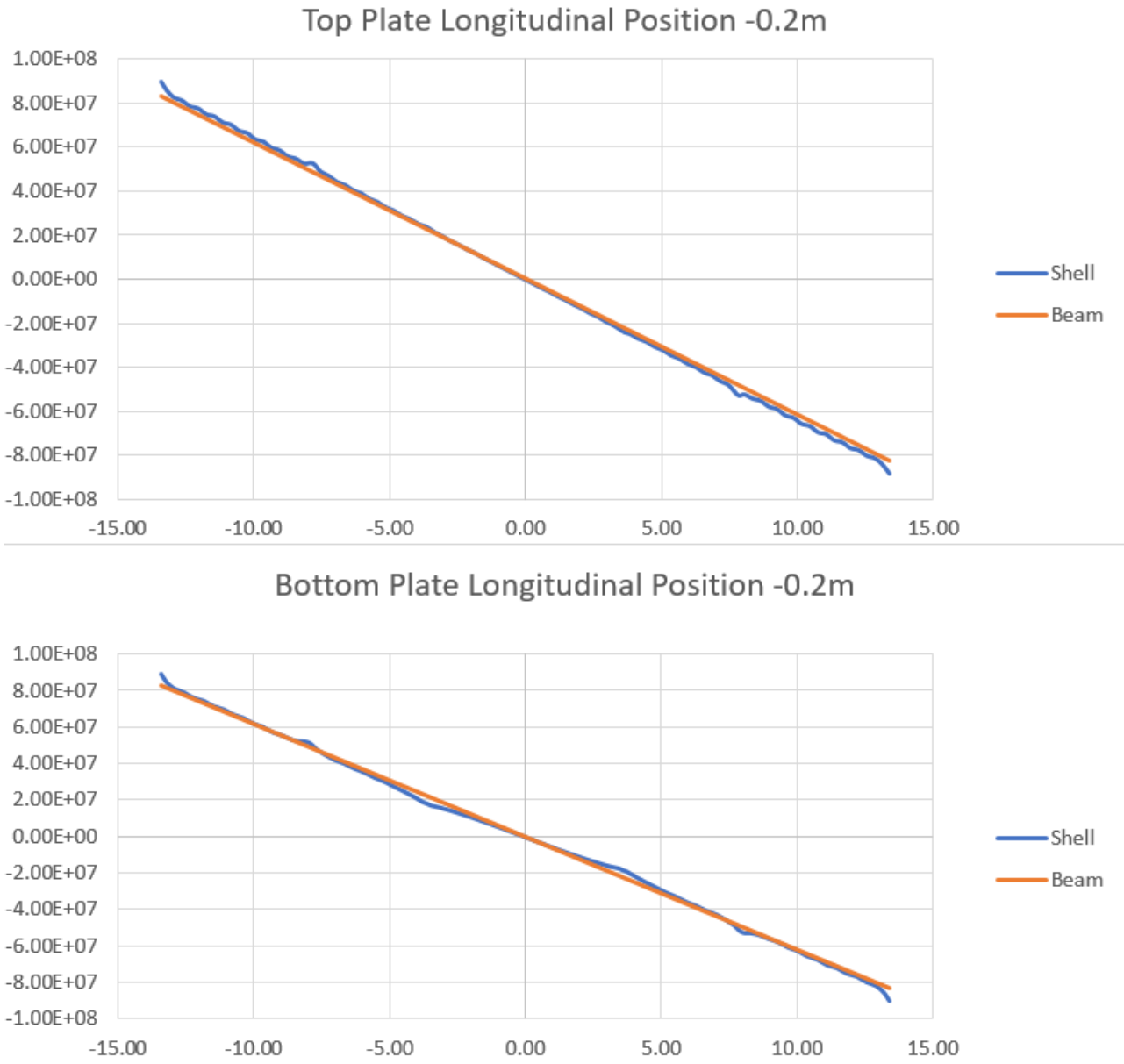
Figure 7-31 Stress comparison from strong axis bending at position -0,2 m

7.3.5 Stress concentration factors

Stress concentration factors (SCF) have been calculated for the eight different stress point locations shown in Figure 7-17.

The results from weak axis bending with a 2 sinus bridge girder deformation are shown in Figure 7-32. Deformation plot can be found in Figure 7-14.

The results from strong axis bending with a ½ sinus bridge girder deformation are shown in Figure 7-33. Deformation plot can be found in Figure 7-15.

AMC-weak-2-sin

AMC - Position 4m from centerline column

	Shell (Mpa)	Beam (Mpa)	SCF
p0	-136	-122	1.11
p1	-117	-94.1	1.24
p2	33.1	29.7	1.11
p3	144	121	1.19
p4	182.0	121	1.50
p5	140	121	1.16
p6	41.3	29.7	1.39
p7	-109	-101	1.08
		Max:	1.50

AMC - Position 16m from centerline column

	Shell (Mpa)	Beam (Mpa)	SCF
p0	-113	-98.1	1.15
p1	-89.6	-74	1.21
p2	34.5	34.5	1.00
p3	125	115	1.09
p4	120.0	115	1.04
p5	132	115	1.15
p6	41.7	34.5	1.21
p7	-90.5	-79.8	1.13
		Max:	1.21

AMC - Position 20m from centerline column

	Shell (Mpa)	Beam (Mpa)	SCF
p0	-93.2	-89.3	1.04
p1	-83.1	-67.6	1.23
p2	31.5	31.5	1.00
p3	128	105	1.22
p4	100.0	105	0.95
p5	129	105	1.23
p6	34.3	31.5	1.09
p7	-82.5	-73.2	1.13
		Max:	1.23

AMC - Position 32m from centerline column

	Shell (Mpa)	Beam (Mpa)	SCF
p0	-70.5	-67.5	1.04
p1	-61.3	-49.1	1.25
p2	42.3	35.1	1.21
p3	110	97.4	1.13
p4	92.4	97.4	0.95
p5	115	97.4	1.18
p6	49.0	35.1	1.40
p7	-64.6	-53.6	1.21
		Max:	1.40

AMC - Position 36m from centerline column

	Shell (Mpa)	Beam (Mpa)	SCF
p0	-69.4	-58.8	1.18
p1	-53.8	-42.6	1.26
p2	32.5	30.5	1.07
p3	99.6	84.5	1.18
p4	89.6	84.5	1.06
p5	107	84.5	1.27
p6	41.1	30.5	1.35
p7	-55.5	-46.5	1.19
		Max:	1.35

Figure 7-32 Stress concentration factors for weak axis bending 2 sinus deformation

AMC-strong-0,5-sin

AMC - Position 0m from centerline column

	Shell (Mpa)	Beam (Mpa)	SCF
p0			
p1	-88.1	-82.7	1.07
p2	-90.1	-82.8	1.09
p3			
p4			
p5			
p6	84.4	82.8	1.02
p7	85.5	82.8	1.03
		Max:	1.09

AMC - Position 16m from centerline column

	Shell (Mpa)	Beam (Mpa)	SCF
p0			
p1	-95.6	-82.7	1.16
p2	-87.8	-82.8	1.06
p3			
p4			
p5			
p6	88	82.8	1.06
p7	91	82.8	1.10
		Max:	1.16

AMC - Position 20m from centerline column

	Shell (Mpa)	Beam (Mpa)	SCF
p0			
p1	-97.8	-82.7	1.18
p2	-102	-82.8	1.23
p3			
p4			
p5			
p6	101	82.8	1.22
p7	92.9	82.8	1.12
		Max:	1.23

AMC - Position 32m from centerline column

	Shell (Mpa)	Beam (Mpa)	SCF
p0			
p1	-106	-90.3	1.17
p2	-97.2	-90.4	1.08
p3			
p4			
p5			
p6	96.6	90.4	1.07
p7	102	90.5	1.13
		Max:	1.17

AMC - Position 36m from centerline column

	Shell (Mpa)	Beam (Mpa)	SCF
p0			
p1	-113	-106	1.07
p2	-121	-106	1.14
p3			
p4			
p5			
p6	121	104	1.16
p7	113	106	1.07
		Max:	1.16

Figure 7-33   Stress concentration factors for strong axis bending 1/2 sinus deformation

7.3.6 Fatigue life for selected points including local stress concentrations

The stress concentration factors for weak and strong axes bending moments are applied at two locations in the support area at Axis 21 and Axis 32. Table 7-1 and Table 7-2 present the applied stress concentration factors and the obtained fatigue life. The fatigue life is reduced about 50% due to local stress concentration.

Table 7-1 Fatigue life of Axis 21 support locations including local stress concentrations

Location	Cross-sections	Weak axis SCF	Strong axis SCF	Fatigue life from screening analysis [years]	Fatigue life including local stress concentration [years]
16 m from centreline column	T1	1.21	1.16	3965	1987
32 m from centreline column	F1	1.25	1.17	2388	1205

Table 7-2 Fatigue life of Axis 32 support locations including local stress concentrations

Location	Cross-sections	Weak axis SCF	Strong axis SCF	Fatigue life from screening analysis [years]	Fatigue life including local stress concentration [years]
16 m from centreline column	T1	1.21	1.16	1687	893
32 m from centreline column	F1	1.25	1.17	1141	603

It may be argued that it is conservative to multiply the stress concentration factor from the local analysis with the typical 1.5 SCF that is assumed to account for eccentricities at buttwelds and welded details like attachments for rails etc. as the stress peaks found in the local analysis are limited in size and one can avoid that buttwelds or attachments are located in areas with increased stresses. But as there are numerous regions with increase in stresses it would be recommended to design with allowance of additional stress concentration from differences from stresses calculated with beam theory.

The example above shows that accounting for the local stress concentration will considerably reduce the fatigue life, however, for most of the bridge it seems that there are sufficient margins to allow for actual stress concentrations. Final conclusions can only be made when also effects from traffic and tidal loads are included.

7.4 Fatigue in stay cables

The effect of fatigue from environmental loads in the pair of stay cables are calculated. The damage is calculated using the recommended detail category as given in Table 3-11. It is found that the fatigue damages in the cables are small, leaving sufficient margins for damage from traffic without further calculations.

7.5 Summary and recommendations fatigue capacity

The independent analyses carried out by DNV GL determines the contribution to damage from environmental loads in the bridge girder. The results from the screening analysis show a minimum fatigue life of 482 years. This number should be reduced with the local stress increase as shown in Section 7.3.5. A reduction similar to the example in Section 7.3.6 could be expected that will bring the fatigue damage from environmental loads close to the required life of 250 years.

The contributions from traffic and tidal variation is not part of the independent analyses by DNV GL. The damages will add only at certain details in the bridge. Tidal variation will only lead to damage close to the ends and traffic will predominantly give damage in the bridge deck. However, the fatigue loading as determined by DNV GL show that it should be expected that in certain areas details as assumed in the fatigue screening may not be allowed even from environmental actions alone.

8 REFERENCES

/1/ AMC, Concept development, floating bridge E39 Bjørnafjorden. Concept evaluation, Appendix A -Drawings binder, 20190630, Report No.: SBJ-33-C5-AMC-90-RE-101, rev. 0. Drawing No.: SBJ-33-C5-AMC-22-DR-012.

/2/ AMC, Concept development, floating bridge E39 Bjørnafjorden. Concept evaluation, Appendix A -Drawings binder, 20190630, Report No.: SBJ-33-C5-AMC-90-RE-101, rev. 0. Drawing No.: SBJ-33-C5-AMC-22-DR-103.

/3/ AMC, Concept evaluation, Appendix F -Global analyses – Modelling and assumptions, 20190524, Report No.: SBJ-32-C5-AMC-90-RE-106, rev. 0. With enclosure "E01_K12_06_designers_format.xlsx".

/4/ AMC, Concept evaluation, Appendix E - Aerodynamics, 20190524, Report No.: SBJ-32-C5-AMC-20-RE-105, rev. 0.

/5/ DNVGL-OS-E301. Position mooring. ; July 2018.

/6/ AMC, Concept evaluation, Appendix I – Fatigue analysis, 20190524, Report No.: SBJ-32-C5-AMC-20-RE-109, rev. 0.

/7/ AMC, Concept evaluation, Appendix M – Anchor systems, 20190524, Report No.: SBJ-32-C5-AMC-20-RE-113, rev. 0.

/8/ SINTEF Ocean. SIMO 4.14.0 User Guide; 2018.

/9/ SINTEF Ocean. RIFLEX 4.14.0 User Guide; 2018.

/10/ SINTEF Ocean. SIMA.3.6.01; 2018.

/11/ Statens vegvesen, MetOcean Design Basis, 20181130, Document No.: SBJ-01-C4-SVV-01-BA-001, rev.1

/12/ Statens vegvesen, Design Basis Bjørnafjorden floating bridge, 20180912, Document No.: SBJ-32-C3-SVV-90-BA-002, rev.F

/13/ NS-EN-1993-1-5:2006, Eurocode 3:Design of steel structures, Part 1-5: Plated structural elements.

/14/ AMC, Concept evaluation – main report, 20190524, Report No.: SBJ-32-C5-AMC-90-RE-100, rev. 0.

/15/ AMC, Preferred solution, K12 - Appendix G – Global analyses - Response, 2019815, Report No.: SBJ-33-C5-AMC-90-RE-107, rev. 0.

/16/ AMC, Preferred solution, K12 - Appendix I – Fatigue analyses, 2019815, Report No.: SBJ-33-C5-AMC-22-RE-109, rev. 0.

/17/ AMC, Preferred solution, K12 - Appendix A -Drawings binder, 20190815, Report No.: SBJ-33-C5-AMC-90-RE-101, rev. 0.

/18/ DNVGL-RP-C203. Fatigue design of offshore steel structures ; April 2016.

/19/   NS-EN-1993-1-9:2005, Eurocode 3:Design of steel structures, Part 1-9: Fatigue.

/20/   AMC, Preferred solution, K12 – main report, 20190815, Report No.: SBJ-33-C5-AMC-90-RE-100, rev. 0.

/21/   B.J. Jonkmann LK. TurbSim User's Guide Version 1.06.00. [Online].; 2012. Available from: https://nwtc.nrel.gov/system/files/TurbSim.pdf.

/22/   Email from Parthasarathi Jena to Vigleik Hansen on March 20, 2019.

APPENDIX A
Structural drawings

The table below contains the main drawings provided in /17/:

Drawing no.	Drawing title
SBJ-33-C5-AMC-22-DR-012	General view, K12
SBJ-33-C5-AMC-22-DR-101	Cable stayed bridge, K12 - Base case layout, plan and elevation
SBJ-33-C5-AMC-22-DR-102	Cable stayed bridge, K12 - Tower, elevation and sections
SBJ-33-C5-AMC-22-DR-103	Cable stayed bridge, K12 - Steel box girder, section and details
SBJ-33-C5-AMC-22-DR-104	Cable stayed bridge, K12 - Concrete box girder, section and details
SBJ-33-C5-AMC-22-DR-105	Cable stayed bridge, K12 - Stay cable system
SBJ-33-C5-AMC-22-DR-106	Cable stayed bridge, K12 - Piers in side span
SBJ-33-C5-AMC-22-DR-201	Abutments, K12 - South, layout and sections
SBJ-33-C5-AMC-22-DR-202	Abutments, K12 - North, layout and sections
SBJ-33-C5-AMC-22-DR-203	Abutments, K12 - South and north, details
SBJ-33-C5-AMC-22-DR-300	Floating Bridge Pontoon, K12 - General Arrangement, Dimensions
SBJ-33-C5-AMC-22-DR-301	Floating Bridge Pontoon, K12 - Arrangement, Tank Plan
SBJ-33-C5-AMC-22-DR-302	Floating Bridge Pontoon, K12 - Pontoon Bottom Plate, Dimension Plate and stiffeners
SBJ-33-C5-AMC-22-DR-303	Floating Bridge Pontoon, K12 - Top-Plate, Dimension Plate and stiffeners
SBJ-33-C5-AMC-22-DR-304	Floating Bridge Pontoon, K12 - Internal Plate, Longitudinal Structure 4000 mm from CL
SBJ-33-C5-AMC-22-DR-305	Floating Bridge Pontoon, K12 - Internal Plate, Longitudinal Structure in CL
SBJ-33-C5-AMC-22-DR-306	Floating Bridge Pontoon, K12 - Pontoon Side, Longitudinal Structure 7450 mm from CL
SBJ-33-C5-AMC-22-DR-307	Floating Bridge Pontoon, K12 - Internal Structure, Transvers Frame No. 02 (No. 19)
SBJ-33-C5-AMC-22-DR-308	Floating Bridge Pontoon, K12 - Internal Structure, Transvers Frame No. 07 (No. 14)
SBJ-33-C5-AMC-22-DR-309	Floating Bridge Pontoon, K12 - Internal Structure, Transvers Frame No. 08 (No. 13)
SBJ-33-C5-AMC-22-DR-310	Floating Bridge Pontoon, K12 - Internal Structure, Transvers Frame No. 09
SBJ-33-C5-AMC-22-DR-351	Floating Bridge Pontoon, K12 - Plan Bottom Deck, Fairlead reinforcement
SBJ-33-C5-AMC-22-DR-352	Floating Bridge Pontoon, K12 - Plan Pontoon deck 11000 ab. Base line, Fairlead reinforcement
SBJ-33-C5-AMC-22-DR-353	Floating Bridge Pontoon, K12 - Longitudinal Structure in CL, Fairlead reinforcement
SBJ-33-C5-AMC-22-DR-354	Floating Bridge Pontoon, K12 - Longitudinal Structure 4000 mm from CL, Fairlead reinforcement
SBJ-33-C5-AMC-22-DR-355	Floating Bridge Pontoon, K12 - Longitudinal Structure 7450 from CL, Fairlead reinforcement
SBJ-33-C5-AMC-22-DR-356	Floating Bridge Pontoon, K12 - Curved Structure Bow and Stern, Fairlead reinforcement
SBJ-33-C5-AMC-22-DR-401	Floating Bridge Girder, K12 - High Part Axis 3-8, Typical Plan
SBJ-33-C5-AMC-22-DR-402	Floating Bridge Girder, K12 - High Part Axis 3-8, Typical Cross-section at Midspan
SBJ-33-C5-AMC-22-DR-403	Floating Bridge Girder, K12 - High Part Axis 3-8, Typical Cross-section at Transition
SBJ-33-C5-AMC-22-DR-404	Floating Bridge Girder, K12 - High Part Axis 3-8, Typical Cross-section above Column
SBJ-33-C5-AMC-22-DR-405	Floating Bridge Girder, K12 - High Part Axis 3-8, Typical Transverse Bulkhead above Column
SBJ-33-C5-AMC-22-DR-406	Floating Bridge Girder, K12 - High Part Axis 3-8, Typical Longitudinal Truss and Bulkhead
SBJ-33-C5-AMC-22-DR-407	Floating Bridge Girder, K12 - High Part Axis 3-8, Typical Longitudinal Detail above Column
SBJ-33-C5-AMC-22-DR-431	Floating Bridge Girder, K12 - Low Part Axis 9-40, Typical Plan
SBJ-33-C5-AMC-22-DR-432	Floating Bridge Girder, K12 - Low Part Axis 9-40, Typical Cross-section at Midspan
SBJ-33-C5-AMC-22-DR-433	Floating Bridge Girder, K12 - Low Part Axis 9-40, Typical Cross-section at Transition
SBJ-33-C5-AMC-22-DR-434	Floating Bridge Girder, K12 - Low Part Axis 9-40, Typical Cross-section above Column
SBJ-33-C5-AMC-22-DR-435	Floating Bridge Girder, K12 - Low Part Axis 9-40, Typical Transverse Bulkhead above Column
SBJ-33-C5-AMC-22-DR-436	Floating Bridge Girder, K12 - Low Part Axis 9-40, Typical Longitudinal Trusses and Bulkheads
SBJ-33-C5-AMC-22-DR-437	Floating Bridge Girder, K12 - Low Part Axis 9-40, Typical Longitudinal Detail above Column
SBJ-33-C5-AMC-22-DR-451	Floating Bridge Girder, K12 - Stiffener Details
SBJ-33-C5-AMC-22-DR-461	Floating Bridge Girder, K12 - End of girder at North Abutment, Plan and Elevation
SBJ-33-C5-AMC-22-DR-462	Floating Bridge Girder, K12 - End of girder at North Abutment, Sections
SBJ-33-C5-AMC-22-DR-471	Floating Bridge Column, K12 - High Part Axis 3 - 8, Structural Arrangement and Dimensions
SBJ-33-C5-AMC-22-DR-481	Floating Bridge Column, K12 - Low Part Axis 9 and above, Structural Arrangement and Dimensions
SBJ-33-C5-AMC-22-DR-491	Floating Bridge High Part, K12 - Axis 3-8, Typical Structural Arrangement
SBJ-33-C5-AMC-22-DR-492	Floating Bridge Low Part, K12 - Axis 9-40, Typical Structural Arrangement
SBJ-33-C5-AMC-22-DR-601	Anchor, K12 - Suction anchor, typical
SBJ-33-C5-AMC-22-DR-701	Mooring, K12 - Mooring line segmentation arrangement

SBJ-33-C5-AMC-22-DR-800	Assembly and installation, K12 - Sections overview
SBJ-33-C5-AMC-22-DR-810	Assembly and installation, K12 - Abutment north
SBJ-33-C5-AMC-22-DR-811	Assembly and installation, K12 - North section installation
SBJ-33-C5-AMC-22-DR-812	Assembly and installation, K12 - Floating bridge installation
SBJ-33-C5-AMC-22-DR-813	Assembly and installation, K12 - Cable stayed bridge, Construction stages
SBJ-33-C5-AMC-22-DR-820	Assembly and installation, K12 - Construction joint, Joint overview
SBJ-33-C5-AMC-22-DR-821	Assembly and installation, K12 - Construction joint, Guide and positioning joint
SBJ-33-C5-AMC-22-DR-822	Assembly and installation, K12 - Construction joint, Positioning joint
SBJ-33-C5-AMC-22-DR-823	Assembly and installation, K12 - Construction joint, Locking joint construction 1 & 2
SBJ-33-C5-AMC-22-DR-824	Assembly and installation, K12 - Construction joint, Locking joint construction 3
SBJ-33-C5-AMC-22-DR-850	Assembly and installation, K12 - Floating bridge assembly site setup in Søreidsvika
SBJ-33-C5-AMC-22-DR-851	Assembly and installation, K12 - Low floating bridge assembly method
SBJ-33-C5-AMC-22-DR-852	Assembly and installation, K12 - High floating bridge assembly method
SBJ-33-C5-AMC-05-DR-900	Road alignments overview
SBJ-33-C5-AMC-05-DR-910	Road alignment K12, Part 1
SBJ-33-C5-AMC-05-DR-911	Road alignment K12, Part 2
SBJ-33-C5-AMC-05-DR-920	Road alignment K12, Detail geometry northern end

APPENDIX B
Geometric description of the bridge

This appendix describes the coordinates for the structure nodes, their boundary conditions and any master-slave pairs.

The geometric input refers to a coordinate system as described in Section 3.1.3.

ID	Bridge geometry and coordinates				Boundary cond. (1=fixed, 0=free)						Master node	Floater
(-)	Acc. (m)	X (m)	Y (m)	Z (m)	x	y	z	rx	ry	rz	ID	ID
AX1	0	-2581.0	1267.8	66.7	1	1	1	1	1	1		
AX1A	40	-2548.3	1244.7	66.4	0	0	0	0	0	0		
AX1B	95	-2503.5	1212.9	65.9	0	0	0	0	0	0		
AX1C_118	150	-2458.6	1181.1	65.4	0	0	0	0	0	0		
INT117	160	-2450.4	1175.3	65.3	0	0	0	0	0	0		
INT116	170	-2442.2	1169.6	65.2	0	0	0	0	0	0		
INT115	180	-2434.1	1163.8	65.1	0	0	0	0	0	0		
INT114	190	-2425.9	1158.0	65.0	0	0	0	0	0	0		
INT113	200	-2417.7	1152.2	64.8	0	0	0	0	0	0		
AX1D	205	-2413.7	1149.3	64.8	0	0	0	0	0	0		
INT112	210	-2409.6	1146.5	64.7	0	0	0	0	0	0		
INT111	220	-2401.4	1140.7	64.6	0	0	0	0	0	0		
INT110	230	-2393.3	1134.9	64.5	0	0	0	0	0	0		
INT109	240	-2385.1	1129.1	64.3	0	0	0	0	0	0		
INT108	250	-2376.9	1123.4	64.2	0	0	0	0	0	0		
AX1E_107	260	-2368.8	1117.6	64.1	0	0	0	0	0	0		
INT106	280	-2352.4	1106.0	63.8	0	0	0	0	0	0		
INT105	300	-2336.1	1094.5	63.5	0	0	0	0	0	0		
INT104	320	-2319.8	1082.9	63.2	0	0	0	0	0	0		
INT103	340	-2303.5	1071.4	62.9	0	0	0	0	0	0		
INT102	360	-2287.1	1059.8	62.5	0	0	0	0	0	0		
INT101	380	-2270.8	1048.3	62.2	0	0	0	0	0	0		
AX2	400	-2254.5	1036.7	61.9	0	1	1	1	0	0		
INT201	420	-2238.2	1025.1	61.5	0	0	0	0	0	0		
INT202	440	-2221.8	1013.6	61.1	0	0	0	0	0	0		
INT203	460	-2205.5	1002.0	60.7	0	0	0	0	0	0		
INT204	480	-2189.2	990.5	60.4	0	0	0	0	0	0		
INT205	500	-2172.9	978.9	59.9	0	0	0	0	0	0		
INT206	520	-2156.5	967.4	59.5	0	0	0	0	0	0		
INT207	540	-2140.2	955.8	59.1	0	0	0	0	0	0		
INT208	560	-2123.9	944.3	58.7	0	0	0	0	0	0		
INT209	580	-2107.6	932.7	58.2	0	0	0	0	0	0		
INT210	600	-2091.2	921.2	57.7	0	0	0	0	0	0		
INT211	620	-2074.9	909.6	57.3	0	0	0	0	0	0		
INT212	640	-2058.6	898.1	56.8	0	0	0	0	0	0		
INT213	660	-2042.3	886.5	56.3	0	0	0	0	0	0		
INT214	680	-2025.9	874.9	55.8	0	0	0	0	0	0		
INT215	700	-2009.6	863.4	55.3	0	0	0	0	0	0		
INT216	720	-1993.3	851.8	54.7	0	0	0	0	0	0		
INT217	740	-1977.0	840.3	54.2	0	0	0	0	0	0		
INT218	760	-1960.6	828.7	53.6	0	0	0	0	0	0		
AX3	780	-1944.3	817.2	53.1	0	0	0	0	0	0		
AX4	905	-1841.0	746.9	49.4	0	0	0	0	0	0		
AX5	1030	-1735.9	679.1	45.6	0	0	0	0	0	0		
AX6	1155	-1629.2	614.0	41.9	0	0	0	0	0	0		
AX7	1280	-1520.9	551.6	38.1	0	0	0	0	0	0		
AX8	1405	-1411.1	491.9	34.4	0	0	0	0	0	0		
AX9	1530	-1299.8	435.0	30.6	0	0	0	0	0	0		
AX10	1655	-1187.2	380.8	26.9	0	0	0	0	0	0		
AX11	1780	-1073.2	329.5	23.4	0	0	0	0	0	0		

AX12	1905	-957.9	281.1	20.8	0	0	0	0	0	0		
AX13	2030	-841.5	235.5	19.0	0	0	0	0	0	0		
AX14	2155	-724.0	192.9	18.1	0	0	0	0	0	0		
AX15	2280	-605.5	153.3	18.0	0	0	0	0	0	0		
AX16	2405	-486.0	116.6	18.0	0	0	0	0	0	0		
AX17	2530	-365.6	82.9	18.0	0	0	0	0	0	0		
AX18	2655	-244.5	52.2	18.0	0	0	0	0	0	0		
AX19	2780	-122.6	24.6	18.0	0	0	0	0	0	0		
AX20	2905	0.0	0.0	18.0	0	0	0	0	0	0		
AX21	3030	123.1	-21.5	18.0	0	0	0	0	0	0		
AX22	3155	246.8	-39.9	18.0	0	0	0	0	0	0		
AX23	3280	370.8	-55.3	18.0	0	0	0	0	0	0		
AX24	3405	495.2	-67.5	18.0	0	0	0	0	0	0		
AX25	3530	619.9	-76.6	18.0	0	0	0	0	0	0		
AX26	3655	744.7	-82.6	18.0	0	0	0	0	0	0		
AX27	3780	869.7	-85.4	18.0	0	0	0	0	0	0		
AX28	3905	994.7	-85.2	18.0	0	0	0	0	0	0		
AX29	4030	1119.6	-81.8	18.0	0	0	0	0	0	0		
AX30	4155	1244.5	-75.3	18.0	0	0	0	0	0	0		
AX31	4280	1369.1	-65.6	18.0	0	0	0	0	0	0		
AX32	4405	1493.4	-52.9	18.0	0	0	0	0	0	0		
AX33	4530	1617.4	-37.1	18.0	0	0	0	0	0	0		
AX34	4655	1741.0	-18.1	18.0	0	0	0	0	0	0		
AX35	4780	1864.0	3.9	18.0	0	0	0	0	0	0		
AX36	4905	1986.5	29.0	18.0	0	0	0	0	0	0		
AX37	5030	2108.3	57.1	18.0	0	0	0	0	0	0		
AX38	5155	2229.3	88.3	17.8	0	0	0	0	0	0		
AX39	5280	2349.5	122.5	16.7	0	0	0	0	0	0		
AX40	5405	2468.9	159.7	14.7	0	0	0	0	0	0		
AX41	5530	2587.3	199.8	11.6	1	1	1	1	1	1		
C_TOP1A		-2548.3	1244.7	62.9	0	0	0	0	0	0	AX1A	
C_TOP1B		-2503.5	1212.9	62.4	0	0	0	0	0	0	AX1B	
C_TOP1C		-2458.6	1181.1	61.9	0	0	0	0	0	0	AX1C_118	
C_TOP1D		-2413.7	1149.3	61.3	0	0	0	0	0	0	AX1D	
C_TOP1E		-2368.8	1117.6	60.6	0	0	0	0	0	0	AX1E_107	
C_TOP03		-1944.3	817.2	49.1	0	0	0	0	0	0	AX3	
C_TOP04		-1841.0	746.9	45.4	0	0	0	0	0	0	AX4	
C_TOP05		-1735.9	679.1	41.6	0	0	0	0	0	0	AX5	
C_TOP06		-1629.2	614.0	37.9	0	0	0	0	0	0	AX6	
C_TOP07		-1520.9	551.6	34.1	0	0	0	0	0	0	AX7	
C_TOP08		-1411.1	491.9	30.4	0	0	0	0	0	0	AX8	
C_TOP09		-1299.8	435.0	26.6	0	0	0	0	0	0	AX9	
C_TOP10		-1187.2	380.8	22.9	0	0	0	0	0	0	AX10	
C_TOP11		-1073.2	329.5	19.4	0	0	0	0	0	0	AX11	
C_TOP12		-957.9	281.1	16.8	0	0	0	0	0	0	AX12	
C_TOP13		-841.5	235.5	15.0	0	0	0	0	0	0	AX13	
C_TOP14		-724.0	192.9	14.1	0	0	0	0	0	0	AX14	
C_TOP15		-605.5	153.3	14.0	0	0	0	0	0	0	AX15	
C_TOP16		-486.0	116.6	14.0	0	0	0	0	0	0	AX16	
C_TOP17		-365.6	82.9	14.0	0	0	0	0	0	0	AX17	
C_TOP18		-244.5	52.2	14.0	0	0	0	0	0	0	AX18	
C_TOP19		-122.6	24.6	14.0	0	0	0	0	0	0	AX19	
C_TOP20		0.0	0.0	14.0	0	0	0	0	0	0	AX20	
C_TOP21		123.1	-21.5	14.0	0	0	0	0	0	0	AX21	
C_TOP22		246.8	-39.9	14.0	0	0	0	0	0	0	AX22	
C_TOP23		370.8	-55.3	14.0	0	0	0	0	0	0	AX23	
C_TOP24		495.2	-67.5	14.0	0	0	0	0	0	0	AX24	
C_TOP25		619.9	-76.6	14.0	0	0	0	0	0	0	AX25	
C_TOP26		744.7	-82.6	14.0	0	0	0	0	0	0	AX26	
C_TOP27		869.7	-85.4	14.0	0	0	0	0	0	0	AX27	
C_TOP28		994.7	-85.2	14.0	0	0	0	0	0	0	AX28	
C_TOP29		1119.6	-81.8	14.0	0	0	0	0	0	0	AX29	
C_TOP30		1244.5	-75.3	14.0	0	0	0	0	0	0	AX30	
C_TOP31		1369.1	-65.6	14.0	0	0	0	0	0	0	AX31	
C_TOP32		1493.4	-52.9	14.0	0	0	0	0	0	0	AX32	
C_TOP33		1617.4	-37.1	14.0	0	0	0	0	0	0	AX33	

C_TOP34		1741.0	-18.1	14.0	0	0	0	0	0	0	AX34	
C_TOP35		1864.0	3.9	14.0	0	0	0	0	0	0	AX35	
C_TOP36		1986.5	29.0	14.0	0	0	0	0	0	0	AX36	
C_TOP37		2108.3	57.1	14.0	0	0	0	0	0	0	AX37	
C_TOP38		2229.3	88.3	13.8	0	0	0	0	0	0	AX38	
C_TOP39		2349.5	122.5	12.7	0	0	0	0	0	0	AX39	
C_TOP40		2468.9	159.7	10.7	0	0	0	0	0	0	AX40	
C_BOT1A		-2548.3	1244.7	49.5	1	1	1	1	1	1		
C_BOT1B		-2503.5	1212.9	39.7	1	1	1	1	1	1		
C_BOT1C		-2458.6	1181.1	28.2	1	1	1	1	1	1		
C_BOT1D		-2413.7	1149.3	19.5	1	1	1	1	1	1		
C_BOT1E		-2368.8	1117.6	4.3	1	1	1	1	1	1		
C_BOT03		-1944.3	817.2	3.5	0	0	0	0	0	0		PAX3
C_BOT04		-1841.0	746.9	3.5	0	0	0	0	0	0		PAX4
C_BOT05		-1735.9	679.1	3.5	0	0	0	0	0	0		PAX5
C_BOT06		-1629.2	614.0	3.5	0	0	0	0	0	0		PAX6
C_BOT07		-1520.9	551.6	3.5	0	0	0	0	0	0		PAX7
C_BOT08		-1411.1	491.9	3.5	0	0	0	0	0	0		PAX8
C_BOT09		-1299.8	435.0	3.5	0	0	0	0	0	0		PAX9
C_BOT10		-1187.2	380.8	3.5	0	0	0	0	0	0		PAX10
C_BOT11		-1073.2	329.5	3.5	0	0	0	0	0	0		PAX11
C_BOT12		-957.9	281.1	3.5	0	0	0	0	0	0		PAX12
C_BOT13		-841.5	235.5	3.5	0	0	0	0	0	0		PAX13
C_BOT14		-724.0	192.9	3.5	0	0	0	0	0	0		PAX14
C_BOT15		-605.5	153.3	3.5	0	0	0	0	0	0		PAX15
C_BOT16		-486.0	116.6	3.5	0	0	0	0	0	0		PAX16
C_BOT17		-365.6	82.9	3.5	0	0	0	0	0	0		PAX17
C_BOT18		-244.5	52.2	3.5	0	0	0	0	0	0		PAX18
C_BOT19		-122.6	24.6	3.5	0	0	0	0	0	0		PAX19
C_BOT20		0.0	0.0	3.5	0	0	0	0	0	0		PAX20
C_BOT21		123.1	-21.5	3.5	0	0	0	0	0	0		PAX21
C_BOT22		246.8	-39.9	3.5	0	0	0	0	0	0		PAX22
C_BOT23		370.8	-55.3	3.5	0	0	0	0	0	0		PAX23
C_BOT24		495.2	-67.5	3.5	0	0	0	0	0	0		PAX24
C_BOT25		619.9	-76.6	3.5	0	0	0	0	0	0		PAX25
C_BOT26		744.7	-82.6	3.5	0	0	0	0	0	0		PAX26
C_BOT27		869.7	-85.4	3.5	0	0	0	0	0	0		PAX27
C_BOT28		994.7	-85.2	3.5	0	0	0	0	0	0		PAX28
C_BOT29		1119.6	-81.8	3.5	0	0	0	0	0	0		PAX29
C_BOT30		1244.5	-75.3	3.5	0	0	0	0	0	0		PAX30
C_BOT31		1369.1	-65.6	3.5	0	0	0	0	0	0		PAX31
C_BOT32		1493.4	-52.9	3.5	0	0	0	0	0	0		PAX32
C_BOT33		1617.4	-37.1	3.5	0	0	0	0	0	0		PAX33
C_BOT34		1741.0	-18.1	3.5	0	0	0	0	0	0		PAX34
C_BOT35		1864.0	3.9	3.5	0	0	0	0	0	0		PAX35
C_BOT36		1986.5	29.0	3.5	0	0	0	0	0	0		PAX36
C_BOT37		2108.3	57.1	3.5	0	0	0	0	0	0		PAX37
C_BOT38		2229.3	88.3	3.5	0	0	0	0	0	0		PAX38
C_BOT39		2349.5	122.5	3.5	0	0	0	0	0	0		PAX39
C_BOT40		2468.9	159.7	3.5	0	0	0	0	0	0		PAX40
TOWERFE		-2267.8	1017.9	0.0	1	1	1	1	1	1		
TOWERFW		-2241.2	1055.5	0.0	1	1	1	1	1	1		
TWRCROBE		-2263.9	1023.4	54.5	0	0	0	0	0	0		
TWRCROBW		-2245.1	1050.0	54.5	0	0	0	0	0	0		
TWRTOPT		-2254.5	1036.7	220.0	0	0	0	0	0	0		
TWRCE01		-2258.8	1030.7	127.0	0	0	0	0	0	0		
TWRCE02		-2258.4	1031.2	132.0	0	0	0	0	0	0		
TWRCE03		-2258.0	1031.7	137.0	0	0	0	0	0	0		
TWRCE04		-2257.7	1032.2	142.0	0	0	0	0	0	0		
TWRCE05		-2257.3	1032.7	147.0	0	0	0	0	0	0		
TWRCE06		-2257.0	1033.2	152.0	0	0	0	0	0	0		
TWRCE07		-2256.6	1033.7	157.0	0	0	0	0	0	0		
TWRCE08		-2256.3	1034.2	162.0	0	0	0	0	0	0		
TWRCE09		-2255.9	1034.7	167.0	0	0	0	0	0	0		
TWRCE10		-2255.6	1035.2	172.0	0	0	0	0	0	0		
TWRCE11		-2255.2	1035.7	177.0	0	0	0	0	0	0		

TWRCE12		-2254.8	1036.2	182.0	0	0	0	0	0	0		
TWRC13		-2254.5	1036.7	187.0	0	0	0	0	0	0		
TWRC14		-2254.5	1036.7	192.0	0	0	0	0	0	0		
TWRC15		-2254.5	1036.7	197.0	0	0	0	0	0	0		
TWRC16		-2254.5	1036.7	202.0	0	0	0	0	0	0		
TWRC17		-2254.5	1036.7	207.0	0	0	0	0	0	0		
TWRC18		-2254.5	1036.7	212.0	0	0	0	0	0	0		
TWRCW01		-2250.2	1042.7	127.0	0	0	0	0	0	0		
TWRCW02		-2250.6	1042.2	132.0	0	0	0	0	0	0		
TWRCW03		-2250.9	1041.7	137.0	0	0	0	0	0	0		
TWRCW04		-2251.3	1041.2	142.0	0	0	0	0	0	0		
TWRCW05		-2251.7	1040.7	147.0	0	0	0	0	0	0		
TWRCW06		-2252.0	1040.2	152.0	0	0	0	0	0	0		
TWRCW07		-2252.4	1039.7	157.0	0	0	0	0	0	0		
TWRCW08		-2252.7	1039.2	162.0	0	0	0	0	0	0		
TWRCW09		-2253.1	1038.7	167.0	0	0	0	0	0	0		
TWRCW10		-2253.4	1038.2	172.0	0	0	0	0	0	0		
TWRCW11		-2253.8	1037.7	177.0	0	0	0	0	0	0		
TWRCW12		-2254.1	1037.2	182.0	0	0	0	0	0	0		
TW_U118		-2255.8	1038.3	212.0	0	0	0	0	0	0	TWRC18	
TW_U117		-2255.6	1038.6	207.0	0	0	0	0	0	0	TWRC17	
TW_U116		-2255.4	1038.9	202.0	0	0	0	0	0	0	TWRC16	
TW_U115		-2255.1	1039.2	197.0	0	0	0	0	0	0	TWRC15	
TW_U114		-2254.9	1039.6	192.0	0	0	0	0	0	0	TWRC14	
TW_U113		-2254.7	1039.9	187.0	0	0	0	0	0	0	TWRC13	
TW_U112		-2254.5	1040.2	182.0	0	0	0	0	0	0	TWRCW12	
TW_U111		-2254.3	1040.4	177.0	0	0	0	0	0	0	TWRCW11	
TW_U110		-2254.1	1040.7	172.0	0	0	0	0	0	0	TWRCW10	
TW_U109		-2253.9	1041.0	167.0	0	0	0	0	0	0	TWRCW09	
TW_U108		-2253.7	1041.3	162.0	0	0	0	0	0	0	TWRCW08	
TW_U107		-2253.5	1041.5	157.0	0	0	0	0	0	0	TWRCW07	
TW_U106		-2253.3	1041.9	152.0	0	0	0	0	0	0	TWRCW06	
TW_U105		-2253.1	1042.2	147.0	0	0	0	0	0	0	TWRCW05	
TW_U104		-2252.8	1042.5	142.0	0	0	0	0	0	0	TWRCW04	
TW_U103		-2252.6	1042.8	137.0	0	0	0	0	0	0	TWRCW03	
TW_U102		-2252.3	1043.2	132.1	0	0	0	0	0	0	TWRCW02	
TW_U101		-2252.1	1043.6	127.1	0	0	0	0	0	0	TWRCW01	
TW_U201		-2248.8	1041.2	127.1	0	0	0	0	0	0	TWRCW01	
TW_U202		-2249.1	1040.9	132.1	0	0	0	0	0	0	TWRCW02	
TW_U203		-2249.3	1040.5	137.0	0	0	0	0	0	0	TWRCW03	
TW_U204		-2249.6	1040.2	142.0	0	0	0	0	0	0	TWRCW04	
TW_U205		-2249.8	1039.9	147.0	0	0	0	0	0	0	TWRCW05	
TW_U206		-2250.0	1039.5	152.0	0	0	0	0	0	0	TWRCW06	
TW_U207		-2250.2	1039.2	157.0	0	0	0	0	0	0	TWRCW07	
TW_U208		-2250.5	1038.9	162.0	0	0	0	0	0	0	TWRCW08	
TW_U209		-2250.7	1038.7	167.0	0	0	0	0	0	0	TWRCW09	
TW_U210		-2250.9	1038.4	172.0	0	0	0	0	0	0	TWRCW10	
TW_U211		-2251.0	1038.1	177.0	0	0	0	0	0	0	TWRCW11	
TW_U212		-2251.2	1037.9	182.0	0	0	0	0	0	0	TWRCW12	
TW_U213		-2251.4	1037.6	187.0	0	0	0	0	0	0	TWRC13	
TW_U214		-2251.6	1037.3	192.0	0	0	0	0	0	0	TWRC14	
TW_U215		-2251.9	1036.9	197.0	0	0	0	0	0	0	TWRC15	
TW_U216		-2252.1	1036.6	202.0	0	0	0	0	0	0	TWRC16	
TW_U217		-2252.3	1036.3	207.0	0	0	0	0	0	0	TWRC17	
TW_U218		-2252.6	1036.0	212.0	0	0	0	0	0	0	TWRC18	
TE_U118		-2256.4	1037.4	212.0	0	0	0	0	0	0	TWRC18	
TE_U117		-2256.6	1037.1	207.0	0	0	0	0	0	0	TWRC17	
TE_U116		-2256.9	1036.8	202.0	0	0	0	0	0	0	TWRC16	
TE_U115		-2257.1	1036.5	197.0	0	0	0	0	0	0	TWRC15	
TE_U114		-2257.3	1036.1	192.0	0	0	0	0	0	0	TWRC14	
TE_U113		-2257.6	1035.8	187.0	0	0	0	0	0	0	TWRC13	
TE_U112		-2257.8	1035.5	182.0	0	0	0	0	0	0	TWRCE12	
TE_U111		-2257.9	1035.3	177.0	0	0	0	0	0	0	TWRCE11	
TE_U110		-2258.1	1035.0	172.0	0	0	0	0	0	0	TWRCE10	
TE_U109		-2258.3	1034.7	167.0	0	0	0	0	0	0	TWRCE09	
TE_U108		-2258.5	1034.5	162.0	0	0	0	0	0	0	TWRCE08	

TE_U107		-2258.7	1034.2	157.0	0	0	0	0	0	0	TWRCE07	
TE_U106		-2259.0	1033.9	152.0	0	0	0	0	0	0	TWRCE06	
TE_U105		-2259.2	1033.5	147.0	0	0	0	0	0	0	TWRCE05	
TE_U104		-2259.4	1033.2	142.0	0	0	0	0	0	0	TWRCE04	
TE_U103		-2259.6	1032.9	137.0	0	0	0	0	0	0	TWRCE03	
TE_U102		-2259.9	1032.5	132.1	0	0	0	0	0	0	TWRCE02	
TE_U101		-2260.2	1032.2	127.1	0	0	0	0	0	0	TWRCE01	
TE_U201		-2256.9	1029.8	127.1	0	0	0	0	0	0	TWRCE01	
TE_U202		-2256.6	1030.2	132.1	0	0	0	0	0	0	TWRCE02	
TE_U203		-2256.4	1030.6	137.0	0	0	0	0	0	0	TWRCE03	
TE_U204		-2256.1	1030.9	142.0	0	0	0	0	0	0	TWRCE04	
TE_U205		-2255.9	1031.2	147.0	0	0	0	0	0	0	TWRCE05	
TE_U206		-2255.7	1031.5	152.0	0	0	0	0	0	0	TWRCE06	
TE_U207		-2255.5	1031.9	157.0	0	0	0	0	0	0	TWRCE07	
TE_U208		-2255.3	1032.1	162.0	0	0	0	0	0	0	TWRCE08	
TE_U209		-2255.1	1032.4	167.0	0	0	0	0	0	0	TWRCE09	
TE_U210		-2254.9	1032.7	172.0	0	0	0	0	0	0	TWRCE10	
TE_U211		-2254.7	1033.0	177.0	0	0	0	0	0	0	TWRCE11	
TE_U212		-2254.5	1033.2	182.0	0	0	0	0	0	0	TWRCE12	
TE_U213		-2254.3	1033.5	187.0	0	0	0	0	0	0	TWRC13	
TE_U214		-2254.1	1033.8	192.0	0	0	0	0	0	0	TWRC14	
TE_U215		-2253.8	1034.2	197.0	0	0	0	0	0	0	TWRC15	
TE_U216		-2253.6	1034.5	202.0	0	0	0	0	0	0	TWRC16	
TE_U217		-2253.4	1034.8	207.0	0	0	0	0	0	0	TWRC17	
TE_U218		-2253.1	1035.1	212.0	0	0	0	0	0	0	TWRC18	
TW_L118		-2450.5	1192.6	64.4	0	0	0	0	0	0	AX1C_118	
TW_L117		-2442.3	1186.8	64.3	0	0	0	0	0	0	INT117	
TW_L116		-2434.2	1181.0	64.2	0	0	0	0	0	0	INT116	
TW_L115		-2426.0	1175.2	64.1	0	0	0	0	0	0	INT115	
TW_L114		-2417.8	1169.4	64.0	0	0	0	0	0	0	INT114	
TW_L113		-2409.7	1163.7	63.8	0	0	0	0	0	0	INT113	
TW_L112		-2401.5	1157.9	63.7	0	0	0	0	0	0	INT112	
TW_L111		-2393.3	1152.1	63.6	0	0	0	0	0	0	INT111	
TW_L110		-2385.2	1146.3	63.5	0	0	0	0	0	0	INT110	
TW_L109		-2377.0	1140.6	63.3	0	0	0	0	0	0	INT109	
TW_L108		-2368.9	1134.8	63.2	0	0	0	0	0	0	INT108	
TW_L107		-2360.7	1129.0	63.1	0	0	0	0	0	0	AX1E_107	
TW_L106		-2344.4	1117.5	62.8	0	0	0	0	0	0	INT106	
TW_L105		-2328.0	1105.9	62.5	0	0	0	0	0	0	INT105	
TW_L104		-2311.7	1094.4	62.2	0	0	0	0	0	0	INT104	
TW_L103		-2295.4	1082.8	61.9	0	0	0	0	0	0	INT103	
TW_L102		-2279.1	1071.2	61.5	0	0	0	0	0	0	INT102	
TW_L101		-2262.7	1059.7	61.2	0	0	0	0	0	0	INT101	
TW_L201		-2230.1	1036.6	60.5	0	0	0	0	0	0	INT201	
TW_L202		-2213.8	1025.0	60.1	0	0	0	0	0	0	INT202	
TW_L203		-2197.4	1013.5	59.7	0	0	0	0	0	0	INT203	
TW_L204		-2181.1	1001.9	59.4	0	0	0	0	0	0	INT204	
TW_L205		-2164.8	990.4	58.9	0	0	0	0	0	0	INT205	
TW_L206		-2148.5	978.8	58.5	0	0	0	0	0	0	INT206	
TW_L207		-2132.1	967.3	58.1	0	0	0	0	0	0	INT207	
TW_L208		-2115.8	955.7	57.7	0	0	0	0	0	0	INT208	
TW_L209		-2099.5	944.2	57.2	0	0	0	0	0	0	INT209	
TW_L210		-2083.2	932.6	56.7	0	0	0	0	0	0	INT210	
TW_L211		-2066.8	921.1	56.3	0	0	0	0	0	0	INT211	
TW_L212		-2050.5	909.5	55.8	0	0	0	0	0	0	INT212	
TW_L213		-2034.2	897.9	55.3	0	0	0	0	0	0	INT213	
TW_L214		-2017.9	886.4	54.8	0	0	0	0	0	0	INT214	
TW_L215		-2001.5	874.8	54.3	0	0	0	0	0	0	INT215	
TW_L216		-1985.2	863.3	53.7	0	0	0	0	0	0	INT216	
TW_L217		-1968.9	851.7	53.2	0	0	0	0	0	0	INT217	
TW_L218		-1952.6	840.2	52.6	0	0	0	0	0	0	INT218	
TE_L118		-2466.7	1169.7	64.4	0	0	0	0	0	0	AX1C_118	
TE_L117		-2458.5	1163.9	64.3	0	0	0	0	0	0	INT117	
TE_L116		-2450.3	1158.1	64.2	0	0	0	0	0	0	INT116	
TE_L115		-2442.2	1152.4	64.1	0	0	0	0	0	0	INT115	
TE_L114		-2434.0	1146.6	64.0	0	0	0	0	0	0	INT114	

TE_L113		-2425.8	1140.8	63.8	0	0	0	0	0	0	INT113	
TE_L112		-2417.7	1135.0	63.7	0	0	0	0	0	0	INT112	
TE_L111		-2409.5	1129.3	63.6	0	0	0	0	0	0	INT111	
TE_L110		-2401.4	1123.5	63.5	0	0	0	0	0	0	INT110	
TE_L109		-2393.2	1117.7	63.3	0	0	0	0	0	0	INT109	
TE_L108		-2385.0	1111.9	63.2	0	0	0	0	0	0	INT108	
TE_L107		-2376.9	1106.2	63.1	0	0	0	0	0	0	AX1E_107	
TE_L106		-2360.5	1094.6	62.8	0	0	0	0	0	0	INT106	
TE_L105		-2344.2	1083.0	62.5	0	0	0	0	0	0	INT105	
TE_L104		-2327.9	1071.5	62.2	0	0	0	0	0	0	INT104	
TE_L103		-2311.6	1059.9	61.9	0	0	0	0	0	0	INT103	
TE_L102		-2295.2	1048.4	61.5	0	0	0	0	0	0	INT102	
TE_L101		-2278.9	1036.8	61.2	0	0	0	0	0	0	INT101	
TE_L201		-2246.3	1013.7	60.5	0	0	0	0	0	0	INT201	
TE_L202		-2229.9	1002.2	60.1	0	0	0	0	0	0	INT202	
TE_L203		-2213.6	990.6	59.7	0	0	0	0	0	0	INT203	
TE_L204		-2197.3	979.1	59.4	0	0	0	0	0	0	INT204	
TE_L205		-2181.0	967.5	58.9	0	0	0	0	0	0	INT205	
TE_L206		-2164.6	956.0	58.5	0	0	0	0	0	0	INT206	
TE_L207		-2148.3	944.4	58.1	0	0	0	0	0	0	INT207	
TE_L208		-2132.0	932.9	57.7	0	0	0	0	0	0	INT208	
TE_L209		-2115.7	921.3	57.2	0	0	0	0	0	0	INT209	
TE_L210		-2099.3	909.8	56.7	0	0	0	0	0	0	INT210	
TE_L211		-2083.0	898.2	56.3	0	0	0	0	0	0	INT211	
TE_L212		-2066.7	886.6	55.8	0	0	0	0	0	0	INT212	
TE_L213		-2050.4	875.1	55.3	0	0	0	0	0	0	INT213	
TE_L214		-2034.0	863.5	54.8	0	0	0	0	0	0	INT214	
TE_L215		-2017.7	852.0	54.3	0	0	0	0	0	0	INT215	
TE_L216		-2001.4	840.4	53.7	0	0	0	0	0	0	INT216	
TE_L217		-1985.1	828.9	53.2	0	0	0	0	0	0	INT217	
TE_L218		-1968.7	817.3	52.6	0	0	0	0	0	0	INT218	
FAIR_01		-843.5	210.6	-6.0	0	0	0	0	0	0	C_BOT13	
FAIR_02		-856.1	215.6	-6.0	0	0	0	0	0	0	C_BOT13	
FAIR_03		-839.6	260.5	-6.0	0	0	0	0	0	0	C_BOT13	
FAIR_04		-826.5	255.5	-6.0	0	0	0	0	0	0	C_BOT13	
FAIR_05		2.5	-24.9	-6.0	0	0	0	0	0	0	C_BOT20	
FAIR_06		-11.3	-22.3	-6.0	0	0	0	0	0	0	C_BOT20	
FAIR_07		-2.5	24.9	-6.0	0	0	0	0	0	0	C_BOT20	
FAIR_08		11.3	22.3	-6.0	0	0	0	0	0	0	C_BOT20	
FAIR_09		876.4	-109.5	-6.0	0	0	0	0	0	0	C_BOT27	
FAIR_10		862.4	-109.4	-6.0	0	0	0	0	0	0	C_BOT27	
FAIR_11		862.9	-61.4	-6.0	0	0	0	0	0	0	C_BOT27	
FAIR_12		876.9	-61.5	-6.0	0	0	0	0	0	0	C_BOT27	
ANCHOR01		-941.3	-312.4	-466.0	1	1	1	1	0	0		
ANCHOR02		-1098.3	-216.4	-449.0	1	1	1	1	0	0		
ANCHOR03		-714.3	915.6	-559.0	1	1	1	1	0	0		
ANCHOR04		-494.3	825.6	-560.0	1	1	1	1	0	0		
ANCHOR05		270.7	-886.4	-491.0	1	1	1	1	0	0		
ANCHOR06		-462.3	-716.4	-491.0	1	1	1	1	0	0		
ANCHOR07		-303.3	774.6	-560.0	1	1	1	1	0	0		
ANCHOR08		385.7	640.6	-485.0	1	1	1	1	0	0		
ANCHOR09		1048.7	-578.4	-367.0	1	1	1	1	0	0		
ANCHOR10		700.7	-683.4	-388.0	1	1	1	1	0	0		
ANCHOR11		710.7	365.6	-442.0	1	1	1	1	0	0		
ANCHOR12		949.7	398.6	-360.0	1	1	1	1	0	0		

APPENDIX C
Pontoons frequency domain analyses results

Pontoon type 1
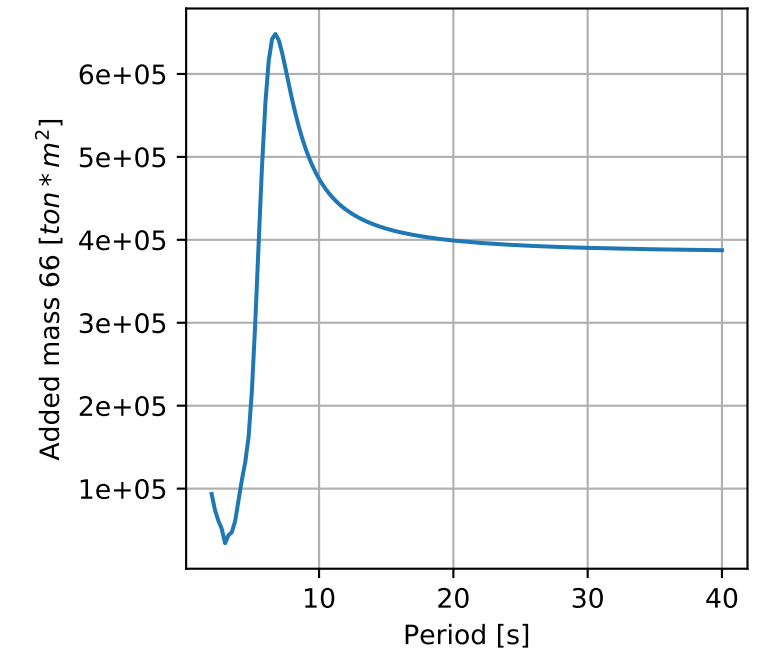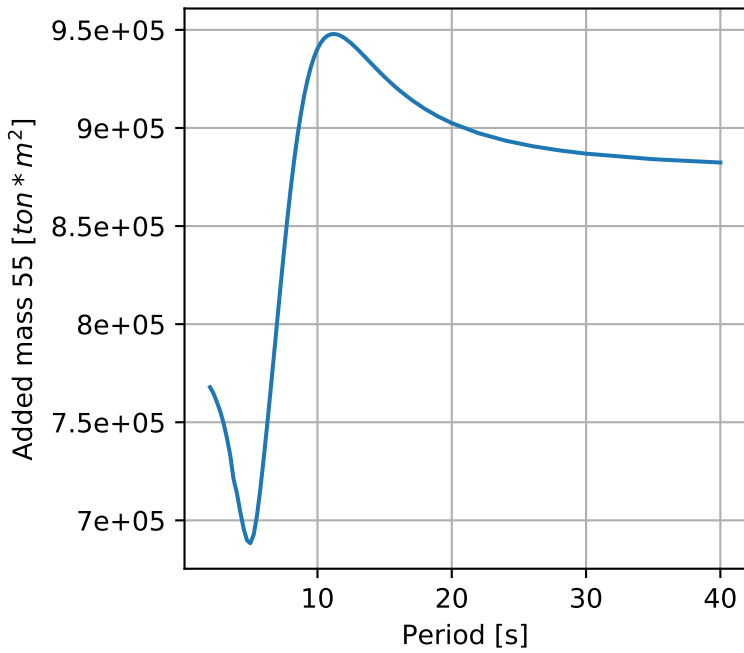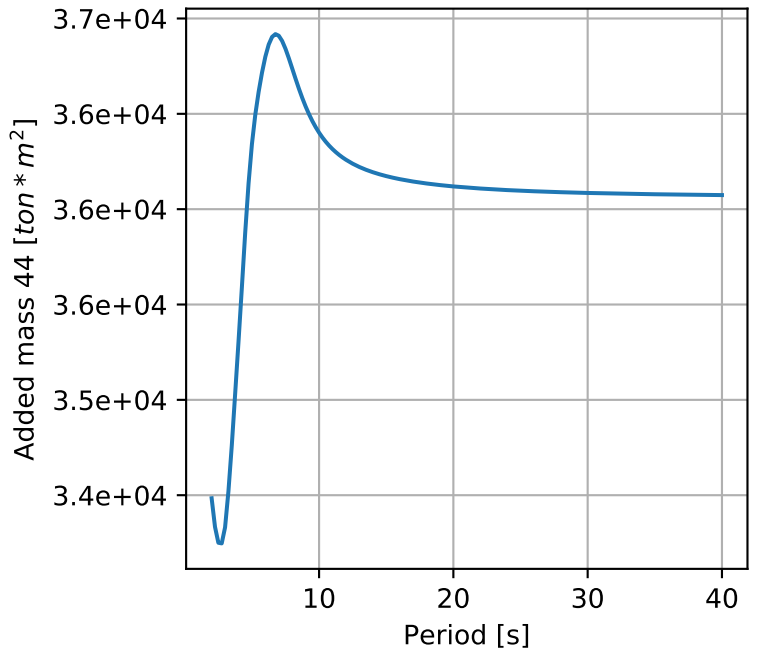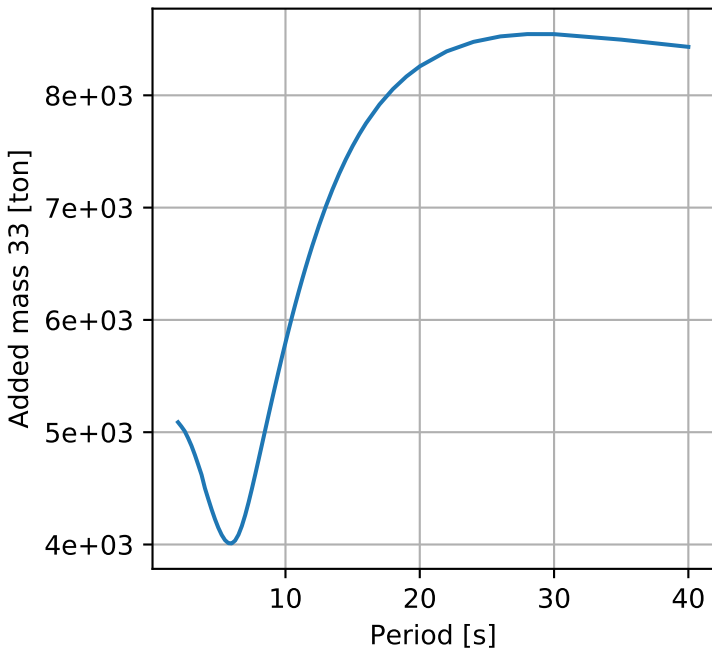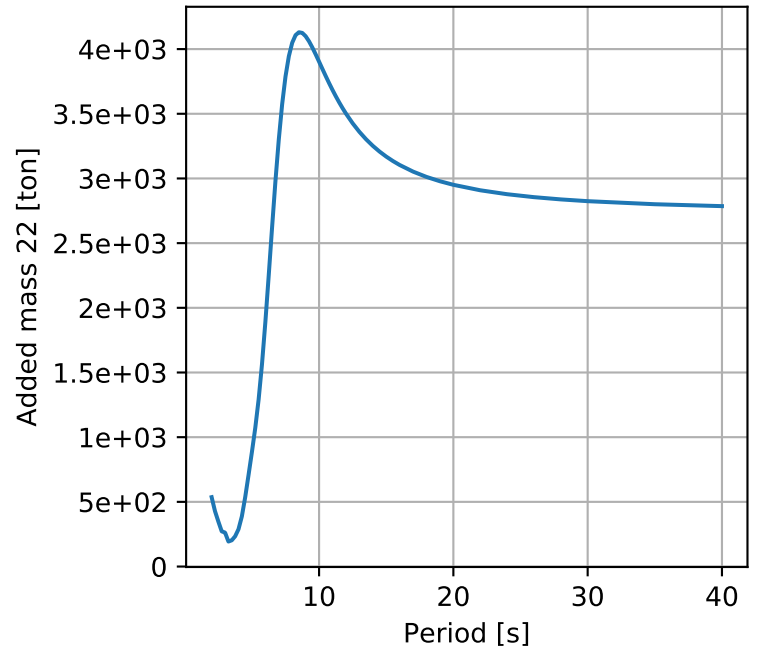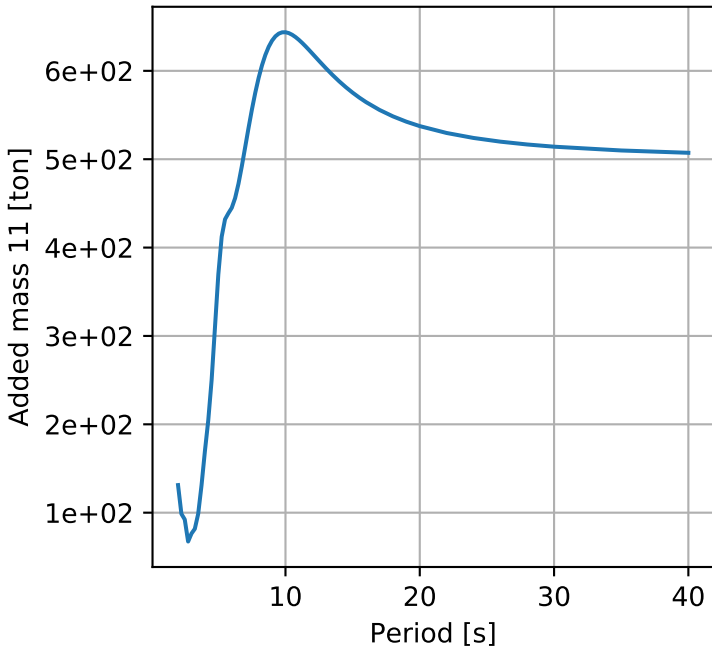
Pontoon type 1
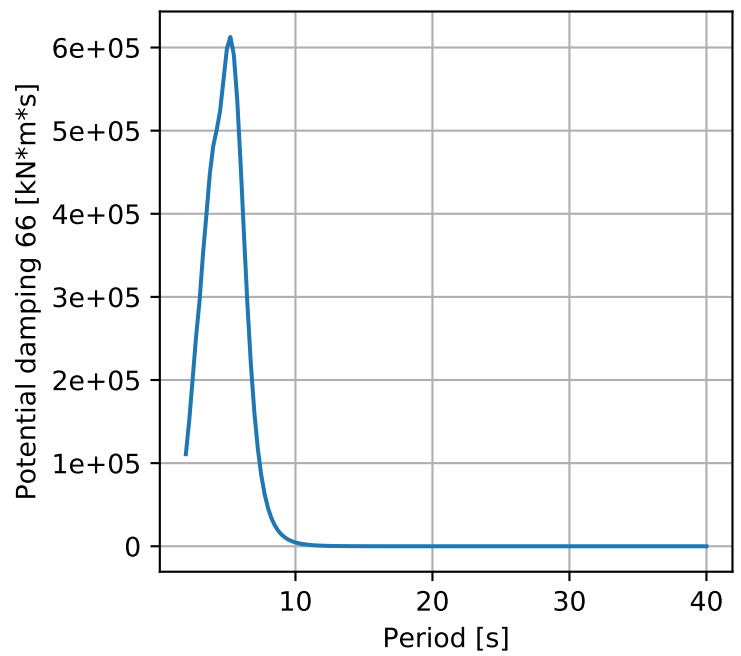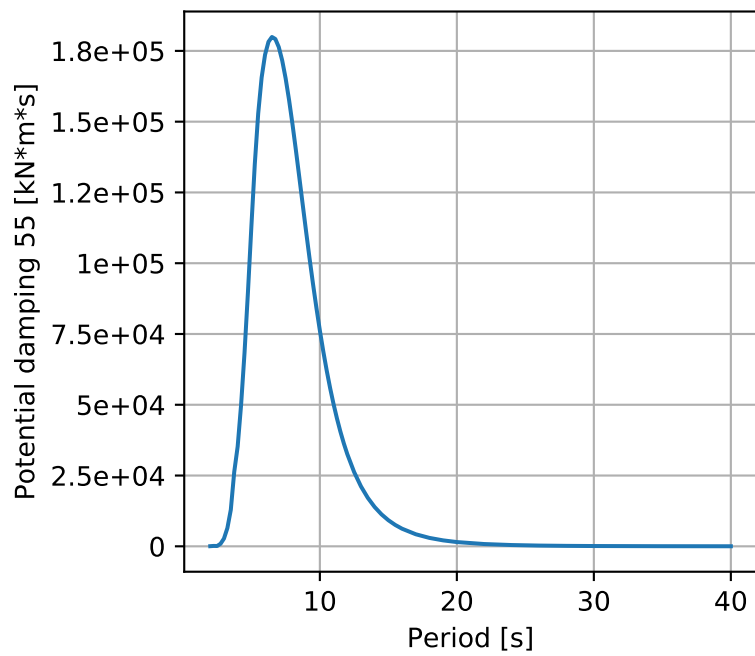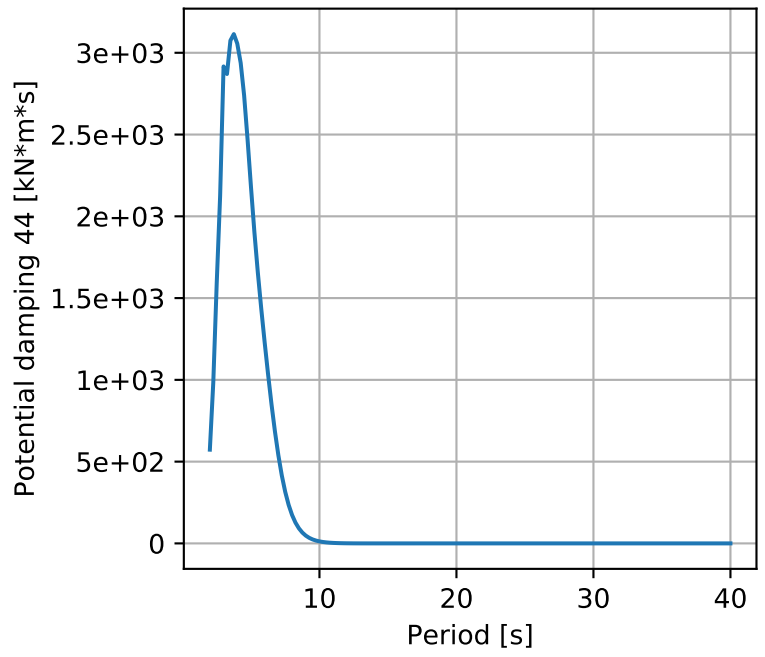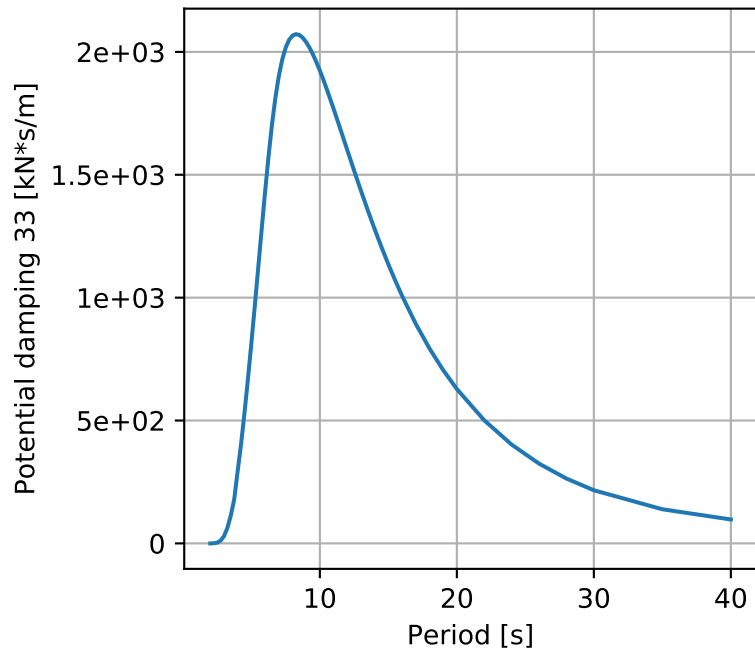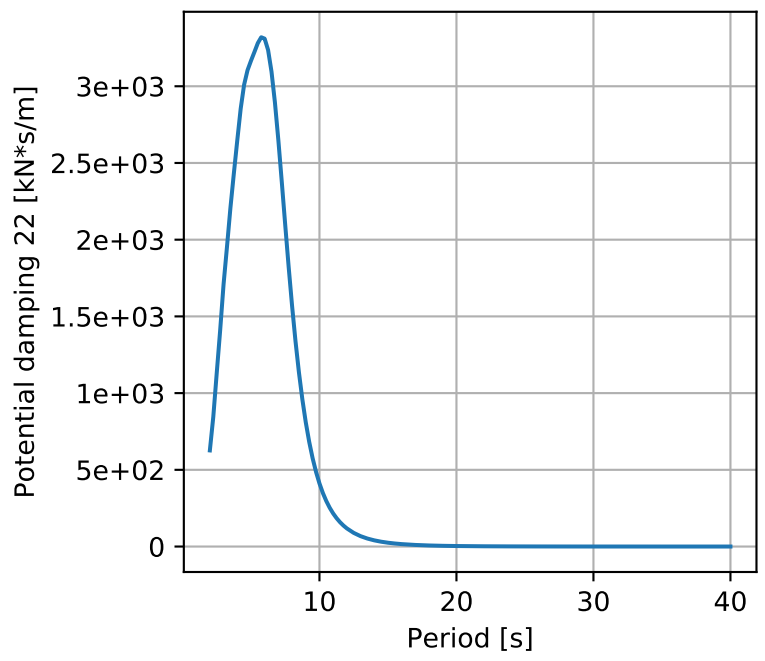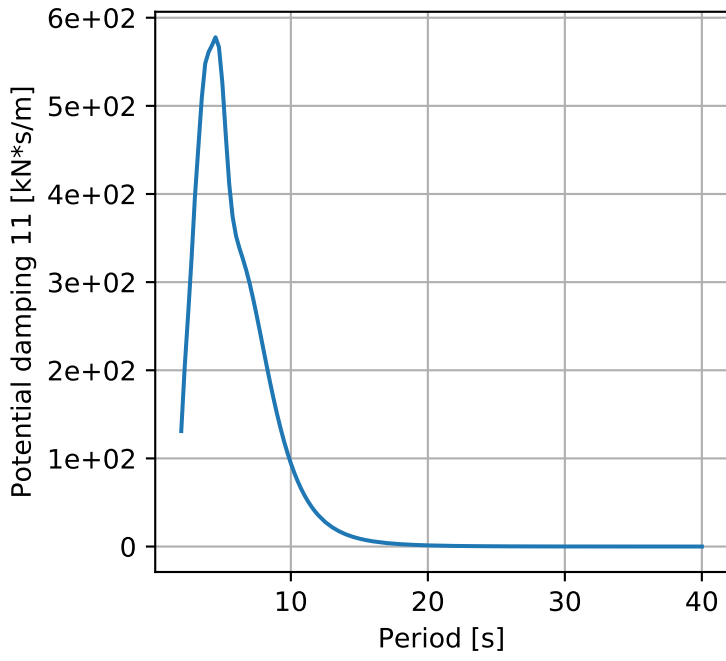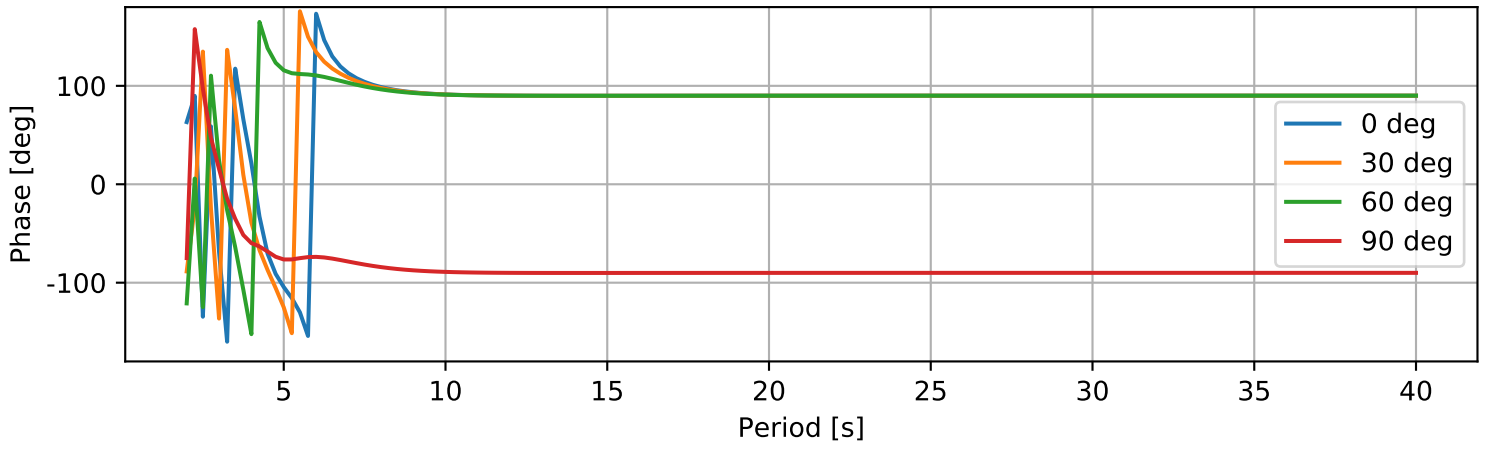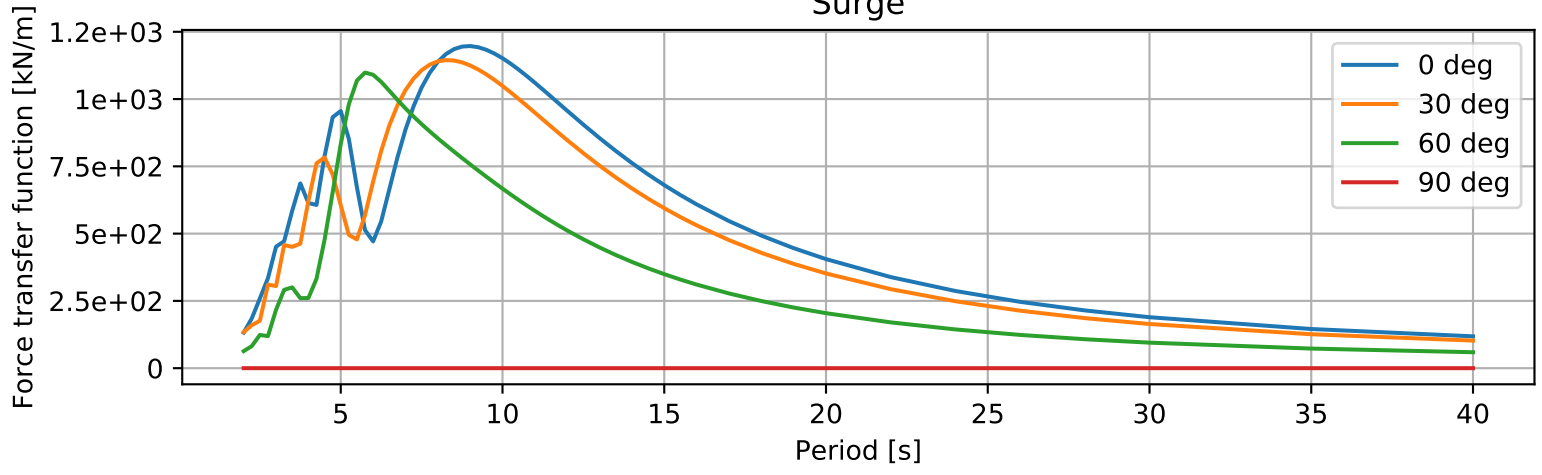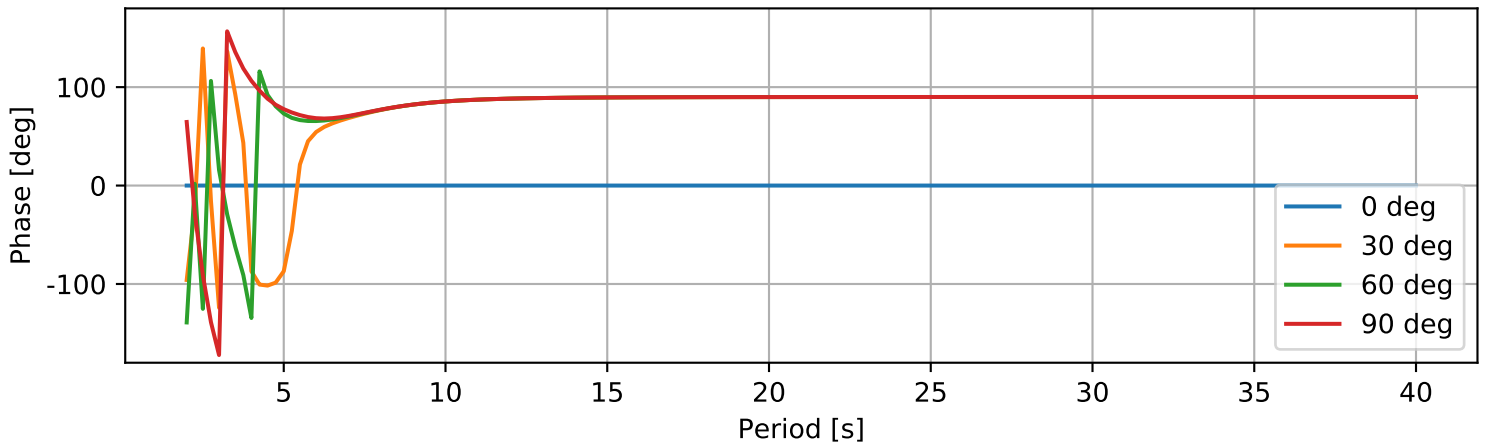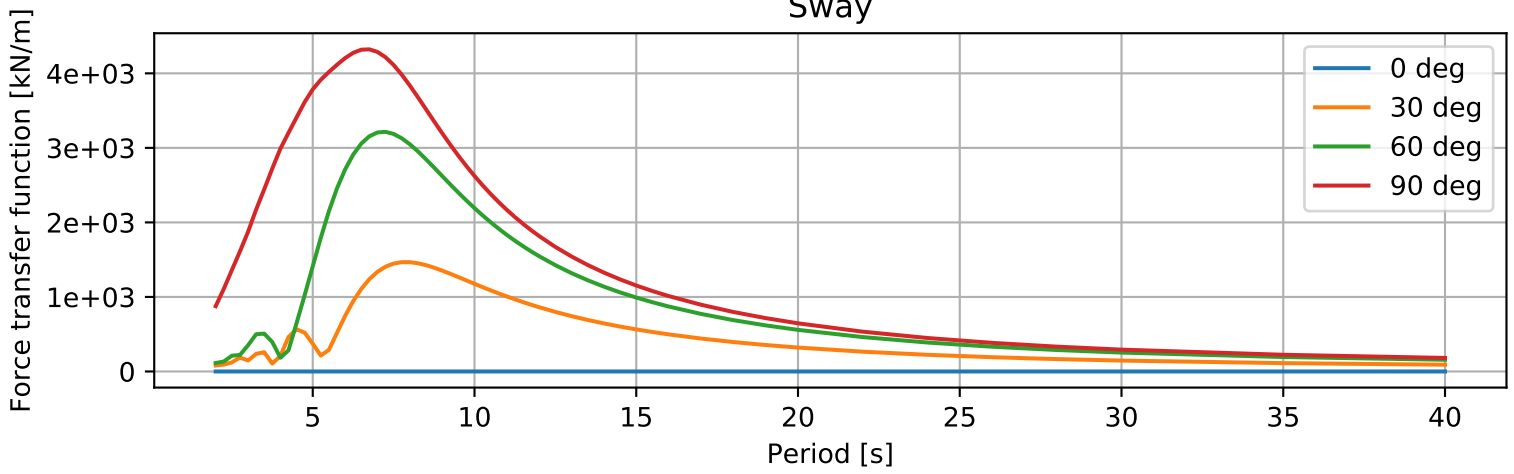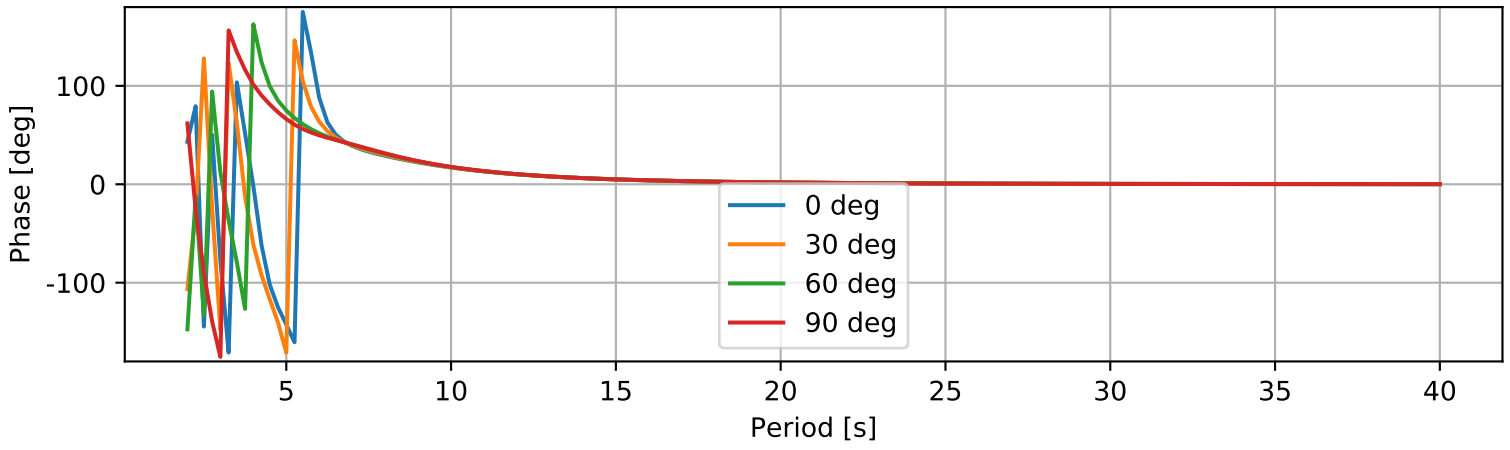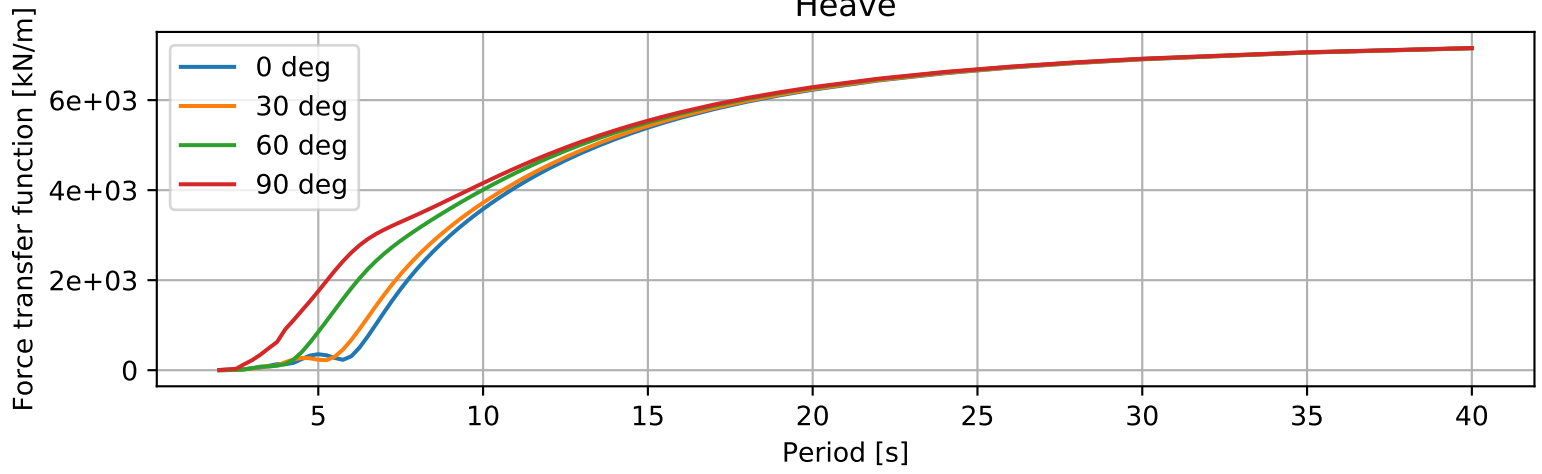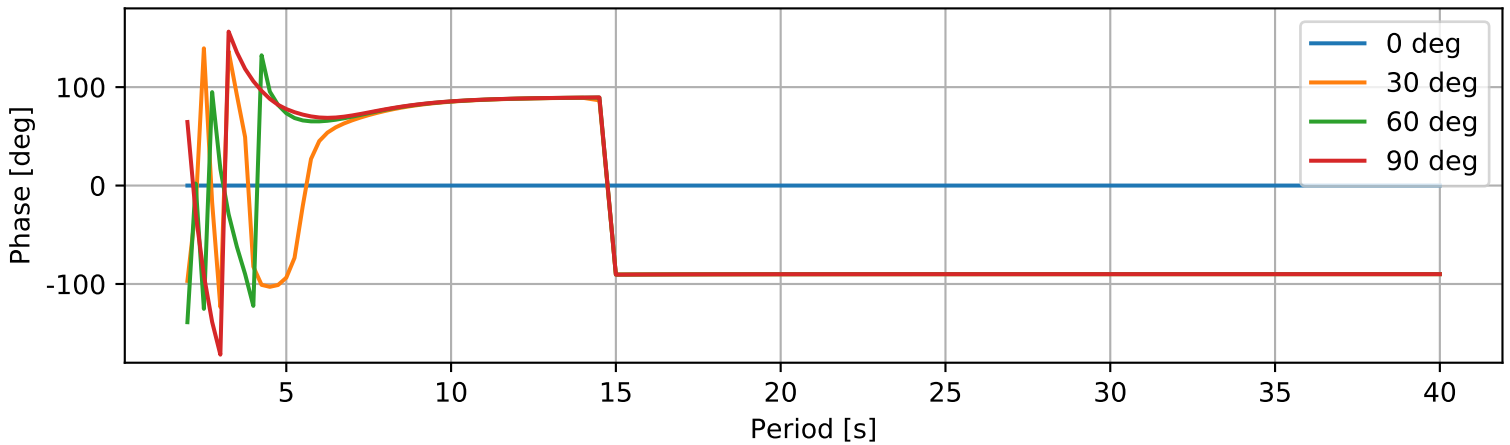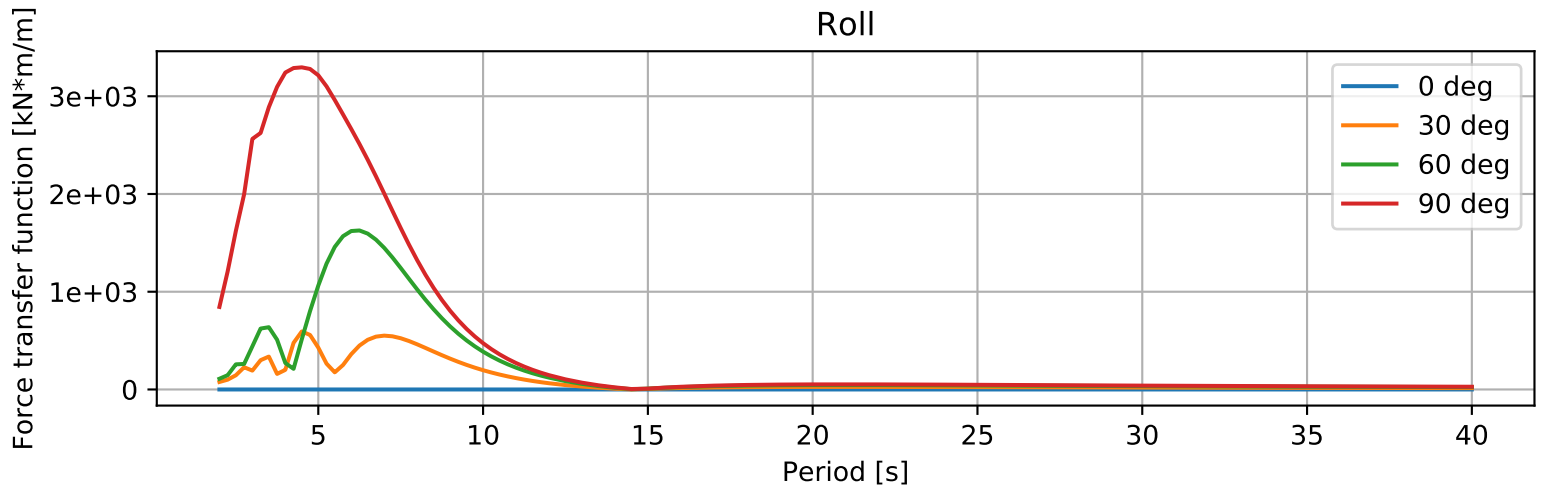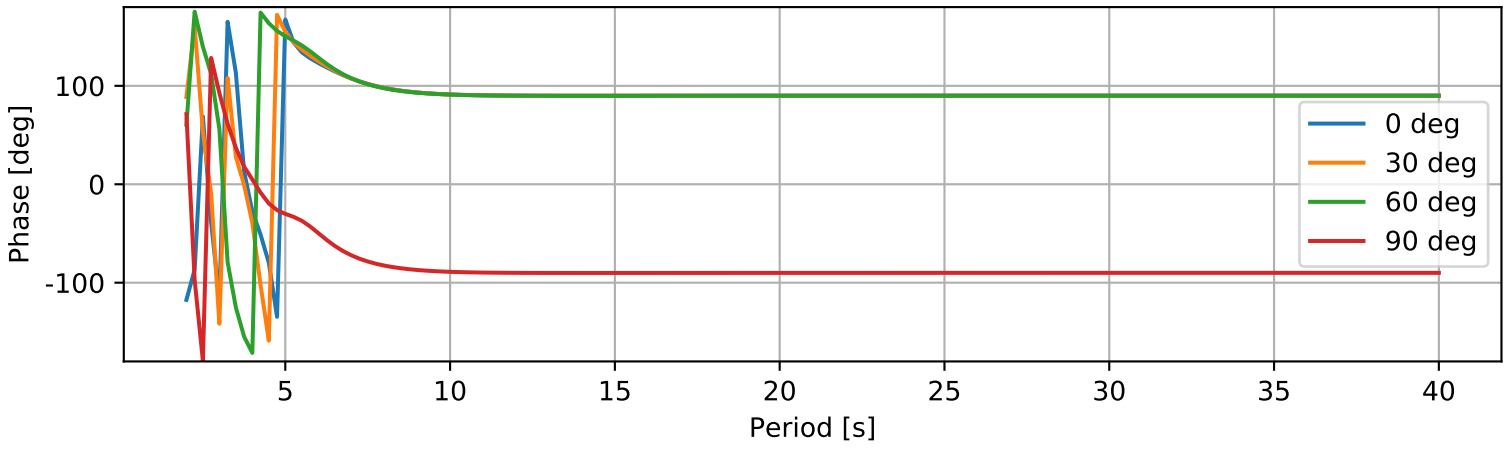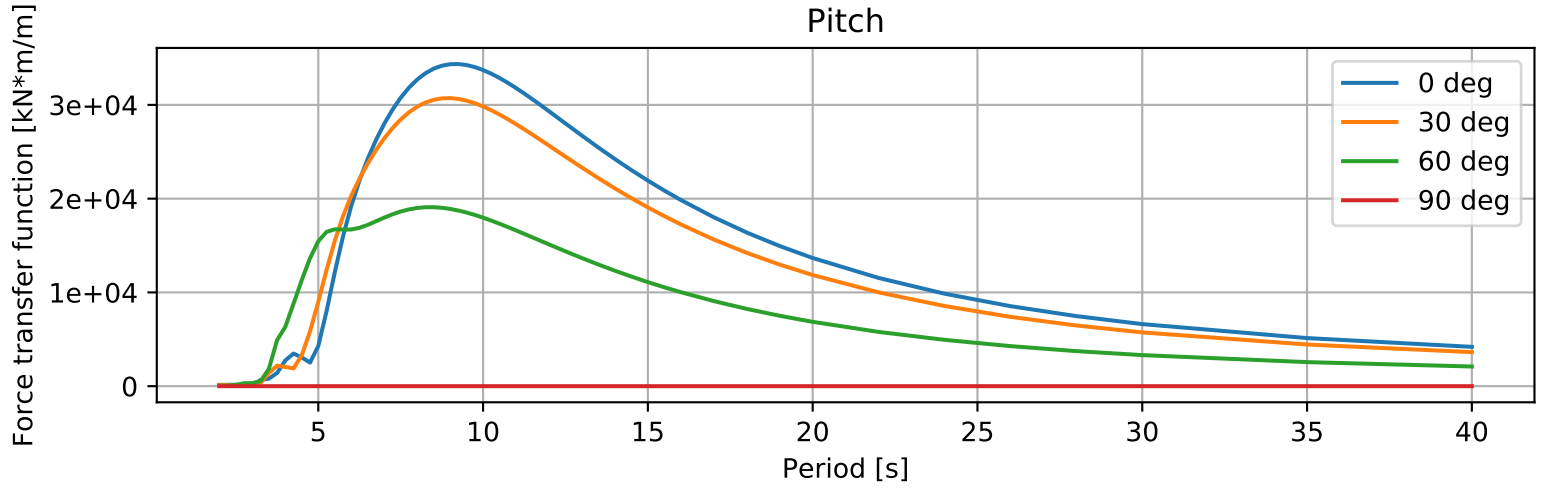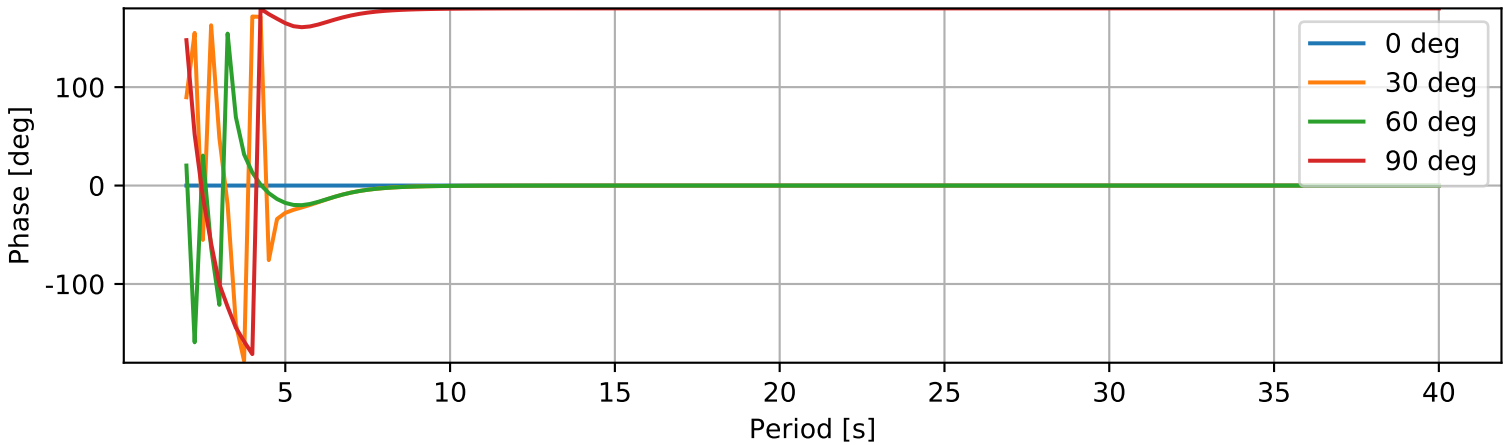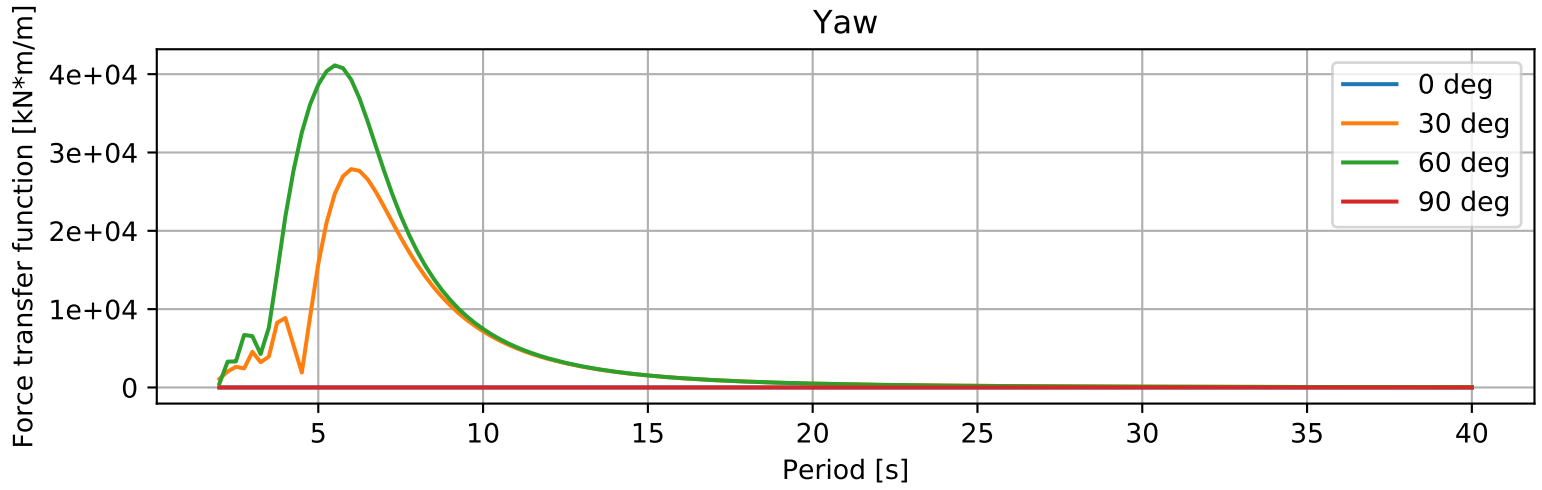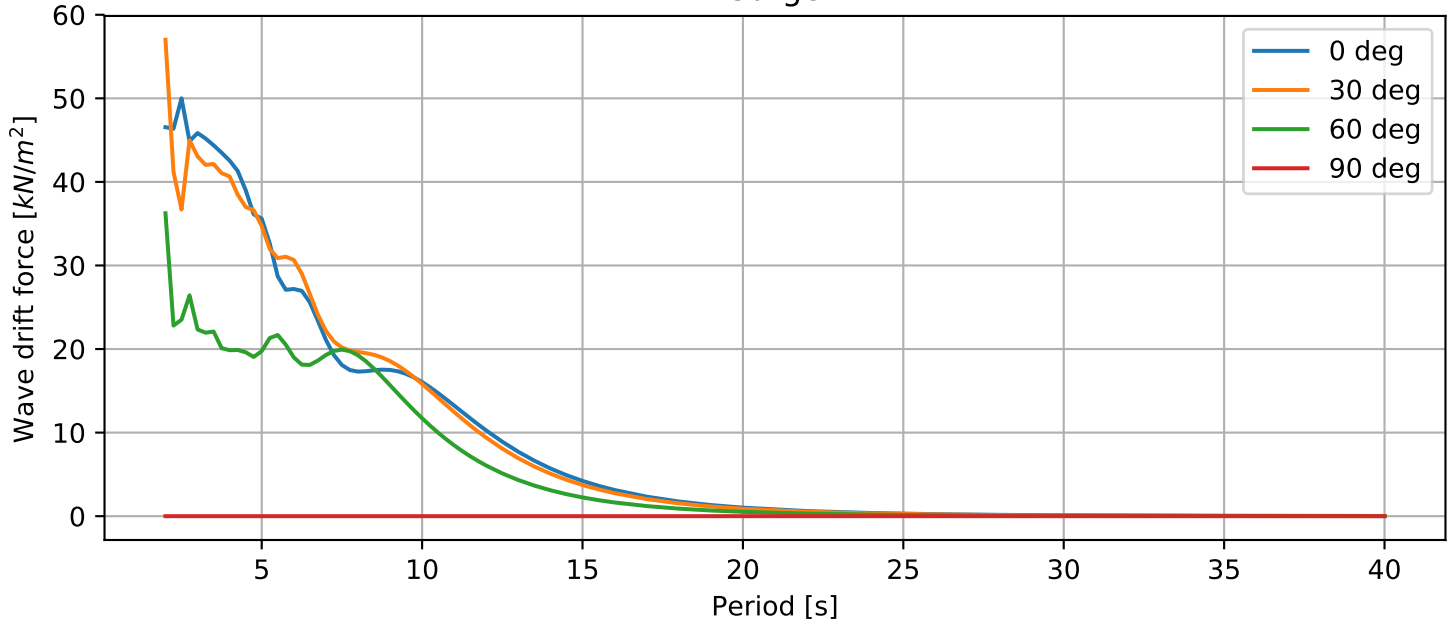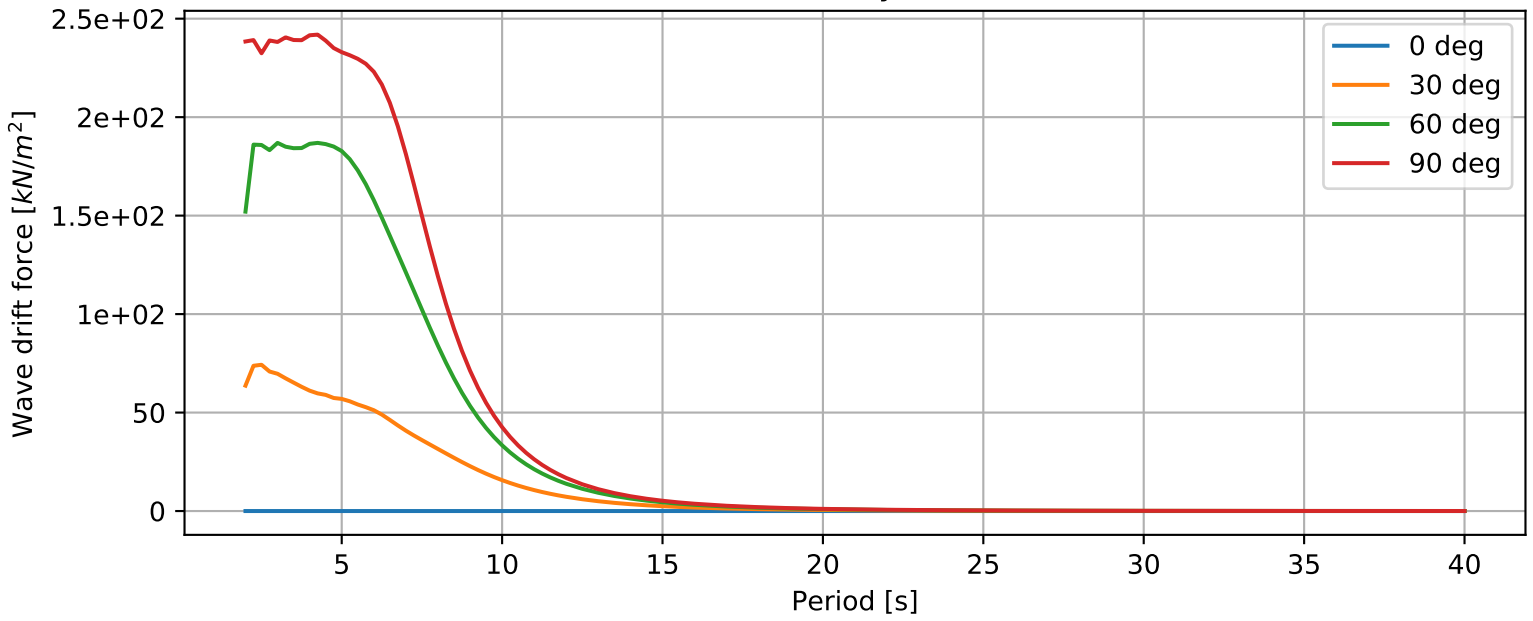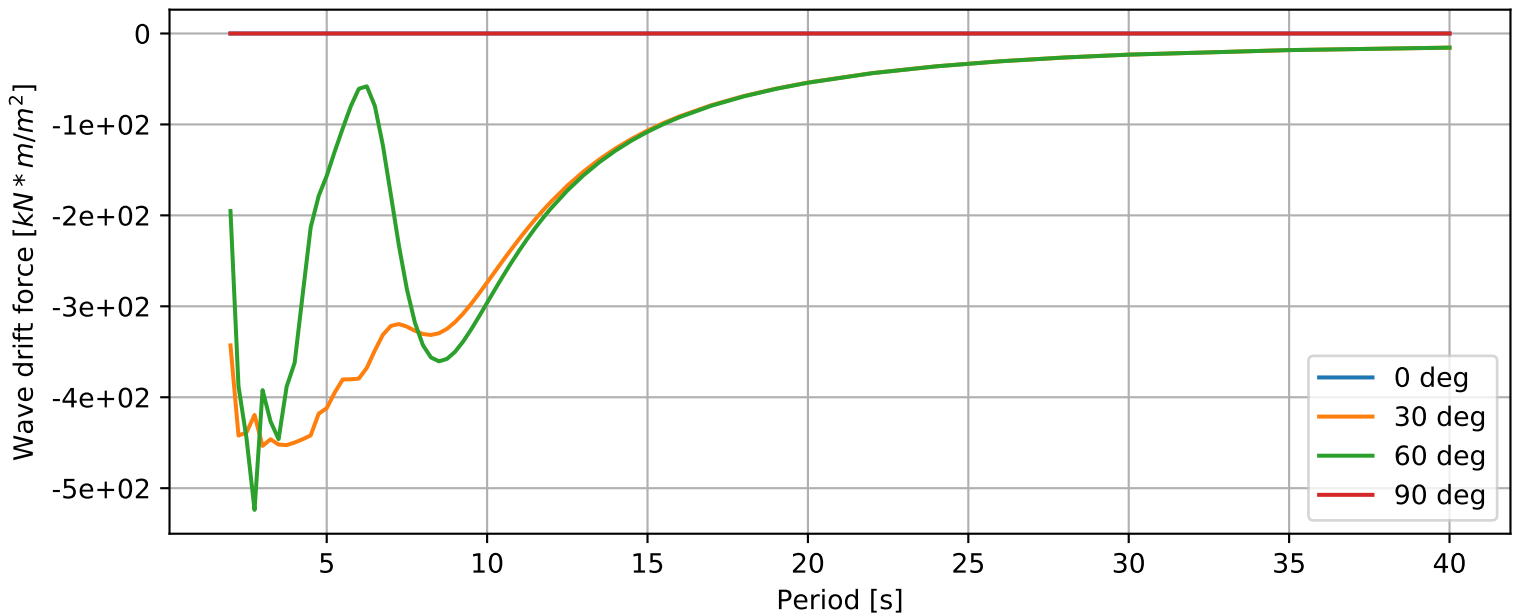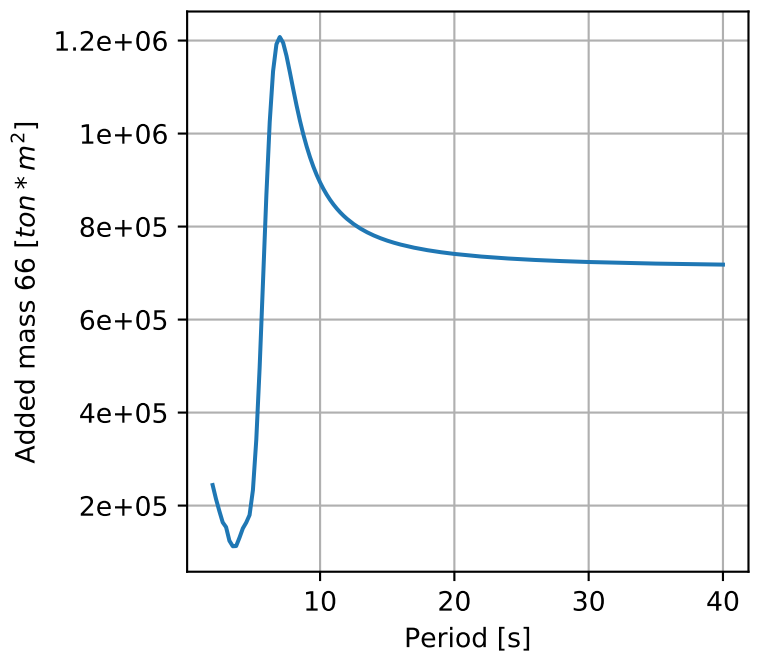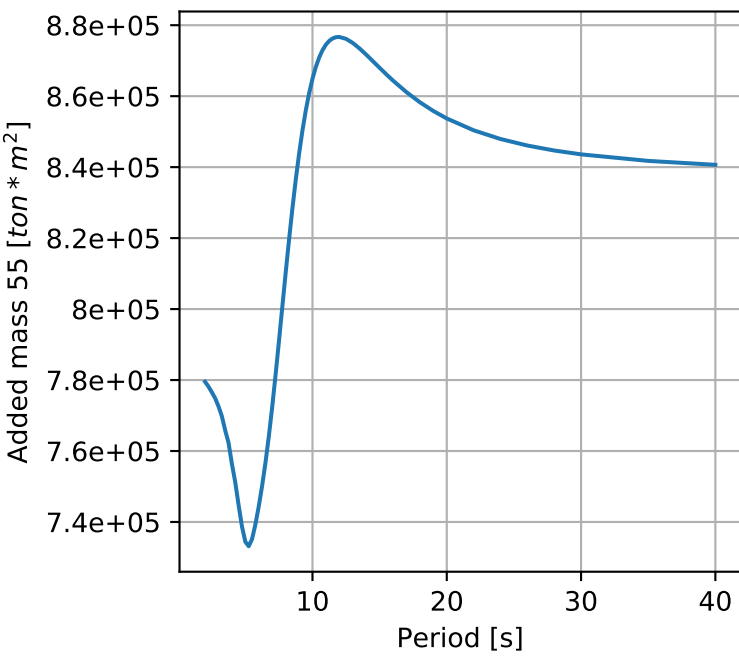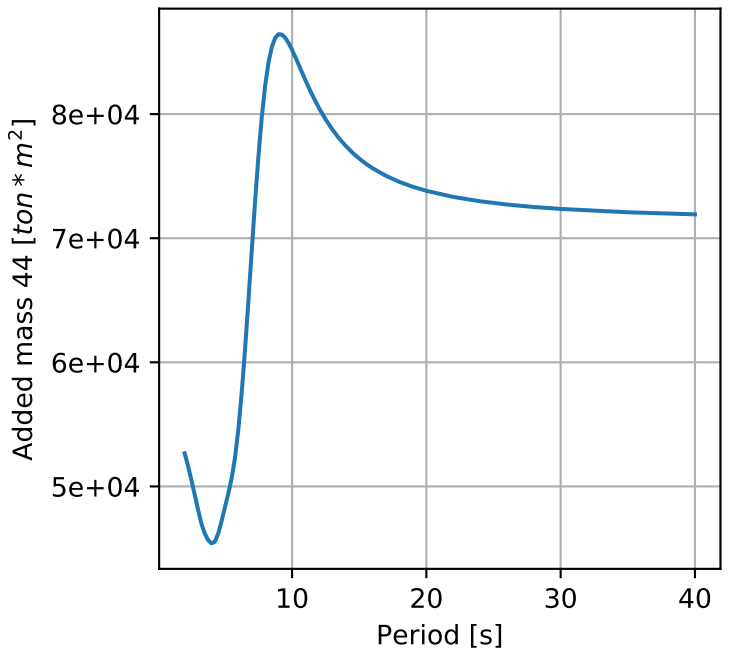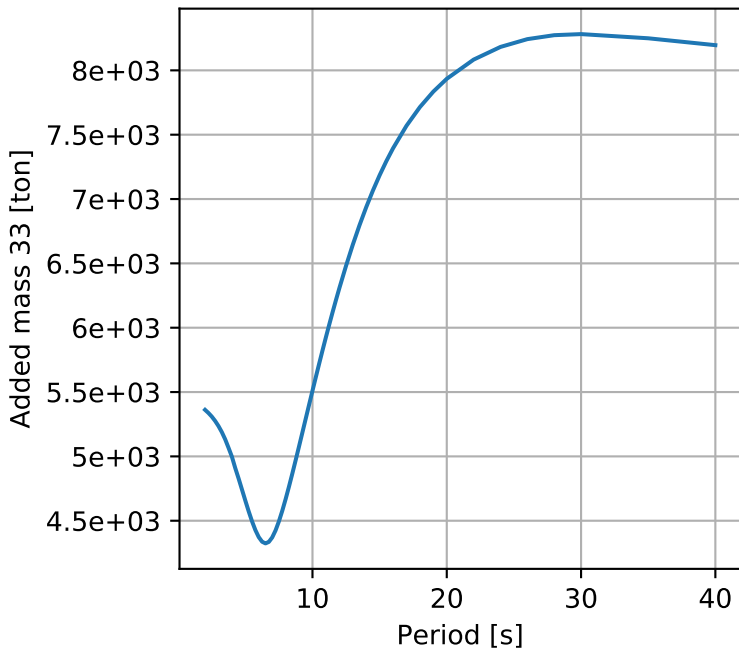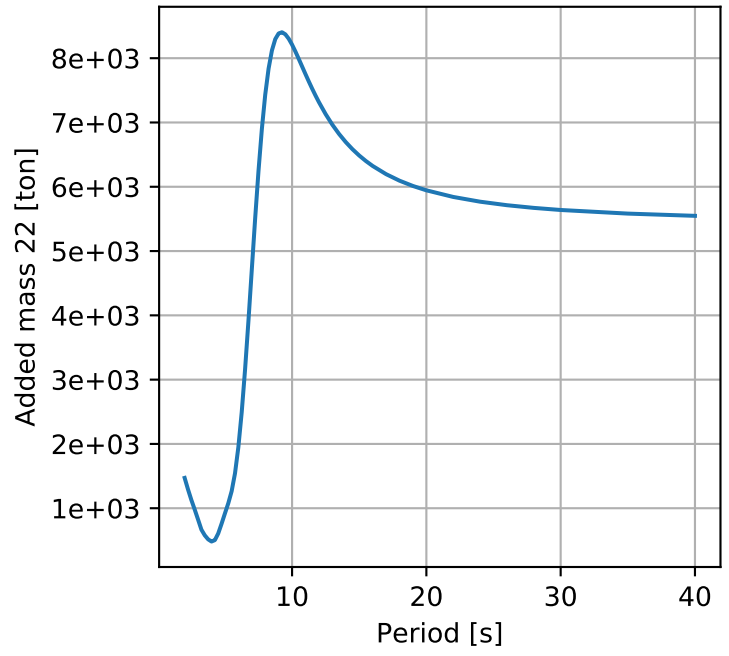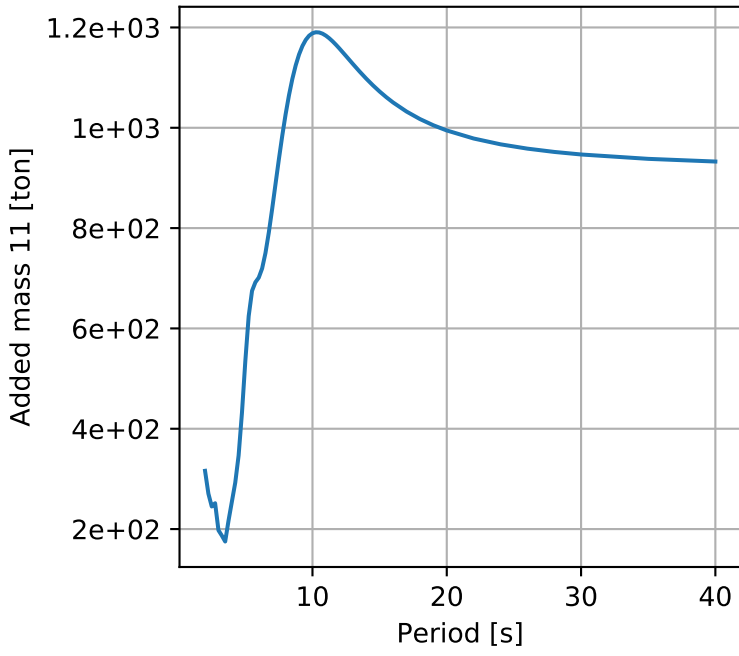
Pontoon type 1
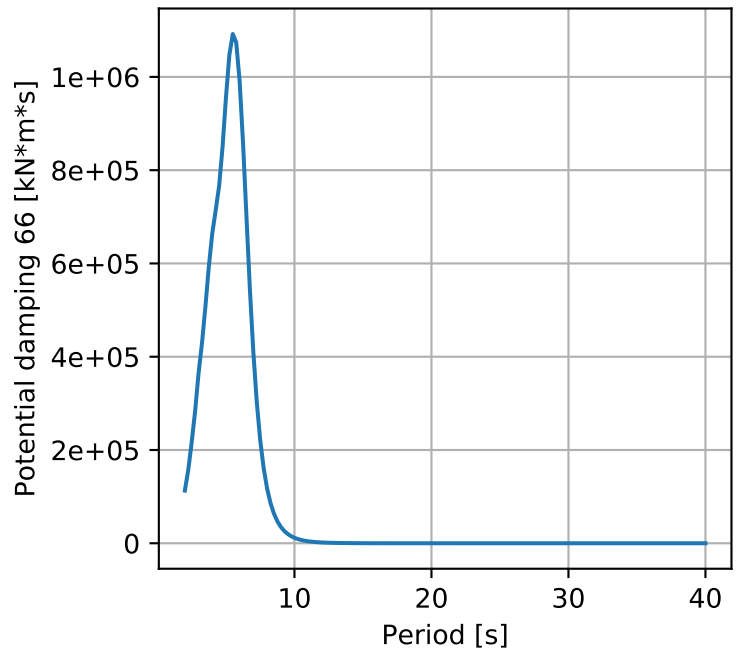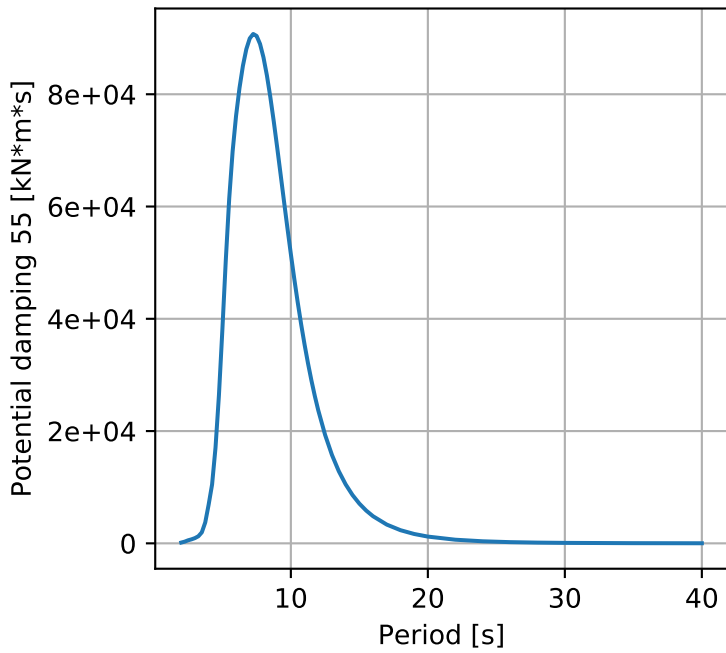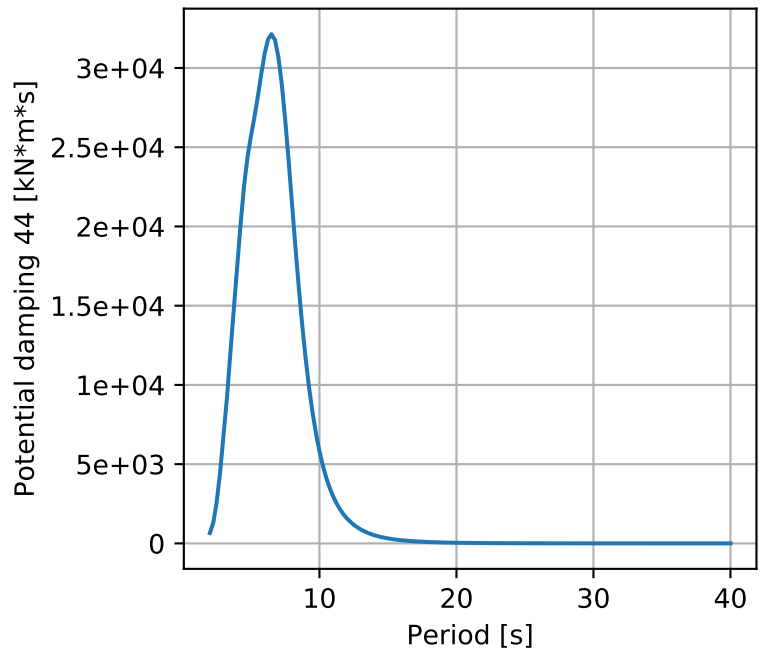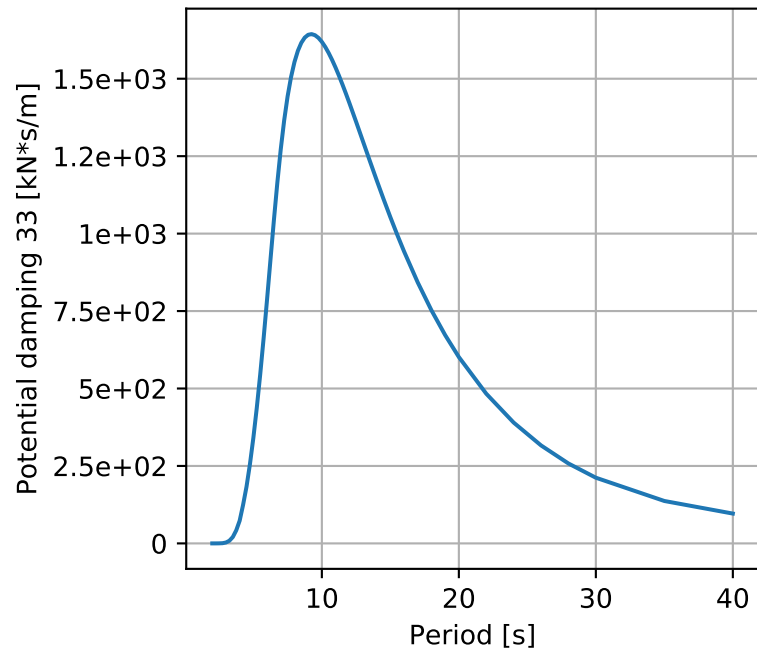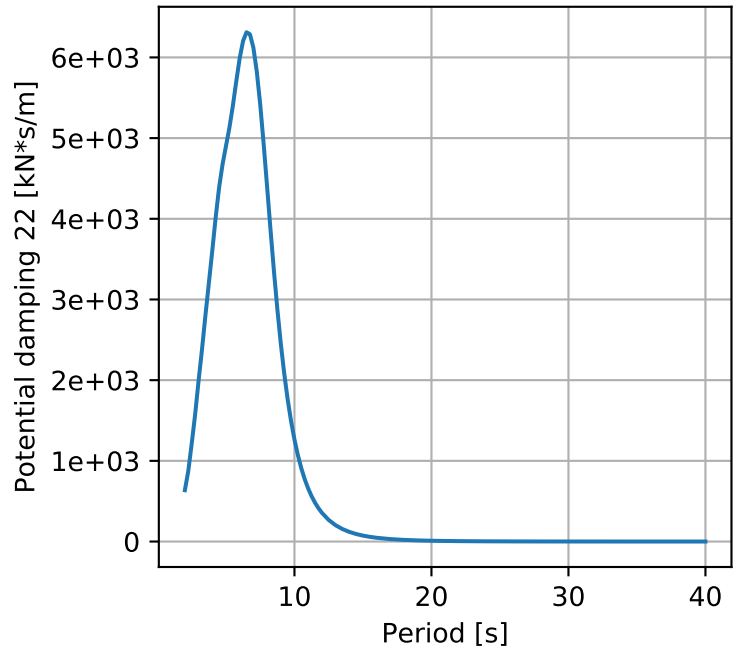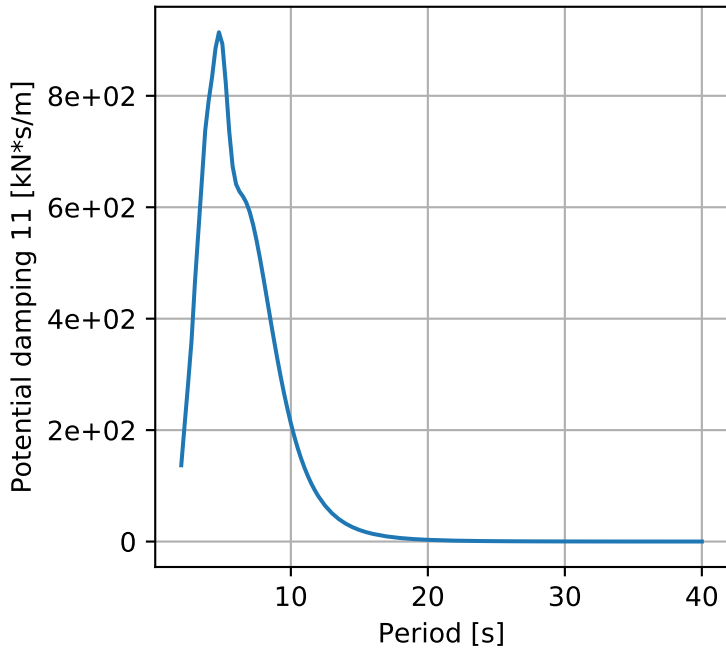
Pontoon type 1
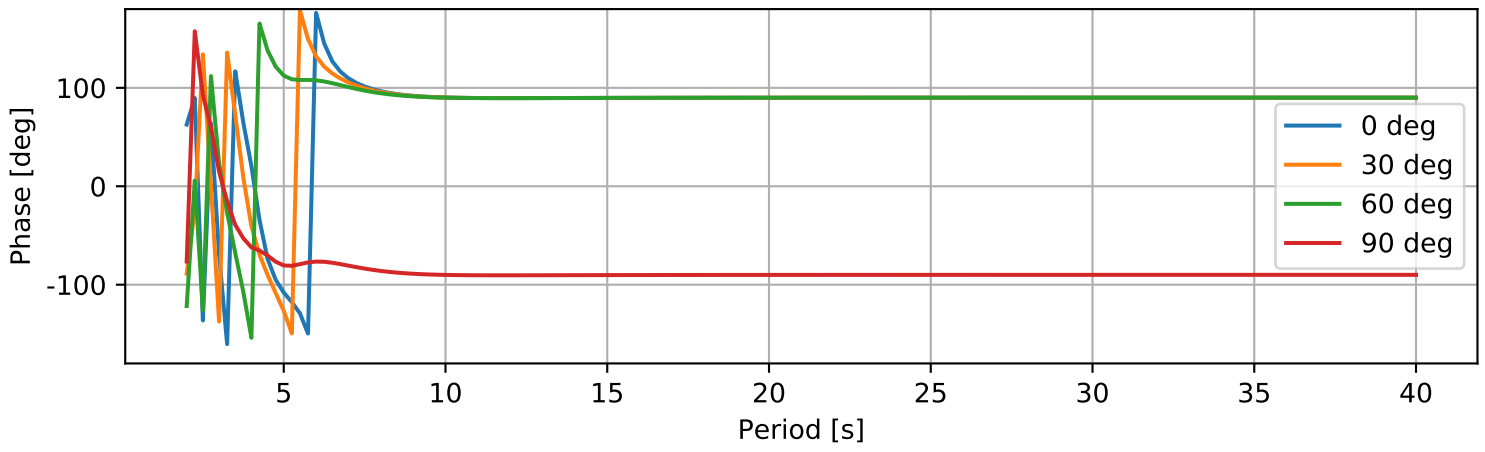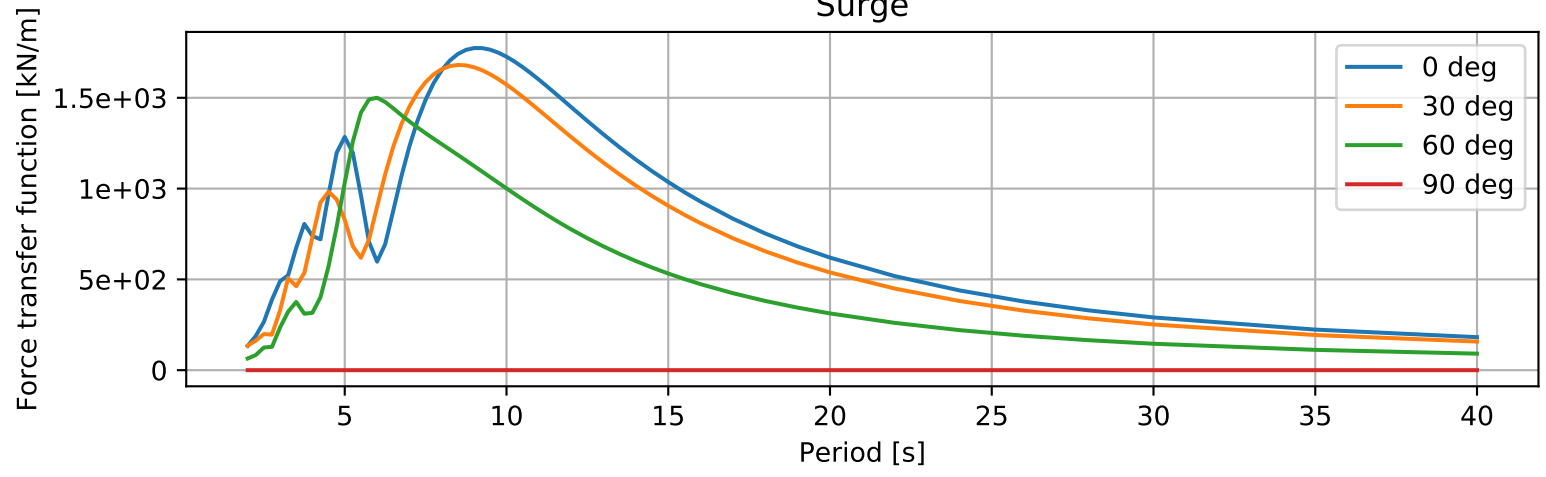
Pontoon type 1
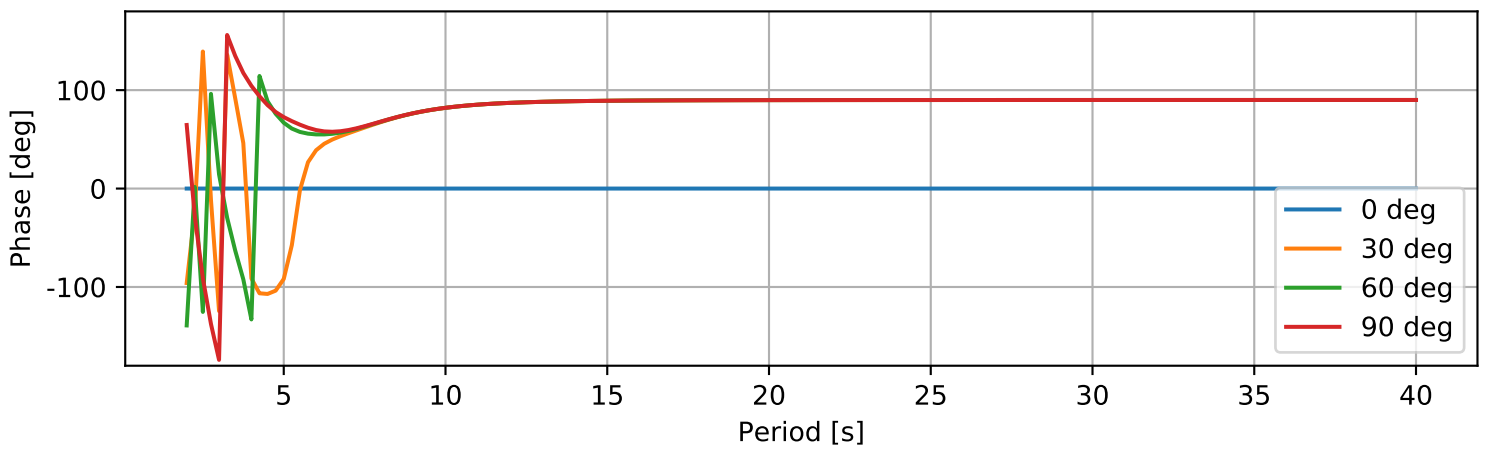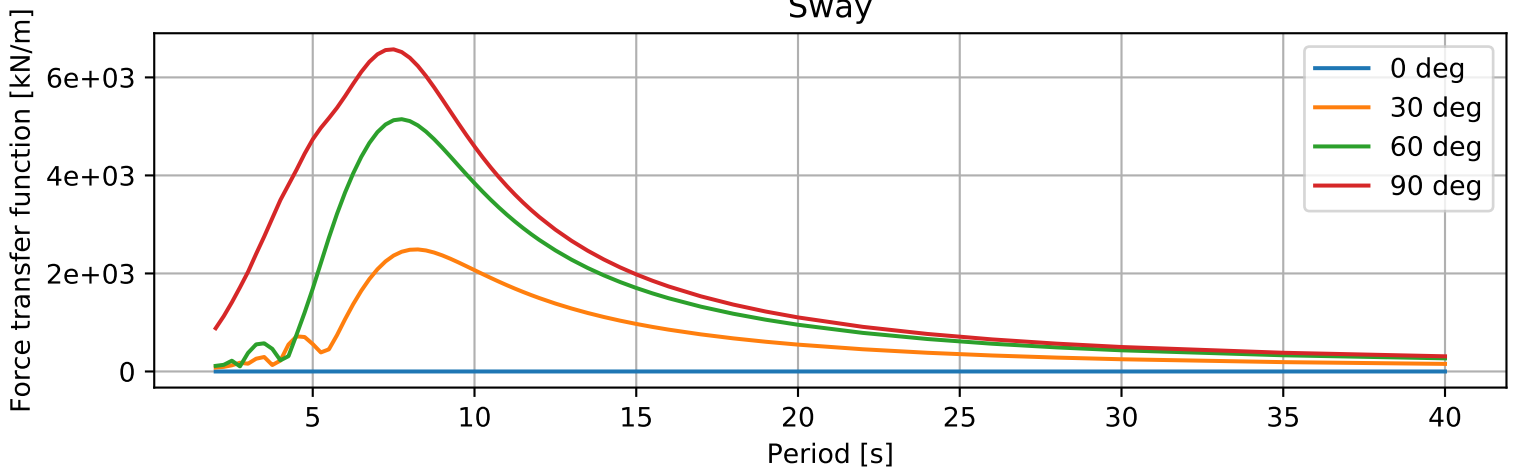
Pontoon type 1
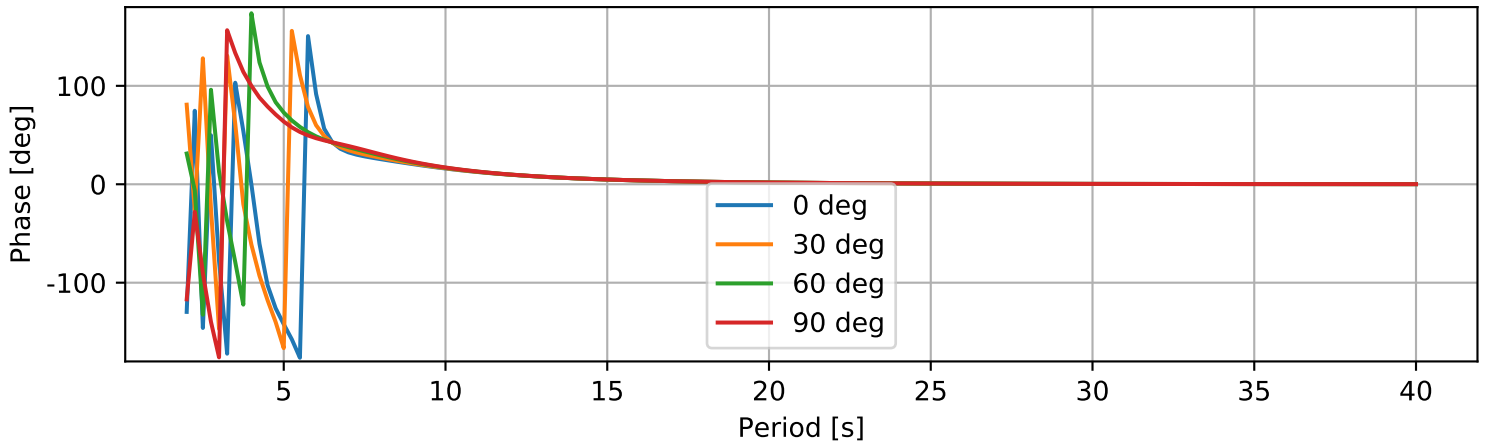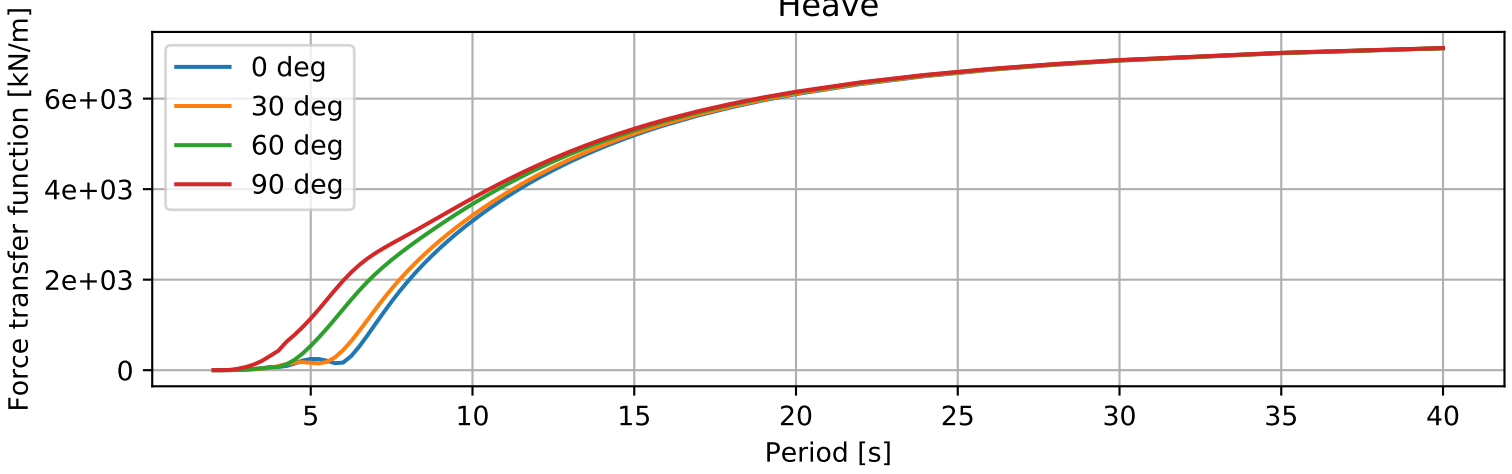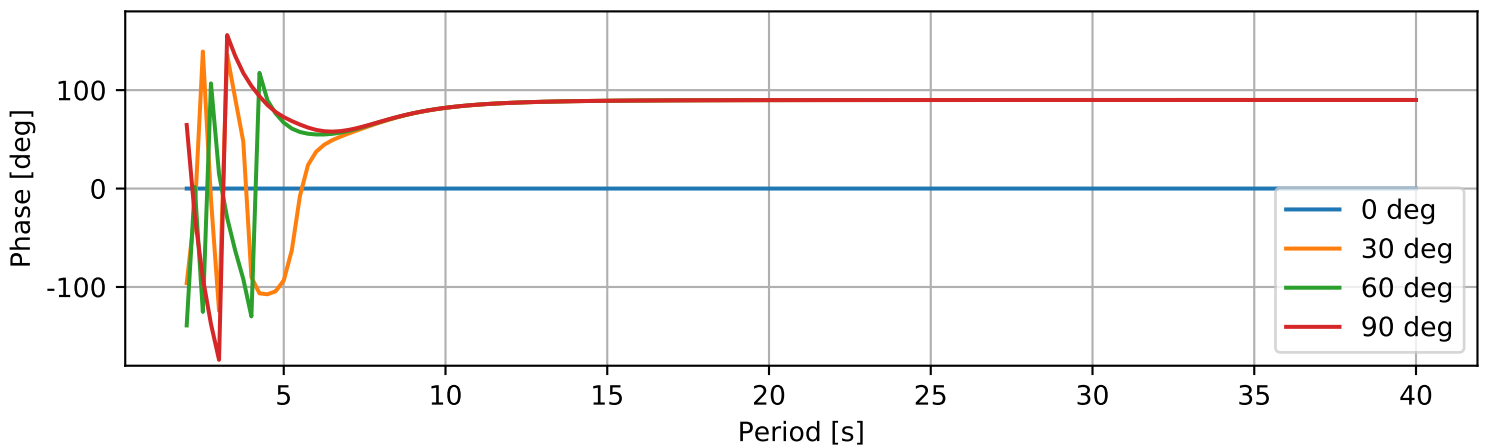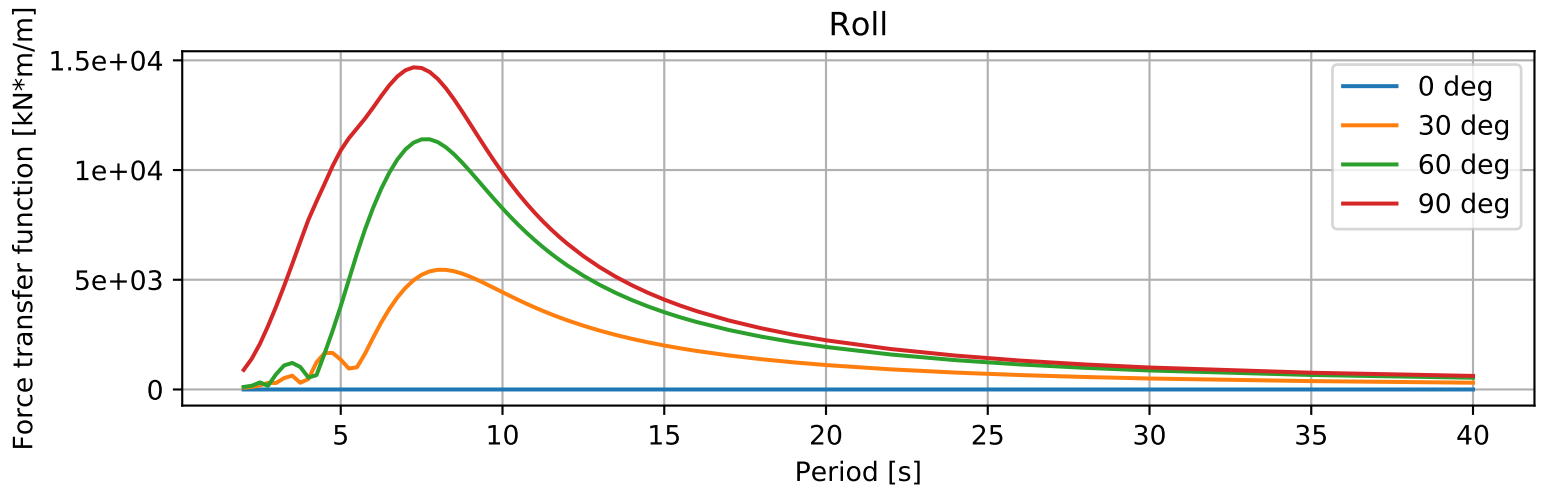
Pontoon type 2

Pontoon type 2
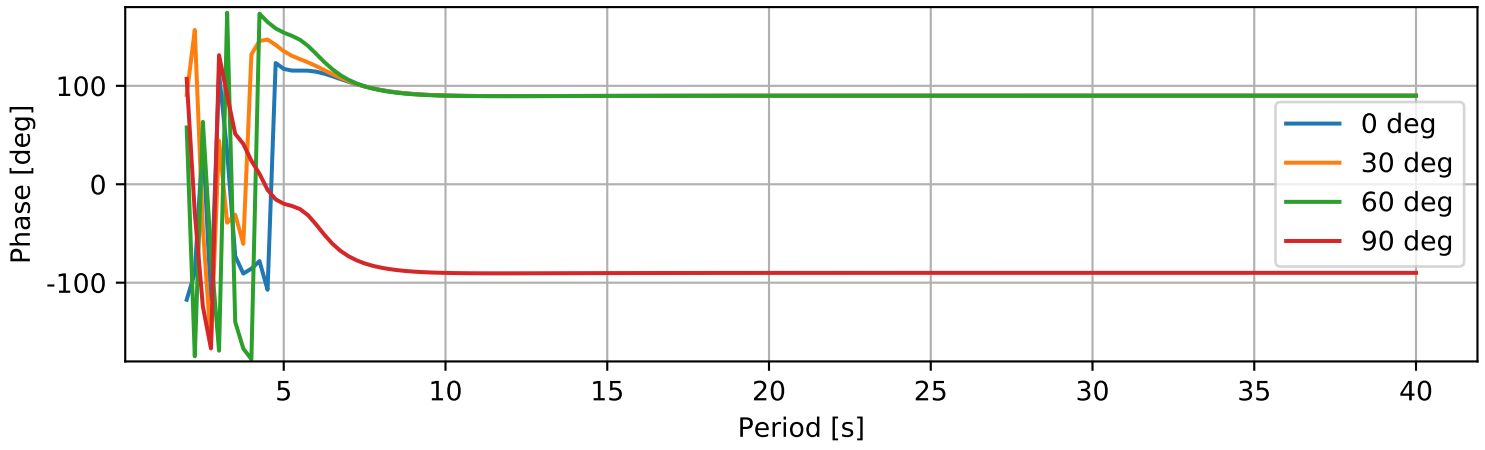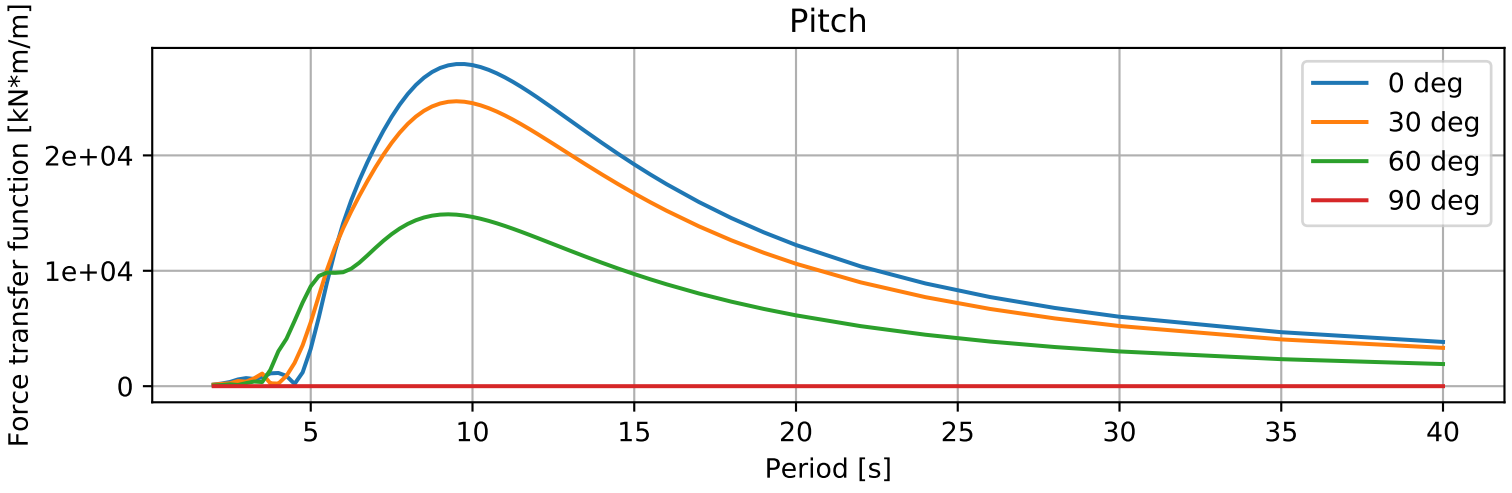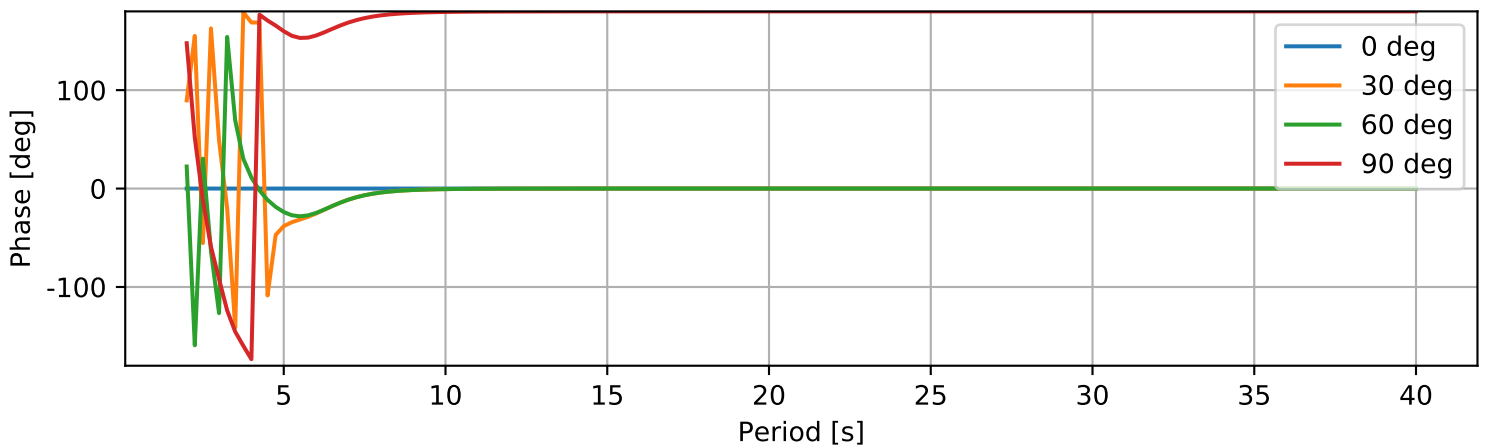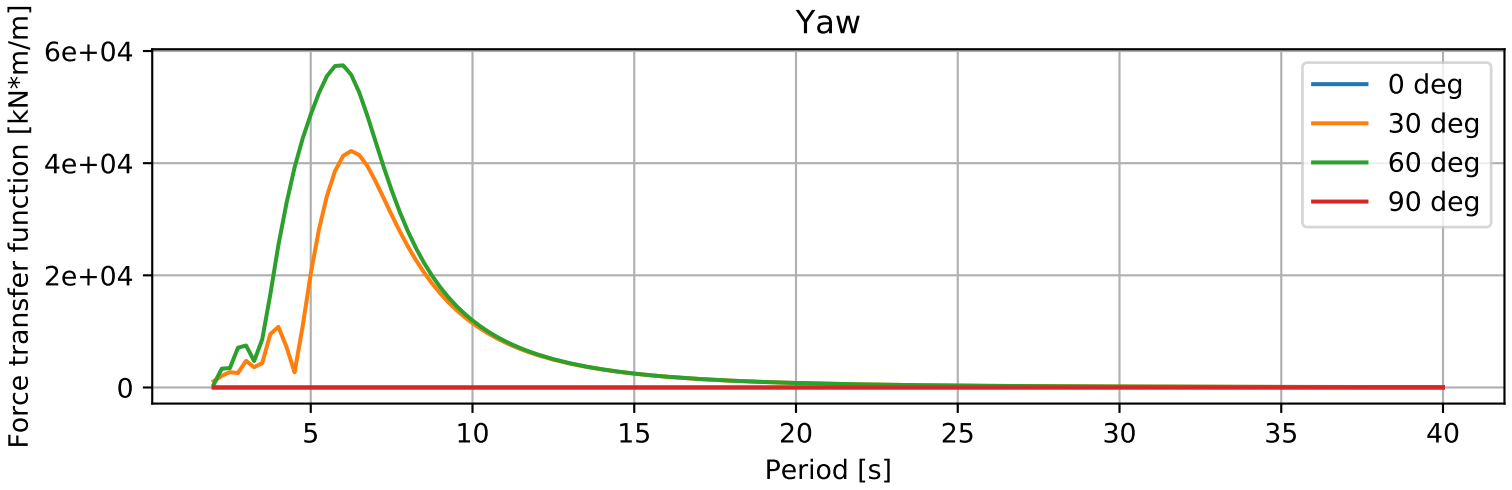
Pontoon type 2

Pontoon type 2

Pontoon type 2
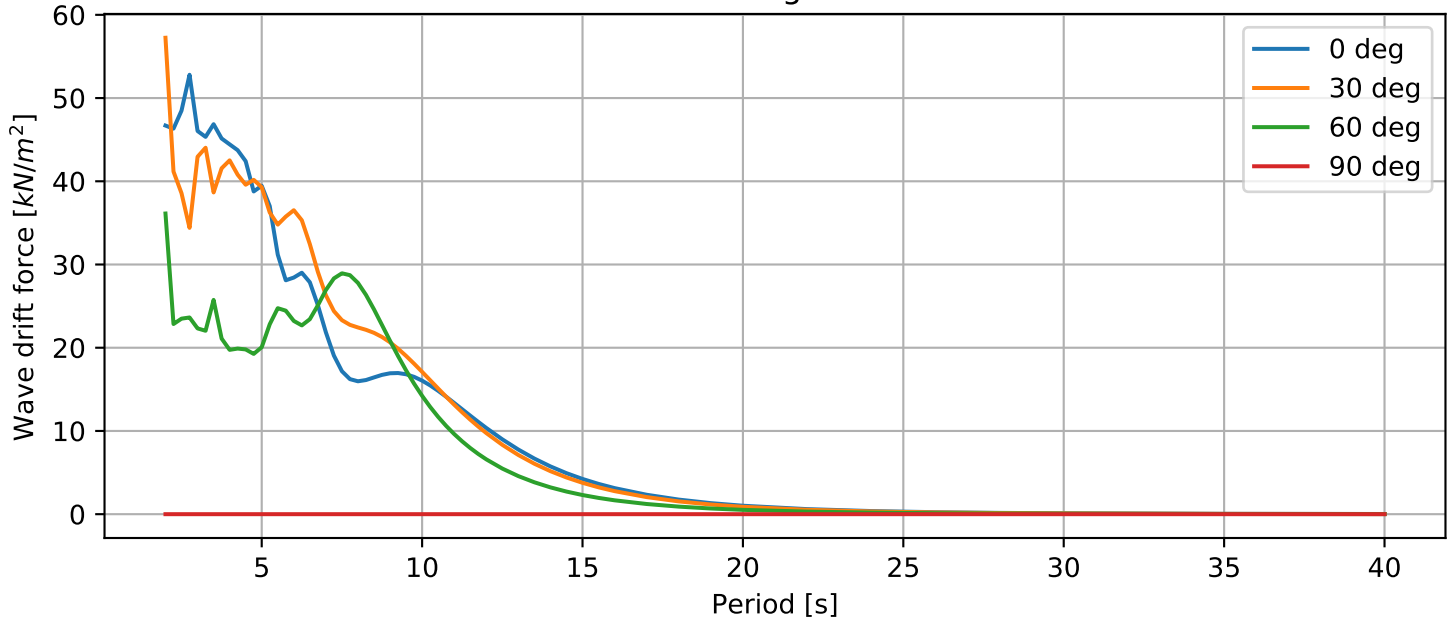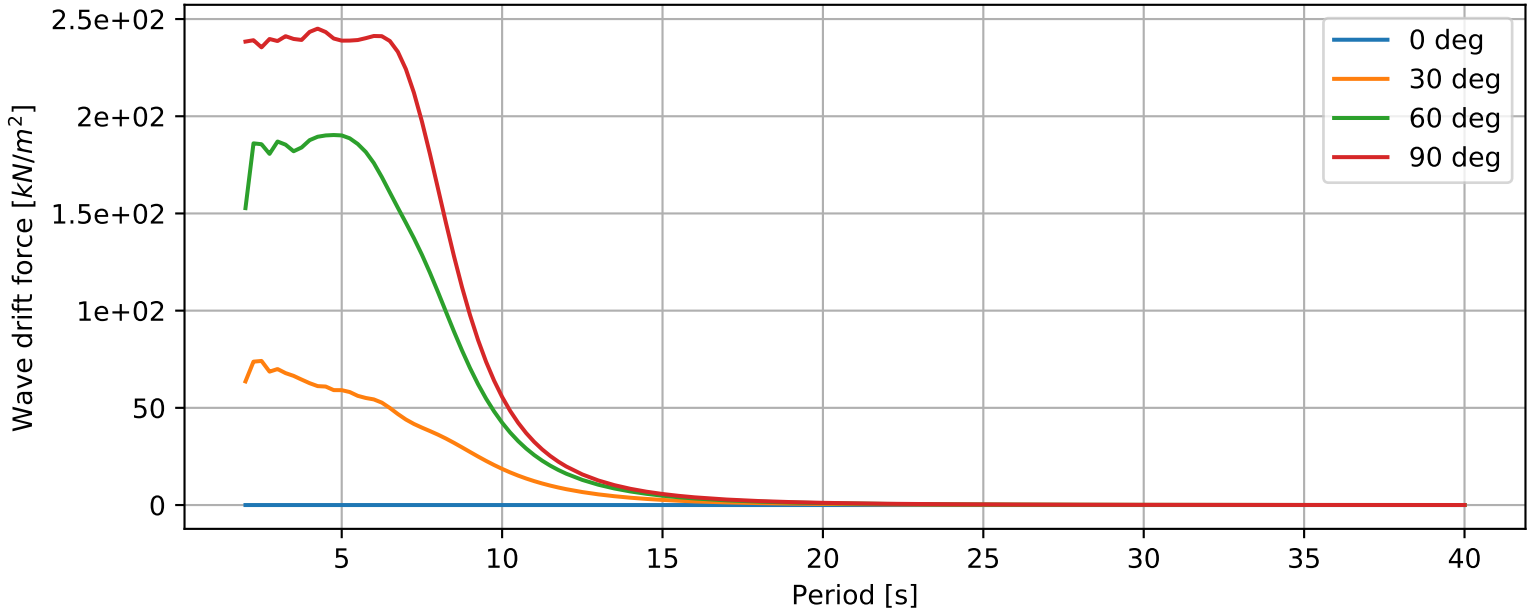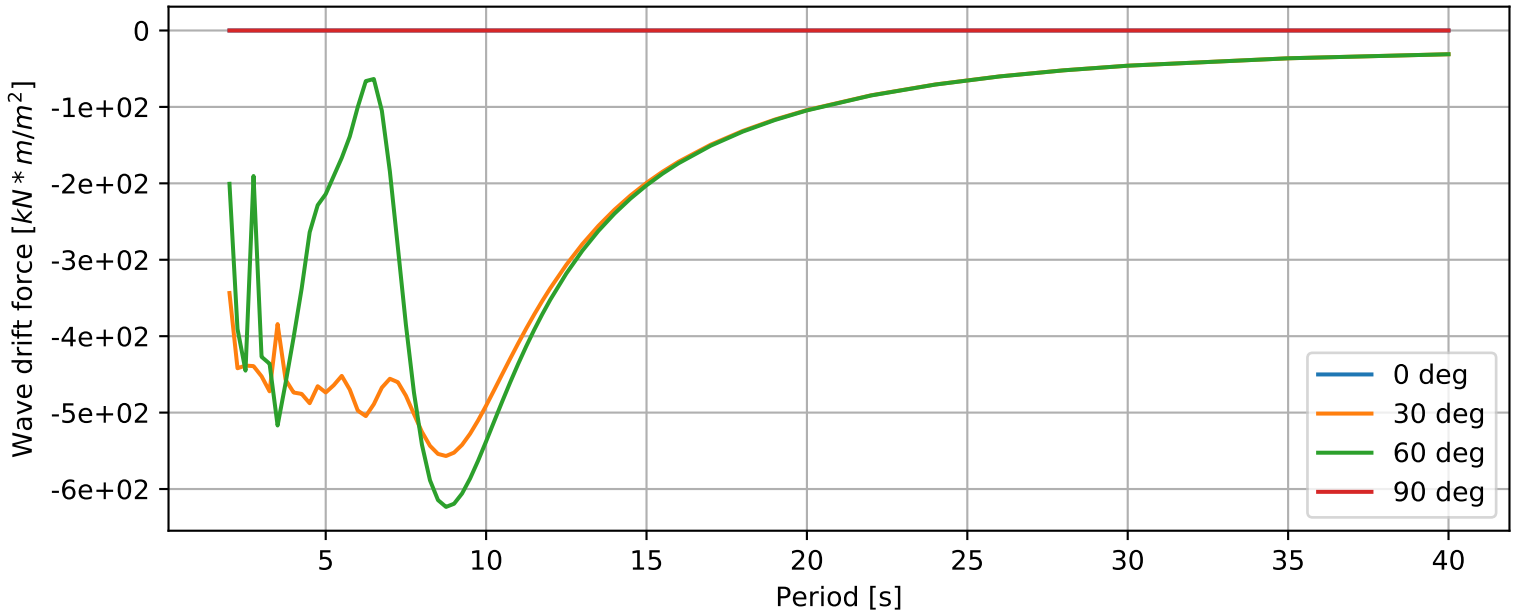
APPENDIX D
Fatigue environmental conditions

ID	HSW	TPW	WADIR	HSS	TPS	SWDIR	UW	WIDIR	Prob
case0001	0.1	1.25	0	0.01	5	0	2.3	0	0.027578
case0002	0.1	1.75	0	0.01	5	0	2.3	0	0.001208
case0003	0.1	2.25	0	0.01	5	0	2.3	0	0.000154
case0004	0.2	1.25	0	0.01	5	0	2.9	0	0.006087
case0005	0.2	1.75	0	0.01	5	0	2.9	0	0.001477
case0006	0.2	2.25	0	0.01	5	0	2.9	0	0.000669
case0007	0.2	2.75	0	0.01	5	0	2.9	0	0.000115
case0008	0.3	1.75	0	0.01	5	0	5.5	0	0.0002
case0009	0.3	2.25	0	0.01	5	0	5.5	0	8.46E-05
case0010	0.3	2.75	0	0.01	5	0	5.5	0	0.000146
case0011	0.3	3.25	0	0.01	5	0	5.5	0	3.08E-05
case0012	0.4	1.75	0	0.01	5	0	6.7	0	1.54E-05
case0013	0.4	2.25	0	0.01	5	0	6.7	0	4.61E-05
case0014	0.4	2.75	0	0.01	5	0	6.7	0	6.92E-05
case0015	0.4	3.25	0	0.01	5	0	6.7	0	2.31E-05
case0016	0.4	3.75	0	0.01	5	0	6.7	0	7.7E-06
case0017	0.5	2.25	0	0.01	5	0	8	0	7.7E-06
case0018	0.5	2.75	0	0.01	5	0	8	0	7.7E-06
case0019	0.5	3.25	0	0.01	5	0	8	0	5.38E-05
case0020	0.5	3.75	0	0.01	5	0	8	0	1.54E-05
case0021	0.6	2.75	0	0.01	5	0	9.3	0	7.7E-06
case0022	0.6	3.25	0	0.01	5	0	9.3	0	2.31E-05
case0023	0.6	3.75	0	0.01	5	0	9.3	0	7.7E-06
case0024	0.7	3.75	0	0.01	5	0	12.2	0	1.54E-05
case0025	0.8	3.75	0	0.01	5	0	11.5	0	1.54E-05
case0026	0.9	3.75	0	0.01	5	0	13.8	0	2.31E-05
case0027	0.1	1.25	30	0.01	5	30	2.3	30	0.021368
case0028	0.1	1.75	30	0.01	5	30	2.3	30	0.000754
case0029	0.1	2.25	30	0.01	5	30	2.3	30	3.08E-05
case0030	0.2	1.25	30	0.01	5	30	2.7	30	0.007995
case0031	0.2	1.75	30	0.01	5	30	2.7	30	0.00077
case0032	0.2	2.25	30	0.01	5	30	2.7	30	0.000531
case0033	0.2	2.75	30	0.01	5	30	2.7	30	3.85E-05
case0034	0.3	1.75	30	0.01	5	30	5.3	30	4.61E-05
case0035	0.3	2.25	30	0.01	5	30	5.3	30	7.69E-05
case0036	0.3	2.75	30	0.01	5	30	5.3	30	6.15E-05
case0037	0.3	3.25	30	0.01	5	30	5.3	30	1.54E-05
case0038	0.4	1.75	30	0.01	5	30	6.4	30	7.7E-06
case0039	0.4	2.25	30	0.01	5	30	6.4	30	4.61E-05
case0040	0.4	2.75	30	0.01	5	30	6.4	30	2.31E-05
case0041	0.4	3.25	30	0.01	5	30	6.4	30	1.54E-05
case0042	0.5	3.25	30	0.01	5	30	9.2	30	3.85E-05
case0043	0.6	3.25	30	0.01	5	30	9.8	30	7.7E-06

case0044	0.1	1.25	60	0.01	5	60	2.6	60	0.011988
case0045	0.1	1.75	60	0.01	5	60	2.6	60	0.001901
case0046	0.1	2.25	60	0.01	5	60	2.6	60	0.000215
case0047	0.2	1.25	60	0.01	5	60	3.5	60	0.007525
case0048	0.2	1.75	60	0.01	5	60	3.5	60	0.00634
case0049	0.2	2.25	60	0.01	5	60	3.5	60	0.002862
case0050	0.2	2.75	60	0.01	5	60	3.5	60	0.0002
case0051	0.3	1.75	60	0.01	5	60	5.1	60	0.000692
case0052	0.3	2.25	60	0.01	5	60	5.1	60	0.002809
case0053	0.3	2.75	60	0.01	5	60	5.1	60	0.000677
case0054	0.3	3.25	60	0.01	5	60	5.1	60	3.08E-05
case0055	0.4	2.25	60	0.01	5	60	6.5	60	0.000608
case0056	0.4	2.75	60	0.01	5	60	6.5	60	0.000808
case0057	0.4	3.25	60	0.01	5	60	6.5	60	0.000131
case0058	0.5	2.75	60	0.01	5	60	7.7	60	0.000292
case0059	0.5	3.25	60	0.01	5	60	7.7	60	9.24E-05
case0060	0.6	2.75	60	0.01	5	60	8.8	60	5.38E-05
case0061	0.6	3.25	60	0.01	5	60	8.8	60	0.000162
case0062	0.7	3.25	60	0.01	5	60	10.4	60	1.54E-05
case0063	0.7	3.75	60	0.01	5	60	10.4	60	1.54E-05
case0064	0.1	1.25	90	0.01	5	90	2.8	90	0.010927
case0065	0.1	1.75	90	0.01	5	90	2.8	90	0.00384
case0066	0.1	2.25	90	0.01	5	90	2.8	90	0.000277
case0067	0.2	1.25	90	0.01	5	90	4.1	90	0.012055
case0068	0.2	1.75	90	0.01	5	90	4.1	90	0.029802
case0069	0.2	2.25	90	0.01	5	90	4.1	90	0.009988
case0070	0.2	2.75	90	0.01	5	90	4.1	90	0.000585
case0071	0.3	1.75	90	0.01	5	90	5.8	90	0.006202
case0072	0.3	2.25	90	0.01	5	90	5.8	90	0.025608
case0073	0.3	2.75	90	0.01	5	90	5.8	90	0.003455
case0074	0.3	3.25	90	0.01	5	90	5.8	90	0.000154
case0075	0.4	2.25	90	0.01	5	90	7.1	90	0.008372
case0076	0.4	2.75	90	0.01	5	90	7.1	90	0.009935
case0077	0.4	3.25	90	0.01	5	90	7.1	90	0.00077
case0078	0.5	2.25	90	0.01	5	90	8.3	90	8.46E-05
case0079	0.5	2.75	90	0.01	5	90	8.3	90	0.007241
case0080	0.5	3.25	90	0.01	5	90	8.3	90	0.002178
case0081	0.5	3.75	90	0.01	5	90	8.3	90	5.38E-05
case0082	0.6	2.75	90	0.01	5	90	9.2	90	0.001362
case0083	0.6	3.25	90	0.01	5	90	9.2	90	0.003278
case0084	0.6	3.75	90	0.01	5	90	9.2	90	0.000223
case0085	0.7	2.75	90	0.01	5	90	10.1	90	6.15E-05
case0086	0.7	3.25	90	0.01	5	90	10.1	90	0.002008
case0087	0.7	3.75	90	0.01	5	90	10.1	90	0.000531
case0088	0.7	4.25	90	0.01	5	90	10.1	90	2.31E-05
case0089	0.8	3.25	90	0.01	5	90	11.2	90	0.000716

case0090	0.8	3.75	90	0.01	5	90	11.2	90	0.000677
case0091	0.8	4.25	90	0.01	5	90	11.2	90	6.15E-05
case0092	0.9	3.25	90	0.01	5	90	12.1	90	0.000131
case0093	0.9	3.75	90	0.01	5	90	12.1	90	0.000616
case0094	0.9	4.25	90	0.01	5	90	12.1	90	8.46E-05
case0095	1	3.25	90	0.01	5	90	13.1	90	1.54E-05
case0096	1	3.75	90	0.01	5	90	13.1	90	0.000323
case0097	1	4.25	90	0.01	5	90	13.1	90	0.000231
case0098	1.1	3.75	90	0.01	5	90	14.6	90	5.38E-05
case0099	1.1	4.25	90	0.01	5	90	14.6	90	0.000123
case0100	1.2	3.75	90	0.01	5	90	15	90	2.31E-05
case0101	1.2	4.25	90	0.01	5	90	15	90	0.000108
case0102	1.3	4.25	90	0.01	5	90	17.1	90	0.000192
case0103	1.3	4.75	90	0.01	5	90	17.1	90	7.7E-06
case0104	1.4	4.25	90	0.01	5	90	15.9	90	1.54E-05
case0105	1.4	4.75	90	0.01	5	90	15.9	90	3.08E-05
case0106	1.5	4.75	90	0.01	5	90	17.1	90	3.85E-05
case0107	1.6	4.75	90	0.01	5	90	19	90	5.38E-05
case0108	0.1	1.25	120	0.01	5	120	2.7	120	0.010988
case0109	0.1	1.75	120	0.01	5	120	2.7	120	0.00267
case0110	0.1	2.25	120	0.01	5	120	2.7	120	6.92E-05
case0111	0.2	1.25	120	0.01	5	120	4.2	120	0.010588
case0112	0.2	1.75	120	0.01	5	120	4.2	120	0.014366
case0113	0.2	2.25	120	0.01	5	120	4.2	120	0.004401
case0114	0.2	2.75	120	0.01	5	120	4.2	120	9.24E-05
case0115	0.3	1.75	120	0.01	5	120	6.1	120	0.004748
case0116	0.3	2.25	120	0.01	5	120	6.1	120	0.008672
case0117	0.3	2.75	120	0.01	5	120	6.1	120	0.001631
case0118	0.3	3.25	120	0.01	5	120	6.1	120	2.31E-05
case0119	0.3	3.75	120	0.01	5	120	6.1	120	7.7E-06
case0120	0.4	1.75	120	0.01	5	120	7.7	120	2.31E-05
case0121	0.4	2.25	120	0.01	5	120	7.7	120	0.004278
case0122	0.4	2.75	120	0.01	5	120	7.7	120	0.004171
case0123	0.4	3.25	120	0.01	5	120	7.7	120	2E-05
case0124	0.5	2.25	120	0.01	5	120	9.1	120	0.000462
case0125	0.5	2.75	120	0.01	5	120	9.1	120	0.002832
case0126	0.5	3.25	120	0.01	5	120	9.1	120	0.000708
case0127	0.5	3.75	120	0.01	5	120	9.1	120	7.7E-06
case0128	0.6	2.75	120	0.01	5	120	10.7	120	0.000977
case0129	0.6	3.25	120	0.01	5	120	10.7	120	0.000931
case0130	0.6	3.75	120	0.01	5	120	10.7	120	7.69E-05
case0131	0.7	2.75	120	0.01	5	120	11.7	120	0.000123
case0132	0.7	3.25	120	0.01	5	120	11.7	120	0.000623
case0133	0.7	3.75	120	0.01	5	120	11.7	120	3.08E-05
case0134	0.7	4.25	120	0.01	5	120	11.7	120	1.54E-05
case0135	0.8	3.25	120	0.01	5	120	12.9	120	0.000431

case0136	0.8	3.75	120	0.01	5	120	12.9	120	0.000177
case0137	0.8	4.25	120	0.01	5	120	12.9	120	1.54E-05
case0138	0.9	3.25	120	0.01	5	120	13.6	120	0.000123
case0139	0.9	3.75	120	0.01	5	120	13.6	120	0.0002
case0140	0.9	4.25	120	0.01	5	120	13.6	120	3.85E-05
case0141	1	3.25	120	0.01	5	120	15	120	2.31E-05
case0142	1	3.75	120	0.01	5	120	15	120	0.0001
case0143	1	4.25	120	0.01	5	120	15	120	1.54E-05
case0144	1.1	3.75	120	0.01	5	120	15.3	120	1.54E-05
case0145	1.1	4.25	120	0.01	5	120	15.3	120	6.92E-05
case0146	1.2	4.25	120	0.01	5	120	17.9	120	7.7E-06
case0147	0.1	1.25	150	0.01	5	150	2.5	150	0.018252
case0148	0.1	1.75	150	0.01	5	150	2.5	150	0.001531
case0149	0.1	2.25	150	0.01	5	150	2.5	150	2.31E-05
case0150	0.2	1.25	150	0.01	5	150	4.3	150	0.011173
case0151	0.2	1.75	150	0.01	5	150	4.3	150	0.01422
case0152	0.2	2.25	150	0.01	5	150	4.3	150	0.002039
case0153	0.2	2.75	150	0.01	5	150	4.3	150	0.000223
case0154	0.3	1.75	150	0.01	5	150	6.5	150	0.012835
case0155	0.3	2.25	150	0.01	5	150	6.5	150	0.00681
case0156	0.3	2.75	150	0.01	5	150	6.5	150	0.001039
case0157	0.3	3.25	150	0.01	5	150	6.5	150	7.69E-05
case0158	0.4	1.75	150	0.01	5	150	8	150	0.000839
case0159	0.4	2.25	150	0.01	5	150	8	150	0.014305
case0160	0.4	2.75	150	0.01	5	150	8	150	0.001562
case0161	0.4	3.25	150	0.01	5	150	8	150	0.000246
case0162	0.4	3.75	150	0.01	5	150	8	150	7.7E-06
case0163	0.4	4.25	150	0.01	5	150	8	150	7.7E-06
case0164	0.5	2.25	150	0.01	5	150	9.6	150	0.006233
case0165	0.5	2.75	150	0.01	5	150	9.6	150	0.004425
case0166	0.5	3.25	150	0.01	5	150	9.6	150	0.000208
case0167	0.6	2.25	150	0.01	5	150	11.2	150	0.000477
case0168	0.6	2.75	150	0.01	5	150	11.2	150	0.005386
case0169	0.6	3.25	150	0.01	5	150	11.2	150	0.000408
case0170	0.6	3.75	150	0.01	5	150	11.2	150	1.54E-05
case0171	0.6	4.25	150	0.01	5	150	11.2	150	7.7E-06
case0172	0.7	2.75	150	0.01	5	150	12.6	150	0.002024
case0173	0.7	3.25	150	0.01	5	150	12.6	150	0.000562
case0174	0.7	3.75	150	0.01	5	150	12.6	150	4.61E-05
case0175	0.7	4.25	150	0.01	5	150	12.6	150	7.7E-06
case0176	0.8	2.75	150	0.01	5	150	14.3	150	0.000308
case0177	0.8	3.25	150	0.01	5	150	14.3	150	0.0009
case0178	0.8	3.75	150	0.01	5	150	14.3	150	2.31E-05
case0179	0.9	2.75	150	0.01	5	150	15.2	150	1.54E-05
case0180	0.9	3.25	150	0.01	5	150	15.2	150	0.0007
case0181	0.9	3.75	150	0.01	5	150	15.2	150	3.08E-05

case0182	1	3.25	150	0.01	5	150	15.7	150	7.69E-05
case0183	1	3.75	150	0.01	5	150	15.7	150	0.0001
case0184	1.1	3.75	150	0.01	5	150	17.6	150	2.31E-05
case0185	1.2	3.75	150	0.01	5	150	18	150	7.7E-06
case0186	0.1	1.25	180	0.01	5	180	2.3	180	0.030848
case0187	0.1	1.75	180	0.01	5	180	2.3	180	0.001962
case0188	0.1	2.25	180	0.01	5	180	2.3	180	3.08E-05
case0189	0.1	2.75	180	0.01	5	180	2.3	180	7.7E-06
case0190	0.2	1.25	180	0.01	5	180	3.9	180	0.011157
case0191	0.2	1.75	180	0.01	5	180	3.9	180	0.008618
case0192	0.2	2.25	180	0.01	5	180	3.9	180	0.003886
case0193	0.2	2.75	180	0.01	5	180	3.9	180	0.000631
case0194	0.3	1.75	180	0.01	5	180	6	180	0.004332
case0195	0.3	2.25	180	0.01	5	180	6	180	0.004509
case0196	0.3	2.75	180	0.01	5	180	6	180	0.002401
case0197	0.3	3.25	180	0.01	5	180	6	180	0.000131
case0198	0.3	3.75	180	0.01	5	180	6	180	1.54E-05
case0199	0.3	4.25	180	0.01	5	180	6	180	7.7E-06
case0200	0.4	1.75	180	0.01	5	180	7.4	180	0.000339
case0201	0.4	2.25	180	0.01	5	180	7.4	180	0.004401
case0202	0.4	2.75	180	0.01	5	180	7.4	180	0.002832
case0203	0.4	3.25	180	0.01	5	180	7.4	180	0.0006
case0204	0.4	3.75	180	0.01	5	180	7.4	180	3.08E-05
case0205	0.5	2.25	180	0.01	5	180	8.9	180	0.00207
case0206	0.5	2.75	180	0.01	5	180	8.9	180	0.002439
case0207	0.5	3.25	180	0.01	5	180	8.9	180	0.001131
case0208	0.5	3.75	180	0.01	5	180	8.9	180	2.31E-05
case0209	0.6	2.25	180	0.01	5	180	10.5	180	0.000292
case0210	0.6	2.75	180	0.01	5	180	10.5	180	0.001724
case0211	0.6	3.25	180	0.01	5	180	10.5	180	0.001085
case0212	0.6	3.75	180	0.01	5	180	10.5	180	8.46E-05
case0213	0.7	2.75	180	0.01	5	180	11.8	180	0.001123
case0214	0.7	3.25	180	0.01	5	180	11.8	180	0.000585
case0215	0.7	3.75	180	0.01	5	180	11.8	180	0.000308
case0216	0.8	2.75	180	0.01	5	180	13.5	180	0.000346
case0217	0.8	3.25	180	0.01	5	180	13.5	180	0.000277
case0218	0.8	3.75	180	0.01	5	180	13.5	180	0.000169
case0219	0.9	2.75	180	0.01	5	180	14.8	180	6.92E-05
case0220	0.9	3.25	180	0.01	5	180	14.8	180	0.000223
case0221	0.9	3.75	180	0.01	5	180	14.8	180	0.000146
case0222	0.9	4.25	180	0.01	5	180	14.8	180	7.7E-06
case0223	1	3.25	180	0.01	5	180	15.4	180	3.08E-05
case0224	1	3.75	180	0.01	5	180	15.4	180	6.92E-05
case0225	1	4.25	180	0.01	5	180	15.4	180	7.7E-06
case0226	1.1	3.75	180	0.01	5	180	15.8	180	7.7E-06
case0227	0.2	1.75	210	0.05	8.5	210	4.1	210	0.008839

case0228	0.1	1.25	210	0.03	7.5	210	2.3	210	0.007857
case0229	0.3	2.25	300	0.07	9.5	300	5.3	300	0.007265
case0230	0.3	2.25	210	0.04	7.5	210	6	210	0.007237
case0231	0.2	1.75	300	0.06	8.5	300	3.9	300	0.007173
case0232	0.4	2.75	300	0.03	10.5	300	6.7	300	0.006997
case0233	0.1	1.25	330	0.03	12.5	330	2.4	330	0.00659
case0234	0.4	2.25	210	0.03	9.5	210	7.5	210	0.006302
case0235	0.2	1.25	210	0.06	9.5	210	4.1	210	0.006228
case0236	0.1	1.25	240	0.03	11.5	240	2.4	240	0.006154
case0237	0.2	1.75	270	0.04	8.5	270	4.2	270	0.005275
case0238	0.5	2.75	210	0.03	13.5	210	9.1	210	0.004544
case0239	0.1	1.25	270	0.05	7.5	270	2.3	270	0.004488
case0240	0.5	2.75	300	0.03	8.5	300	8	300	0.004359
case0241	0.2	2.25	300	0.07	8.5	300	3.9	300	0.004201
case0242	0.1	1.25	300	0.08	9.5	300	2.4	300	0.004118
case0243	0.6	3.25	300	0.09	10.5	300	9.2	300	0.003961
case0244	0.3	1.75	210	0.04	11.5	210	6	210	0.003952
case0245	0.2	2.25	330	0.03	6.5	330	3.3	330	0.003896
case0246	0.4	2.75	210	0.05	9.5	210	7.5	210	0.003859
case0247	0.2	1.75	240	0.04	10.5	240	4.2	240	0.003665
case0248	0.4	2.25	300	0.08	10.5	300	6.7	300	0.003332
case0249	0.3	2.75	300	0.04	12.5	300	5.3	300	0.003202
case0250	0.2	1.75	330	0.03	14.5	330	3.3	330	0.002971
case0251	0.2	1.25	240	0.07	10.5	240	4.2	240	0.002953
case0252	0.2	1.25	270	0.1	10.5	270	4.2	270	0.002832
case0253	0.2	2.25	210	0.04	13.5	210	4.1	210	0.002758
case0254	0.4	2.25	240	0.09	9.5	240	8.2	240	0.002406
case0255	0.2	1.25	300	0.05	12.5	300	3.9	300	0.00223
case0256	0.5	3.25	300	0.04	14.5	300	8	300	0.002184
case0257	0.7	3.25	300	0.04	9.5	300	10.5	300	0.002119
case0258	0.2	1.25	330	0.1	11.5	330	3.3	330	0.001934
case0259	0.3	1.75	240	0.03	15.5	240	6.5	240	0.001925
case0260	0.3	1.75	300	0.05	11.5	300	5.3	300	0.001842
case0261	0.7	3.25	210	0.11	10.5	210	12.3	210	0.001795
case0262	0.4	2.25	270	0.06	7.5	270	7.6	270	0.001721
case0263	0.3	2.25	270	0.05	14.5	270	6	270	0.001573
case0264	0.6	3.25	210	0.05	13.5	210	10.5	210	0.001555
case0265	0.6	2.75	210	0.11	11.5	210	10.5	210	0.001546
case0266	0.3	2.75	330	0.12	11.5	330	5.3	330	0.001527
case0267	0.3	2.25	330	0.06	10.5	330	5.3	330	0.001351
case0268	0.3	2.25	240	0.08	8.5	240	6.5	240	0.001324
case0269	0.3	1.75	270	0.04	15.5	270	6	270	0.001305
case0270	0.4	2.75	330	0.09	11.5	330	6.6	330	0.001268
case0271	0.3	2.75	210	0.05	15.5	210	6	210	0.001259
case0272	0.8	3.75	300	0.06	12.5	300	11.4	300	0.001166
case0273	0.5	2.75	270	0.1	9.5	270	8.8	270	0.00112

case0274	0.1	1.75	300	0.13	11.5	300	2.4	300	0.001074
case0275	0.1	1.75	330	0.05	10.5	330	2.4	330	0.001046
case0276	0.5	2.75	240	0.12	10.5	240	9.6	240	0.001009
case0277	0.9	3.75	300	0.03	5.5	300	12.6	300	0.000991
case0278	0.8	3.25	300	0.16	12.5	300	11.4	300	0.000731
case0279	0.6	2.75	240	0.06	11.5	240	11.2	240	0.000684
case0280	0.6	2.75	270	0.06	14.5	270	10.3	270	0.000684
case0281	0.2	2.75	330	0.08	11.5	330	3.3	330	0.000675
case0282	0.6	2.75	300	0.15	12.5	300	9.2	300	0.000657
case0283	0.4	3.25	300	0.05	16.5	300	6.7	300	0.00062
case0284	0.5	3.25	330	0.07	11.5	330	7.8	330	0.00061
case0285	0.1	1.75	210	0.06	13.5	210	2.3	210	0.000601
case0286	0.5	2.25	240	0.06	15.5	240	9.6	240	0.000601
case0287	0.2	2.75	300	0.14	12.5	300	3.9	300	0.000601
case0288	0.8	3.25	210	0.04	6.5	210	13.5	210	0.000583
case0289	0.7	3.75	300	0.06	16.5	300	10.5	300	0.000573
case0290	0.5	3.25	210	0.07	7.5	210	9.1	210	0.000564
case0291	0.4	3.25	330	0.04	16.5	330	6.6	330	0.000555
case0292	0.1	1.75	270	0.13	12.5	270	2.3	270	0.000518
case0293	1	3.75	300	0.03	16.5	300	13.7	300	0.000509
case0294	0.3	1.75	330	0.13	10.5	330	5.3	330	0.000472
case0295	0.9	3.75	210	0.07	12.5	210	15	210	0.000462
case0296	0.5	2.25	270	0.07	16.5	270	8.8	270	0.000462
case0297	0.1	1.75	240	0.14	11.5	240	2.4	240	0.000444
case0298	0.6	3.25	330	0.17	12.5	330	8.9	330	0.00037
case0299	0.8	3.75	210	0.11	9.5	210	13.5	210	0.000361
case0300	0.7	2.75	240	0.07	13.5	240	12.7	240	0.000314
case0301	0.2	2.25	270	0.12	12.5	270	4.2	270	0.000305
case0302	0.1	2.25	330	0.07	15.5	330	2.4	330	0.000296
case0303	0.4	2.25	330	0.07	14.5	330	6.6	330	0.000287
case0304	0.4	2.75	270	0.09	8.5	270	7.6	270	0.000268
case0305	0.7	2.75	270	0.05	17.5	270	11.6	270	0.00025
case0306	0.1	2.25	300	0.16	11.5	300	2.4	300	0.00025
case0307	0.8	3.25	270	0.03	17.5	270	13	270	0.000231
case0308	0.5	2.75	330	0.18	12.5	330	7.8	330	0.000231
case0309	0.2	2.75	210	0.07	17.5	210	4.1	210	0.000222
case0310	0.8	3.25	240	0.15	11.5	240	14.4	240	0.000213
case0311	0.6	3.75	300	0.04	17.5	300	9.2	300	0.000203
case0312	0.7	3.25	270	0.06	17.5	270	11.6	270	0.000176
case0313	1.1	4.25	300	0.08	13.5	300	14.9	300	0.000176
case0314	0.9	3.25	270	0.16	13.5	270	14.5	270	0.000176
case0315	0.3	3.25	330	0.08	7.5	330	5.3	330	0.000166
case0316	0.5	2.25	210	0.08	12.5	210	9.1	210	0.000166
case0317	0.7	3.75	330	0.08	15.5	330	10.2	330	0.000166
case0318	0.4	3.25	210	0.1	12.5	210	7.5	210	0.000166
case0319	1	4.25	300	0.11	12.5	300	13.7	300	0.000166

case0320	0.3	3.25	300	0.15	13.5	300	5.3	300	0.000166
case0321	1	3.75	210	0.06	18.5	210	16	210	0.000157
case0322	0.9	3.25	300	0.08	14.5	300	12.6	300	0.000157
case0323	0.9	4.25	300	0.08	16.5	300	12.6	300	0.000157
case0324	0.9	3.25	240	0.09	12.5	240	15.4	240	0.000157
case0325	1.2	4.25	300	0.14	10.5	300	15.7	300	0.000157
case0326	1.1	3.75	300	0.03	18.5	300	14.9	300	0.000148
case0327	0.7	3.75	210	0.05	18.5	210	12.3	210	0.000139
case0328	1	3.25	270	0.07	18.5	270	15.7	270	0.000139
case0329	0.7	2.75	210	0.19	12.5	210	12.3	210	0.000129
case0330	0.6	3.75	330	0.08	18.5	330	8.9	330	0.00012
case0331	0.7	3.25	240	0.09	18.5	240	12.7	240	0.00012
case0332	0.7	3.25	330	0.17	11.5	330	10.2	330	0.00012
case0333	0.5	3.75	300	0.08	17.5	300	8	300	0.000111
case0334	0.9	3.25	210	0.14	13.5	210	15	210	0.000111
case0335	0.2	2.25	240	0.17	13.5	240	4.2	240	0.000111
case0336	0.5	2.25	300	0.04	18.5	300	8	300	0.000102
case0337	0.8	3.75	330	0.12	9.5	330	10.6	330	0.000102
case0338	0.4	2.75	240	0.18	13.5	240	8.2	240	0.000102
case0339	1	3.75	270	0.13	13.5	270	15.7	270	9.2E-05
case0340	1	3.25	240	0.09	13.5	240	16.3	240	7.4E-05
case0341	0.6	3.25	270	0.13	9.5	270	10.3	270	7.4E-05
case0342	1.3	4.25	300	0.17	14.5	300	16.6	300	5.5E-05
case0343	0.7	2.75	300	0.18	11.5	300	10.5	300	5.5E-05
case0344	1.4	4.25	300	0.09	14.5	300	18.5	300	4.6E-05
case0345	0.5	3.75	330	0.09	15.5	330	7.8	330	4.6E-05
case0346	1.1	3.75	270	0.09	16.5	270	17.5	270	4.6E-05
case0347	0.8	2.75	240	0.1	8.5	240	14.4	240	4.6E-05
case0348	0.3	2.75	270	0.1	17.5	270	6	270	4.6E-05
case0349	1.1	3.25	270	0.19	13.5	270	17.5	270	4.6E-05
case0350	1.2	3.75	270	0.2	14.5	270	18	270	4.6E-05
case0351	1.1	4.25	210	0.21	14.5	210	17.2	210	4.6E-05
case0352	0.1	2.25	270	0.03	19.5	270	2.3	270	3.7E-05
case0353	0.5	2.25	330	0.1	18.5	330	7.8	330	3.7E-05
case0354	0.1	2.25	210	0.11	13.5	210	2.3	210	3.7E-05
case0355	0.3	3.25	210	0.11	17.5	210	6	210	3.7E-05
case0356	0.6	2.75	330	0.16	14.5	330	8.9	330	3.7E-05
case0357	0.7	4.25	300	0.04	5.5	300	10.5	300	2.8E-05
case0358	0.8	4.25	300	0.09	17.5	300	11.4	300	2.8E-05
case0359	0.2	2.75	270	0.1	14.5	270	4.2	270	2.8E-05
case0360	0.8	2.75	270	0.1	15.5	270	13	270	2.8E-05
case0361	1.2	3.75	300	0.1	16.5	300	15.7	300	2.8E-05
case0362	0.6	3.75	210	0.12	18.5	210	10.5	210	2.8E-05
case0363	1.1	3.75	210	0.15	10.5	210	17.2	210	2.8E-05
case0364	0.2	3.25	330	0.15	14.5	330	3.3	330	2.8E-05
case0365	0.9	3.75	330	0.18	15.5	330	11.4	330	2.8E-05

case0366	1	4.25	210	0.19	14.5	210	16	210	2.8E-05
case0367	0.4	1.75	240	0.2	13.5	240	8.2	240	2.8E-05
case0368	1.1	3.25	240	0.03	20.5	240	18.4	240	1.8E-05
case0369	0.2	3.25	300	0.05	6.5	300	3.9	300	1.8E-05
case0370	0.4	3.75	300	0.08	19.5	300	6.7	300	1.8E-05
case0371	0.4	1.75	330	0.09	7.5	330	6.6	330	1.8E-05
case0372	1.4	4.75	300	0.11	18.5	300	18.5	300	1.8E-05
case0373	1.7	4.75	300	0.12	13.5	300	21.3	300	1.8E-05
case0374	0.8	4.25	330	0.12	14.5	330	10.6	330	1.8E-05
case0375	0.9	4.25	330	0.13	17.5	330	11.4	330	1.8E-05
case0376	0.5	3.25	270	0.14	17.5	270	8.8	270	1.8E-05
case0377	0.9	3.75	270	0.14	18.5	270	14.5	270	1.8E-05
case0378	1.3	3.75	270	0.15	17.5	270	21.6	270	1.8E-05
case0379	0.6	4.25	300	0.16	10.5	300	9.2	300	1.8E-05
case0380	0.2	3.25	210	0.18	14.5	210	4.1	210	1.54E-05
case0381	0.5	3.75	210	0.19	15.5	210	9.1	210	1.54E-05
case0382	0.9	4.25	210	0.19	18.5	210	15	210	1.54E-05
case0383	1.2	4.25	210	0.21	12.5	210	20.9	210	1.54E-05
case0384	0.6	3.25	240	0.04	19.5	240	11.2	240	9E-06
case0385	0.4	1.75	270	0.06	19.5	270	7.6	270	9E-06
case0386	1.4	3.75	270	0.1	13.5	270	22.5	270	9E-06
case0387	1.3	3.75	300	0.11	14.5	300	16.6	300	9E-06
case0388	1.3	4.75	300	0.11	16.5	300	16.6	300	9E-06
case0389	1.5	4.25	300	0.12	8.5	300	19.9	300	9E-06
case0390	1.5	4.75	300	0.12	15.5	300	19.9	300	9E-06
case0391	1.6	4.75	300	0.12	17.5	300	18.2	300	9E-06
case0392	0.4	3.75	330	0.13	14.5	330	6.6	330	9E-06
case0393	0.8	3.25	330	0.13	18.5	330	10.6	330	9E-06
case0394	0.4	1.75	210	0.14	14.5	210	7.5	210	7.7E-06
case0395	0.4	3.75	210	0.14	15.5	210	7.5	210	7.7E-06
case0396	1	3.25	210	0.15	15.5	210	16	210	7.7E-06
case0397	1.2	3.75	210	0.15	18.5	210	20.9	210	7.7E-06
case0398	1.3	4.25	210	0.16	15.5	210	21.5	210	7.7E-06
case0399	1.4	4.25	210	0.16	17.5	210	16.8	210	7.7E-06
case0400	0.1	2.25	240	0.16	18.5	240	2.4	240	7.7E-06
case0401	0.3	3.25	240	0.17	15.5	240	6.5	240	7.7E-06
case0402	1	3.75	240	0.18	18.5	240	16.3	240	7.7E-06
case0403	1.2	3.25	240	0.19	17.5	240	17.2	240	7.7E-06
case0404	1.2	3.75	240	0.2	11.5	240	17.2	240	7.7E-06
case0405	0.8	3.75	270	0.2	12.5	270	13	270	7.7E-06
case0406	0.9	2.75	270	0.21	11.5	270	14.5	270	7.7E-06
case0407	1.3	4.25	270	0.21	13.5	270	21.6	270	7.7E-06
case0408	1.4	4.25	270	0.21	15.5	270	22.5	270	7.7E-06
case0409	1.5	3.75	270	0.21	16.5	270	18.7	270	7.7E-06
case0410	1.5	4.25	270	0.22	14.5	270	18.7	270	7.7E-06
case0411	1	3.25	300	0.23	12.5	300	13.7	300	7.7E-06

case0412	1.2	4.75	300	0.01	5	300	15.7	300	7.7E-06
case0413	1.8	4.75	300	0.01	5	300	21.2	300	7.7E-06
case0414	1.9	4.75	300	0.01	5	300	24.9	300	7.7E-06
case0415	1.9	5.25	300	0.01	5	300	24.9	300	7.7E-06
case0416	0.3	3.75	330	0.01	5	330	5.3	330	7.7E-06
case0417	0.6	4.25	330	0.01	5	330	8.9	330	7.7E-06
case0418	0.2	1.75	210	0.01	5	210	4.1	210	0.016523
case0419	0.1	1.25	210	0.01	5	210	2.3	210	0.015919
case0420	0.3	2.25	300	0.01	5	300	5.3	300	0.015057
case0421	0.3	2.25	210	0.01	5	210	6	210	0.014585
case0422	0.2	1.75	300	0.01	5	300	3.9	300	0.013611
case0423	0.4	2.75	300	0.01	5	300	6.7	300	0.0087
case0424	0.1	1.25	330	0.01	5	330	2.4	330	0.007099
case0425	0.4	2.25	210	0.01	5	210	7.5	210	0.00724
case0426	0.2	1.25	210	0.01	5	210	4.1	210	0.006352
case0427	0.1	1.25	240	0.01	5	240	2.4	240	0.00628
case0428	0.2	1.75	270	0.01	5	270	4.2	270	0.007075
case0429	0.5	2.75	210	0.01	5	210	9.1	210	0.007282
case0430	0.1	1.25	270	0.01	5	270	2.3	270	0.007215
case0431	0.5	2.75	300	0.01	5	300	8	300	0.00726
case0432	0.2	2.25	300	0.01	5	300	3.9	300	0.007125
case0433	0.1	1.25	300	0.01	5	300	2.4	300	0.005446
case0434	0.6	3.25	300	0.01	5	300	9.2	300	0.005134
case0435	0.3	1.75	210	0.01	5	210	6	210	0.005097
case0436	0.2	2.25	330	0.01	5	330	3.3	330	0.004983
case0437	0.4	2.75	210	0.01	5	210	7.5	210	0.004728
case0438	0.2	1.75	240	0.01	5	240	4.2	240	0.004476
case0439	0.4	2.25	300	0.01	5	300	6.7	300	0.003886
case0440	0.3	2.75	300	0.01	5	300	5.3	300	0.004008
case0441	0.2	1.75	330	0.01	5	330	3.3	330	0.003616
case0442	0.2	1.25	240	0.01	5	240	4.2	240	0.003534
case0443	0.2	1.25	270	0.01	5	270	4.2	270	0.003032
case0444	0.2	2.25	210	0.01	5	210	4.1	210	0.003006
case0445	0.4	2.25	240	0.01	5	240	8.2	240	0.00318
case0446	0.2	1.25	300	0.01	5	300	3.9	300	0.003264
case0447	0.5	3.25	300	0.01	5	300	8	300	0.003294
case0448	0.7	3.25	300	0.01	5	300	10.5	300	0.003298
case0449	0.2	1.25	330	0.01	5	330	3.3	330	0.003414
case0450	0.3	1.75	240	0.01	5	240	6.5	240	0.003015
case0451	0.3	1.75	300	0.01	5	300	5.3	300	0.002798
case0452	0.7	3.25	210	0.01	5	210	12.3	210	0.002453
case0453	0.4	2.25	270	0.01	5	270	7.6	270	0.002396
case0454	0.3	2.25	270	0.01	5	270	6	270	0.002444
case0455	0.6	3.25	210	0.01	5	210	10.5	210	0.002246
case0456	0.6	2.75	210	0.01	5	210	10.5	210	0.002194
case0457	0.3	2.75	330	0.01	5	330	5.3	330	0.002205

case0458	0.3	2.25	330	0.01	5	330	5.3	330	0.00205
case0459	0.3	2.25	240	0.01	5	240	6.5	240	0.00207
case0460	0.3	1.75	270	0.01	5	270	6	270	0.001981
case0461	0.4	2.75	330	0.01	5	330	6.6	330	0.001879
case0462	0.3	2.75	210	0.01	5	210	6	210	0.001881
case0463	0.8	3.75	300	0.01	5	300	11.4	300	0.001666
case0464	0.5	2.75	270	0.01	5	270	8.8	270	0.001527
case0465	0.1	1.75	300	0.01	5	300	2.4	300	0.001496
case0466	0.1	1.75	330	0.01	5	330	2.4	330	0.001386
case0467	0.5	2.75	240	0.01	5	240	9.6	240	0.001292
case0468	0.9	3.75	300	0.01	5	300	12.6	300	0.00121
case0469	0.8	3.25	300	0.01	5	300	11.4	300	0.001285
case0470	0.6	2.75	240	0.01	5	240	11.2	240	0.001324
case0471	0.6	2.75	270	0.01	5	270	10.3	270	0.001309
case0472	0.2	2.75	330	0.01	5	330	3.3	330	0.00121
case0473	0.6	2.75	300	0.01	5	300	9.2	300	0.001205
case0474	0.4	3.25	300	0.01	5	300	6.7	300	0.001219
case0475	0.5	3.25	330	0.01	5	330	7.8	330	0.001221
case0476	0.1	1.75	210	0.01	5	210	2.3	210	0.001107
case0477	0.5	2.25	240	0.01	5	240	9.6	240	0.001107
case0478	0.2	2.75	300	0.01	5	300	3.9	300	0.00103
case0479	0.8	3.25	210	0.01	5	210	13.5	210	0.000948
case0480	0.7	3.75	300	0.01	5	300	10.5	300	0.00095
case0481	0.5	3.25	210	0.01	5	210	9.1	210	0.000852
case0482	0.4	3.25	330	0.01	5	330	6.6	330	0.000853
case0483	0.1	1.75	270	0.01	5	270	2.3	270	0.000851
case0484	1	3.75	300	0.01	5	300	13.7	300	0.000845
case0485	0.3	1.75	330	0.01	5	330	5.3	330	0.000713
case0486	0.9	3.75	210	0.01	5	210	15	210	0.000715
case0487	0.5	2.25	270	0.01	5	270	8.8	270	0.0006
case0488	0.1	1.75	240	0.01	5	240	2.4	240	0.000525
case0489	0.6	3.25	330	0.01	5	330	8.9	330	0.000561
case0490	0.8	3.75	210	0.01	5	210	13.5	210	0.000562
case0491	0.7	2.75	240	0.01	5	240	12.7	240	0.000602
case0492	0.2	2.25	270	0.01	5	270	4.2	270	0.000603
case0493	0.1	2.25	330	0.01	5	330	2.4	330	0.000558
case0494	0.4	2.25	330	0.01	5	330	6.6	330	0.000552
case0495	0.4	2.75	270	0.01	5	270	7.6	270	0.000547
case0496	0.7	2.75	270	0.01	5	270	11.6	270	0.000535
case0497	0.1	2.25	300	0.01	5	300	2.4	300	0.000519
case0498	0.8	3.25	270	0.01	5	270	13	270	0.0005
case0499	0.5	2.75	330	0.01	5	330	7.8	330	0.000438
case0500	0.2	2.75	210	0.01	5	210	4.1	210	0.00044
case0501	0.8	3.25	240	0.01	5	240	14.4	240	0.000379
case0502	0.6	3.75	300	0.01	5	300	9.2	300	0.000382
case0503	0.7	3.25	270	0.01	5	270	11.6	270	0.000378

case0504	1.1	4.25	300	0.01	5	300	14.9	300	0.000339
case0505	0.9	3.25	270	0.01	5	270	14.5	270	0.000324
case0506	0.3	3.25	330	0.01	5	330	5.3	330	0.000311
case0507	0.5	2.25	210	0.01	5	210	9.1	210	0.000296
case0508	0.7	3.75	330	0.01	5	330	10.2	330	0.000296
case0509	0.4	3.25	210	0.01	5	210	7.5	210	0.000219
case0510	1	4.25	300	0.01	5	300	13.7	300	0.000219
case0511	0.3	3.25	300	0.01	5	300	5.3	300	0.000211
case0512	1	3.75	210	0.01	5	210	16	210	0.000197
case0513	0.9	3.25	300	0.01	5	300	12.6	300	0.000174
case0514	0.9	4.25	300	0.01	5	300	12.6	300	0.000174
case0515	0.9	3.25	240	0.01	5	240	15.4	240	0.000166
case0516	1.2	4.25	300	0.01	5	300	15.7	300	0.000166
case0517	1.1	3.75	300	0.01	5	300	14.9	300	0.00016
case0518	0.7	3.75	210	0.01	5	210	12.3	210	0.000161
case0519	1	3.25	270	0.01	5	270	15.7	270	0.00013
case0520	0.7	2.75	210	0.01	5	210	12.3	210	0.000109
case0521	0.6	3.75	330	0.01	5	330	8.9	330	0.000118
case0522	0.7	3.25	240	0.01	5	240	12.7	240	0.000103
case0523	0.7	3.25	330	0.01	5	330	10.2	330	9.54E-05
case0524	0.5	3.75	300	0.01	5	300	8	300	7.36E-05
case0525	0.9	3.25	210	0.01	5	210	15	210	6.59E-05
case0526	0.2	2.25	240	0.01	5	240	4.2	240	5.82E-05
case0527	0.5	2.25	300	0.01	5	300	8	300	5.95E-05
case0528	0.8	3.75	330	0.01	5	330	10.6	330	5.95E-05
case0529	0.4	2.75	240	0.01	5	240	8.2	240	5.18E-05
case0530	1	3.75	270	0.01	5	270	15.7	270	6.18E-05
case0531	1	3.25	240	0.01	5	240	16.3	240	7.21E-05
case0532	0.6	3.25	270	0.01	5	270	10.3	270	6.44E-05
case0533	1.3	4.25	300	0.01	5	300	16.6	300	6.8E-05
case0534	0.7	2.75	300	0.01	5	300	10.5	300	4.5E-05
case0535	1.4	4.25	300	0.01	5	300	18.5	300	5.4E-05
case0536	0.5	3.75	330	0.01	5	330	7.8	330	5.4E-05
case0537	1.1	3.75	270	0.01	5	270	17.5	270	4.63E-05
case0538	0.8	2.75	240	0.01	5	240	14.4	240	3.86E-05
case0539	0.3	2.75	270	0.01	5	270	6	270	3.86E-05
case0540	1.1	3.25	270	0.01	5	270	17.5	270	3.86E-05
case0541	1.2	3.75	270	0.01	5	270	18	270	3.86E-05
case0542	1.1	4.25	210	0.01	5	210	17.2	210	3.09E-05
case0543	0.1	2.25	270	0.01	5	270	2.3	270	3.99E-05
case0544	0.5	2.25	330	0.01	5	330	7.8	330	3.99E-05
case0545	0.1	2.25	210	0.01	5	210	2.3	210	3.22E-05
case0546	0.3	3.25	210	0.01	5	210	6	210	3.22E-05
case0547	0.6	2.75	330	0.01	5	330	8.9	330	3.22E-05
case0548	0.7	4.25	300	0.01	5	300	10.5	300	3.35E-05
case0549	0.8	4.25	300	0.01	5	300	11.4	300	3.35E-05

case0550	0.2	2.75	270	0.01	5	270	4.2	270	2.58E-05
case0551	0.8	2.75	270	0.01	5	270	13	270	2.58E-05
case0552	1.2	3.75	300	0.01	5	300	15.7	300	2.58E-05
case0553	0.6	3.75	210	0.01	5	210	10.5	210	1.81E-05
case0554	1.1	3.75	210	0.01	5	210	17.2	210	1.81E-05
case0555	0.2	3.25	330	0.01	5	330	3.3	330	1.81E-05
case0556	0.9	3.75	330	0.01	5	330	11.4	330	1.81E-05
case0557	1	4.25	210	0.01	5	210	16	210	1.05E-05
case0558	0.4	1.75	240	0.01	5	240	8.2	240	1.05E-05
case0559	1.1	3.25	240	0.01	5	240	18.4	240	2.05E-05
case0560	0.2	3.25	300	0.01	5	300	3.9	300	2.05E-05
case0561	0.4	3.75	300	0.01	5	300	6.7	300	2.05E-05
case0562	0.4	1.75	330	0.01	5	330	6.6	330	2.05E-05
case0563	1.4	4.75	300	0.01	5	300	18.5	300	1.28E-05
case0564	1.7	4.75	300	0.01	5	300	21.3	300	1.28E-05
case0565	0.8	4.25	330	0.01	5	330	10.6	330	1.28E-05
case0566	0.9	4.25	330	0.01	5	330	11.4	330	1.28E-05
case0567	0.5	3.25	270	0.01	5	270	8.8	270	5.1E-06
case0568	0.9	3.75	270	0.01	5	270	14.5	270	5.1E-06
case0569	1.3	3.75	270	0.01	5	270	21.6	270	5.1E-06
case0570	0.6	4.25	300	0.01	5	300	9.2	300	5.1E-06
case0571	0.6	3.25	240	0.01	5	240	11.2	240	6.4E-06
case0572	0.4	1.75	270	0.01	5	270	7.6	270	6.4E-06
case0573	1.4	3.75	270	0.01	5	270	22.5	270	6.4E-06
case0574	1.3	3.75	300	0.01	5	300	16.6	300	6.4E-06
case0575	1.3	4.75	300	0.01	5	300	16.6	300	6.4E-06
case0576	1.5	4.25	300	0.01	5	300	19.9	300	6.4E-06
case0577	1.5	4.75	300	0.01	5	300	19.9	300	6.4E-06
case0578	1.6	4.75	300	0.01	5	300	18.2	300	6.4E-06
case0579	0.4	3.75	330	0.01	5	330	6.6	330	6.4E-06
case0580	0.8	3.25	330	0.01	5	330	10.6	330	6.4E-06

APPENDIX E
Stress factors

		C_xA [m^-2]	C_xMS [m^-3]	C_xMW [m^-3]	C_τz [m^-2]	C_τy [m^-2]	C_τMtor [m^-3]
Column AX 3-8	Point 0	0.518	-0.012	-0.398	0	1.606	0.331
	Point 1	0.518	0.11	-0.307	3.575	0	0.331
	Point 2	0.518	0.11	0.09	4.286	0	0.265
	Point 3	0.518	0.066	0.395	0	0.833	-0.241
	Point 4	0.518	0.003	0.395	0	1.188	-0.241
	Point 5	0.518	-0.061	0.395	0	0.833	-0.241
	Point 6	0.518	-0.105	0.09	4.286	0	-0.265
	Point 7	0.518	-0.105	-0.329	3.575	0	-0.331
Column AX 9-40	Point 0	0.558	-0.013	-0.425	0	1.627	0.433
	Point 1	0.558	0.123	-0.327	3.857	0	0.433
	Point 2	0.558	0.123	0.099	4.723	0	0.379
	Point 3	0.558	0.074	0.426	0	0.913	-0.265
	Point 4	0.558	0.003	0.426	0	1.324	-0.265
	Point 5	0.558	-0.068	0.426	0	0.913	-0.265
	Point 6	0.558	-0.117	0.099	4.723	0	-0.379
	Point 7	0.558	-0.117	-0.351	3.857	0	-0.433
Transition AX 3-8	Point 0	0.644	-0.016	-0.432	0	1.652	0.331
	Point 1	0.644	0.133	-0.324	8.428	0	0.379
	Point 2	0.644	0.133	0.147	9.943	0	0.379
	Point 3	0.644	0.08	0.509	0	1.12	-0.331
	Point 4	0.644	0.002	0.509	0	1.614	-0.331
	Point 5	0.644	-0.075	0.509	0	1.12	-0.331
	Point 6	0.644	-0.129	0.147	9.943	0	-0.379
	Point 7	0.644	-0.129	-0.35	8.428	0	-0.379
Transition AX 9-40	Point 0	0.644	-0.016	-0.432	0	1.652	0.331
	Point 1	0.644	0.133	-0.324	8.428	0	0.379
	Point 2	0.644	0.133	0.147	9.943	0	0.379
	Point 3	0.644	0.08	0.509	0	1.12	-0.331
	Point 4	0.644	0.002	0.509	0	1.614	-0.331
	Point 5	0.644	-0.075	0.509	0	1.12	-0.331
	Point 6	0.644	-0.129	0.147	9.943	0	-0.379
	Point 7	0.644	-0.129	-0.35	8.428	0	-0.379
Midspan AX 3-8	Point 0	0.713	-0.018	-0.448	0	1.648	0.331
	Point 1	0.713	0.147	-0.328	8.485	0	0.379
	Point 2	0.713	0.147	0.195	9.936	0	0.379
	Point 3	0.713	0.088	0.598	0	1.28	-0.379
	Point 4	0.713	0.002	0.598	0	1.84	-0.379
	Point 5	0.713	-0.084	0.598	0	1.28	-0.379
	Point 6	0.713	-0.143	0.195	9.936	0	-0.379
	Point 7	0.713	-0.143	-0.357	8.485	0	-0.379
Midspan AX 9-40	Point 0	0.747	-0.019	-0.456	0	1.686	0.331
	Point 1	0.747	0.155	-0.328	10.018	0	0.442
	Point 2	0.747	0.155	0.23	11.575	0	0.442
	Point 3	0.747	0.093	0.659	0	1.461	-0.442
	Point 4	0.747	0.002	0.659	0	2.11	-0.442
	Point 5	0.747	-0.088	0.659	0	1.461	-0.442
	Point 6	0.747	-0.151	0.23	11.575	0	-0.442
	Point 7	0.747	-0.151	-0.358	10.018	0	-0.442
H1	Point 0	0.764	-0.017	-0.564	0	1.624	0.388
	Point 1	0.764	0.157	-0.39	8.727	0	0.388
	Point 2	0.764	0.157	0.173	13.434	0	0.518
	Point 3	0.764	0.095	0.794	0	1.501	-0.518
	Point 4	0.764	0.004	0.794	0	2.114	-0.518
	Point 5	0.764	-0.086	0.794	0	1.501	-0.518
	Point 6	0.764	-0.148	0.173	13.434	0	-0.518
	Point 7	0.764	-0.148	-0.425	8.727	0	-0.388
H2	Point 0	0.606	-0.013	-0.468	0	1.31	0.31
	Point 1	0.606	0.125	-0.336	6.867	0	0.31
	Point 2	0.606	0.125	0.089	8.062	0	0.31
	Point 3	0.606	0.075	0.557	0	0.899	-0.31

	Point 4	0.606	0.003	0.557	0	1.28	-0.31
	Point 5	0.606	-0.068	0.557	0	0.899	-0.31
	Point 6	0.606	-0.118	0.089	8.062	0	-0.31
	Point 7	0.606	-0.118	-0.363	6.867	0	-0.31
D-D	Point 0	0.597	-0.011	-0.408	0	1.733	0.303
	Point 1	0.597	0.1	-0.324	2.132	0	0.303
	Point 2	0.597	0.1	0.327	2.405	0	0.212
	Point 3	0.597	0.059	0.327	0	0.917	-0.212
	Point 4	0.597	0.002	0.327	0	1.23	-0.212
	Point 5	0.597	-0.055	0.327	0	0.917	-0.212
	Point 6	0.597	-0.096	0.327	2.405	0	-0.212
	Point 7	0.597	-0.096	-0.347	2.132	0	-0.303
E-E	Point 0	0.353	-0.005	-0.32	1.736	0.817	0.265
	Point 1	0.353	0.053	-0.234	1.736	0.817	0.265
	Point 2	0.353	0.053	0.243	1.736	0.817	0.186
	Point 3	0.353	0.024	0.243	1.736	0.817	-0.186
	Point 4	0.353	0	0.243	1.736	0.817	-0.186
	Point 5	0.353	-0.023	0.243	1.736	0.817	-0.186
	Point 6	0.353	-0.053	0.243	1.736	0.817	-0.186
	Point 7	0.353	-0.053	-0.254	1.736	0.817	-0.265

APPENDIX F
Fatigue lives

Fatigue lives in years induced by normal stress and shear stress are given in the tables below. Noted that position in the table is the horizontal distance from abutment south.

Table 8-1   Fatigue lives along the bridge girder. Normal stress is applied.

Position	axis	Point0	Point1	Point2	Point3	Point4	Point5	Point6	Point7
400	A2	1817000	1136	1135	8352	2544000	11880	1379	1380
780	A3	510.1	1216	16340	482.5	502.3	481.7	16700	959.4
805		1409	2383	7937	609.7	655.6	609.1	7335	1948
821		3510	3178	5515	848.9	954.1	846.4	4950	2684
864		13770	6222	9670	4380	5916	4471	8639	5308
880		8210	8295	21440	6077	7738	6342	21040	6944
905	A4	1272	2370	15510	1304	1431	1299	15300	1922
930		3222	3290	7249	1448	1713	1459	6922	2692
946		6716	3392	4713	1622	2088	1663	4598	2798
989		10970	4598	6641	3138	4619	3472	6893	3884
1005		6857	5997	14260	4387	5997	4838	15990	5030
1030	A5	1247	2074	9759	1096	1272	1147	11740	1605
1054		2985	2359	4324	1109	1408	1178	4875	1976
1070		5934	2121	2729	1183	1628	1254	3034	1941
1114		11330	2619	3495	2868	4568	2966	3953	2656
1130		7567	3837	7108	4520	6649	4627	8736	3884
1155	A6	1494	1728	5026	1303	1591	1322	6609	1505
1179		3491	1601	2276	1243	1748	1309	2833	1444
1195		6740	1355	1511	1243	1980	1344	1871	1273
1239		11730	1998	2370	2690	5032	3058	2923	1968
1255		8087	3328	5306	4464	7317	4934	6927	3287
1279	A7	1749	1818	4788	1457	1830	1509	6174	1651
1304		4107	1666	2451	1390	1977	1457	2956	1659
1320		8000	1456	1727	1399	2212	1471	2063	1527
1363		13900	2342	2835	3116	5826	3547	3553	2405
1379		9570	3979	6344	5195	8660	5917	8572	3911
1404	A8	2083	2166	5469	1702	2205	1838	7408	1886
1428		4697	1923	2688	1551	2304	1741	3475	1809
1444		8139	1356	1437	1060	1677	1206	1844	1359
1496		12400	2419	3030	3034	5300	3411	3870	2555
1512		5985	2531	4218	3337	5292	3650	5750	2712
1528	A9	2106	1666	3843	1607	2129	1675	5096	1686
1544		4203	1908	3025	1506	2075	1574	3730	1983
1560		7617	1456	1691	1078	1570	1138	2051	1592
1620		15230	3151	4056	3823	6515	4302	5158	3418
1636		6950	3284	5625	4018	6191	4456	7703	3482
1652	A10	2401	2128	5035	1842	2384	1942	6773	2070
1668		4993	2428	3798	1759	2371	1854	4689	2476

1684		9668	1785	2044	1293	1858	1370	2445	1946
1744		17360	3233	4068	4372	7371	4783	4918	3512
1760		7493	3364	5444	4473	6753	4861	7101	3583
1776	A11	2774	2304	4842	2169	2780	2265	6289	2242
1792		5521	2605	3824	2040	2705	2133	4569	2577
1808		10490	1950	2163	1501	2120	1587	2531	2000
1868		27070	5041	6128	7106	12470	8060	7121	4954
1883		11460	5685	9226	7204	10910	8037	11510	5481
1899	A12	3827	3831	9063	3158	3970	3333	11160	3386
1915		6899	4594	7513	2738	3446	2857	8306	4083
1931		11160	3563	4190	1765	2247	1823	4425	3308
1991		23470	6334	9029	6368	8868	6154	8969	6345
2007		10850	5777	11000	6636	8860	6443	12100	6012
2023	A13	4289	3492	8385	3358	4165	3249	9313	3451
2039		9339	4387	7141	3314	4213	3197	7059	4207
2054		17190	3419	4076	2285	3014	2225	3881	3252
2114		20410	6091	8621	5810	8379	5942	8248	5690
2130		10190	5724	10760	6478	9098	6699	11410	5518
2146	A14	4647	3745	8622	3564	4562	3567	9190	3541
2161		10920	4012	5945	3717	5175	3701	5822	3725
2177		23460	2617	2893	2882	4662	2906	2834	2422
2237		21820	3709	4442	5632	10600	6287	4649	3256
2252		8717	3720	5745	5334	8794	6017	6575	3343
2268	A15	3252	2529	4996	2387	3253	2588	5766	2172
2284		7413	2811	3810	2404	3531	2629	4067	2377
2300		15890	1988	2070	1865	3092	2076	2202	1736
2359		23990	3884	4801	5615	10510	6139	5087	3535
2375		8978	3978	6717	5347	8428	5737	7746	3760
2390	A16	3309	2702	6083	2456	3227	2519	7129	2447
2406		7403	3080	4534	2451	3438	2539	4945	2751
2422		15660	2197	2372	1886	2952	2008	2601	2021
2481		24950	3852	4639	5727	11480	6680	5370	3551
2497		9687	3877	6160	5530	9426	6297	7760	3651
2512	A17	3424	2595	5354	2418	3327	2594	6786	2339
2528		7788	2830	3905	2377	3522	2584	4620	2570
2544		16900	1945	2032	1795	3011	2013	2396	1862
2603		25170	3393	4112	5618	11380	6571	4842	3461
2618		9912	3579	5612	5586	9565	6417	7122	3701
2634	A18	3641	2557	5174	2614	3582	2806	6508	2500
2649		7980	2795	4016	2582	3749	2773	4662	2811
2665		16970	1999	2237	1993	3209	2153	2555	2113
2724		33150	4791	5950	8058	15540	8907	7124	5015
2739		12690	5373	8897	7914	12470	8544	11600	5597
2755	A19	4438	3839	8747	3359	4261	3435	11420	3707
2770		9014	4672	7277	3109	4004	3163	8805	4588
2786		17020	3659	4150	2179	2910	2225	4948	3799

2844		30760	7891	10690	8101	12400	8633	13530	8228
2860		12320	7425	14060	7936	11150	8424	19350	7493
2876	A20	4806	4712	11340	3543	4486	3740	15720	4296
2891		10500	5984	9359	3493	4547	3700	11990	5678
2906		20340	4560	5118	2506	3431	2688	6386	4722
2965		30220	6903	9368	7901	13290	8804	11180	7122
2980		13810	6355	11280	8311	13290	9252	14380	6413
2996	A21	5970	4115	8722	4156	5750	4386	10820	4008
3011		13170	3965	5679	3958	5990	4166	6420	4001
3027		25940	2388	2662	2774	4803	2923	2929	2514
3085		31900	3037	3790	6786	15770	7290	4164	3242
3100		13420	3189	4837	6932	13810	7552	5777	3482
3115	A22	5273	2386	4222	3307	5103	3486	5066	2435
3131		11650	2413	3236	3145	5313	3320	3573	2425
3146		23000	1638	1791	2219	4255	2371	1942	1668
3204		30090	3521	4440	6475	13820	6897	4905	3562
3219		12630	3901	6456	6880	12350	7212	7743	4065
3235	A23	5107	2968	6149	3362	4819	3397	7428	2919
3250		11670	3297	4819	3326	5150	3372	5314	3188
3265		24060	2367	2642	2465	4313	2554	2852	2320
3323		26780	4425	5802	6304	12950	7318	6420	4105
3338		11120	4422	7759	6265	11290	7300	9327	4101
3353	A24	4400	3068	6580	2862	4170	3176	7982	2681
3369		10210	3255	4626	2842	4525	3157	5162	2886
3384		22400	2167	2319	2164	3986	2408	2541	2023
3441		27810	3141	4044	6204	13370	6244	4287	3195
3456		10970	3192	5303	6183	11060	6195	6091	3418
3472	A25	4190	2341	4665	2833	4004	2813	5427	2352
3487		8781	2552	3616	2668	4008	2675	3870	2443
3502		18010	1861	2028	1979	3351	2042	2145	1762
3559		46080	4973	6106	9452	23270	10580	6310	4458
3574		18070	5735	9519	9730	18380	10630	10500	5341
3589	A26	6277	4386	9440	4090	5770	4309	10660	3767
3605		10820	5016	7811	3366	4682	3466	7936	4188
3619		16690	3806	4315	2075	2912	2124	4287	3234
3676		43350	7151	9192	9374	19710	11090	9268	5925
3691		21160	6964	11260	10100	20630	12610	12620	5831
3707	A27	8241	4579	8208	4050	6621	4934	9726	3570
3722		15810	5217	6564	3581	5903	4374	7269	3879
3736		23520	3718	3537	2186	3608	2679	3979	2838
3793		32980	6582	8288	7830	15500	9214	8678	5297
3808		19530	6584	11010	10200	19880	11720	12320	5793
3823	A28	11700	4989	9175	6611	11400	7241	10410	4458
3838		24040	4803	6426	6017	11540	6619	6751	4223
3853		37390	2970	3176	3764	8046	4188	3340	2698
3909		28340	4243	5529	7002	15170	7798	6037	4030

3924		14800	4411	7378	7897	15670	8825	8820	4380
3939	A29	7123	3366	6478	4073	6551	4405	7916	3212
3954		15650	3499	4842	3813	6746	4183	5530	3339
3969		29270	2395	2580	2604	5210	2925	2943	2378
4025		31090	4131	5561	6444	13980	7286	6619	4446
4039		13800	4217	7634	6903	13110	7719	9870	4673
4054	A30	5844	3089	6673	3349	5152	3637	8705	3217
4069		12350	3224	4765	3088	5174	3440	5856	3388
4084		22380	2184	2408	2128	4015	2466	2964	2368
4140		28270	3171	4025	5635	15130	7312	5227	3350
4154		12900	3190	5179	6002	13980	7609	7170	3412
4169	A31	5559	2320	4335	3029	5391	3573	5918	2384
4184		11700	2193	2978	2745	5438	3264	3763	2307
4198		20860	1381	1500	1840	4142	2197	1845	1524
4254		25870	1988	2523	4323	12530	5049	3033	2278
4268		12050	2146	3354	4742	11700	5509	4333	2495
4283	A32	5204	1709	3011	2510	4564	2778	3879	1861
4298		11420	1687	2232	2326	4748	2614	2671	1808
4312		21290	1141	1225	1625	3851	1876	1444	1241
4367		23090	2225	2822	4486	12480	5242	3343	2330
4382		10400	2493	4098	4961	11220	5626	5188	2627
4397	A33	4394	1989	3976	2589	4240	2684	4935	2012
4411		9309	2129	3105	2483	4355	2541	3523	2151
4425		17240	1554	1766	1817	3529	1864	1942	1613
4480		24420	3236	4293	5412	12540	5823	4709	3128
4495		10900	3432	6023	5566	11010	6046	7126	3270
4509	A34	4477	2545	5419	2641	4056	2734	6319	2289
4524		9392	2689	3921	2466	4088	2559	4227	2401
4538		16850	1874	2047	1746	3237	1841	2182	1727
4592		23080	2812	3709	5044	12170	5325	3964	2713
4607		10590	2829	4854	5335	11060	5591	5621	2847
4621	A35	4379	2083	4139	2581	4136	2641	4848	1994
4636		9102	2149	3019	2360	4171	2479	3316	2005
4650		16110	1493	1609	1619	3272	1782	1772	1414
4704		21820	3050	3937	4762	11320	5669	4493	2870
4718		10280	3373	6019	5281	10420	6110	7336	3285
4732	A36	4447	2750	5857	2620	4078	2991	7408	2439
4747		9246	3360	4921	2484	4029	2915	5873	2936
4761		16580	2750	2926	1808	3114	2200	3515	2491
4815		24040	7804	12560	6878	11550	8017	13880	7399
4829		11030	7615	20620	7209	10710	8111	23720	7332
4843	A37	4794	5385	19100	3289	4320	3707	22210	4677
4857		9626	6603	13090	3055	4160	3460	14150	5900
4871		16040	4957	6060	2121	3050	2402	6526	4605
4925		22600	5694	8180	6182	11690	7197	8739	5063
4939		11100	5014	9720	6388	11350	7408	11170	4543

4953	A38	5139	3348	7316	3153	4762	3494	8418	2966
4967		10530	3296	4759	2816	4730	3154	5098	2849
4981		16420	2112	2268	1789	3337	2022	2424	1856
5034		15150	3196	4431	3843	7354	4138	4568	2802
5048		7932	3275	6305	4426	7667	4669	6931	2992
5062	A39	3995	2549	5689	2493	3610	2510	6347	2245
5076		10290	3067	4466	2794	4514	2845	4617	2644
5090		23190	2261	2437	2431	4892	2592	2522	2010
5142		12140	2374	3402	3316	6614	3580	3601	2232
5156		5478	1951	3773	3038	5739	3280	4336	1920
5170	A40	2315	1210	2655	1435	2281	1491	3066	1173
5244		26080	741.8	726.1	4298	72310	6139	908	868.5
5271		3612	2431	2153	7870	12810	8892	2379	2096
5277	A41								

Table 8-2 Fatigue lives along the bridge girder. Shearstress is applied.

Position	axis	Point0	Point1	Point2	Point3	Point4	Point5	Point6	Point7
400	A2	1.18E+09	65630	96060	24690	8312	132400	635600	1277000
780	A3	5.57E+08	96410	79870	28380	8504	71640	686400	29330
805		58590	2.42E+08	30050	79560	33800	17360	226600	4418
821		236100	58260	152700	201900	233900	74920	53680	4323
864		132800	97500	113400	169500	1.25E+08	226000	227700	4486
880		129600	39670	56240	16190	397500	6570000	693400	29930
905	A4	3.13E+08	118700	45120	35370	8192	76140	843700	72400
930		85700	1.64E+08	46880	96830	76290	18370	277700	10470
946		360700	28980	87750	372600	389400	157800	65480	10060
989		238800	84700	153200	101700	1.79E+09	478900	278200	9905
1005		257600	41800	65060	34830	215400	3764000	847900	67410
1030	A5	2.09E+08	122900	69300	43550	17710	148500	731900	22820
1054		119200	1.01E+08	64090	147600	129200	36370	241400	3570
1070		498200	48470	54230	182500	176900	211700	57380	3460
1114		366700	46580	202100	221900	1.63E+09	634300	233800	3453
1130		396600	37560	81300	33770	228700	2180000	709300	22150
1155	A6	1.74E+08	70290	90600	62160	32260	226500	496600	89070
1179		135900	55330000	71780	87400	57960	53310	164000	12840
1195		554700	63300	35830	1660000	181000	164600	39820	12380
1239		492300	67930	401200	407000	1.7E+09	496800	164200	12310
1255		495500	21200	102500	73520	442800	1275000	497700	85270
1279	A7	5.34E+08	44690	96310	37910	13620	168800	457900	61990
1304		80300	31620000	78220	33380	59680	39770	150500	8952
1320		326400	70460	1403000	9145000	426200	191200	36090	8781
1363		539300	89210	239300	173900	98180000	581100	156900	9129
1379		510400	30790	149900	134600	684000	751100	478800	62910
1404	A8	6.55E+08	48430	95180	5046	14690	185300	670800	132000
1428		44510	18320000	93760	64220	139900	44230	221200	18180
1444		181000	76310	30940	14610000	507800	144900	52210	8345
1496		315700	96940	39410	183800	65300000	431500	219000	18220
1512		292600	40290	90270	57130	509500	457700	670100	22910
1528	A9	73050000	85000	109400	8748	33040	157600	808600	22870
1544		50110	10760000	79600	24920	166900	37760	269100	18960
1560		205100	93570	63440	23690000	652200	64660	62910	8709
1620		177800	95260	4774	402700	40020000	194000	243900	18820
1636		181500	42810	586400	60730	557300	281700	739300	23180
1652	A10	67700000	129300	96270	4052	40330	64740	799400	51060
1668		78240	6333000	56990	92480	213300	15770	264300	38590
1684		319800	83310	23880	35800000	761800	111700	62750	17450
1744		201300	110100	8643	513400	23830000	336500	282000	39080
1760		198000	41270	4740	134400	474800	173800	864300	53070
1776	A11	67130000	114000	74440	13120	49200	113900	2064000	93450
1792		120400	3681000	48900	66630	250500	27420	679400	65410
1808		495400	59180	90940	45840000	445400	168600	164100	28710

1868		321700	100100	3943	631800	14180000	507200	813800	58900
1883		340200	47200	8418	169700	193700	109400	2535000	87170
1899	A12	23660000	98870	64260	9891	59210	165500	1366000	42350
1915		112700	2170000	65350	22690	148200	40380	445400	33990
1931		471900	49390	69440	6.03E+08	262900	179900	103000	15270
1991		497900	78140	13160	764200	8213000	541300	360100	32550
2007		520300	43040	3922	208100	341100	71150	1054000	42150
2023	A13	25490000	72760	78850	17490	36770	183200	156500	41780
2039		108600	1253000	92010	22690	86070	43840	401400	31490
2054		436800	62620	133900	5.11E+08	269100	193200	8871	14500
2114		468700	66330	10340	467600	4923000	582900	41550	32140
2130		473600	34210	12810	251300	493000	47580	654800	40620
2146	A14	28300000	45460	101300	17910	20180	193000	8384	83430
2161		76590	714400	114300	53020	88470	45930	4501	59270
2177		305400	86190	22800	3.52E+09	552500	238300	18550	26980
2237		424100	79190	17950	254400	2965000	721000	90000	62250
2252		402700	29040	9984	154100	551200	1991000	1225000	88570
2268	A15	30410000	65810	125000	36710	21650	236700	18830	111100
2284		42800	417700	217800	90180	180700	56130	9571	73000
2300		178200	112700	51740	3.1E+09	756500	199700	6295	31870
2359		299800	102100	18520	274300	1791000	601400	29870	70940
2375		290800	34380	8125	83820	581000	38560	10670000	112400
2390	A16	30880000	86150	203000	59040	41470	205800	6242	138800
2406		70040	258700	104000	41880	249400	49260	3264	81730
2422		281900	231500	93640	3.25E+09	602600	140800	24050	35300
2481		177900	129800	37630	513000	1082000	424300	113500	82500
2497		186700	44130	8393	90440	713200	91750	2.56E+08	144400
2512	A17	28150000	99920	114800	31520	61560	139800	24480	165100
2528		83760	169100	289000	42050	197900	34250	12690	96140
2544		336000	140000	42630	1.8E+08	669200	139700	16290	41050
2603		275100	207400	64110	793300	653700	424300	78730	89380
2618		266100	54760	16710	170700	618300	29400	1.87E+09	153800
2634	A18	23250000	117200	11590	33570	47430	132400	16190	100600
2649		94160	507200	1270000	90390	219400	31960	8312	68390
2665		380300	22060	42400	1.17E+08	494500	199200	35680	30350
2724		334500	125000	34180	613900	405300	603400	108400	65120
2739		341200	84490	28160	261700	418900	115900	1.79E+09	95180
2755	A19	17280000	141000	22330	60600	51160	203700	34830	56970
2770		109900	10810	11560000	119700	164400	48180	8504	43300
2786		448700	5141	82050	68320000	234000	200000	33800	19550
2844		380400	113600	32200	657500	252500	596200	102800	42170
2860		396900	51450	15280	202000	398700	78120	1.18E+10	58450
2876	A20	11810000	118300	8445	72670	42300	229000	33770	61880
2891		139400	22360	3.35E+08	143000	77120	53380	8192	44800
2906		574900	9539	111300	38280000	395900	223700	76290	20470
2965		449200	5126	56000	537900	157200	681700	233900	45780

2980		470700	5438	14850	216300	615000	169500	3.02E+09	61350
2996	A21	7608000	78760	32170	79740	18550	206800	73520	107500
3011		128100	8178	6.92E+09	163300	130500	49450	17710	74750
3027		528100	4090	145200	21390000	581900	728900	129200	33840
3085		572000	9328	70320	230800	99630	2276000	389400	77250
3100		578600	9647	25430	177400	688400	101700	4.53E+08	114500
3115	A22	4737000	62860	22710	88990	32040	579100	134600	160300
3131		86900	31870	6.27E+09	93430	191800	142200	32260	95500
3146		346800	14500	169000	11610000	634200	309400	57960	41670
3204		516300	4075	83850	406000	65050	895800	176900	94550
3219		489800	4203	30870	76590	618500	221900	8.6E+08	162600
3235	A23	2981000	82550	12150	61940	45720	380600	57130	138400
3250		65130	23410	2.32E+10	58380	208700	88870	13620	89430
3265		251600	11020	104700	6570000	693400	37190	59680	39430
3323		336100	14200	92830	566700	43620	654800	181000	88860
3338		319100	14520	35410	134100	1724000	407000	1.17E+09	137600
3353	A24	1865000	157900	12110	41240	50120	317300	60730	141100
3369		73970	46210	6.26E+09	60990	227700	7978	14690	88770
3384		286300	19820	57930	3764000	847900	81480	139900	38540
3441		245900	10700	69830	635600	1759000	9145000	426200	84410
3456		246300	10620	39290	188700	1153000	173900	74830000	133800
3472	A25	1155000	222300	28390	43360	53680	4064	134400	106800
3487		123800	12120	5.13E+08	113400	278200	16810	33040	71640
3502		528700	20080	63030	2180000	709300	26700	166900	31270
3559		287400	8966	43590	686400	34330	14610000	507800	61950
3574		312100	19400	30160	210100	121700	183800	65880000	97060
3589	A26	724500	254800	48540	72980	65480	8693	169700	53180
3605		222000	27590	8.74E+08	162200	233800	5643	40330	41360
3619		1020000	42820	105200	1275000	497700	100100	213300	18740
3676		552000	9106	43560	843700	82770	23690000	652200	38520
3691		637100	19580	19400	226600	7523	402700	51360000	53560
3707	A27	467800	112800	22300	98260	57380	2932	208100	86230
3722		375500	50470	1.16E+09	132900	164200	21300	49200	56380
3736		1420000	74710	161500	751100	478800	68420	250500	25950
3793		1025000	19070	69420	731900	26180	35800000	761800	57830
3808		1021000	42430	19570	277700	17050	513400	35890000	83670
3823	A28	311000	289000	22370	73930	39820	11300	251300	110700
3838		182400	22540	74880000	134600	156900	14170	59210	72520
3853		629800	37100	133800	457700	670100	95720	148200	33530
3909		1281000	32950	100700	496600	102500	45840000	445400	77260
3924		1011000	70220	31270	241400	5580	631800	22750000	116100
3939	A29	746200	10660000	48830	78310	36090	7246	154100	125500
3954		34990	22750	67490000	102800	219000	31690	36770	80670
3969		191400	35760	138000	281700	739300	88850	86070	36490
4025		561500	16600	75660	457900	67510	6.03E+08	262900	82610
4039		413400	35200	44280	164000	21710	764200	12450000	130400

4054	A30	16160	95260000	64220	67990	52210	7558	83820	144300
4069		15870	44600	52610000	55690	243900	29450	20180	88820
4084		15700	65450	107400	173800	864300	198500	88470	39240
4140		16230	16340	79660	670800	148400	5.11E+08	269100	88530
4154		16340	36490	32350	150500	14040	467600	7211000	148400
4169	A31	32520	2.56E+09	77980	39940	62910	7179	90440	173300
4184		31490	60150	35820000	86730	282000	65180	21650	95470
4198		30650	85020	54070	109400	2535000	327000	180700	41380
4254		30570	29740	73290	808600	87640	3.52E+09	552500	93510
4268		30940	70490	34230	221200	30670	254400	4262000	171600
4283	A32	11890	4.67E+10	88440	61210	62750	15140	170700	155200
4298		11770	78450	22050000	117300	813800	109400	41470	87860
4312		11580	103400	88620	71150	1054000	147200	249400	38170
4367		11800	37470	42680	799400	186700	3.1E+09	756500	84960
4382		11980	88510	32480	269100	29370	274300	2515000	148000
4397	A33	48140	4.58E+10	50620	78520	164100	27510	261700	106600
4411		48190	91850	11890000	131200	360100	48610	61560	67220
4425		47550	116800	116100	47580	654800	153800	197900	29850
4480		48270	43750	58770	2064000	341600	3.25E+09	602600	64030
4495		48860	99590	19430	264300	62420	513000	1451000	101900
4509	A34	38270	4.48E+10	31400	81040	103000	11480	202000	90280
4524		37470	56150	6825000	140700	41550	51140	47430	57450
4538		36480	81640	129400	1991000	3046000	371000	219400	25480
4592		36460	49430	76500	1366000	144100	1.8E+08	669200	56660
4607		36380	113000	27060	679400	113900	793300	812700	90880
4621	A35	71720	1.17E+10	32870	77540	8871	12630	216300	115400
4636		68750	30920	4020000	167800	90000	122900	51160	69390
4650		67020	48400	137800	38560	4409000	422200	164400	30520
4704		65620	35350	81690	156500	155000	1.17E+08	494500	68250
4718		16160	73250	34910	445400	47780	613900	455500	119400
4732	A36	17180	6.84E+08	61640	87420	18550	29300	177400	164700
4747		70650	34040	2404000	142400	29870	140300	42300	93970
4761		69830	49910	167500	91750	6431000	543200	77120	40630
4815		70500	21580	78080	8384	352900	68320000	234000	86850
4829		17280	46990	36260	401400	51750	657500	248600	166300
4843	A37	41290	1.01E+09	88480	77880	6295	34510	76590	198900
4857		173900	57240	1431000	103000	113500	178900	18550	103000
4871		173000	81240	149100	29400	8875000	649000	130500	44100
4925		177200	22270	88330	18830	436700	38280000	395900	100700
4939		42430	49150	34040	4501	118500	537900	133900	205200
4953	A38	76480	1.25E+09	72900	61600	24050	41340	134100	411300
4967		320700	87740	832500	88630	78730	214400	32040	170900
4981		315800	120600	107400	115900	10840000	383200	191800	73070
5034		304900	36500	80920	6242	523200	21390000	581900	184100
5048		72100	85690	38190	9571	145000	230800	75320	419000
5062	A39	35730	3.48E+08	73210	53750	16290	50400	188700	248200

5076		151400	73240	486200	117800	108400	128300	45720	105300
5090		148000	93090	90260	78120	1.38E+08	222300	208700	45350
5142		147000	52890	65440	24480	638000	11610000	634200	102100
5156		34500	118200	35020	3264	173900	406000	46120	192800
5170	A40	33180	3.1E+08	55620	63960	35680	31900	210100	39820
5244		135800	75210	275000	163400	102800	73440	50120	607500
5271		31690	91260	28700	12690	212100	566700	30230	654800
5277	A41								

About DNV GL

DNV GL is a global quality assurance and risk management company. Driven by our purpose of safeguarding life, property and the environment, we enable our customers to advance the safety and sustainability of their business. We provide classification, technical assurance, software and independent expert advisory services to the maritime, oil & gas, power and renewables industries. We also provide certification, supply chain and data management services to customers across a wide range of industries. Operating in more than 100 countries, our experts are dedicated to helping customers make the world safer, smarter and greener.